



The
University
Of
Sheffield.

Batch and containerless crystallisation of L-glutamic acid in the presence and absence of amino acid additives

A thesis submitted to the University of Sheffield
for the degree of Doctor of Philosophy in the Faculty of Engineering

by

Michal Rusin

Department of Chemical and Biological Engineering
University of Sheffield

July 2013

Abstract

Despite significant advances in recent years, our fundamental understanding and the ability to predict and control the polymorphic outcome of the crystallisation process remains limited. The aim of this work is to investigate how manipulation of the process conditions and application of new experimental strategies may provide new modes of polymorph selection during crystallisation from solution.

In the first part of this thesis, batch crystallisation of pure and glycine-doped L-glutamic acid was investigated using single-photon laser light scattering and synchrotron wide angle X-ray scattering (WAXS) techniques. Surprisingly, in the presence of the additive, a marked increase in the amount of homogeneously nucleated β was observed, ultimately leading to a significant enhancement in the polymorphic transformation rate. Thus, for the first time, it was demonstrated that the crystallisation rates of one amino acid can be promoted using another amino acid as a doping material.

The second part of this work focuses on the containerless crystallisation of L-glutamic acid from a droplet in an acoustic levitator. Using *in-situ* WAXS and Raman spectroscopy measurements, it was found that, contrary to the Ostwald's rule of stages, the more stable β is the first and only polymorph that forms. The metastable α did not nucleate even in the presence of the additives that have previously been reported to stabilise the metastable polymorph. It was postulated that the previously unreported selective crystallisation is due to a lower nucleation barrier for β at the surface of a droplet when compared to the centrosymmetric bulk.

The entirely new effects presented in this work demonstrate how changing the crystallisation conditions may perturb the initial series of nucleation events and ultimately have a significant effect on the subsequent polymorphic transformation and thus on the crystallisation process as a whole. Furthermore, these original findings open new avenues of research and raise many fundamental questions on how nature finds intriguing ways to help crystallisation of the more stable polymorphic form. From the industrial standpoint, the insights derived from this study may contribute to the design of new nucleation and transformation modulators.

Acknowledgements

First and foremost, I would like to express my gratitude to my supervisor, Dr Rile Ristic, for his unreserved support, expertise and encouragement throughout this project, for many stimulating discussions and his insistence on excellence. I would also like to acknowledge Dr Bruce Ewan and Dr Luciana De Matos for their help at various stages of my PhD.

Furthermore, I would like to extend my gratitude to Dr Franziska Emmerling and her research group at the BAM Institute in Berlin for giving me the opportunity to access the synchrotron facilities and for assistance provided during data collection at BESSY II.

On a personal level, I would like to thank my family and friends for their encouragement, patience and support.

Table of contents

Introduction.....	14
Project objectives	16
Key contributions.....	17
Thesis structure	18
1. Theoretical background	19
1.1 Crystals and crystal structures	19
1.1.1 Crystalline and amorphous state	19
1.1.2 Unit cell.....	20
1.1.3 Miller indices	20
1.2 Structural imperfections in crystals	22
1.2.1 Point defects.....	22
1.2.2 Line defects.....	23
1.2.3 Surface defects	26
1.2.4 Volume defects	26
1.3 Driving force for crystallisation.....	26
1.3.1 Solubility curves	26
1.3.2 Supersaturation	28
1.4 Nucleation	29
1.4.1 Primary homogeneous nucleation.....	30
1.4.2 Primary heterogeneous nucleation.....	33
1.4.3 Secondary nucleation	34
1.5 Crystal growth.....	34
1.5.1 Adsorption layer theories and spiral growth.....	36
1.5.2 Birth and spread model	37
1.5.3 Continuous growth.....	40
1.6 Polymorphism.....	40
1.6.1 Types of polymorphism	40

1.6.2 The phase rule	41
1.6.3 Ostwald's rule	41
1.6.4 Enantiotropism and monotropism	42
1.6.5 Commercial importance of polymorphism	42
2. L-Glutamic acid as a model compound.....	44
2.1 Amino acids	44
2.2 Selection criteria	45
2.3 Molecular and crystal structure.....	47
2.4 The existing approaches to study crystallisation	51
2.5 Primary factors affecting the crystallisation of L-glutamic acid	56
2.6 Crystallisation kinetics.....	57
2.7 Polymorphic transformation mechanism	57
2.8 Reactive crystallisation of L-glutamic acid.....	59
2.9 Additives as secondary determinants in the crystallisation process	60
3. Experimental methods	64
3.1 Materials used	64
3.2 Apparatus and experimental techniques	64
3.2.1 Batch crystallisation.....	64
3.2.1.1 Nucleation time measurements	65
3.2.1.2 In-house studies of polymorphic transformation	67
3.2.1.3 Synchrotron-based studies of growth and polymorphic transformation.....	68
3.2.2 Acoustic levitation	68
3.2.3 Synchrotron Wide-Angle X-ray Scattering	70
3.2.4 Raman Spectroscopy.....	73
3.2.5 Droplet volume monitoring.....	74
3.2.6 Solution concentration evolution	74
3.3 Experimental procedures	76
3.3.1 Batch crystallisation.....	76
3.3.1.1 Nucleation time measurements	76
3.3.1.2 In-house studies of polymorphic transformation	77
3.3.1.3 Synchrotron-based studies of growth and polymorphic transformation.....	78
3.3.2 Acoustic levitation	78

4. Nucleation and polymorphic transformation studies of pure and glycine-doped L-glutamic acid	81
4.1 Polymorphic transformation of L-glutamic acid in the presence and absence of glycine additive	81
4.1.1 Pure L-glutamic acid solution	81
4.1.2 L-Glutamic acid doped with glycine	83
4.2 Nucleation of L-glutamic acid in the presence and absence of glycine additive	87
4.2.1 The effect of glycine on the nucleation time of L-glutamic acid	87
4.2.2 The effect of glycine on the surface free energy and critical nucleus radius of L-glutamic acid	90
4.3 Scanning Electron Microscopy and High Performance Liquid Chromatography of pure and glycine doped L-glutamic acid samples	95
4.4 Discussion	96
4.5 Conclusions	100
5. Evolutionary behaviour of the polymorphic mole fractions during crystallisation of pure and glycine-doped L-glutamic acid	101
5.1 WAXS as a tool to monitor the mole fraction evolutions of the crystallising L-glutamic acid	101
5.1.1 Evidence of the effect of the additive	101
5.1.2 Assessment of the mole fraction evolutions	102
5.2 Mole fraction evolutions of α and β polymorphs during crystallisation of the pure and glycine-doped solutions of L-glutamic acid	106
5.2.1 Region I: pure solution of L-glutamic acid	111
5.2.2 Region I: L-glutamic acid solution doped with glycine	112
5.2.3 Region II: pure solution of L-glutamic acid	114
5.2.4 Region II: L-glutamic acid solution doped with glycine	116
5.2.5 Region III: pure solution of L-glutamic acid	119
5.2.6 Region III: L-glutamic acid doped with glycine	121
5.2.7 Region IV: pure solution of L-glutamic acid	122
5.2.8 Region IV: L-glutamic acid solution doped with glycine	123
5.3 Determination of the polymorphic transformation time from WAXS data	124
5.4 Conclusions	125
6. Crystallisation of L-glutamic acid in an acoustic levitator	127
6.1 Containerless crystallisation of pure L-glutamic acid solution	127
6.1.1 Wide Angle X-ray Scattering	127

6.1.2 Raman spectroscopy measurements	131
6.1.3 Sample volume and aspect ratio	132
6.2 Molar concentration and crystallised mole fraction evolutions.....	134
6.2.1 Assessment method.....	134
6.2.2 Physical meaning of the key points on the evolution curves	135
6.2.3 Chemical potential and the irreversible change in entropy.....	139
6.3 Why is β -L-glutamic acid the only polymorph that forms in an acoustic levitator?....	141
6.3.1 Thermodynamic consideration of nucleation in the bulk	142
6.3.2 Crystallisation from a levitated droplet in the light of classical nucleation theory	144
6.3.5 Qualitative rationale for selective crystallisation of β -L-glutamic acid in an acoustic levitator	145
6.4 Containerless crystallisation of L-glutamic acid solution doped with additives.....	147
6.4.1 Results.....	147
6.4.2 Discussion	152
6.5 Conclusions.....	154
7. Conclusions.....	156
8. Further work.....	159
8.1 Investigation of the mechanism leading to the enhanced primary nucleation of β -L-glutamic acid in the presence of glycine additive	159
8.2 Molecular dynamics modelling to determine the order parameters leading to selective nucleation of β -L-glutamic acid in a levitated droplet	161
References.....	163

List of figures

Figure 1.1	Schematic structures of amorphous and crystalline SiO ₂	21
Figure 1.2	Schematic representations of structural motifs in a crystal lattice	21
Figure 1.3	A parallel-sided unit cell in a space lattice and the notation for the sides and angles	22
Figure 1.4	Various lattice planes described using Miller indices	24
Figure 1.5	Schematic representation of common point defects: interstitial impurity, substitutional impurity, vacancy	24
Figure 1.6	Movement of an edge dislocation through a crystal.....	25
Figure 1.7	A screw dislocation	25
Figure 1.8	Two types of grain boundaries: tilt, twist.....	27
Figure 1.9	Development of an inclusion	27
Figure 1.10	The solubility-supersolubility diagram and change in supersaturation on cooling, solvent evaporation, combined cooling and solvent evaporation.....	29
Figure 1.11	Classification of nucleation mechanisms	32
Figure 1.12	Free energy diagram for nucleation explaining the existence of a critical nucleus	32
Figure 1.13	Equilibrium shape of a liquid droplet on a substrate surface	35
Figure 1.14	Ratio of free energies of heterogeneous and homogeneous nucleation as a function of the contact angle.....	35
Figure 1.15	Kossel's model of a growing crystal showing flat surfaces, steps, kinks, and three stages of the crystal growth: bulk transport, boundary layer diffusion, incorporation of the crystallising entity.....	38
Figure 1.16	Development of a growth spiral starting from a screw dislocation	38
Figure 1.17	The Burton-Cabrera-Frank supersaturation-growth relationship: parabolic growth law, linear growth law	39
Figure 1.18	Development of the polynuclear growth by the birth and spread mechanism ...	39
Figure 1.19	Solubility curves in monotropic and enantiotropic systems.....	42
Figure 2.1	General structure of an α -amino acid	45
Figure 2.2	Skeletal structure of L-glutamic acid in its neutral and zwitterionic form	48
Figure 2.3	Conformation of L-glutamic acid in the α and the β crystal structure.	49

Figure 2.4	Packing structures of α - and β -L-glutamic acid.....	50
Figure 2.5	Experimentally observed X-ray diffraction patterns of the α and the β form of L-glutamic acid	52
Figure 2.6	Experimentally observed Raman spectra of the α and the β form of L-glutamic acid.....	53
Figure 2.7	Microscope images showing the α and the β L-glutamic acid crystal morphology.....	54
Figure 2.8	Solubility curves of L-glutamic acid polymorphs.....	54
Figure 2.9	Concentration change during crystallisation of L-glutamic acid at 45°C.....	58
Figure 2.10	Morphological change of the α crystal during growth	58
Figure 2.11	Crystal morphologies of α - and β -L-glutamic acid.....	58
Figure 3.1	Front view of the experimental set-up for the nucleation time studies	66
Figure 3.2	Side view of the experimental set-up for the nucleation time studies	66
Figure 3.3	Experimental set-up used in the growth and polymorphic transformation studies	69
Figure 3.4	Detailed view of the flow cell used in the growth and polymorphic transformation studies.....	69
Figure 3.5	A droplet of L-glutamic acid solution suspended in air using an acoustic levitator.....	71
Figure 3.6	Schematic representation of the principle of acoustic levitation	71
Figure 3.7	Schematic representation of the set-up used in the levitated droplet experiment	72
Figure 3.8	Equivalent points on the conductivity plot obtained during batch crystallisation of L-glutamic acid at 45°C and on the solubility curves	75
Figure 3.9	Relationship between solution conductivity and concentration of L-glutamic acid.....	75
Figure 3.10	Single-photon laser light scattering data on the induction time of L-glutamic acid ($\sigma = 0.5$) obtained in one of the nucleation experiments for pure solution.	77
Figure 4.1	Concentration evolution curve for batch crystallisation of pure L-glutamic acid.....	84
Figure 4.2	Concentration evolution curve for batch crystallisation of L-glutamic acid doped with 1250 ppm of glycine	84
Figure 4.3	Concentration evolution curve for batch crystallisation of L-glutamic acid doped with 2500 ppm of glycine	85
Figure 4.4	Concentration evolution curve for batch crystallisation of L-glutamic acid doped with 5000 ppm of glycine	85
Figure 4.5	Concentration evolution curve for batch crystallisation of L-glutamic acid doped with 7500 ppm of glycine	86
Figure 4.6	Single-photon laser light scattering data on the induction time of L-glutamic acid ($\sigma = 0.5$) obtained in one of the nucleation experiments for pure solution.	88

Figure 4.7	Single-photon laser light scattering data on the induction time of L-glutamic acid ($\sigma = 0.5$) obtained in one of the nucleation experiments for solution doped with 1250 ppm of glycine	88
Figure 4.8	Single-photon laser light scattering data on the induction time of L-glutamic acid ($\sigma = 0.5$) obtained in one of the nucleation experiments for solution doped with 2500 ppm of glycine	89
Figure 4.9	Single-photon laser light scattering data on the induction time of L-glutamic acid ($\sigma = 0.5$) obtained in one of the nucleation experiments for solution doped with 5000 ppm of glycine	89
Figure 4.10	Single-photon laser light scattering data on the induction time of L-glutamic acid ($\sigma = 0.5$) obtained in one of the nucleation experiments for solution doped with 7500 ppm of glycine	90
Figure 4.11	Plot of the dependence of $\ln \tau$ on $T^{-3}(\ln S)^{-2}$ obtained for nucleation of pure L-glutamic acid solution	92
Figure 4.12	Plot of the dependence of $\ln \tau$ on $T^{-3}(\ln S)^{-2}$ obtained for nucleation of L-glutamic acid solution doped with 1250 ppm of glycine	92
Figure 4.13	Plot of the dependence of $\ln \tau$ on $T^{-3}(\ln S)^{-2}$ obtained for nucleation of L-glutamic acid solution doped with 2500 ppm of glycine	93
Figure 4.14	Plot of the dependence of $\ln \tau$ on $T^{-3}(\ln S)^{-2}$ obtained for nucleation of L-glutamic acid solution doped with 5000 ppm of glycine	93
Figure 4.15	Plot of the dependence of $\ln \tau$ on $T^{-3}(\ln S)^{-2}$ obtained for nucleation of L-glutamic acid solution doped with 7500 ppm of glycine	94
Figure 4.16	Plot of the dependence of surface free energy, γ , on the level of glycine additive	94
Figure 4.17.	SEM images of samples extracted shortly after the crystallisation process was started, i.e. at the beginning of region I: crystallisation without glycine and with 2500 ppm of glycine as an additive	97
Figure 4.18.	SEM image of β crystals growing on the $\{011\}$ and $\{111\}$ type faces of α -L-glutamic acid as a result of secondary nucleation of the more stable polymorph in region II.....	100
Figure 5.1	Time-resolved WAXS spectra of L-glutamic acid crystallising from pure solution	103
Figure 5.2	Time-resolved WAXS spectra of L-glutamic acid crystallising from solution doped with 5000 ppm of glycine	103
Figure 5.3	Mole fraction evolution of dissolved L-glutamic acid determined using two independent methods: from conductivity data and from WAXS data.....	106
Figure 5.4	Mole fraction evolutions of the crystallised phases and dissolved L-glutamic acid determined for pure solution.....	107
Figure 5.5	The rate of change (first derivative) of mole fraction evolutions of the crystallised phases of L-glutamic acid determined for pure solution	107
Figure 5.6	Mole fraction evolutions of the crystallised phases and dissolved L-glutamic acid determined for solution doped with 2500 ppm of glycine.....	108

Figure 5.7	The rate of change (first derivative) of mole fraction evolutions of the crystallised phases of L-glutamic acid determined for solution doped with 2500 ppm of glycine	108
Figure 5.8	Mole fraction evolutions of the crystallised phases and dissolved L-glutamic acid determined for solution doped with 5000 ppm of glycine	109
Figure 5.9	The rate of change (first derivative) of mole fraction evolutions of the crystallised phases of L-glutamic acid determined for solution doped with 5000 ppm of glycine	109
Figure 5.10	Mole fraction evolutions of the crystallised phases and dissolved L-glutamic acid determined for solution doped with 7500 ppm of glycine	110
Figure 5.11	The rate of change (first derivative) of mole fraction evolutions of the crystallised phases of L-glutamic acid determined for solution doped with 7500 ppm of glycine	110
Figure 5.12	Schematic representation of formation of an etch pit at screw dislocation outcrop	114
Figure 5.13	SEM image of fragmented β -L-glutamic acid crystals extracted in region III .	120
Figure 6.1	Time evolution of WAXS spectra for crystallisation of pure L-glutamic acid.	128
Figure 6.2	Selected WAXS patterns and Raman spectra for crystallisation of pure L-glutamic acid	129
Figure 6.3	Selected images of the shadow of the sample used to determine the change in its volume with time for a typical pure L-glutamic acid crystallisation experiment	130
Figure 6.4	Change in volume of the sample as a function of time for a typical pure L-glutamic acid crystallisation experiment	133
Figure 6.5	Change in the aspect ratio and the horizontal and vertical diameters of the sample as a function of time for a typical pure L-glutamic acid crystallisation experiment	133
Figure 6.6	Molar concentration and crystallised mole fraction evolution curves determined for a typical pure L-glutamic acid solution crystallising from a droplet	136
Figure 6.7	The rate of change (first derivative) of concentration and crystallised mole fraction evolution curves determined for a typical pure L-glutamic acid solution crystallising from a droplet	136
Figure 6.8	The rate of change of the rate of change (second derivative) of concentration and crystallised mole fraction evolution curves determined for a typical pure L-glutamic acid solution crystallising from a droplet	137
Figure 6.9	Irreversible change of entropy for a typical pure L-glutamic acid solution crystallising from a droplet	141
Figure 6.10	Schematic representation of the change of enthalpy and entropy during crystallisation of α and β polymorphs of L-glutamic acid	143
Figure 6.11	Evolution of solution concentration in a levitated droplet	146

Figure 6.12	Schematic representation of the balance of attractive forces in the bulk and at the surface of a droplet	146
Figure 6.13	Selected WAXS spectra for a typical crystallisation of L-glutamic acid doped with 2500 ppm of glycine	148
Figure 6.14	Selected WAXS spectra for a typical crystallisation of L-glutamic acid doped with 10000 ppm of glycine	148
Figure 6.15	Selected WAXS spectra for a typical crystallisation of L-glutamic acid doped with 2500 ppm of L-alanine	149
Figure 6.16	Selected WAXS spectra for a typical crystallisation of L-glutamic acid doped with 10000 ppm of L-alanine	149
Figure 6.17	Selected WAXS spectra for a typical crystallisation of L-glutamic acid doped with 2500 ppm of L-phenylalanine	150
Figure 6.18	Selected WAXS spectra for a typical crystallisation of L-glutamic acid doped with 10000 ppm of L-phenylalanine	150

List of tables

Table 2.1	Twenty common naturally-occurring amino acids and their classification.....	46
Table 2.2	Crystallographic data of L-glutamic acid polymorphs.....	48
Table 3.1	Chemicals used in the experiments	65
Table 3.2	Chemical composition of all investigated solutions	79
Table 5.1	Effect of various levels of glycine on the polymorphic transformation of L-glutamic acid	125
Table 6.1	Average values of the nucleation and crystal growth time during crystallisation of L-glutamic acid in the acoustic levitator in the presence of additives	152

Introduction

Crystallisation is a complex process where a particular substance undergoes a phase transition from solution, melt or more rarely vapour to the crystalline solid state. The solid resulting from the process, a crystal, has an ordered internal arrangement of molecules. Some molecules, however, have the ability to adopt different arrangements in the solid state. This phenomenon is commonly referred to as polymorphism and can greatly complicate efforts to control the crystalline form of the compound of interest. Despite many years of scientific endeavour, our fundamental understanding of the molecular mechanisms occurring in the crystallisation of polymorphic materials from solution remains one of the greatest challenges in science. Fortunately, the recent advances in both experimental and computational methods are beginning to provide new insights into the crystallisation process.

Over the past years, there has been an increased interest in controlling the crystallisation pathways using molecular additives. It has been shown that such additives can influence nucleation and growth rates and even lead to selective formation of a particular polymorphic form. The latter appears to be of critical importance since different polymorphs may have very different physical properties, such as solubility, crystal morphology or melting point. Since molecular crystals make up a large number of substances produced by the chemical industry, from pharmaceuticals and cosmetics through food and agricultural products to specialty chemicals, the ability to manipulate the crystal structure and therefore material properties is of great academic and industrial interest.

The initial motivation for this work was to investigate the previously unreported polymorphic transformation promoting effect of glycine serendipitously discovered by the author during studies on the influence of various amino acid additives on the crystallisation process of L-glutamic acid. The goal was to provide insights into the underlying molecular mechanisms responsible for the observed effect and, in particular, explore the effect of the additive on the nucleation process, the most critical stage which defines the overall time dependent crystallisation evolution of the system. Additionally, during the course of the project, the opportunity arose to, for the first time, study the crystallisation behaviour of L-glutamic acid

from a droplet of solution suspended in an acoustic levitator. The containerless crystallisation technique is considered to be of particular interest since it allows exploring the nucleation and crystal growth phenomena without any surface contributions of a conventional reaction vessel.

We believe that the findings from this research would be interesting and stimulating for both industrial and scientific communities. The generic nature of the work presented in this thesis should open new research avenues for a comprehensive appreciation of the overall complexity of the crystallisation of polymorphic materials, from clean metastable solution via polymorphic transformation to stable crystalline phase. The insights derived from these studies could facilitate the design of potent new synthetic nucleation and transformation modulators for diverse polymorphic systems. Ultimately, this would allow better control of the polymorph selection process in a wide range of crystalline materials.

Project objectives

In light of the presented research challenges, the following aims and objectives have been set for this project:

- (i) At constant initial supersaturation and crystallisation temperature, investigate the effect of various levels of glycine on the nucleation and polymorphic transformation times of L-glutamic acid.
- (ii) Determine mole fractions and the corresponding mole fraction rates evolutions of metastable α and stable β form of L-glutamic acid for the conditions defined in (i).
- (iii) Compare these evolutions with the simultaneously measured concentration evolutions and find a correlation between them.
- (iv) Find the physical reasons and mechanism by which the additive enhances the kinetics of growth/dissolution of the two forms, and hence the polymorphic transformation time.
- (v) Establish the concentration range at which the promoting effect of glycine is present.
- (vi) At constant crystallisation temperature and starting from saturated solution, investigate nucleation and growth of L-glutamic acid during crystallisation from a pure droplet and in the presence of additives.
- (vii) Propose a qualitative model explaining why under conditions defined in (vi) the nucleation process results in formation of a different polymorph than expected.
- (viii) Examine the effect of additives on the growth process for the conditions defined in (vi) and determine a mechanism by which the additives operate.

Key contributions

The key contributions of this work are:

- (i) For the first time, it was demonstrated that glycine used as an additive promotes primary nucleation of the stable β form of L-glutamic acid, ultimately leading to a significant increase in the subsequent polymorphic transformation.
- (ii) It was shown that, contrary to the Ostwald's rule of stages, the more stable β is the first and only polymorph that forms during crystallisation of L-glutamic acid from a levitated droplet.

Thesis structure

Following the introduction, this thesis is organised into the following chapters.

Chapter 1 introduces the basic concepts in the field of crystallisation and presents the main nucleation and crystal growth theories on which this research is based. *Chapter 2* contains a literature review covering the crystal structures and physical data of L-glutamic acid polymorphs and surveys previous work related to the topic of this study. The experimental methods, procedures and materials used in this work are outlined in *Chapter 3*.

Chapters 4 and *5* cover batch crystallisation studies of L-glutamic acid. In *Chapter 4*, the effect of various levels of glycine on the nucleation and polymorphic transformation rates is investigated using laser light scattering and concentration monitoring techniques. The evolution of polymorphic mole fractions studied under the same experimental conditions using WAXS is presented and thoroughly discussed in *Chapter 5*.

Chapter 6 considers nucleation and crystal growth of L-glutamic acid during crystallisation from a levitated droplet. Studies of pure solution and solution doped with various levels of other amino acid additives were carried out using *in-situ* WAXS, Raman spectroscopy and droplet size monitoring techniques.

The final conclusions and recommendations for further work are presented in *Chapters 7* and *8*, respectively.

Chapter 1

Theoretical background

Crystallisation is a complex process where a particular substance undergoes a phase transition from liquid, melt or rarely gas to the solid state with an ordered three-dimensional molecular array that we call a crystal. The crystallisation process can be divided into three stages: generation of the supersaturation condition, nucleation and crystal growth. The following chapter provides essential background and introduces concepts related to nucleation and crystal growth.

1.1 Crystals and crystal structures

1.1.1 Crystalline and amorphous state

In the solid state, one of the three general states of matter, molecules are packed closely together, the intermolecular interactions are strong and, consequently, atomic motion is confined to vibration about a mean position. At a given temperature, a solid material has fixed shape and volume. The structure of a solid is rigid and generally resists compression very strongly.

Depending on the structural order of a solid, it can be classified as amorphous or crystalline. In an amorphous solid, structural units are arranged in a random manner and there is no long-range atomic order, although some local ordering can still be present (*Figure 1.1a*). Atoms of a crystalline solid are arranged in regular repeating three-dimensional pattern (*Figure 1.1b*) (McKie and McKie, 1974). The regular repetition of the individual entities over distances equivalent to many thousands of atomic dimensions gives rise to characteristic properties of crystalline materials:

- Strictly defined melting point
- Variation of physical properties with the direction in which they are measured (anisotropy)

- Constant angles between crystal faces for a given crystalline material
- Crystal symmetry

1.1.2 Unit cell

A perfect crystal is composed of atoms, molecules or ions arranged in a pattern that repeats regularly in space. Points in a periodic pattern that represent these structural units and all have identical surroundings are called lattice points. An atom or a group of atoms may be associated with a lattice point but does not necessarily need to lie on it. An infinite array of lattice points in three-dimensional space defines the basic crystal structure.

The smallest repeat unit within the lattice that can be used to build the entire crystal is denoted as a unit cell. The unit cell in a lattice can be selected in a variety of ways but the one with sides that have the shortest lengths and are most nearly perpendicular is most commonly chosen. For instance, in a lattice shown in *Figure 1.2*, the rectangular unit cell would normally be chosen.

In a three-dimensional unit cell, the lengths of the sides are denoted a , b and c and the angles between bc , ac and ab sides are denoted α , β and γ , respectively (*Figure 1.3*).

1.1.3 Miller indices

The spatial orientation of lattice planes can be mathematically described in terms of their axial intercepts using Miller indices. Such mathematical notation uses three integer numbers h , k , and l , defined by:

$$h = \frac{a}{X}, \quad k = \frac{b}{Y}, \quad l = \frac{c}{Z} \quad (1.1)$$

where X , Y and Z are the axial intercepts, and a , b and c are the corresponding unit cell lengths.

The values of h , k and l are usually written as (hkl) , noting that negative values are designated with a bar over the number, as in $\bar{2}$ for -2 (Cullity and Stock, 2001). A set of example lattice planes with corresponding description using Miller indices is given in *Figure 1.4*.

It is generally accepted that indices of a particular face are written either unenclosed – as 312 – or in round brackets – (312). Indices in braces – {312} – denote a family of parallel planes and square brackets – [312] – are used to define zone axis direction (Phillips, 1963).

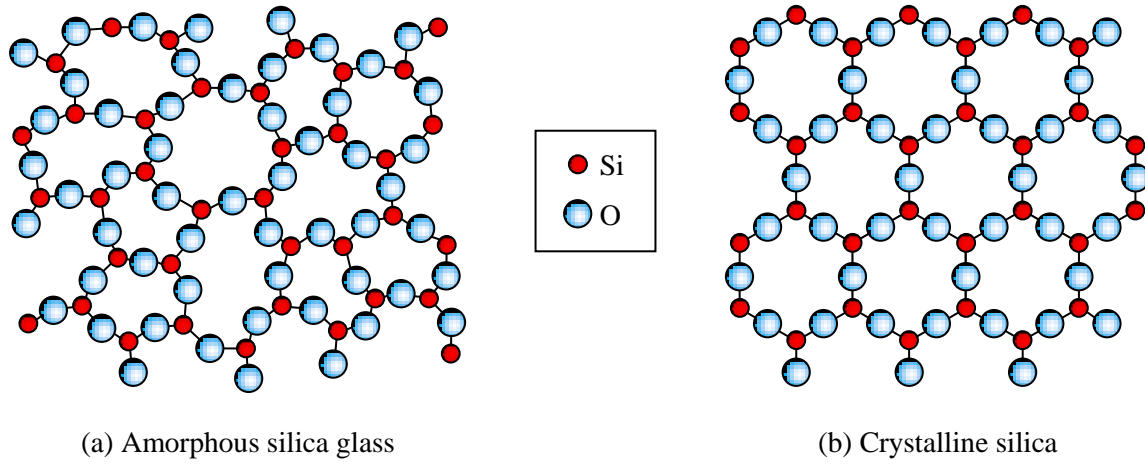


Figure 1.1 Schematic structures of amorphous and crystalline SiO_2

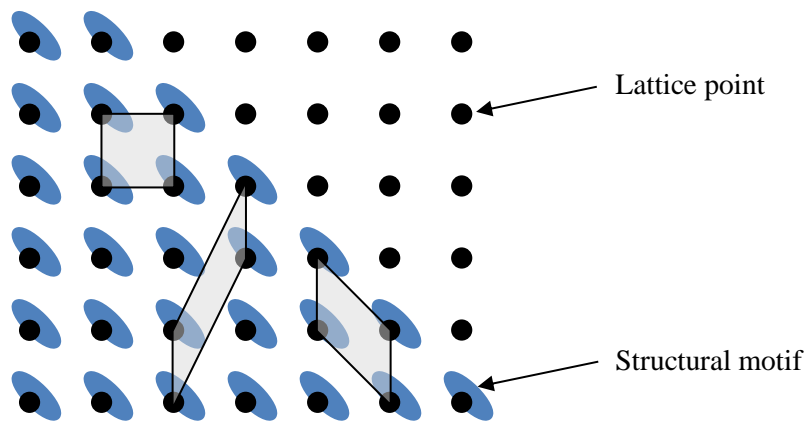


Figure 1.2 Schematic representations of structural motifs in a crystal lattice

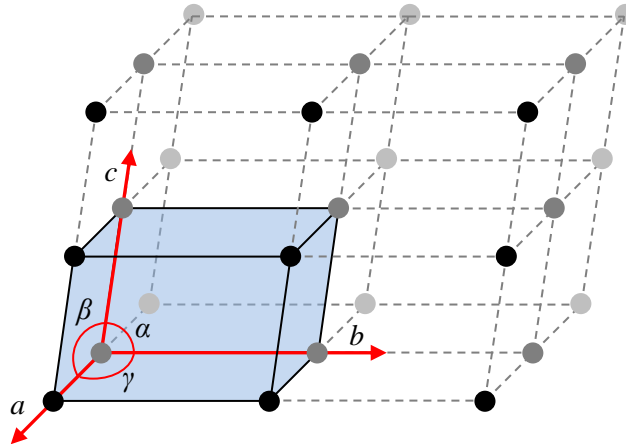


Figure 1.3 A parallel-sided unit cell in a space lattice and the notation for the sides and angles

The Miller indices can also readily be used to calculate the separation of planes. For a general orthorhombic lattice, the separation d_{hkl} of the $\{hkl\}$ planes is given by:

$$\frac{1}{d_{hkl}^2} = \frac{h^2}{a^2} + \frac{k^2}{b^2} + \frac{l^2}{c^2} \quad (1.2)$$

1.2 Structural imperfections in crystals

The most important feature of a crystalline solid is a very regular arrangement of atoms and molecules in space. However, in real crystals this regularity is often disturbed by imperfections. Although only a very small fraction of atoms is usually affected, defects can give rise to important chemical and mechanical properties of crystalline materials and also influence the crystal growth process (Mullin, 2001).

There are four main classes of crystal lattice defects: zero-dimensional (point defects), one-dimensional (line defects), two-dimensional (surface defects) and three-dimensional (volume defects).

1.2.1 Point defects

Point defects are not extended in space in any dimension and typically involve a few extra or missing atoms. They can be classified into three types (*Figure 1.5*):

- Vacancies are lattice sites from which units are simply missing, leaving ‘holes’ in the structure. These units may be atoms, molecules or ions.

- Interstitials are foreign atoms that occupy sites in the spaces between the crystal lattice atoms. The interstices are usually small and the occurrence of interstitial defects often leads to a distortion of the lattice.
- Substitutional impurities are foreign units that substitute for matrix atoms.

A vacancy, with no corresponding interstitial atom, is sometimes called a Schottky defect, whereas a single interstitial atom is referred to as an anti-Schottky imperfection. A combination of defects consisting of one vacancy and one interstitial is called a Frenkel imperfection (Cracknell, 1969).

1.2.2 Line defects

The two main types of line defects are edge and screw dislocations. Most crystals have large number of dislocations. They can form during crystal growth (grown-in dislocations) or during mechanical deformation (mechanical dislocations). Both edge and screw dislocations are responsible for slip or shearing in crystals.

An edge dislocation is a defect where one plane of atoms terminates in the middle of the crystal. This causes the stacking of the atom sheets to be distorted for a few layers on either side of the extra half layer. An edge dislocation can very easily move thorough a crystal; this process is illustrated in *Figure 1.6a* below. If a sideways force is applied to the bottom layers of the crystalline structure, atom A may move further away from atom B and closer to atom C. As a result, the bond between A and B breaks, a new bond is formed between A and C, and the dislocation moves one atomic distance to the right (*Figure 1.6b*). The process continues until the dislocation has reached the edge of the crystal (*Figure 1.6c*). The direction and magnitude of slip is characterised by the Burgers vector.

When the atoms are displaced along the dislocation line, rather than at right angles to it, we speak of a screw dislocation. This type of lattice distortion plays an important role in the crystal growth mechanism. If a single atom becomes attached to the crystal surface it will not be held on very firmly and might become detached again. However, if this extra atom arrives to the end of a screw dislocation, it is much more firmly attached to the crystal since it is anchored by more than one of its faces (*Figure 1.7*). The attachment of growth units to the face of the dislocation results in the development of a spiral growth pattern.

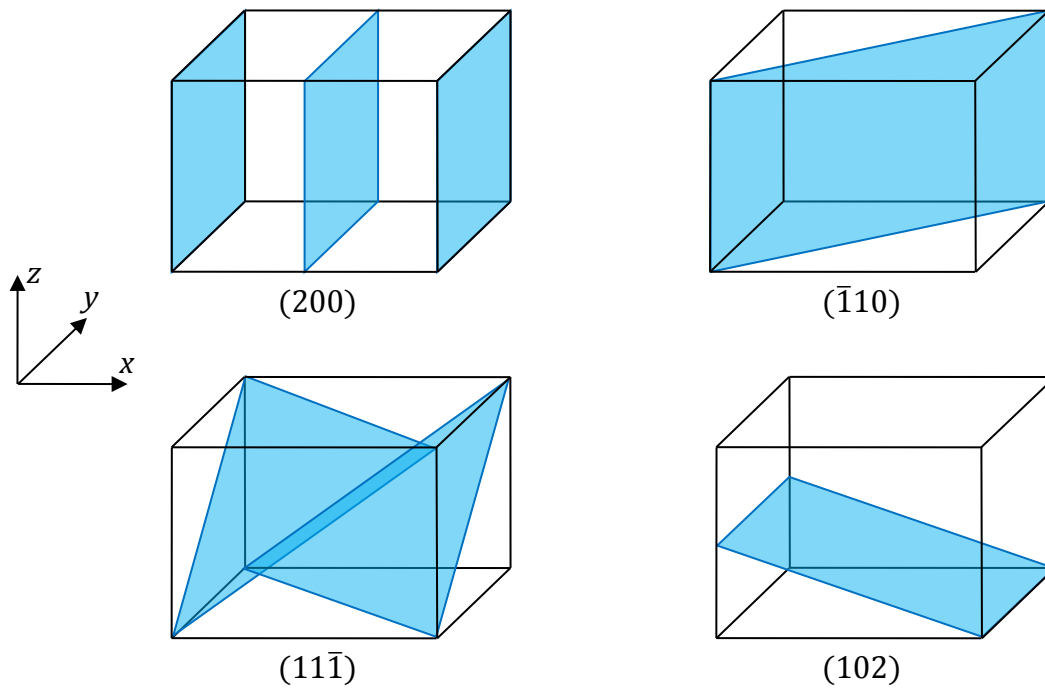


Figure 1.4 Various lattice planes described using Miller indices

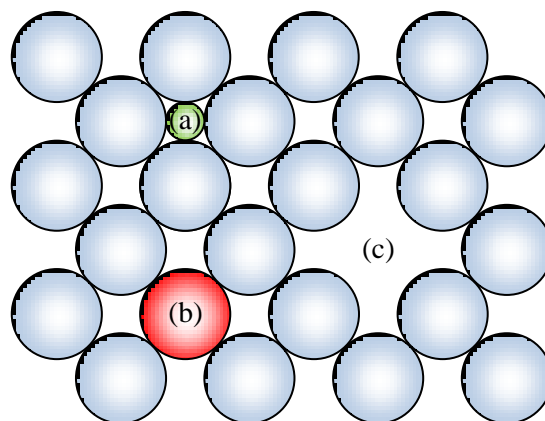


Figure 1.5 Schematic representation of common point defects: (a) interstitial impurity, (b) substitutional impurity, (c) vacancy

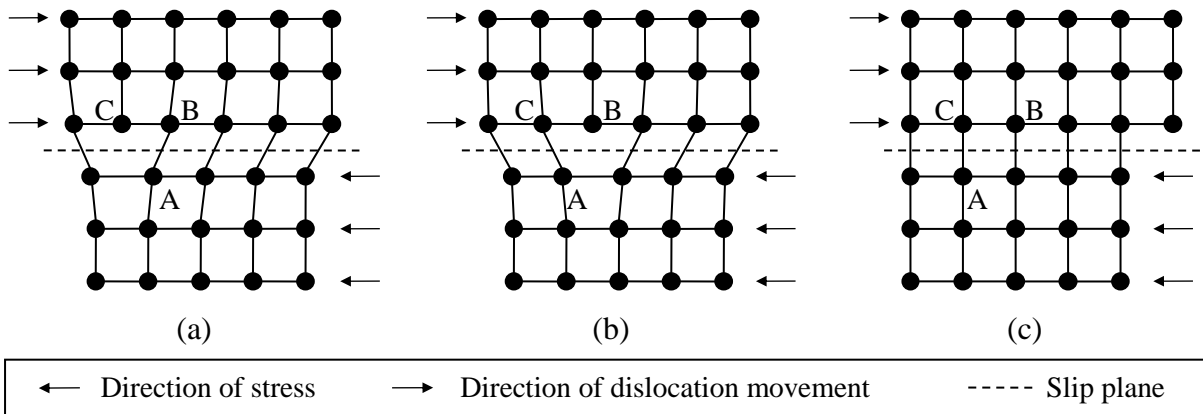


Figure 1.6 *Movement of an edge dislocation through a crystal*

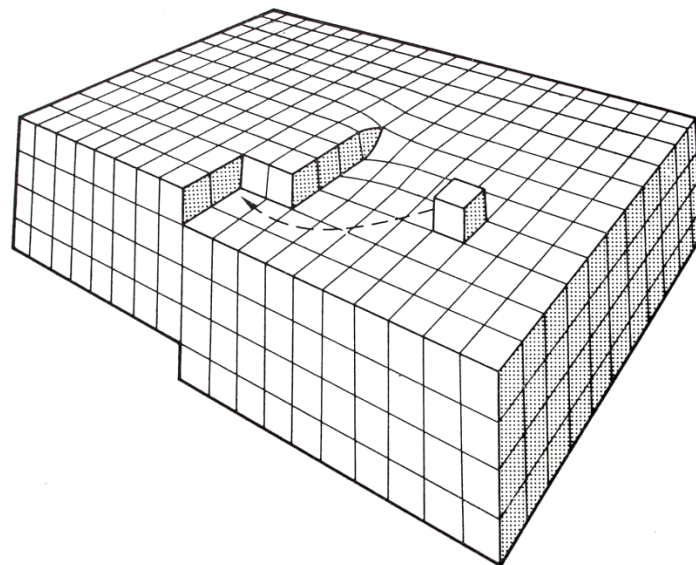


Figure 1.7 *A screw dislocation (Cracknell, 1969)*

1.2.3 Surface defects

Grain boundaries are defined as the mismatch regions on the interface between crystals having different crystallographic orientations. They usually occur when two individual crystals meet during the growth process. Aside from irregular growth, surface defects can also be produced as a result of mechanical or thermal stresses.

Two types of boundaries, tilt and twist, can be distinguished depending on the degree of mismatching between the grains (*Figure 1.8*). A low-angle tilt boundary can be considered to be a line of dislocations. A twist boundary with a small degree of misalignment is equivalent to a succession of parallel screw dislocations (Mullin, 2001).

1.2.4 Volume defects

Volume defects, often referred to as inclusions, are pockets of foreign solid, liquid or gas impurities entrapped inside a crystal. They can be divided into two classes: primary, associated with growth and constituting samples of fluid in which crystal grew, and secondary, formed later often as a result of crystal cracking and incorporation of mother liquor. Volume defects can take different forms and shapes, such as bubbles, fjords (parallel channels), veils (thin sheets of small bubbles) and negative crystals (faceted inclusions), and most frequently they are randomly distributed throughout the crystal. Large and fast growing crystals are more likely to develop inclusions (Mullin, 2001).

Cavities are usually formed at a face centre. This phenomenon was described by Bunn (1949), Humphreys-Owen (1949) and Denbigh and White (1966) who discovered that the diffusion field around a small crystal tends to develop spherical symmetry and as a result more solute is transported to the centre. However, when the crystal grows beyond a certain size, the corners and edges grow more rapidly than the face centres; growth layers are generated on the macroface, grow inwards and meet to seal the inclusion (*Figure 1.9*).

1.3 Driving force for crystallisation

1.3.1 Solubility curves

Solubility is a measure of the maximum amount of solid that can be dissolved in a volume of liquid at a specific temperature and pressure. Solubility of a substance is commonly expressed as a mass concentration, in grams of solute per kilogram of solvent or in grams of solute per 100 millilitres of solvent. A plot of the solubility data versus temperature produces

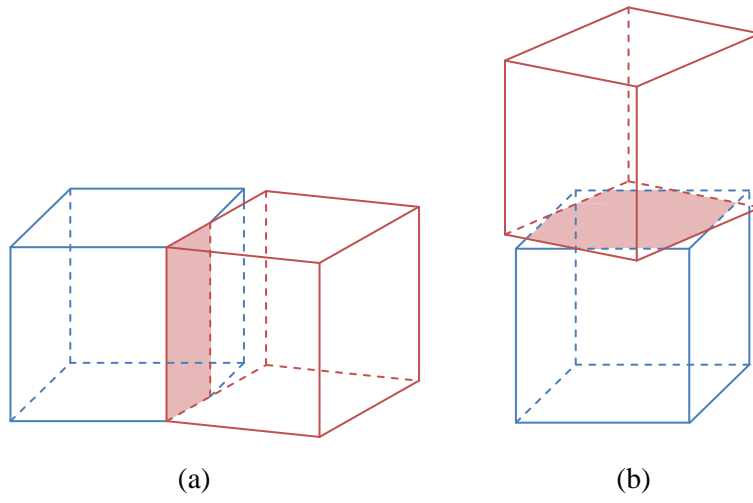


Figure 1.8 Two types of grain boundaries: (a) tilt, (b) twist

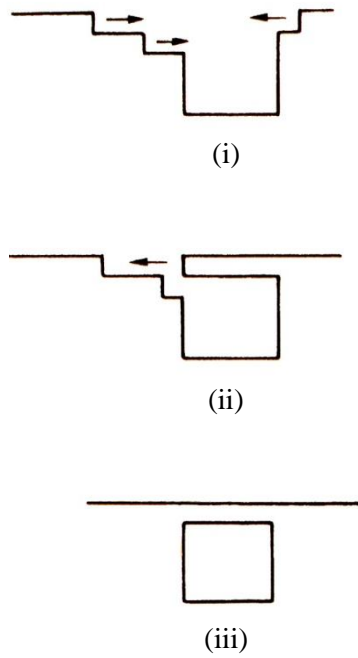


Figure 1.9 Development of an inclusion

the solubility curve that corresponds to the saturation concentration of a solute in a particular solvent.

For the majority of substances, the solubility of a solute in a solvent increases with temperature, but a few exceptions to this rule are known. Since accurate solubility measurements demand laboratory facilities and can be very time consuming, many equations have been proposed to predict the solubility data but none has been found to be of general applicability. While for some systems simple techniques of interpolation and extrapolation can yield data comparable to experimental results, for others the estimated data can only be used for rough assessment (Mullin, 2001). For that reason, an experimental determination of solubility is usually preferred.

1.3.2 Supersaturation

A saturated solution is at thermodynamic equilibrium with the solid phase at a given conditions of temperature and pressure. It is, however, possible to prepare a solution where the amount of dissolved solid is greater than the saturation equilibrium value. The state of supersaturation is essential for both nucleation and crystal growth to occur.

The relationship between supersaturation and probability of spontaneous crystallisation can be represented on a solubility-supersolubility diagram (*Figure 1.10*) which can be divided into three zones:

- (i) The stable zone, where the solution is unsaturated and crystallisation is impossible.
- (ii) The metastable zone, where the solution is supersaturated but where spontaneous crystallisation is improbable; however, growth of a seed crystal placed in the metastable solution would occur.
- (iii) The labile zone, where spontaneous crystallisation is probable but not inevitable.

A supersaturated solution can be prepared by slow cooling of a hot concentrated solution without agitation or by evaporation of a solvent. In the former method, supersaturation is created by a drop of temperature solution that reduces the solubility of the solute. In the latter, the state of solution supersaturation is achieved by removing a certain amount of solvent and consequently increasing the solute concentration. In practice, however, a combination of both methods is often employed.

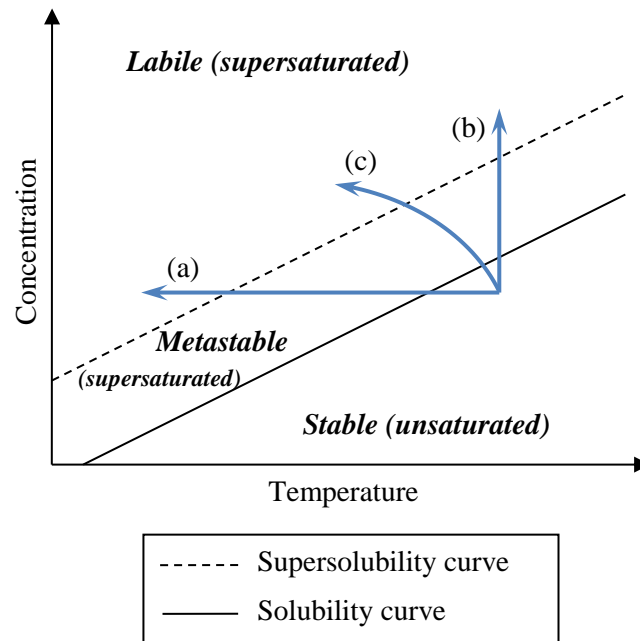


Figure 1.10 The solubility-supersolubility diagram and change in supersaturation on (a) cooling, (b) solvent evaporation, (c) combined cooling and solvent evaporation

There are several ways to express the supersaturation of a system but the two most common are the supersaturation ratio, S , and the relative supersaturation, σ . These quantities are defined by:

$$S = \frac{c}{c^*} \quad (1.3)$$

$$\sigma = S - 1 = \frac{c - c^*}{c^*} \quad (1.4)$$

where c is the solution concentration and c^* is the equilibrium saturation at the given temperature.

1.4 Nucleation

The condition of supersaturation alone is not sufficient cause for a system to begin to crystallise. The formation of the new phase requires the existence of minute solid bodies, embryos, nuclei or seeds, that act as crystallisation centres (Jancic and Grootscholten, 1984). The nucleation process may be induced artificially by agitation, ultrasonic irradiation, electric and magnetic fields or extreme pressures.

Nucleation in systems that do not contain crystalline matter is referred to as ‘primary’ nucleation. Primary nucleation can occur spontaneously (homogeneous) or it may be induced by foreign particles (heterogeneous). On the other hand, the process of formation of nuclei in the vicinity of crystals present in the supersaturated system is described as ‘secondary’ nucleation.

1.4.1 Primary homogeneous nucleation

In homogeneous nucleation, in order to form a stable nucleus, the constituent molecules not only have to aggregate into a fixed orientated lattice but also resist the tendency to redissolve. The actual process of formation of nuclei is hard to envisage. It is, however, believed that a nucleus arises from a sequence of molecular additions rather than from simultaneous collision of the required number of molecules. A newly formed cluster becomes stable when the nucleus achieves a certain critical size after which nucleation and subsequent nucleus growth occur. Nuclei that fail to grow above the critical size become unstable and redissolve into the bulk of the fluid (Mullin, 2001).

The classical theory of nucleation developed from the work of Gibbs (1948), Volmer (1939) and Becker and Döring (1935) is based on the condensation of a vapour to a liquid but can also be extended to crystallisation from solutions and melts. According to the classical theory, the overall excess free energy, ΔG , between a small spherical solid particle of solute of radius r and the solute in solution is equal to the sum of the surface excess free energy, ΔG_S (a positive quantity), and the volume excess free energy, ΔG_V (a negative quantity). Thus,

$$\Delta G = \Delta G_S + \Delta G_V \quad (1.5)$$

$$\Delta G = 4\pi r^2 \gamma + \frac{4}{3}\pi r^3 \Delta G_v \quad (1.6)$$

where ΔG_v is the free energy change of the transformation per unit volume and γ is the interfacial tension.

A plot of ΔG versus nucleus radius size, r , is shown in *Figure 1.12*. The maximum value, ΔG_{crit} , which corresponds to the critical nucleus, r_c , can be obtained by maximising the *Equation 1.6* above, i.e. when $d\Delta G / dr = 0$. Thus,

$$\frac{d\Delta G}{dr} = 8\pi r \gamma + 4\pi r^2 \Delta G_v = 0 \quad (1.7)$$

and therefore,

$$r_c = \frac{-2\gamma}{\Delta G_v} \quad (1.8)$$

where ΔG_v is a negative quantity. Hence, combining equations 1.6 and 1.8 we get

$$\Delta G_{crit} = \frac{16\pi\gamma^3}{3(\Delta G_v)^2} = \frac{4\pi\gamma r_c^2}{3} \quad (1.9)$$

The rate of nucleation, J , i.e. the number of nuclei formed per unit time per unit volume, can be expressed in the form of the Arrhenius reaction velocity equation commonly used for the rate of thermally activated process (Mullin, 2001):

$$J = K \exp(-\Delta G/kT) \quad (1.10)$$

where K is the kinetic factor, k is the Boltzmann constant and T is the temperature.

The Gibbs-Thomson relationship for a non-electrolyte can be expressed as

$$\ln S = \frac{2\gamma v}{kTr} \quad (1.11)$$

Consequently,

$$\frac{2\gamma}{r} = \frac{kT \ln S}{v} \quad (1.12)$$

where S is the supersaturation and v is the molecular volume.

Subsequent substitution of *Equation 1.12* into *Equation 1.8* gives

$$-\Delta G_v = \frac{2\gamma}{r_c} = \frac{kT \ln S}{v} \quad (1.13)$$

and from *Equation 1.9*,

$$\Delta G_{crit} = \frac{16\pi\gamma^3 v^3}{3(kT \ln S)^2} \quad (1.14)$$

Substituting ΔG_{crit} into the Arrhenius equation gives

$$J = K \exp \left[-\frac{16\pi\gamma^3 v^2}{3k^3 T^3 (\ln S)^2} \right] \quad (1.15)$$

The above relationship indicates that the rate of nucleation is a function of three system variables, namely, interfacial tension γ , degree of supersaturation S , and temperature T . It should also be noted that the geometrical factor $16\pi/3$ in the equation above is only valid for

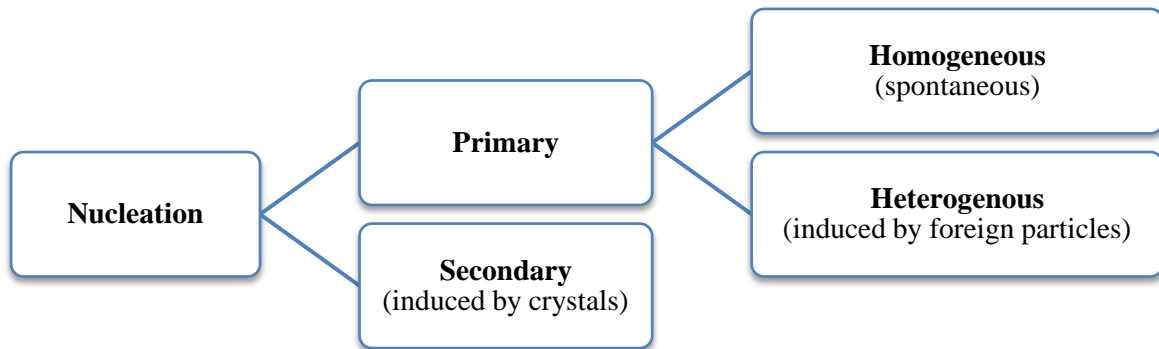


Figure 1.11 Classification of nucleation mechanisms

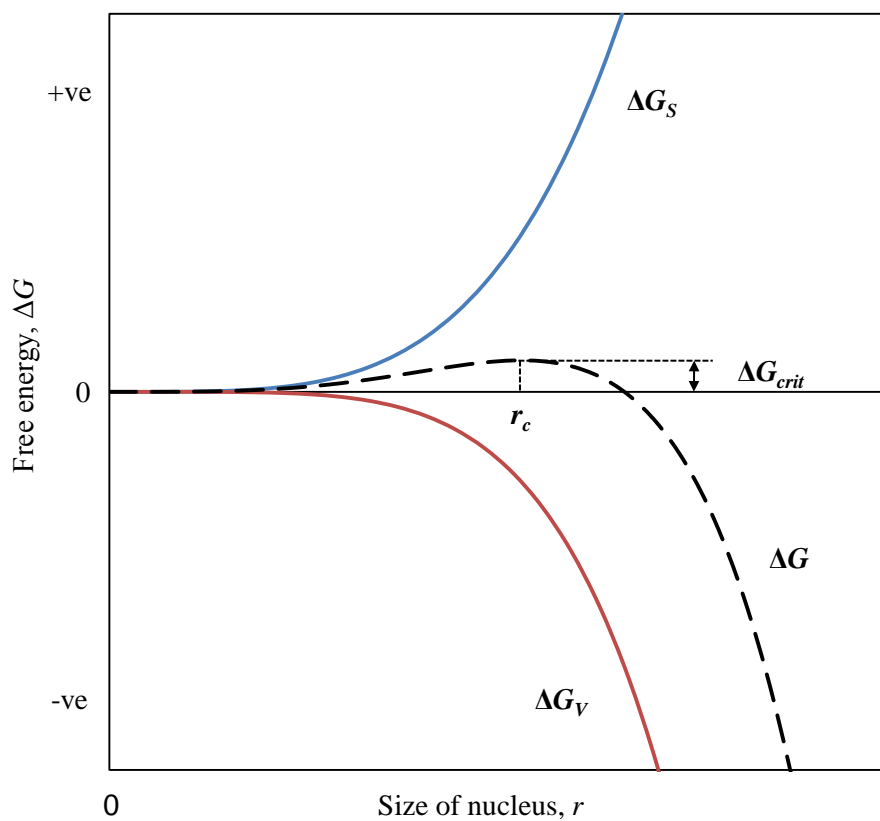


Figure 1.12 Free energy diagram for nucleation explaining the existence of a critical nucleus (ΔG is the overall excess free energy, ΔG_s is the surface excess free energy, ΔG_v is the volume excess free energy and r is the radius of a spherical solid particle of solute)

the case of a spherical nuclei and must be replaced by an appropriate value if a different shape of a nuclei is assumed, e.g. 32 for a cube.

From *Equation 1.13*, the radius, r_{crit} , of a spherical critical size nucleus can be calculated:

$$r_{crit} = \frac{2\gamma v}{kT \ln S} \quad (1.16)$$

Since for a given volume the nucleation rate is inversely proportional to the induction time ($J \propto 1/\tau$) (Van Hook and Bruno, 1949, Nielsen, 1964), *Equation 1.15* can be rearranged:

$$\ln \tau = A + \frac{16\pi\gamma^3 v^2}{3k^3} \frac{1}{T^3 (\ln S)^2} \quad (1.17)$$

where A is constant. Consequently, the value of γ can be calculated from the slope of the obtained linear dependence of $\ln \tau$ on $T^{-3}(\ln S)^{-2}$.

1.4.2 Primary heterogeneous nucleation

Since it is virtually impossible to achieve a solution completely free of foreign bodies, such as dust particles, a true homogeneous nucleation is generally an uncommon event. The presence of foreign bodies can induce nucleation at lower degrees of supercooling or supersaturation than those required for spontaneous nucleation. As a result, the overall free energy change associated with heterogeneous formation of a critical nucleus, $\Delta G'_{crit}$, must be less than the corresponding free energy change under the homogeneous condition, ΔG_{crit} , i.e.

$$\Delta G'_{crit} = \varphi \Delta G_{crit} \quad (1.18)$$

where the factor φ is less than unity.

When considering homogeneous nucleation, a spherical shape of the droplet was assumed. During heterogeneous nucleation, one should consider a liquid droplet on a smooth surface of a substrate. A segment of a sphere with the curvature radius r and the projected radius $r \sin \theta$, where θ is the wetting angle, is presented in *Figure 1.13*. With the specific surface energies of the droplet, σ , the substrate, σ_s , and the substrate-droplet interface, σ_i , the equilibrium condition can be expressed as (Mullin, 2001):

$$\sigma_s = \sigma_i + \sigma \cos \theta \quad (1.19)$$

and thus

$$\cos \theta = \frac{\sigma_s - \sigma_i}{\sigma} \quad (1.20)$$

The relationship between the factor φ and the angle θ was established by Volmer (1939) as:

$$\varphi = \frac{(2 + \cos \theta)(1 - \cos \theta)^2}{4} \quad (1.21)$$

From the plot of the above function (*Figure 1.14*), it can be deduced that for the case of complete non-affinity between the crystalline solid and the foreign solid surface, i.e. $\theta = 180^\circ$, the overall free energies of homogeneous and heterogeneous nucleation are the same. For the case of partial affinity, when $0^\circ < \theta < 180^\circ$, $\Delta G'_{crit}$ is lower than ΔG_{crit} . Finally, for the case of complete affinity, $\theta = 0^\circ$, that corresponds to the seeding of a supersaturated solution with crystals of the required crystalline product, no nuclei have to be formed in the solution as the nucleation free energy is zero.

1.4.3 Secondary nucleation

At a lower supersaturation level, the nucleation process can readily be promoted by addition of seed crystals of the solute. Formation of a new crystal solely because of the prior presence of seed crystals is called secondary nucleation.

Secondary nucleation can occur by a number of different mechanisms (Constable, 1968):

- *initial breeding* – when a new crystal is introduced into a supersaturated solution, a crystalline dust from its surfaces may be sweep off and these can then become new growth centres
- *needle breeding* – the out-growths of crystals that grow in the form of needles are weak and after detachment or breaking can act as nucleation sites
- *polycrystalline breeding* – where secondary nuclei result from fragmentation of a weak polycrystalline mass
- *collision breeding* – a process resulting from the interaction between a growing crystals and the crystalliser walls, a stirrer or impeller, or other crystals

For materials of high and moderate solubility, collision breeding is considered to be the most significant nucleation mechanism in crystallisers (Davey and Garside, 2000).

1.5 Crystal growth

As a result of exposure to supersaturated solution, the surface of stable nuclei, i.e. those that grew larger than the critical size, begins to grow since the number of growth units joining the surface is greater than then the number leaving. The ability to capture approaching molecules

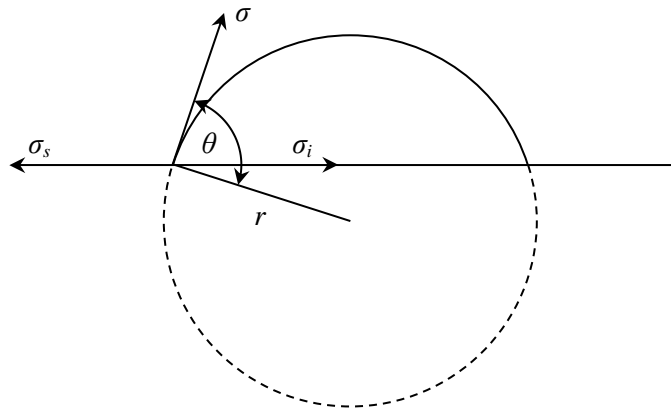


Figure 1.13 Equilibrium shape of a liquid droplet on a substrate surface (θ is the wetting angle, r is the radius of a droplet, and σ , σ_s , and σ_i are specific surface energies of the droplet, the substrate and the substrate-droplet interface, respectively)

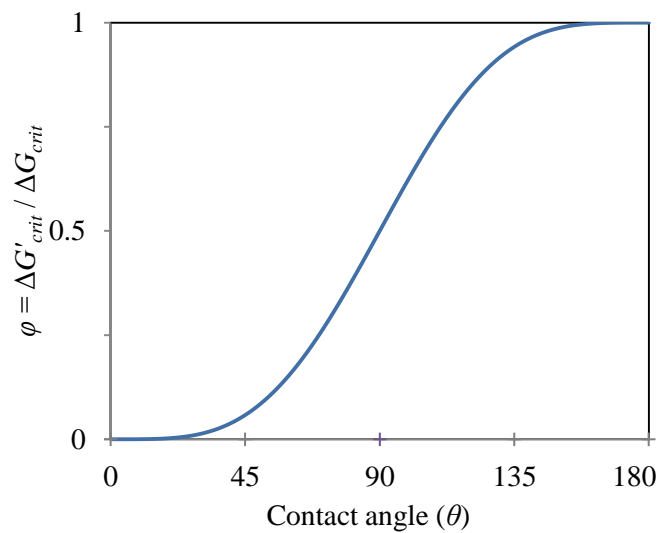


Figure 1.14 Ratio of free energies of heterogeneous and homogeneous nucleation as a function of the contact angle

and their subsequent incorporation into the crystal surface depends on the number and strength of interactions between the surface and the growth unit and can be quantified using the α factor originally defined by Jackson (1958) and later refined by Jetten et al. (1984):

$$\alpha = \xi \left(\frac{\Delta H_f}{RT} - \ln x_{eq} \right) \quad (1.22)$$

where ξ is the surface anisotropy factor, ΔH_f is the heat of fusion and x_{eq} is the solubility.

If the value of α is less than 3, the surface of a crystal contains many kink and step sites and every growth unit arriving at the surface becomes incorporated into the crystal. Hence, the growth is continuous. Values of α between 3 and 5 indicate a decrease in the inherent roughness of the interface and thus some of the growth units that arrive at the surface do not find a growth site and either return to the solution phase or join other growth units to form surface islands or nuclei. The latter mechanism is referred to as a birth and spread model. If the value of α is greater than 5, the molecular surface of a crystal is flat and the growth can only take place if a step can be formed in a low-energy process. Structural defects, in particular screw dislocation, provide such a route and the growth usually proceeds by the screw dislocation mechanism (Davey, 1982).

1.5.1 Adsorption layer theories and spiral growth

The adsorption layer theory, originally postulated by Volmer (1939), holds that the units of the crystallising substance that arrive at the surface of a growing crystal do not get incorporated into the crystal structure immediately but are able to migrate over the crystal face and will link into the lattice in positions where attractive forces are greatest. Three distinct stages can be identified in the process:

- (i) Bulk transport of the growth units to the adsorption layer.
- (ii) Diffusion of the solute molecules to the surface of the growing crystal.
- (iii) Desolvation and adsorption of the crystallising entities onto the growing surface.

A model suggested by Kossel (1934) represents a flat crystal surface as made up of moving layers of monoatomic height, termed steps, which may contain kinks (*Figure 1.15*). The loosely adsorbed growth units are most easily incorporated at kinks as they have more potential binding sites than steps and faces and consequently the system can gain more energy when joining occurs at kinks. As the crystallising units get incorporated to the surface, the kinks move along the step and the face is eventually completed. A fresh step is created by surface nucleation and usually starts at the corners.

Accordingly, the growth of a crystal should be fastest when its faces are entirely covered with kinks and its rate should decrease as the face continues to grow and the number of kinks decreases. It can indeed be observed that broken crystal surfaces rapidly heal and then proceed to grow at much slower rates. On the other hand, however, it was also noticed that at low supersaturations, far below those needed to induce surface nucleation, crystals of certain species, such as iodine, grow at much greater rates than those predicted by Kossel's model, indicating that the latter is unreasonable for growth at moderate to low supersaturation (Mullin, 2001).

To account for the above observations, Frank (1949) postulated that the majority of crystals grow with imperfections and the ideal layer-by-layer growth is uncommon. Dislocations cause steps to be formed and therefore promote growth. Frank (1949) considers the screw dislocations to be particularly important for crystal growth as they eliminate the necessity for surface nucleation. The emergent step of a dislocation spiral extends over only a part of the crystal surface but it winds up during growth to create a growth hillock and the surface grows as if it was covered with kinks (*Figure 1.16*). Hence, the latter mechanism is referred to as a spiral growth model.

The mechanism of growth based on dislocation theory was further studied by Burton, Cabrera and Frank (1951) who mathematically described the relationship between crystal growth rate and supersaturation:

$$R = A \sigma^2 \tanh(B/\sigma) \quad (1.23)$$

Where R is the crystal growth rate, σ is supersaturation, and A and B are complex temperature-dependent constants which include parameters depending on step spacings. From the supersaturation-growth rate relationship it can be seen that at low supersaturation the BCF equation approximates to $R \propto \sigma^2$ but at high supersaturation to $R \propto \sigma$, i.e. the growth law changes from parabolic to linear as the supersaturation increases (*Figure 1.17*).

1.5.2 Birth and spread model

The 'birth and spread' (B+S) mechanism is based on two-dimensional nucleation, followed by the lateral spread of the monolayers (Ohara and Reid, 1973). In the B+S model, growth develops from surface nucleation that can occur at the edges, in the corners and on the faces of a crystal. Further surface nuclei can develop on the top of the growing monolayer, even before the spread is finished (*Figure 1.18*).

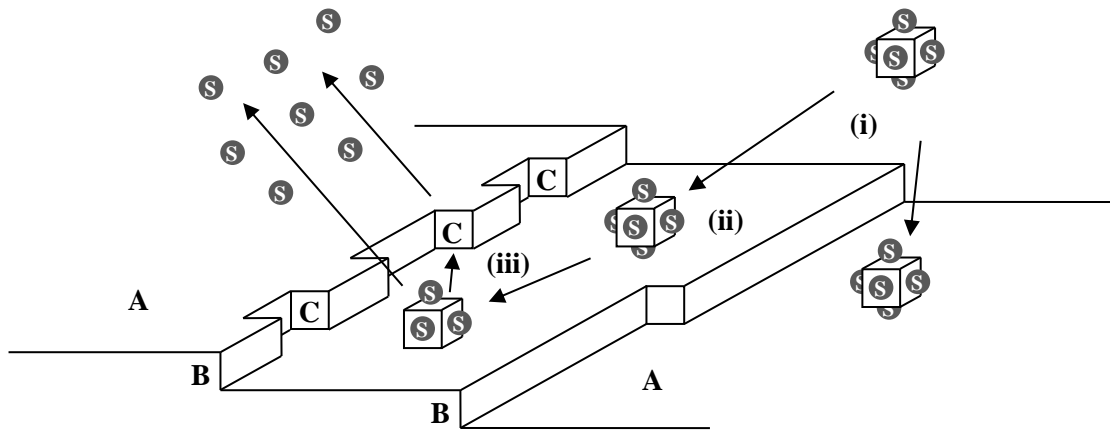


Figure 1.15 Kossel's model of a growing crystal showing (A) flat surfaces, (B) steps, (C) kinks, and three stages of the crystal growth: (i) bulk transport, (ii) boundary layer diffusion, (iii) incorporation of the crystallising entity

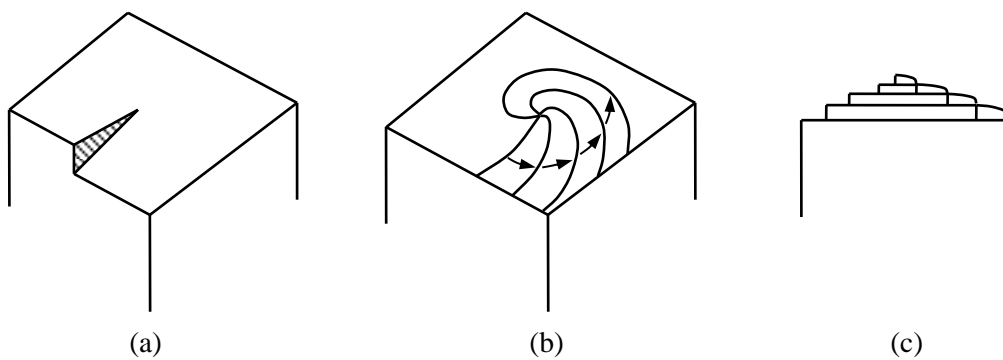


Figure 1.16 Development of a growth spiral starting from a screw dislocation (Mullin, 2001)

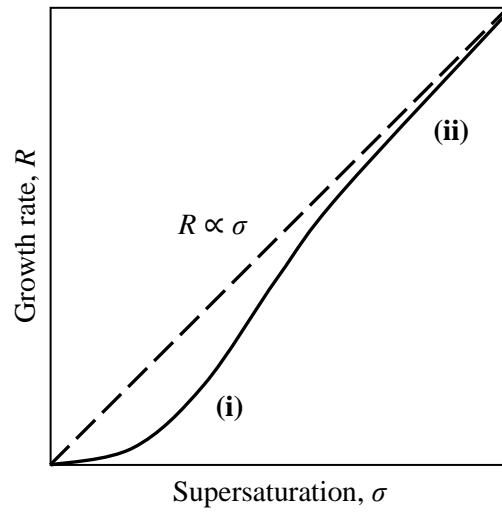


Figure 1.17 The Burton-Cabrera-Frank supersaturation-growth relationship: (i) parabolic growth law, (ii) linear growth law

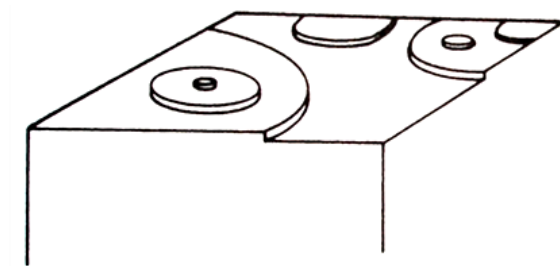


Figure 1.18 Development of the polynuclear growth by the birth and spread mechanism (Mullin, 2001)

The relationship between a face growth velocity and supersaturation in the B+S model can be expressed as

$$R = A_1 \sigma^{5/6} \exp(A_2/\sigma) \quad (1.24)$$

where R is the face growth rate normal to the plane of the face, and A_1 and A_2 are system-related constants.

Mullin (2001) indicates that the terms ‘nuclei on nuclei’ (NON) and ‘polynuclear growth’ are sometimes used in the literature to describe growth behaviour analogous to the birth and spread model.

1.5.3 Continuous growth

When the surface of a growing crystal is rough at the molecular level, i.e. when the surface contains many kink and step sites, every growth unit arriving at the surface will become incorporated into the growing crystal face because of no energy barrier for binding (Davey and Garside, 2000). In such case, the linear growth rate R normal to the surface is proportional to the supersaturation and can be expressed as

$$R = \beta \sigma \quad (1.25)$$

where β is a system-related constant.

1.6 Polymorphism

A substance is said to exhibit polymorphism when it is capable of crystallising into different, but chemically identical, crystalline forms. Although different polymorphs of a given substance have identical composition, they may exhibit different physical properties, such as solubility, melting point, density, colour or bioavailability. Different crystalline forms exhibited by one substance may be the consequence of variation in the crystallisation temperature or a change of solvent.

1.6.1 Types of polymorphism

During the crystallisation process molecules attempt to minimise their free energies. Structural differences between the crystalline lattices originate from alternative ways in which the molecules pack within the crystal. The crystal packing may be driven by intermolecular interaction (enthalpy) or by consideration of entropy, leading to a different structure in each case (Davey and Garside, 2000).

Depending on the mechanisms of origin, polymorphism can be classified as packing and conformational. Packing polymorphism results from various arrangements of conformationally rigid molecules. Distinct conformational states of the same molecule can also lead to different crystal forms and then we speak of conformational polymorphism. Most organic crystals, however, have a mixed origin and exhibit differences in both conformational and packing arrangement of the constituent molecules (Hilfiker, 2006).

1.6.2 The phase rule

On the basis of thermodynamic principles, Gibbs (1876, 1878) formulated the phase rule that relates the number of components, C , phases, P , and degrees of freedom of a system, F , by means of the equation:

$$F = C - P + 2 \quad (1.26)$$

The number of degrees of freedom in the above equation is the number of system variables, such as temperature, pressure and concentration, which must be fixed in order to specify the equilibrium state.

The Gibbs phase rule may also be used to characterise polymorphic behaviour of a substance. Since two polymorphic forms constitute two homogeneous phases, i.e. $C = 1$ and $P = 2$, the system has only one degree of freedom. Thus, at constant pressure, equilibrium between the two polymorphs occurs at a fixed temperature, whereas at constant temperature it occurs at a fixed pressure. Moreover, since the number of degrees of freedom cannot be negative, a maximum of three polymorphs can be in equilibrium with each other.

1.6.3 Ostwald's rule

In the early 19th century it was first observed that rapid cooling may lead to formation of unstable crystals whose form is different to the one which would normally be expected. This type of behaviour was generalised by Ostwald (1893, 1897) who proposed a 'rule of stages' which states that upon crystallisation a system will initially adopt the crystal structure which leads to the smallest loss in free energy and that these crystals will subsequently transform stepwise to the most stable crystal form. In other words, the resulting reaction is, in fact, not the one that is thermodynamically most likely, but the one that has the fastest rate. However, as noted by Ostwald, the theory is not universal and exceptions to the 'rule' exist, e.g. slow cooling of supersaturated 1,3-dioleoyl-2-palmitoyl glycerol solution (Bayes-Garcia et al., 2011).

Although a number of studies attempted to provide a theoretical explanation for Ostwald's theory, the 'rule' still lacks a definite theoretical proof. It does, however, operate often enough to be regarded as important for large-scale precipitation processes.

1.6.4 Enantiotropism and monotropism

Depending on the ability to transform reversibly or irreversibly from one form to another, polymorphic systems can be classified as enantiotropic and monotropic, respectively.

The term monotropic is used to describe a system where crystal forms are not interconvertible, i.e. one polymorph, because of lower solubility, is more stable than the other (*Figure 1.19a*). If, however, one polymorphic form can be reversibly changed into another by varying the temperature or pressure, the system is said to be enantiotropic (*Figure 1.19b*).

Bernstein (2002) points out that the determination of whether a particular substance exhibits mono- or enantiotropic behaviour is particularly important when choosing crystallisation strategy as additional precautions may need to be taken to preserve the stable form or to prevent undesirable transformation.

1.6.5 Commercial importance of polymorphism

Polymorphism plays an important role in a number of industries, including pharmaceuticals, foods, dyes, pigments and explosives. In the chemical industries the demand for high yields and high production rates requires operation of the processes far from equilibrium, thus intensifying the tendency to form metastable structures. Because each polymorphic form has its own unique combination of mechanical, thermal and physical properties, insufficient understanding of solid-state properties can lead to serious setbacks. It is thus important to

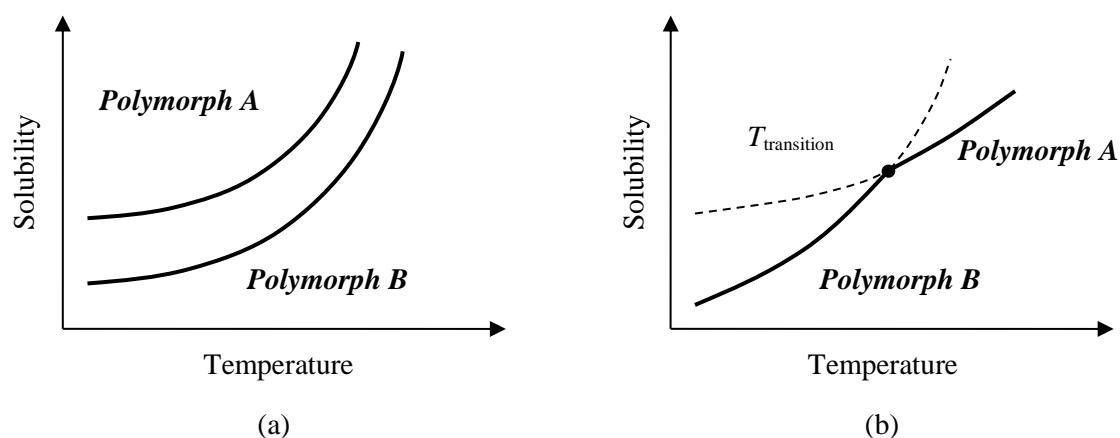


Figure 1.19 Solubility curves in (a) monotropic and (b) enantiotropic systems (Davey and Garside, 2000)

recognise and be able to control the phenomenon of polymorphism, and in consequence manufacture materials with well-defined properties (Davey and Garside, 2000, Bernstein, 2002).

The awareness of importance of polymorphism is most evident in the field of pharmaceuticals. An in-depth study of the polymorphic forms is caused by the strict quality control requirements. Using a thermodynamically unstable polymorph in the production of tablets or creams may sometimes be the reason why undesirable changes into the thermodynamically stable form take place in such formulations after a time of storage, potentially leading to a complete loss of activity of a particular substance. On the other hand, some thermodynamically unstable modifications which show a very low transition tendency can intentionally be applied to take advantage of specific properties they may possess (Henck and Kuhnert-Brandstatter, 1999).

Since the development of a new drug from a promising lead compound to a marketed product is a long and expensive process, the intellectual property implications are another important reason for an intensive investigation of polymorphism in the pharmaceutical industry (Hilfiker, 2006). Since a particular crystalline form of a drug can possess considerable chemical, physical or biological advantages over the market competitors, granting and maintenance of exclusive patent rights to a particular polymorph may have considerable economic consequences.

Chapter 2

L-Glutamic acid as a model compound

L-Glutamic acid was chosen as a model system for investigation of the effect of change in the process conditions and experimental strategy on the nucleation, growth and solution-mediated transformation of its polymorphs. The following chapter outlines the physical data and chemical characteristics of the model compound and presents a thorough review of the literature published to date concerning crystallisation of L-glutamic acid.

2.1 Amino acids

Amino acids are difunctional molecules containing, as their name implies, both amino and carboxyl groups. Two amino acid molecules can join together by a condensation reaction to form a peptide bond, C(O)NH. Amino acids are the basic building blocks of proteins. A protein may consist of a hundred or more amino acid units. All twenty amino acids are involved in the synthesis of proteins but humans can produce only ten of them. The remaining ten have to be supplied by the diet (McMurry, 1996).

The twenty common naturally-occurring amino acids are α -amino acids and all, except for proline which does not contain a primary amino group, have a general formula $\text{H}_2\text{NCHRCOOH}$. In α -amino acids, both the amino group and the carboxyl group are attached to the same carbon atom, which is called the α -carbon. The other two substituents of the α -carbon are hydrogen atom and an organic side chain group R (*Figure 2.1*). Therefore, all amino acids except for glycine, where R = H, are chiral. While both D- and L- amino acids exist in nature, only the L- form is found in proteins synthesised by the human body (Clayden, 2001).

Depending on the nature of the side chain group, amino acids can be divided into 7 classes (*Table 2.1*):

- Aliphatic amino acids: have open, sometimes branched side chains
- Aliphatic hydroxyl amino acids: contain hydroxyl group in their side chains

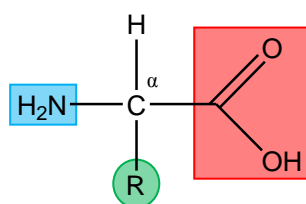


Figure 2.1 General structure of an α -amino acid

- Basic amino acids: side chains contain basic amino groups
- Acidic amino acids and amide derivatives: contain an additional carboxyl group or an amide group in their side chains
- Aromatic amino acids: side chains contain aromatic rings
- Sulphur containing amino acids: contain sulphur atoms in the side chains
- Cyclic amino acid: proline is the only amino acid whose side group is cyclic and links to the α -amino group

2.2 Selection criteria

L-Glutamic acid, often abbreviated as L-Glu or LGA, is one of the proteinogenic amino acids and plays an important role in the human body. It is the most important neurotransmitter in the vertebrate nervous system and a key molecule in cellular metabolism. Commercially, L-glutamic acid is used as a substrate of many pharmaceuticals, cosmetics and agricultural products. In the form of its sodium salt, monosodium glutamate, L-glutamic acid is used as a major flavour enhancing component of foods with a meaty, savoury taste.

L-Glutamic acid is a typical polymorphic compound that can exist in two crystalline forms. Since the system has been widely studied in the past, extensive structural, thermodynamic and kinetic data is available. The two polymorphs of L-glutamic acid are known to undergo solution-mediated transformation but have been reported to be stable in the solid state. The X-ray diffraction patterns and Raman spectra of the two forms are easily distinguishable from one another. While the solubility of L-glutamic acid is low and thus only relatively small amounts of material need to be used to prepare the experimental solutions, it is soluble enough to not cause difficulties when weighing out samples using a typical laboratory balance. Furthermore, when standard laboratory procedures are followed, L-glutamic acid does not pose toxicity concerns.

Table 2.1 Twenty common naturally-occurring amino acids and their classification

Aliphatic amino acids				
$\begin{array}{c} \text{O} \\ \parallel \\ \text{H}_2\text{N}-\text{CH}-\text{C}-\text{OH} \\ \\ \text{H} \\ \text{Glycine} \end{array}$	$\begin{array}{c} \text{O} \\ \parallel \\ \text{H}_2\text{N}-\text{CH}-\text{C}-\text{OH} \\ \\ \text{CH}_3 \\ \text{Alanine} \end{array}$	$\begin{array}{c} \text{O} \\ \parallel \\ \text{H}_2\text{N}-\text{CH}-\text{C}-\text{OH} \\ \\ \text{CH}-\text{CH}_3 \\ \\ \text{CH}_3 \\ \text{Valine} \end{array}$	$\begin{array}{c} \text{O} \\ \parallel \\ \text{H}_2\text{N}-\text{CH}-\text{C}-\text{OH} \\ \\ \text{CH}_2 \\ \\ \text{CH}-\text{CH}_3 \\ \\ \text{CH}_3 \\ \text{Leucine} \end{array}$	$\begin{array}{c} \text{O} \\ \parallel \\ \text{H}_2\text{N}-\text{CH}-\text{C}-\text{OH} \\ \\ \text{CH}-\text{CH}_3 \\ \\ \text{CH}_2 \\ \\ \text{CH}_3 \\ \text{Isoleucine} \end{array}$
Aliphatic hydroxyl amino acids		Basic amino acids		
$\begin{array}{c} \text{O} \\ \parallel \\ \text{H}_2\text{N}-\text{CH}-\text{C}-\text{OH} \\ \\ \text{CH}_2 \\ \\ \text{OH} \\ \text{Serine} \end{array}$	$\begin{array}{c} \text{O} \\ \parallel \\ \text{H}_2\text{N}-\text{CH}-\text{C}-\text{OH} \\ \\ \text{CH}-\text{OH} \\ \\ \text{CH}_3 \\ \text{Threonine} \end{array}$	$\begin{array}{c} \text{O} \\ \parallel \\ \text{H}_2\text{N}-\text{CH}-\text{C}-\text{OH} \\ \\ \text{CH}_2 \\ \\ \text{N} \\ \diagup \quad \diagdown \\ \text{C} \quad \text{C} \\ \diagdown \quad \diagup \\ \text{H} \end{array}$ <p>Histidine</p>	$\begin{array}{c} \text{O} \\ \parallel \\ \text{H}_2\text{N}-\text{CH}-\text{C}-\text{OH} \\ \\ \text{CH}_2 \\ \\ \text{CH}_2 \\ \\ \text{CH}_2 \\ \\ \text{CH}_2 \\ \\ \text{NH}_2 \\ \text{Lysine} \end{array}$	$\begin{array}{c} \text{O} \\ \parallel \\ \text{H}_2\text{N}-\text{CH}-\text{C}-\text{OH} \\ \\ \text{CH}_2 \\ \\ \text{CH}_2 \\ \\ \text{CH}_2 \\ \\ \text{NH} \\ \\ \text{C}=\text{NH} \\ \\ \text{NH}_2 \\ \text{Arginine} \end{array}$
Acidic amino acids and amide derivatives				Cyclic amino acid
$\begin{array}{c} \text{O} \\ \parallel \\ \text{H}_2\text{N}-\text{CH}-\text{C}-\text{OH} \\ \\ \text{CH}_2 \\ \\ \text{C}=\text{O} \\ \\ \text{OH} \\ \text{Aspartic acid} \end{array}$	$\begin{array}{c} \text{O} \\ \parallel \\ \text{H}_2\text{N}-\text{CH}-\text{C}-\text{OH} \\ \\ \text{CH}_2 \\ \\ \text{CH}_2 \\ \\ \text{C}=\text{O} \\ \\ \text{OH} \\ \text{Glutamic acid} \end{array}$	$\begin{array}{c} \text{O} \\ \parallel \\ \text{H}_2\text{N}-\text{CH}-\text{C}-\text{OH} \\ \\ \text{CH}_2 \\ \\ \text{C}=\text{O} \\ \\ \text{NH}_2 \\ \text{Asparagine} \end{array}$	$\begin{array}{c} \text{O} \\ \parallel \\ \text{H}_2\text{N}-\text{CH}-\text{C}-\text{OH} \\ \\ \text{CH}_2 \\ \\ \text{CH}_2 \\ \\ \text{C}=\text{O} \\ \\ \text{NH}_2 \\ \text{Glutamine} \end{array}$	$\begin{array}{c} \text{O} \\ \parallel \\ \text{C}-\text{OH} \\ \\ \text{HN} \\ \diagup \quad \diagdown \\ \text{C} \quad \text{C} \\ \diagdown \quad \diagup \\ \text{C} \end{array}$ <p>Proline</p>
Aromatic amino acids			Sulphur containing amino acids	
$\begin{array}{c} \text{O} \\ \parallel \\ \text{H}_2\text{N}-\text{CH}-\text{C}-\text{OH} \\ \\ \text{CH}_2 \\ \\ \text{C}_6\text{H}_5 \\ \text{Phenylalanine} \end{array}$	$\begin{array}{c} \text{O} \\ \parallel \\ \text{H}_2\text{N}-\text{CH}-\text{C}-\text{OH} \\ \\ \text{CH}_2 \\ \\ \text{C}_8\text{H}_6\text{N}_2 \\ \text{Tryptophan} \end{array}$	$\begin{array}{c} \text{O} \\ \parallel \\ \text{H}_2\text{N}-\text{CH}-\text{C}-\text{OH} \\ \\ \text{CH}_2 \\ \\ \text{C}_6\text{H}_4 \\ \\ \text{OH} \\ \text{Tyrosine} \end{array}$	$\begin{array}{c} \text{O} \\ \parallel \\ \text{H}_2\text{N}-\text{CH}-\text{C}-\text{OH} \\ \\ \text{CH}_2 \\ \\ \text{CH}_2 \\ \\ \text{S} \\ \\ \text{CH}_3 \\ \text{Methionine} \end{array}$	$\begin{array}{c} \text{O} \\ \parallel \\ \text{H}_2\text{N}-\text{CH}-\text{C}-\text{OH} \\ \\ \text{CH}_2 \\ \\ \text{SH} \\ \text{Cysteine} \end{array}$

The above-mentioned characteristics of L-glutamic acid make it a good candidate for a model system, both from scientific and industrial perspective. Additionally, since many amino acids have, to some extent, similar structure and all contain both amino and carboxyl groups, the findings of this research can potentially be applied to other compounds belonging to this class, such as L-aspartic acid that contains one fewer CH₂ group than the model compound considered in this work, consequently making the study an even more valuable contribution to science.

2.3 Molecular and crystal structure

The molecular formula of L-glutamic acid is C₅H₉NO₄ and its molar mass is 147.13 g mol⁻¹. L-Glutamic acid, like all other amino acids, comprises of both amine and carboxylic acid functional groups (C(NH₂)(COOH)) and a characteristic side chain (CH₂CH₂COOH). In the crystal lattice as well as in the aqueous solution, as a result of a proton transfer from the carboxylic acid end to the amino group, the functional groups are present in their charged forms, COO⁻ and NH₃⁺, respectively (*Figure 2.2*). Although the atom groups carry formal positive and negative charges, the molecule remains neutral as a whole. The latter state is referred to as a zwitterionic form.

L-Glutamic acid is a polymorphic compound and its molecules can adopt two different conformations in the solid state, denoted α and β . The crystal structure of the α form was first reported by Bernal (1931) and the β polymorph was later discovered by Hirokawa (1955). The unit cell parameters, originally determined using X-ray diffraction, were later refined by Lehmann et al. (1972) and Lehmann and Nunes (1980) using neutron diffraction data and are summarised in *Table 2.2*. Both polymorphs have primitive orthorhombic unit cells and belong to $P2_12_12_1$ space group. Furthermore, Hirayama et al. (1980) also proposed three hypothetical intermediate molecular conformations that might explain the mechanism of the α to β transition.

L-Glutamic acid molecules crystallise in their zwitterionic state with molecular packing of both forms dominated by intermolecular hydrogen bonding. The most significant difference between the two structures is the adopted molecular conformation (Bernstein, 1991). The torsional angles τ_1 and τ_2 , defined by carbons 1, 2, 3, 4 and 2, 3, 4, 5, respectively, have values of 59.3° and 68.3° in the α structure and -171.5° and -73.1° in the β polymorph and are shown in *Figure 2.3*. The packing structures of the α and β crystal forms, generated using CCDC Mercury software, are shown in *Figure 2.4*. As a result of

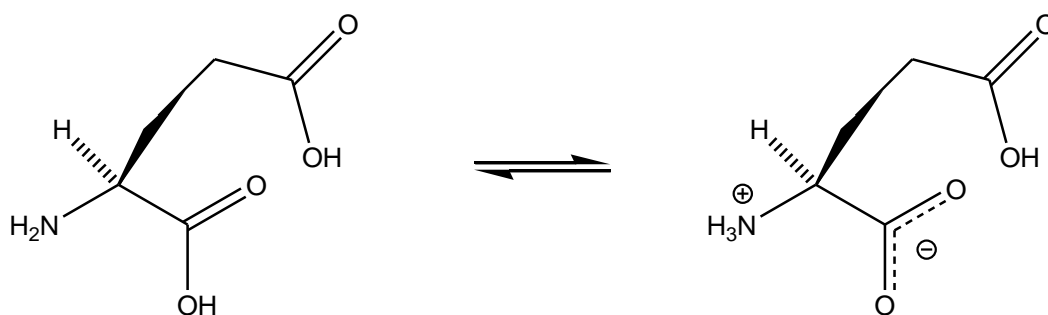
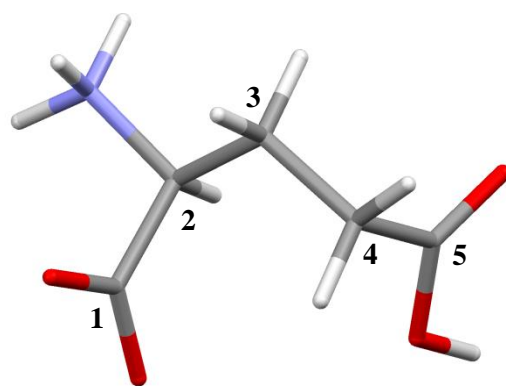


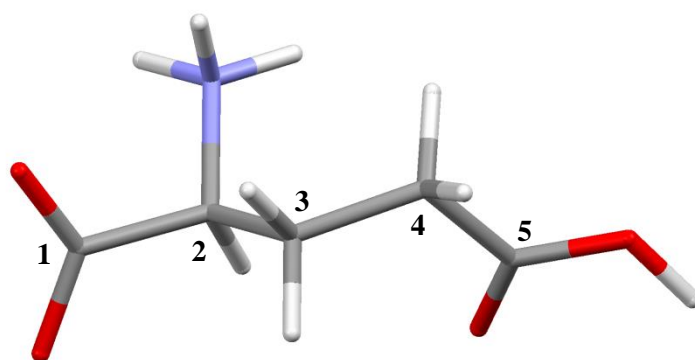
Figure 2.2 Skeletal structure of *L*-glutamic acid in its (left) neutral and (right) zwitterionic form

Table 2.2 Crystallographic data of *L*-glutamic acid polymorphs

Polymorph	α (metastable)	β (stable)
Crystal system	Orthorhombic	Orthorhombic
Space group	$P2_12_12_1$	$P2_12_12_1$
Unit cell lengths (\AA)	a 10.282(10) b 8.779(8) c 7.068(7)	a 5.159(5) b 17.30(2) c 6.948(7)
Unit cell angles	α 90° β 90° γ 90°	α 90° β 90° γ 90°
Number of molecules per unit cell	4	4

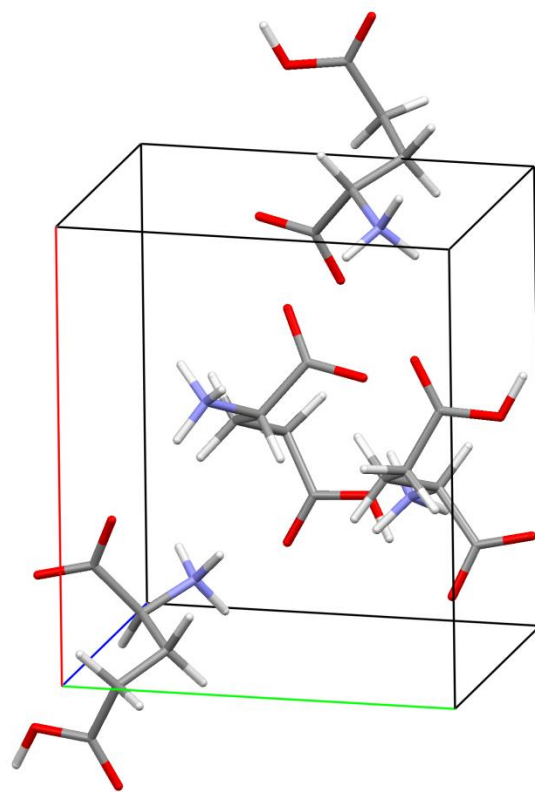


α -L-glutamic acid

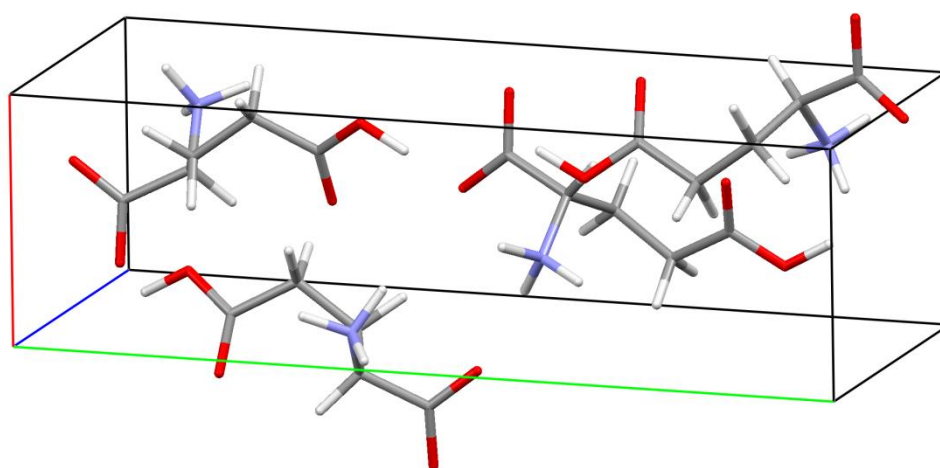


β -L-glutamic acid

Figure 2.3 Conformation of L-glutamic acid in (top) the α and (bottom) the β crystal structure.
Colouring convention: grey – carbon, red – oxygen, blue – nitrogen, white – hydrogen.



α -L-glutamic acid



β -L-glutamic acid

Figure 2.4 Packing structures of (top) α and (bottom) β L-glutamic acid. Colouring convention: grey – carbon, red – oxygen, blue – nitrogen, white – hydrogen.

these characteristic molecular arrangements and large conformational differences in the crystal lattice, the two polymorphs of L-glutamic acid have unique X-ray diffraction patterns (*Figure 2.5*) (Lehmann et al., 1972, Lehmann and Nunes, 1980) and Raman spectra (*Figure 2.6*) (Dhamelincourt and Ramírez, 1991, Ono et al., 2004) that can be used to perform phase identification.

The two crystal forms have very distinct morphologies. The α form crystals are prismatic (*Figure 2.7a*) and are thus preferable for industrial handling since they filter and wash easily. On the other hand, the β polymorph crystals are acicular (*Figure 2.7b*) and because of their needle-like shape tend to break and pack as an impervious layer causing difficulties in downstream processing.

The relative stability of the two polymorphs of L-glutamic acid was determined from solubility (Sakata, 1961b) and enthalpy measurements (Sakata and Takenouchi, 1963). Later studies by Hirayama et al. (1980) showed that the molecular conformation adopted in the β polymorph is more stable and favourable than the one in the α form. The two polymorphs of L-glutamic acid are related monotropically (Kitamura, 1989). Kinetics favours the formation of the metastable form, while thermodynamics favours formation of the stable form (Bernstein, 2002). During typical batch crystallisation, in agreement with the Ostwald's rule of stages, it was observed that it is the less stable α polymorph that nucleates and grows first and then undergoes a solution-mediated transformation where the stable β crystals grow at the expense of the metastable α dissolving (Cardew and Davey, 1985, Kitamura, 1989). The solubility data for the two polymorphs of L-glutamic acid reported by Kitamura (1989) is shown in *Figure 2.8*.

2.4 The existing approaches to study crystallisation

Previous work aimed at understanding and controlling the polymorphic outcome from crystallisation processes can be classified into two fundamentally different approaches:

- (i) studies of kinetic features of solution-mediated transformation (Cardew and Davey, 1985, Davey et al., 1985, Davey et al., 1986, Davey et al., 2002),
- (ii) studies based on control of crystal polymorphism with the assistance of stereospecific nucleation inhibitors (Weissbuch et al., 1991, Lahav and Leiserowitz, 1993), which may be used to prevent the nucleation of undesired polymorphic structures (Staab et al., 1990, Weissbuch et al., 1994, Davey et al., 1997).

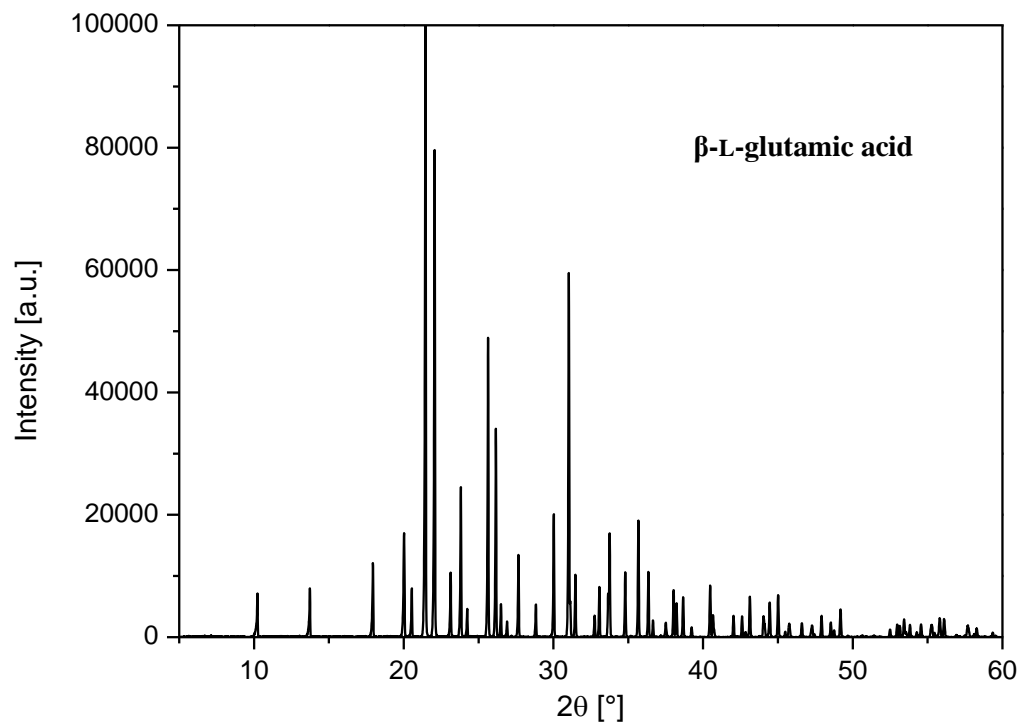
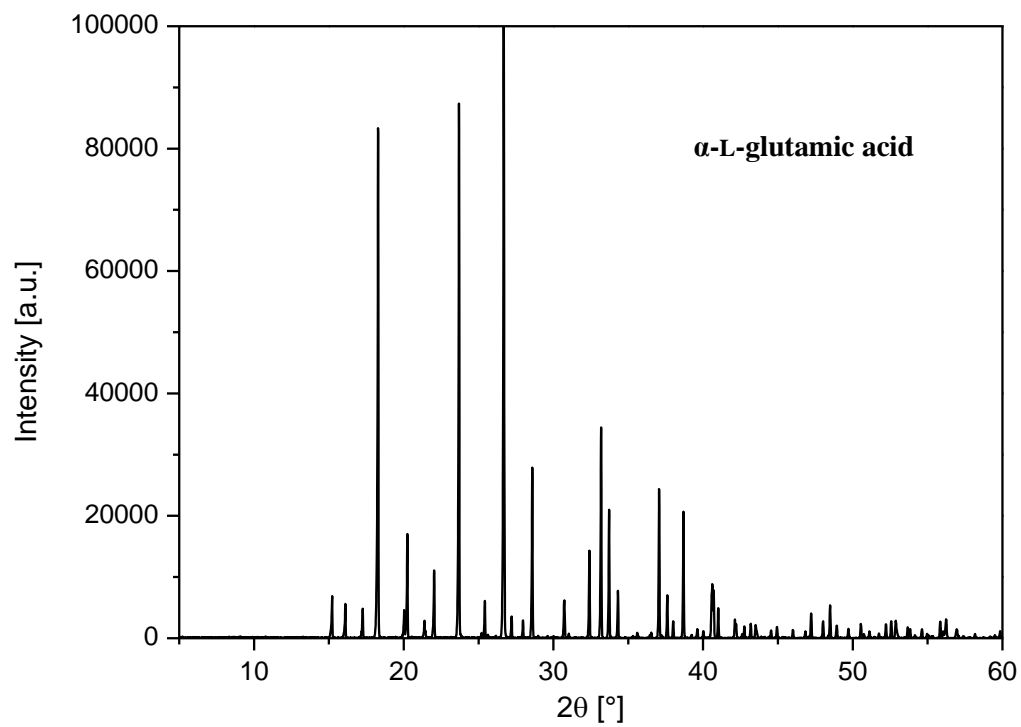


Figure 2.5 Experimentally observed X-ray diffraction patterns of (top) the α and (bottom) the β form of L-glutamic acid

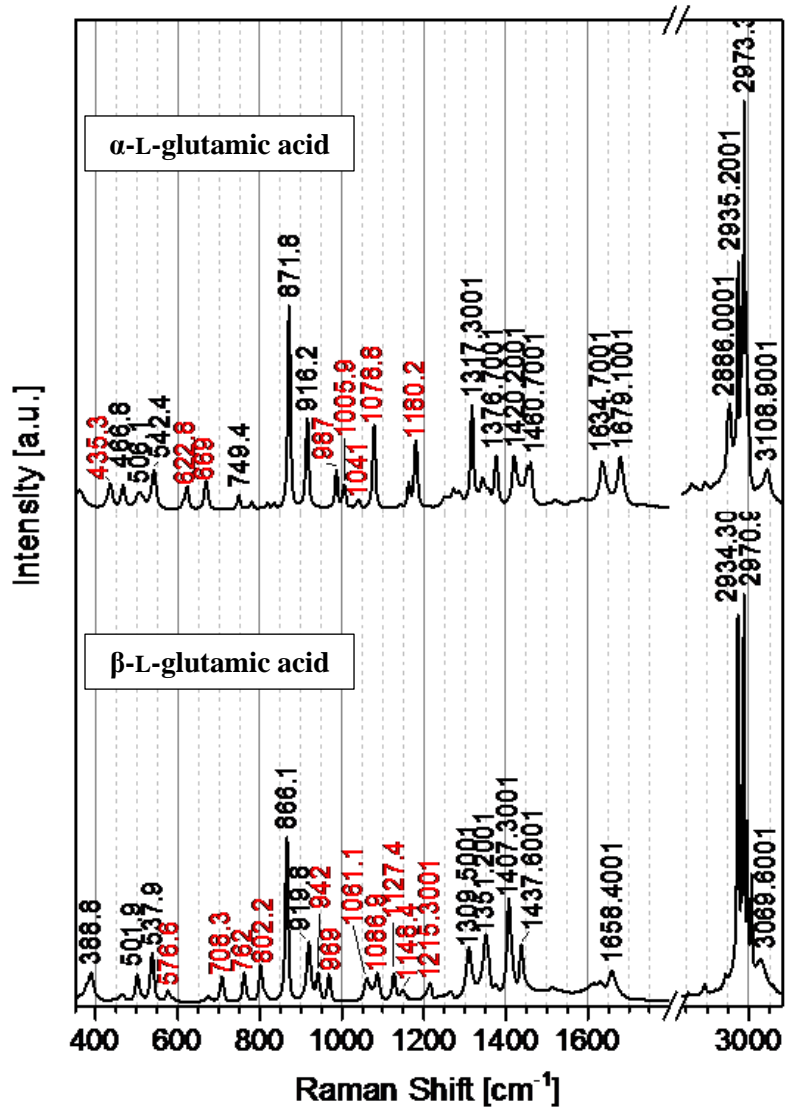


Figure 2.6 Experimentally observed Raman spectra of (top) the α and (bottom) the β form of L-glutamic acid

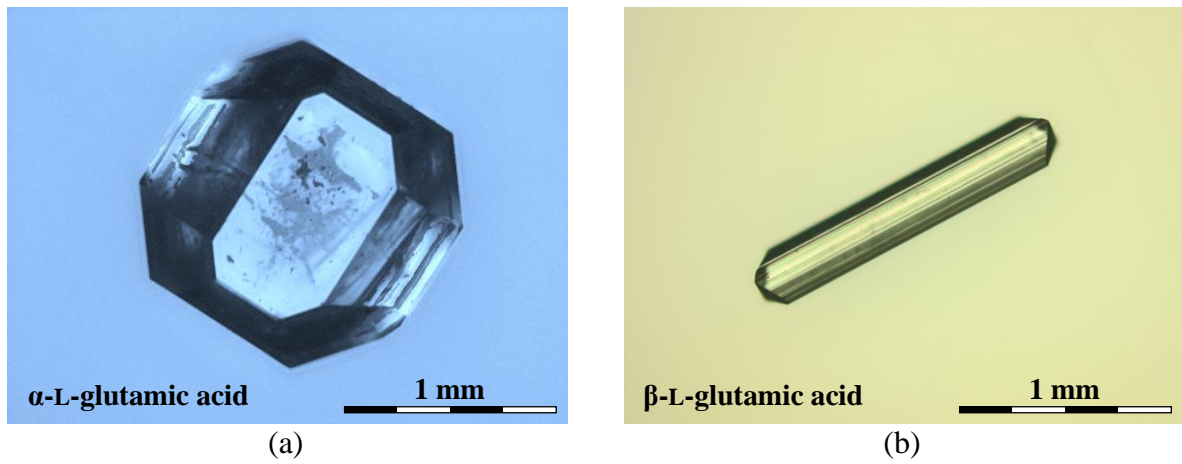


Figure 2.7 Microscope images showing (a) the α and (b) the β L-glutamic acid crystal morphology

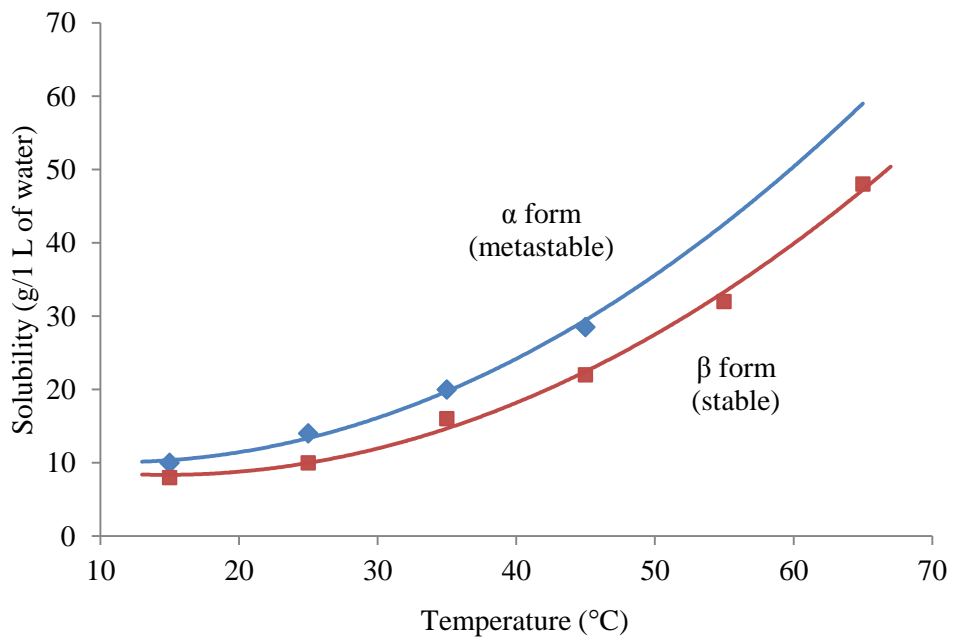


Figure 2.8 Solubility curves of L-glutamic acid polymorphs (Kitamura, 1989)

The former approach has revealed that kinetic studies of the solution-mediated phase transformation between metastable and stable polymorphs is controlled by the crystallisation rate of a stable form. A model has been developed for this type of phase transformation based on the assumption that the starting point for the transformation is a slurry of monosized crystals of a metastable phase in contact with a saturated solution containing nuclei of a stable phase (Cardew and Davey, 1985). In this simplistic view, as the ‘nuclei’ grow, the solution concentration falls below the solubility of the metastable phase and becomes undersaturated with respect to this phase. The crystals of the metastable phase thus dissolve producing supersaturation for the continued growth of the stable phase, and the process continues until all metastable phase has disappeared and the solution composition has fallen to the solubility of the stable phase. The concurrence of dissolution/growth processes would suggest that at least during some period of the transformation the growth and dissolution rates of the two phases must be balanced. Thus, using the mass balance rate of the two phases leads to qualitatively expected supersaturation-time plateau which characterises solution mediated polymorphic transformation (Davey et al., 1986). Further progress of the knowledge in this area has shown that the stable phase nuclei, known as the secondary nuclei (Garside and Davey, 1980), are created at the surfaces of the metastable crystalline phases (Cashell et al., 2003a). However, a mechanism of their formation is still poorly understood (Ferrari and Davey, 2004).

The latter approach, based on stereospecific nucleation inhibitors, assumes *a priori* that clusters are present whose packing mirrors the known crystal structures of the polymorphs. Under this assumption, doping materials have been successfully designed to control the polymorphic outcome by selective inhibition of unwanted structures using the concept of tailor-made additives. However, such results suffer from a notable ambiguity in their interpretation, since the additives may be active during the nucleation or growth process, or during both. Hence, even with its relative simplicity and elegance, the above model does not provide information on the structure of self-assembled clusters in solution and the kinetics of their formation (Davey et al., 2001).

In spite of the fact that the two approaches, (i) and (ii), have considerably advanced the knowledge in the area, the issues such as time evolution and the mechanism of the process at each stage, which includes initial nucleation of both phases from a metastable state of clear solution, their growth prior to solution-mediated transformation and the transformation

process itself, still need a substantial amount of attention. In particular, the coupling between different stages and how a selected additive may be used to tune the overall process.

2.5 Primary factors affecting the crystallisation of L-glutamic acid

It has been shown that the outcome of the crystallisation process of L-glutamic acid can be controlled by manipulation of the crystallisation parameters, such as temperature, supersaturation, cooling rate and agitation. Ono et al. (2004) demonstrated that when saturated solution of L-glutamic acid at 80°C is cooled rapidly to 25°C, predominantly the metastable α crystals are obtained. On the other hand, when the solution saturated at 90°C is cooled slowly, the nucleation of the stable β crystals takes place between 40°C and 50°C (Sakata, 1961a). Moreover, Kitamura (1989) showed that the temperature effect on the relative nucleation rates of the polymorphs in the crystallisation of L-glutamic acid is much more remarkable than the effect of supersaturation ratio. At temperatures lower than 25°C the α form is predominant. However, at constant supersaturation ratio, the nucleation rate of α decreases as the temperature is increased. Above 60°C the crystallisation process yields mainly the more stable β polymorph. Cashell et al. (2004) investigated the effect of agitation rate on the crystallisation of L-glutamic acid under the same conditions, cooling of supersaturated solution from 80°C to 45°C. It was shown that while without agitation β is the only polymorph that is formed, slow agitation speed results in approximately 57% stabilisation of the metastable form and high agitation rate leads to exclusive formation of the α polymorph.

The polymorphic composition of solution changes during the crystallisation process as the initially nucleated α crystals undergo transformation to the β form. The α polymorph remains in solution for a long period of time if kept at low temperature but the transformation rate increases as the temperature of solution is increased (Kitamura, 1989, Ono et al., 2004). The transformation mechanism is believed to be 'solution-mediated' (Cardew and Davey, 1985) since the dry α crystals are indefinitely stable if separated from their mother liquor immediately after crystallisation (Kitamura, 1989, Davey et al., 1997).

Kitamura (1989) divided the crystallisation process of L-glutamic acid into four stages (*Figure 2.9*). In Region I the decrease in solution concentration is due to the nucleation and growth of both polymorphs. Region II begins when the saturation level of the α polymorph is attained and is characterised by nearly constant solution concentration since the β form nucleates and grows at the expense of dissolution of α , i.e. the polymorphic transformation

occurs. The driving force for the formation of β is the difference in solubility between the two polymorphs. Moreover, Garti and Zour (1997) argue that the rate-determining step is the growth of the more stable form and not the dissolution of α . If this was not the case and β nucleated faster than α dissolved, a decrease in solution concentration would be observed. Region II ends when α crystals are completely dissolved. In Region III the stable form continues to grow until solution concentration achieves the solubility level of β . In Region IV the growth stops as the driving force for further crystallisation of β no longer exists.

2.6 Crystallisation kinetics

The growth kinetics and morphological change of α to β polymorph of a single crystal of L-glutamic acid were investigated using optical (Kitamura and Ishizu, 2000) and atomic force microscopy (AFM) (Kitamura and Onuma, 2000). The growth rates of α crystal in the [110], [010] and [001] directions, and that of β crystals in the [100] direction were established to be controlled by surface reaction. The dependence of the growth rate on the relative supersaturation indicated that the growth mechanism of both α and β polymorphs belongs to the birth and spread mechanism rather than the spiral growth mechanism.

Furthermore, Kitamura and Ishizu (2000) also observed morphological changes in the growth of α seed crystal (*Figure 2.10*) and postulated that they are caused by a differences in the dependence of the growth rate on the supersaturation between (111) and (110) faces, indicating the important contribution of the kinetic process to the morphological change.

Crystal morphologies of the two polymorphic forms of L-glutamic acid are shown in *Figure 2.11*. The fastest growing faces for α and β are (111) and (101), respectively (Davey et al., 1997). At the same supersaturation and at 25°C, the growth rate of the (111) face of the α crystal is several times greater than that of the (101) face of β . It was suggested that the higher growth rate of α may be due to the large kinetic factor and low edge free energy of the metastable form. It was also observed that the ratio of the growth rate of β to α increases with increasing solution supersaturation (Kitamura and Ishizu, 2000).

2.7 Polymorphic transformation mechanism

Kitamura and Funahara (1994) observed that the β form crystals tend to appear at the surface of the crystallising solution and suggested that nucleation of the β form may occur at the surface. In later work by Garti and Zour (1997), it was postulated that the nucleation process

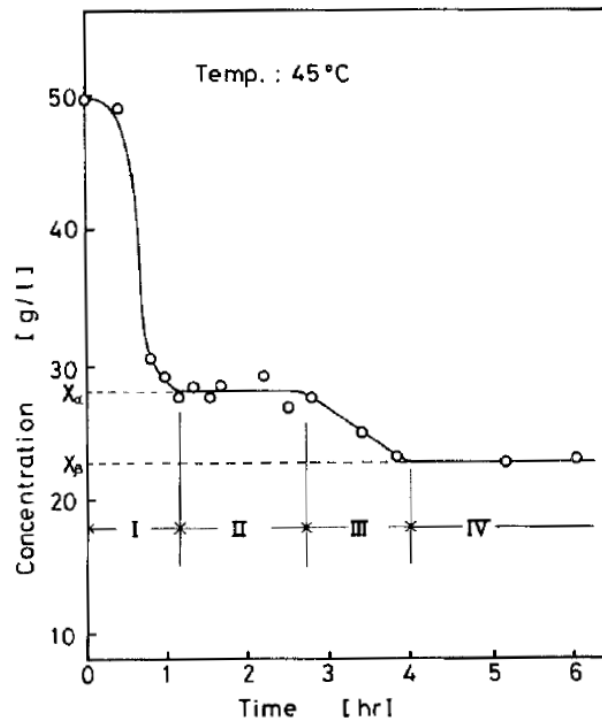


Figure 2.9 Concentration change during crystallisation of *L*-glutamic acid at 45°C (Kitamura, 1989)

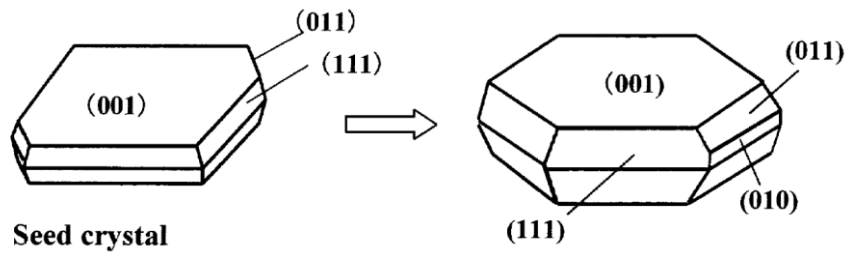


Figure 2.10 Morphological change of the α crystal during growth (Kitamura and Ishizu, 2000)

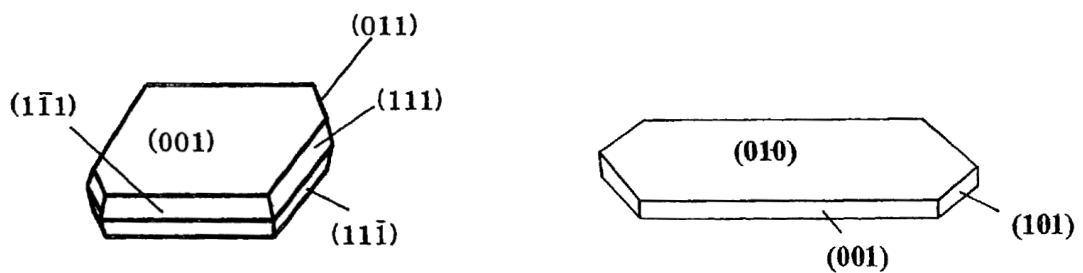


Figure 2.11 Crystal morphologies of (left) α - and (right) β -*L*-glutamic acid (Kitamura, 2002)

is heterogeneous, whereby secondary nucleation of the β polymorph takes place at the surface of the existing α crystals. The experimental evidence for the latter was provided by Cashell et al. (2003a) using a combination of scanning electron microscopy (SEM) and Raman spectroscopy. In further studies, Cashell et al. (2003b) also showed that both α and β forms of L-glutamic acid nucleate in the initial stage of cooling crystallisation and, due to the faster growth of α favoured by kinetics, the small amount of β initially nucleated on the surface of the metastable polymorph may become encapsulated in the α crystal. The secondary nucleation of β was later investigated by Ferrari and Davey (2004) who postulated that the observed phenomenon is caused by poor conformational discrimination at the {111}-type faces of α ultimately leading to the surface nucleation of β .

Cashell et al. (2004) demonstrated that prolonged agitation during slow cooling may be sufficient to disrupt nucleation of the β form crystals on the surface of the α polymorph. It was noted that when solutions are continuously agitated the α crystals that are formed are of poor quality and lack the necessary well-formed crystallographic facets on which the β form could nucleate. The latter observation further supports the mechanism of secondary nucleation of β on the surface of α crystals originally postulated by Garti and Zour (1997) and elaborated by Cashell et al. (2003a) and Ferrari and Davey (2004).

2.8 Reactive crystallisation of L-glutamic acid

In the cooling crystallisation process considered above the maximum driving force that can be achieved is limited by the solubility of L-glutamic acid in water. Moreover, as pointed out by Roelands et al. (2005), the starting point of nucleation during cooling the solution to the desired temperature cannot be exactly determined. Roelands et al. (2005) argue that pH-shift precipitation from a solution of sodium L-glutamate and sulphuric acid using a Y-shaped mixing tee with a static mixer inserted in the outflow tube has the advantage of a well-defined high initial supersaturation and can be used as an alternative method for crystallisation of L-glutamic acid. Further studies by Roelands et al. (2007), using the latter technique, showed that at supersaturation less than 13 without post-mixing aggregated crystals of β are formed while post-stirring generates the metastable α polymorph. At supersaturations greater than 17, with and without post-stirring, formation of smooth spheres was first observed which later transformed into rough spherulitic crystals of the β phase. Roelands et al. (2007) proposed that at the higher investigated supersaturation range the spheres are droplets formed by highly metastable liquid-liquid phase separation from which the stable β subsequently nucleates. It

was also postulated that at the lower supersaturation range without post-stirring the aggregates of β form according to the same mechanism, whereas with post-stirring the liquid-liquid phase separation is disrupted because concentration fluctuations are equalised by mixing and the metastable α nucleates directly from the homogenised solution.

2.9 Additives as secondary determinants in the crystallisation process

While solution supersaturation, temperature and stirring rate are considered to be the primary factors affecting the outcome of the crystallisation process, Kitamura (2002) identified additives as the secondary determinants. The effect of doping materials is comprised of the effect on the nucleation and that on the growth. Therefore, in order to understand the underlying mechanism of additives action, both processes should be examined separately. However, the only report where the effect of amino acid additives on the nucleation of L-glutamic acid was investigated is the work by Kitamura and Funahara (1994) who noted that L-phenylalanine increases the nucleation time of both polymorphic forms but no mechanistic explanation was provided. On the other hand, the effect of amino acid additives on the growth process of L-glutamic acid has long been a subject of study. Moreover, it has been demonstrated that the difference in relative kinetics can be used to manipulate the outcome of the crystallisation process.

Using an optical and atomic force (AFM) microscopy, Kitamura and Ishizu (1998) showed that when L-phenylalanine is added to the crystallising solution the growth rate of α in the [111] direction is suppressed. While it was observed that the new (110) face appears, the growth rate of the (001) face seemed not to be influenced by the presence of the additive. It was speculated that the (001) face may not be affected because L-phenylalanine cannot be adsorbed because of the repulsion between the phenyl group and the carboxyl acid groups in the (001) face. Moreover, growth hindering of the (101) face of β was also observed. For both polymorphs the growth hampering effect increases with increasing concentration. The critical concentration of L-phenylalanine at which the growth of α stops is about twice that for β , indicating the preferential inhibition of the growth of β (Kitamura and Ishizu, 1998).

Kitamura and Funahara (1994) observed that the precipitation ratio of α in the initial stage of crystallisation increases with the concentration of L-phenylalanine and the additive can be used to hinder the polymorphic transformation and almost entirely suppress the formation of the stable polymorph. However, no effect was observed when D-phenylalanine was used as an additive. The latter implies that the effect is highly stereoselective. It was postulated that

the L- isomer can adsorb on the crystal surface through the common part of amino acid and can hinder further attachment of L-glutamic acid growth units with the phenyl ring which cannot be incorporated into the crystal structure. On the other hand, the adsorption of the D- isomer is not possible because the configuration of the common group is not compatible with that in the bulk crystal and hence no effect on the growth is observed.

In further studies, the effect of other amino acids was investigated. Kitamura and Nakamura (2001) demonstrated that three hydrophobic amino acids, L-valine, L-isoleucine and L-leucine, can also be used to hamper the crystallisation rate of α -L-glutamic acid. The effect of the former additive was most pronounced whereas that of the latter was smallest. It was suggested that the effect of L-valine is due to the high adsorption density and the readiness of forming inclusions, rather than the steric hindrance of the substituted groups. On the other hand, it was the methyl group at the β carbon that seemed to effectively inhibit the growth of L-glutamic acid when L-isoleucine and L-leucine were used as the doping material. Cashell et al. (2005) identified that at high concentration levels a range of amino acids, namely L-aspartic acid, L-lysine, L-arginine, L-cysteine, L-serine and L-methionine, a significant amount of the additive uptake is observed causing significant changes in the α form morphology. It was demonstrated that the {011} and {001} facets disappear and the {110} and {111} facets emerge. Accordingly, it was postulated that the molecules of the doping material are preferentially attached to the slowest growing {110} and {111} facets and thus stabilise the metastable form by disrupting β developing on the surface of α . Moreover, Cashell et al. (2005) indicated that the presence of a bulky phenyl side chain in L-phenylalanine and L-tyrosine is an essential feature in achieving stabilisation of the metastable polymorph at low additive levels. The hindering effect of additives on the growth of the three dominant faces of β -L-glutamic acid was investigated by Sano et al. (1997) and was found to be stronger in the {010} and {001} faces than in the {101} face. The observed growth inhibition was in the decreasing order of L-phenylalanine, L-lysine, L-aspartic acid and L-alanine, and for L-phenylalanine and L-aspartic acid was found to significantly increase when the level of the additive was increased. However, the overall discriminating capacity of the β form for the recognition of the additive molecules was found to be lower than in the α polymorph. Therefore, it was concluded the selective crystallisation of L-glutamic acid in the presence of the additives can be attributed to the difference in the inhibitory effects on the two dominant faces of the metastable form.

In addition to the kinetic consideration of the effect of additives discussed above, another approach that received considerable attention is the concept of ‘tailor-made’ additives. The latter was introduced by Addadi et al. (1982) who showed that additives can be ‘tailored’, i.e. carefully selected on a purely structural basis, to carry out a specific task in the crystallisation process. In this approach, a habit modifying additive should have structural characteristics of the host molecule, i.e. similar groups participating in hydrogen bonding, but should also have a modified part that differs in some way. Thus, once incorporated into the structure, ‘tailor-made’ additives will disrupt the bonding sequences present in the crystal and disturb the growth of specific faces (Black et al., 1986).

In later studies, Davey et al. (1997) demonstrated that additives can be successfully chosen on the basis of conformational recognition to inhibit the appearance of the stable β polymorph of L-glutamic acid by selectively binding to and hindering the fastest growing faces of β crystals without affecting the fast growing faces of the metastable form. Davey et al. (1997) showed that 1,5-dicarboxylic acids that mimic the β form conformation, namely transglutamic acid and trimesic acid, could enter the surface with its carboxyl functionalities substituting for those of L-glutamic acid. The missing amino group would not be noticed until the next growth layer was laid down when its absence or substitution for a bulkier moiety would disrupt the growth of β , yielding the metastable α crystals as the main outcome of the crystallisation process. The attempts to use α -like additives, such as glutaric acid and 2-methylglutaric acid and hence directly crystallise the stable β polymorph were, however, unsuccessful.

Generally, additives may not only inhibit the crystallisation of an unwanted polymorph, but can also lead to new and unexpected phenomena irrespective of whether the crystallising material is polymorphic or non-polymorphic. There has been a widely accepted view that molecular modifiers in solution are capable of directing growth morphology, but have only neutral or inhibitory effects on primary nucleation and growth kinetics (Elhadj et al., 2006). While the former view remains largely unchallenged (Galkin and Vekilov, 2000), the latter was recently questioned by *in-situ* atomic force microscopy (AFM) studies on biomineralisation of calcite which have shown that two acidic proteins (isolated and purified from abalone shell nacre) dramatically accelerate calcite growth while still altering the surface morphology through interactions with specific atomic steps on the (104) face (Elhadj et al., 2006, Fu et al., 2005). Following this discovery, additional evidence of a growth accelerating effect has been demonstrated for the same material grown in the presence of

synthetically designed small model peptides (peptoids) (Chen et al., 2011). In spite of the scarcity of the data that exists on nucleation and crystal growth enhancement, one may ask a more general question, 'Should accelerating effects occur for the primary nucleation of polymorphic materials in the presence of selectively chosen molecular modifiers, and how this initial condition may influence, at the later stage, the kinetics of solution-mediated transformation of metastable to stable polymorphic form?' Giving an answer to this question is central to the ability to control the transformation process between polymorphs of crystalline materials in a wide range of consumer products from foods, through cosmetics to pharmaceuticals.

Chapter 3

Experimental methods

The nucleation, growth and polymorphic transformation processes during batch and containerless crystallisation of L-glutamic acid were investigated using a range of experimental techniques, including, but not limited to, single-photon laser light scattering, synchrotron wide angle X-ray scattering and Raman spectroscopy. The following chapter provides the essential background on the principles behind the methods and apparatus that were employed, and describes the materials and experimental procedures used in this study.

3.1 Materials used

All chemicals used were of analytical grade and used as received from the supplier, and are listed in *Table 3.1*. All solutions were prepared using purified and deionised water.

3.2 Apparatus and experimental techniques

3.2.1 Batch crystallisation

Crystallisation plays an important role in a range of industries, especially those manufacturing pharmaceuticals, cosmetics, specialty chemicals and foods. Just like any other production process, crystallisation can be operated in two modes, batch and continuous. The advantage of batch crystallisation is that it yields materials of high purity, narrow crystal size distribution and relatively large crystal size. Unlike the continuous mode, batch processes are relatively flexible and allow for changing product specification. Moreover, as batch operations are repetitive in nature, information from previous runs can be used to improve future operations, allowing trouble-free production for the manufacturers. For those reasons, they are preferred in industries where materials of low volume and high value, such as pharmaceuticals, are manufactured.

Table 3.1 Chemicals used in the experiments

Chemical name	Purity	Supplier	Batch number
L-Glutamic acid	$\geq 99.0\%$	VWR International Ltd.	K35376147609
Glycine	$\geq 99.7\%$	VWR International Ltd.	K34798166542
L-Alanine	$\geq 99.0\%$	Sigma-Aldrich Company Ltd.	K39066207835
L-Phenylalanine	$\geq 99.0\%$	Sigma-Aldrich Company Ltd.	K37363256808

3.2.1.1 Nucleation time measurements

The most common technique employed to study the nucleation process is measurement of the change in solution turbidity as light is transmitted through the sample. When solution nucleates, fewer photons of the original beam propagate towards the detector located opposite the light source. Accordingly, the moment when a drop in the measured light intensity occurs can be assumed to correspond to the onset of the nucleation process. In practice, however, since the extinction of light must be sufficient to cause a detectable change in the transmitted light intensity, the recorded increase in turbidity is not only due to nucleation but also due to growth of the newly formed crystals (Hartel, 2001).

An alternative and a more robust approach to study the nucleation process are light scattering techniques. In this work a variation of a static light scattering method with a novel light detection system is employed. While the light scattering methods typically use analogue photon counting, a single-photon counting technique used in this study provides better resolution of solution fluctuations and a higher signal to noise ratio (Becker, 2010). The latter characteristics make single-photon detection a promising system for the nucleation measurements since it is the low intensity scattering that is produced in the early stage of formation of a solid phase during crystallisation from solution.

The experimental apparatus used to measure the nucleation time of pure and glycine-doped L-glutamic acid from solution consists of a laser source, a set of apertures and lenses to focus and direct the light beam, a crystallisation cell where the nucleation takes place and a system that detects and quantifies the intensity of the scattered light (*Figures 3.1 and 3.2*).

The light source is a 150 mW Omnicrome Argon-Ion laser (wavelength: 514 nm). The light is collimated which limits the spread of the beam as it propagates. The laser beam is focused

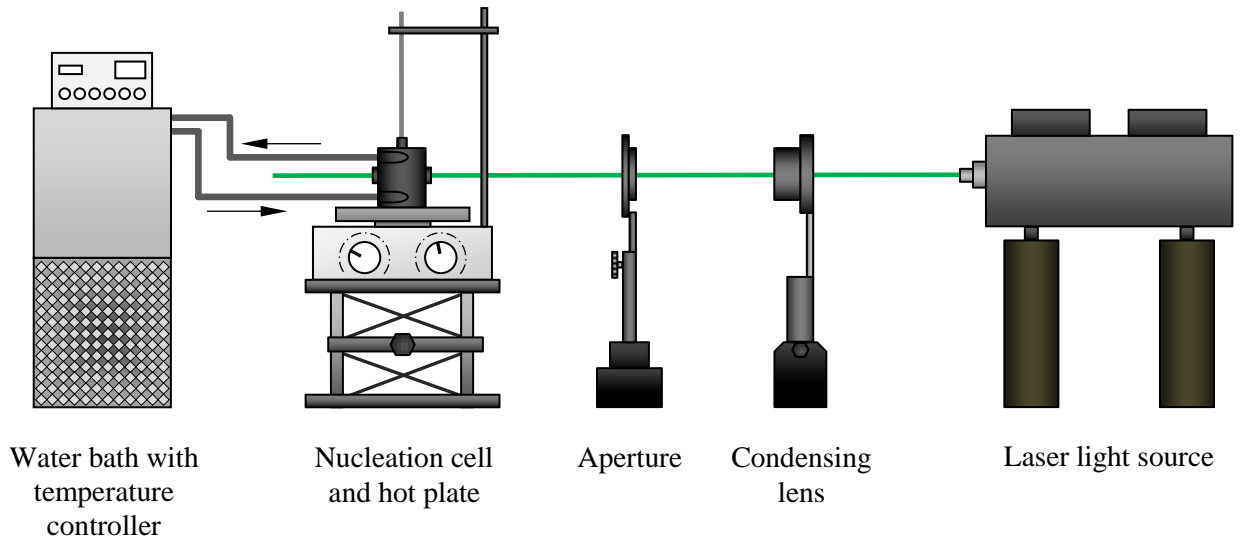


Figure 3.1 Front view of the experimental set-up for the nucleation time studies

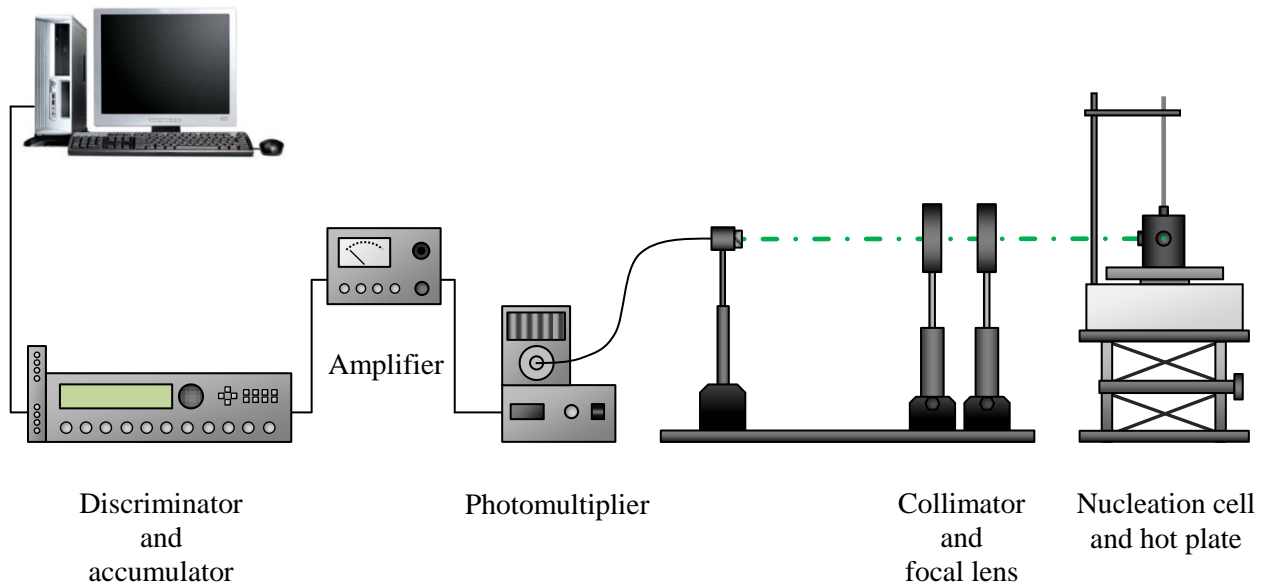


Figure 3.2 Side view of the experimental set-up for the nucleation time studies

using an 80 mm diameter focus lens with a 250 mm focal length and an aperture to shape the beam.

The nucleation cell is an 80 mL jacketed glass crystalliser with three windows made of 1.5 mm thick borosilicate glass. Two of the windows are parallel and on opposite sides of the cell and the third window is perpendicular to them. The temperature of water in the jacket is controlled using a Huber Ministat 240 water bath. The nucleation cell is covered in black tape to reduce reflections and potential detection of light scattered at other angles. The solution was agitated using a magnetic stirring bar and the temperature in the cell was measured using a thermocouple connected to an IKA-Werke RET Control-Visc hotplate.

The laser light passes through the two parallel windows and interacts with solution in the cell leading to light scattering. Any light that scatters through the window perpendicular to the direction of the beam passes through a collimator and a focal lens (both 80 mm, focal lengths of 300 mm and 500 mm) to the detection apparatus. The collimated light is focused on the exposed end of a 120 μm diameter multi-mode optical fibre that transmits the signal to the Thorn EMI Electron Tubes (FACT 50) Photomultiplier.

Within the photomultiplier individual photons collide with a photocathode, which is held at a 1.1 kV negative voltage, resulting in the release of a photoelectron. The released electrons collide with alkali metal cathode plates, known as dynodes, which are also held at a high negative potential resulting in multiple electrons being released for each collision. This process results in an amplified voltage peak being produced by each collected photon.

The electrical signal is then sent through a Stanford Research Systems SR440 DC-300MHz amplifier, with a total gain of 25, into a Stanford Research Systems S400 photon counter which processes the signal and sums up the number of photon pulses detected over a predefined period of time. A discrimination level of 10 mV was set for the system to disregard any signal below the threshold voltage.

The signal from the photon counter is sent using a National Instruments SCC-68 Interface Card to a computer running a custom-written LabView software that continuously records the experimental data. Every 1 V pulse that is recorded corresponds to 999 photons detected.

3.2.1.2 In-house studies of polymorphic transformation

Crystallisation was performed in a 500 mL jacketed round bottom glass reactor equipped with a Hanna Instruments HI-76310 probe for conductivity and temperature monitoring. The probe was calibrated using Jenway Calibration Standard (12880 $\mu\text{S}/\text{cm}$ at 25°C), and was

attached to a Hanna Instruments HI-2300 Microprocessor Conductivity Meter and a computer with data recording software. During the experiments, the top of the crystalliser was sealed in order to prevent evaporation of the solvent and contamination of solution. The temperature of the water jacket was controlled by a programmable Huber CC230 thermostatic water bath.

An external circulation loop was used to ensure homogeneity of the vessel contents. The solution was being withdrawn from the bottom of the crystalliser and then pumped back to the top of the vessel by an Iwaki MD10 magnetic drive pump, at a constant flow rate of 1.6 L per minute. Chemically inert silicon rubber tubing was used to connect the crystalliser and the pump.

3.2.1.3 Synchrotron-based studies of growth and polymorphic transformation

Moreover, when experiments were performed at the synchrotron facility, an additional jacketed glass flow cell was incorporated into the circulation loop to position the crystallising solution in the synchrotron beam and enable continuous sampling. The incident X-rays passed through the windows in the centre of the cell where the solution was flowing. The windows were made of a thin Kapton film (25 μm), aligned parallel and separated by a distance of 1 mm.

The experimental set-up is schematically shown in *Figure 3.3* and a detailed view of the flow cell is presented in *Figure 3.4*.

3.2.2 Acoustic levitation

Over the past years, acoustic levitation has increasingly been used to study crystallisation phenomena in a variety of materials. In contrast to the traditionally used batch reactors where the solution is rapidly mixed and the crystal nuclei form as a result of homo- and heterogeneous nucleation, the former approach has the advantage of holding the sample without contact with container walls thus allowing for an essentially homogeneous process as adsorption of solute molecules on the foreign bodies, such as container walls or blades of the agitator, is avoided. Acoustic levitation has been successfully employed to study crystallisation phenomena *in-situ* using energy dispersive X-ray spectroscopy (EDX) (Leiterer et al., 2006), small- and wide-angle X-ray diffraction (SAXS/WAXS) (Delissen et al., 2008, Wolf et al., 2008) or Raman spectroscopy (Klimakow et al., 2010, Radnik et al., 2011). Moreover, since the technique circumvents the need for a sample container, some of the problems intrinsic to the conventional experimental methods, such as scattering and contributions from the sample container, are not present.

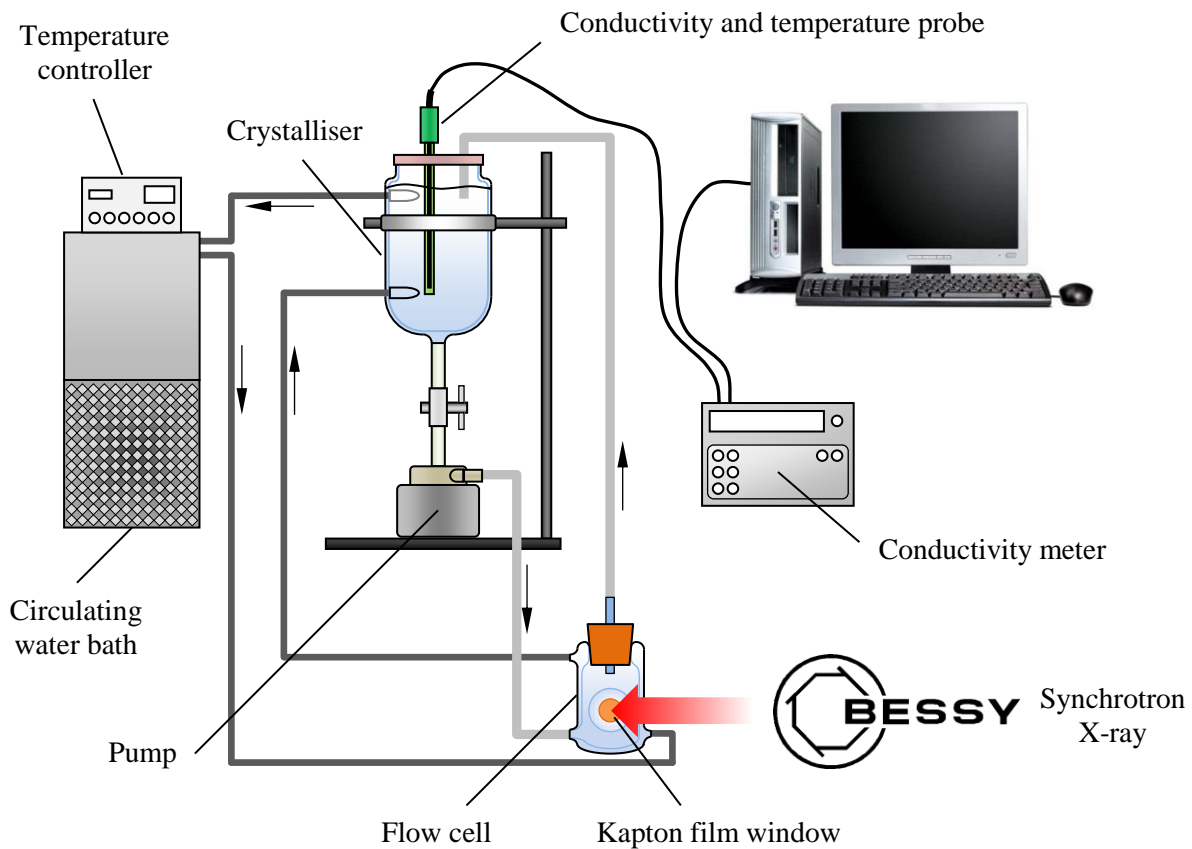


Figure 3.3 *Experimental set-up used in the growth and polymorphic transformation studies*

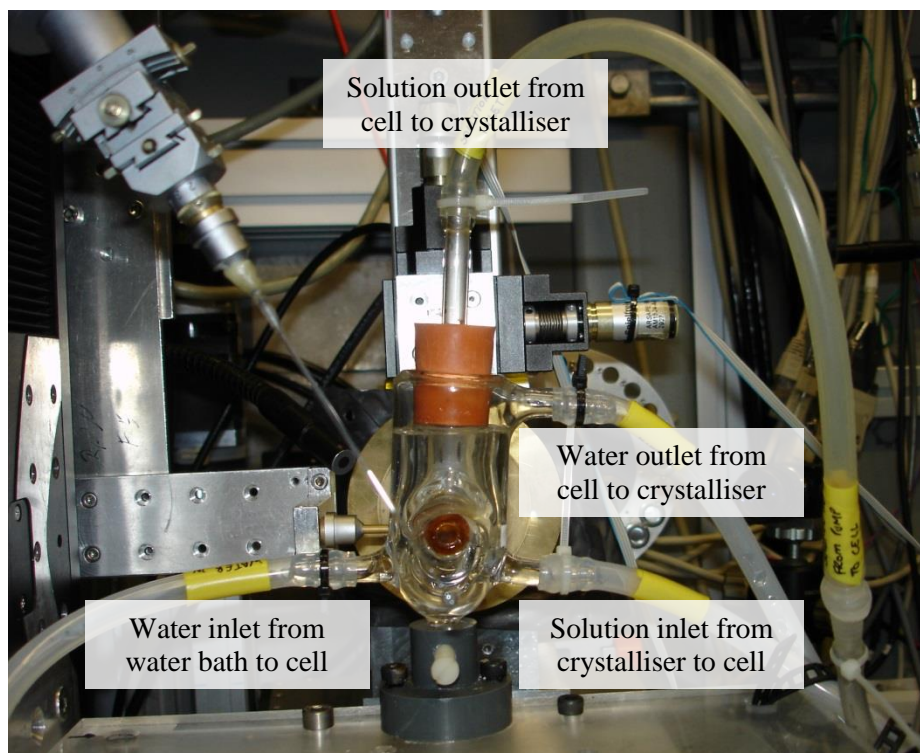


Figure 3.4 *Detailed view of the flow cell used in the growth and polymorphic transformation studies*

An acoustic levitator (tec5, Oberursel, Germany), consisting of a sonotrode and a reflector, was used as a sample holder (*Figure 3.5*). The sonotrode emits an ultrasonic wave with a frequency of 58 kHz and a sound pressure level of 156 dB. When the sonotrode and the reflector (a concave acoustic mirror) are adjusted concentrically and at a distance of multiple of half the wavelength ($d = n\lambda / 2$), a standing wave with equidistant nodal points is formed in the gap between the transducer and the reflector (*Figure 3.6*). In several pressure nodes of this wave, as a result of axial radiation pressure and radial Bernoulli stress, a dissolved sample droplet with an effective diameter of less than half wavelength can be placed and held in a levitated position (Vandaele et al., 2005). When a liquid sample is levitated, gradual evaporation of the solvent occurs and the concentration of the solute increases with time. As a result of an increase in solution supersaturation, crystal nucleation and subsequent growth are induced. Acoustic levitation can therefore be employed to investigate the crystallisation phenomena in liquid samples of small volume without the influence of the sample container.

The containerless crystallisation was investigated *in-situ* using wide-angle X-ray diffraction (WAXS) and Raman spectroscopy techniques. The change in droplet volume was monitored using a telecentric infrared flash light and recorded by a CCD camera on the other side of the droplet (*Figure 3.7*). The ambient temperature at the sample position was $296 \text{ K} \pm 1 \text{ K}$. The relative humidity was $55\% \pm 5\%$. A series of tests by Klimakow et al. (2010), using the same experimental set-up, indicated that the temperature and pressure conditions in the direct environment of the droplet show only minimal deviations from the conditions prevailing in the experimental hutch and the measured positional displacement was smaller than $20 \mu\text{m}$. The sample remains in a fixed position during the measurement even after evaporation of the solvent.

3.2.3 Synchrotron Wide-Angle X-ray Scattering

Synchrotron radiation is the electromagnetic radiation emitted when a current of charged particles, typically electrons, travel in curved path at relativistic speeds, i.e. near the speed of light. Some of the radiation from the bending magnets, and most or all of the radiation from specially designed wiggler and undulator insertion devices, leaves the ring through tangential ports called beam lines that allow radiation to pass experimental stations located outside the ring (Winick, 1995).

The synchrotron radiation is extremely intense over a broad range of wavelengths, extending from the microwave region into the hard X-ray band of the electromagnetic spectrum, and its

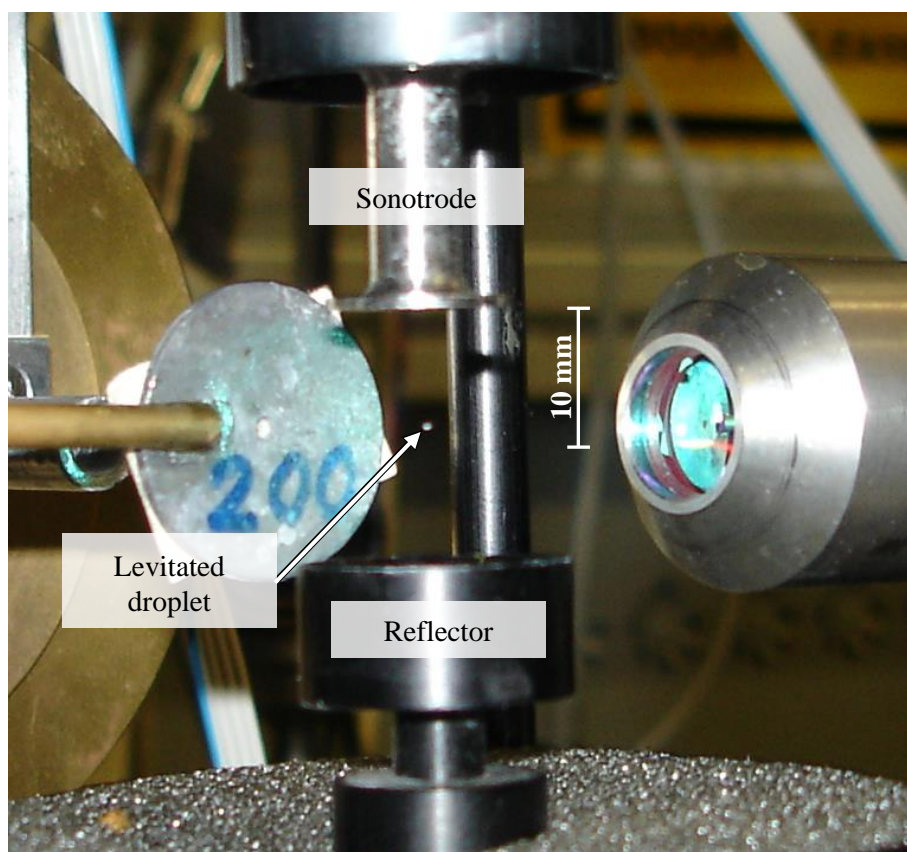


Figure 3.5 A droplet of L-glutamic acid solution suspended in air using an acoustic levitator

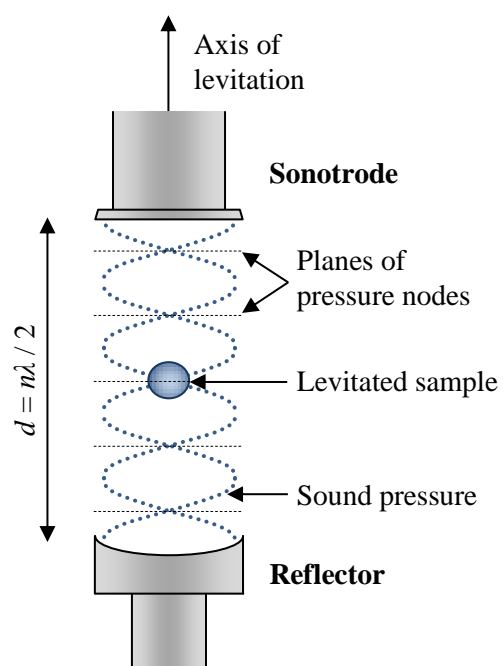


Figure 3.6 Schematic representation of the principle of acoustic levitation

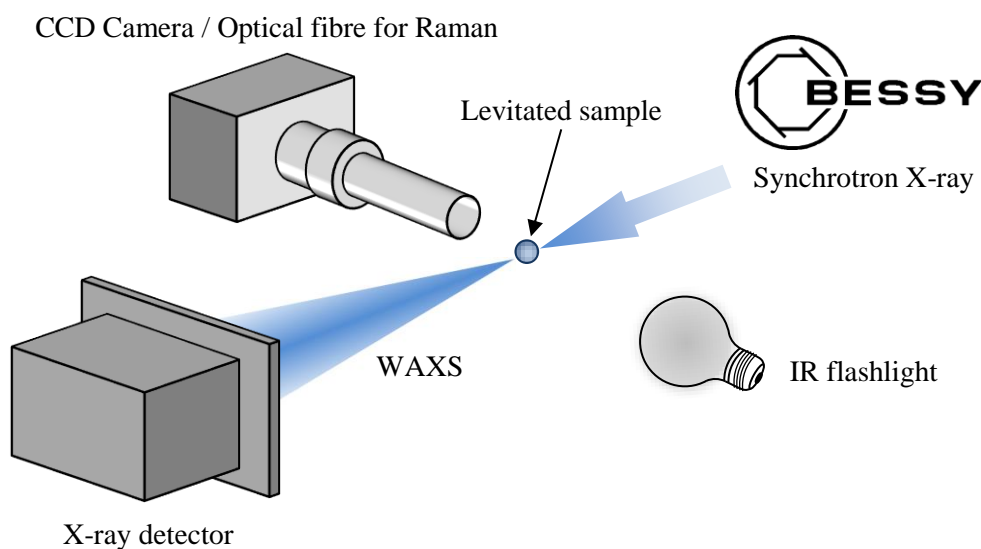


Figure 3.7 Schematic representation of the set-up used in the levitated droplet experiment

intensity is several orders of magnitude higher than the radiation produced by conventional laboratory sources. Moreover, high collimation (small angular divergence of the beam), polarisation, high brilliance and pulsed-time structure make synchrotron radiation a powerful tool for studies of dynamic systems in a wide range of disciplines, ranging from condensed matter physics and materials science through to biology and medicine.

In this work, the *in-situ* time-resolved WAXS measurements are employed to probe the batch and containerless crystallisation of L-glutamic acid from solution in the presence and absence of other amino acid additives. WAXS data would provide information to examine the mole fraction time evolutions and the time-dependent kinetic evolutions of the two crystallising/dissolving polymorphs and thus the role of the additives on the intensification of these processes, including solution-mediated transformation times.

When X-rays pass through a crystal they interact with the investigated sample and are scattered on electrons of atoms that make up a crystal (Glatter and Kratky, 1982). The scattered X-ray waves can interfere constructively and destructively along certain directions of space. Diffraction is observed when X-rays scattered by the families of planes have a difference in phase equal to an integer number of wavelengths, i.e. when the Bragg condition is met (Cullity and Stock, 2001), i.e. when $n\lambda = 2d_{hkl} \sin(\theta)$, where n is the order of reflection, λ is the wavelength, d_{hkl} is the distance between atomic planes and θ is the angle of reflection. Otherwise, destructive interference occurs and scattered radiation is cancelled along a particular direction and no reflections are observed. The shape (crystal system) and size (lattice parameters) of the unit cell determine the diffraction directions. The result is

a pattern of peaks which is unique to a specific material. The scattering at angles 2θ larger than 5° provides information on molecular and atomic ordering and is referred to as wide angle X-ray scattering (WAXS).

The Wide-Angle X-ray Scattering (WAXS) spectra were recorded *in-situ* at the synchrotron microfocus beamline (μ -Spot, BESSY II, the Helmholtz Centre Berlin for Materials and Energy, Germany) in order to determine the crystallised mass fractions of the metastable and stable forms of L-glutamic acid. A circular beam adjusted to the centre of the droplet with a cross section of $100\ \mu\text{m}$ at photon flux of $1 \times 10^9\ \text{s}^{-1}$ at a ring current of 100 mA was used. All experiments were carried out using a double crystal monochromator (Si 111). The beam energy was 12.0 keV which corresponds to a wavelength of $1.0332\ \text{\AA}$. The WAXS patterns were recorded 200 mm behind the sample with a two-dimensional X-ray detector (MarMosaic, CCD 3072×3072 pixels and a point spread function width of about $100\ \mu\text{m}$).

The scattered radiation collected on a flat plate detector leads to formation of diffraction rings around the beam axis, the so called Debye-Scherrer rings (Debye and Scherrer, 1916). The obtained scattering data was corrected for background scattering and converted into diagrams of scattered intensities, I , as a function of the scattering vector, q , (q is defined as $q = 4\pi \sin(\theta) / \lambda$, where θ is the scattering angle between the beam axis and the ring and λ is the radiation wavelength) using the FIT2D software package. For phase analysis, the scattering vector was converted into the 2θ values (Cu $K\alpha$ radiation $\lambda = 1.5418\ \text{\AA}$). The scanning range was 6 to 60 degrees 2θ . The X-ray data acquisition time was 15 seconds.

3.2.4 Raman Spectroscopy

Raman spectroscopy is a spectroscopy technique for measuring characteristic vibrational modes of molecular groups. Raman scattering is a two-photon inelastic light scattering process. The incident photon is of much greater energy than the vibrational quantum energy, and loses part of its energy to the molecular vibration with the remaining energy scattered as a photon with reduced frequency. The interaction between light and matter is an off-resonance condition involving the Raman polarisability of the molecule (Larkin, 2011).

Spectrometric analysis of the scattered radiation shows strong Rayleigh line at the unmodified frequency of radiation used to excite the sample but also contains frequencies arrayed above and below the frequency of the Rayleigh line. The Raman lines are generally weak in intensity, approximately 0.001% of the source (Bugay and Williams, 1995). Raman bands at wavenumbers less than the Rayleigh line are called Stokes lines, while anti-Stokes

lines occur at greater wavenumbers than the source of radiation. Since the anti-Stokes lines are less intense, the Stokes portion of the spectrum is generally used. The differences between the Rayleigh line and the Raman line frequencies correspond to the vibrational frequencies present in the molecules of the sample. The Raman vibrational bands are characterised by their frequency, intensity and band shape and are unique to a particular molecule (Larkin, 2011). The abscissa of the spectrum is usually labelled as wavenumber or Raman shift (cm^{-1}).

The Raman spectra of the levitated droplet were recorded *in-situ* using a RXN Raman Spectrometer (Kaiser Optical Systems, Ecully, France) equipped with a thermoelectrically cooled CCD detector and a fibre optic probe. The samples were excited using a 785 nm diode laser and with a maximum power of 70 mW. The laser beam was focused on a droplet with a spot diameter of 1 mm and a focal distance of 178 mm. The Raman scattered light was collected in a 180° backscattering geometry. Spectra were recorded between 350 cm^{-1} and 3300 cm^{-1} with a time resolution of 30 seconds.

3.2.5 Droplet volume monitoring

The change in position, shape and volume of a droplet were monitored using a telecentric infrared flashlight and recorded by a microscope equipped with a CCD camera on the opposite side of the droplet (*Figure 3.7*). Because of the strong absorption of water in the infrared region ($\lambda = 880 \text{ nm}$), a shadow of the droplet is observed and the area of the shadow could be measured. The rotational symmetry around the axis of levitation allowed estimation of the volume of the droplet from the area of the shadow using the formula for the volume of an ellipsoid of rotation, $V = 4\pi / 3a^2b$, where a and b are the width and height of the droplet shadow, respectively. The measured volumes were converted to mL using the calibration data obtained with standardised spheres (Delissen et al., 2008). The images of the droplet were taken every 1 minute.

3.2.6 Solution concentration evolution

The conductivity measurements can be related to the concentration of L-glutamic acid in solution. The initial conductivity (point A in *Figure 3.8*) corresponds to the original concentration of the supersaturated L-glutamic acid solution that was prepared. The value at the beginning of the first plateau on the conductivity curve (point B in *Figure 3.8*) coincides with the solubility of the metastable form. The final conductivity (point C in *Figure 3.8*) corresponds to the solubility concentration of the stable polymorph. The relationship between solution conductivity and concentration, plotted in *Figure 3.9*, is approximately linear and the

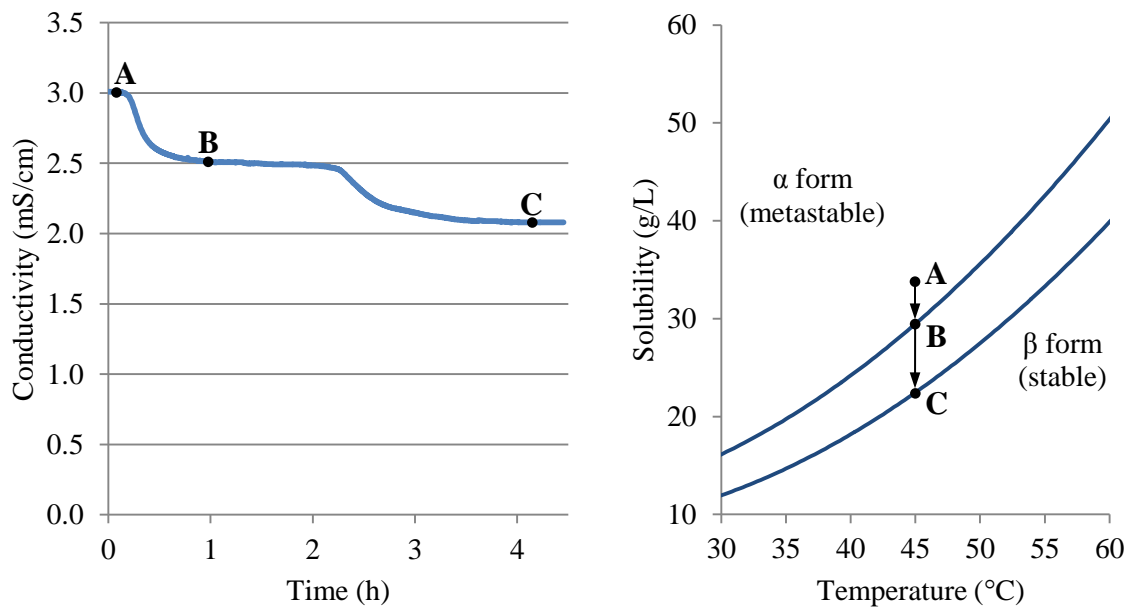


Figure 3.8 Equivalent points on the conductivity plot obtained during batch crystallisation of *L*-glutamic acid at 45°C and on the solubility curves by Kitamura (1989)

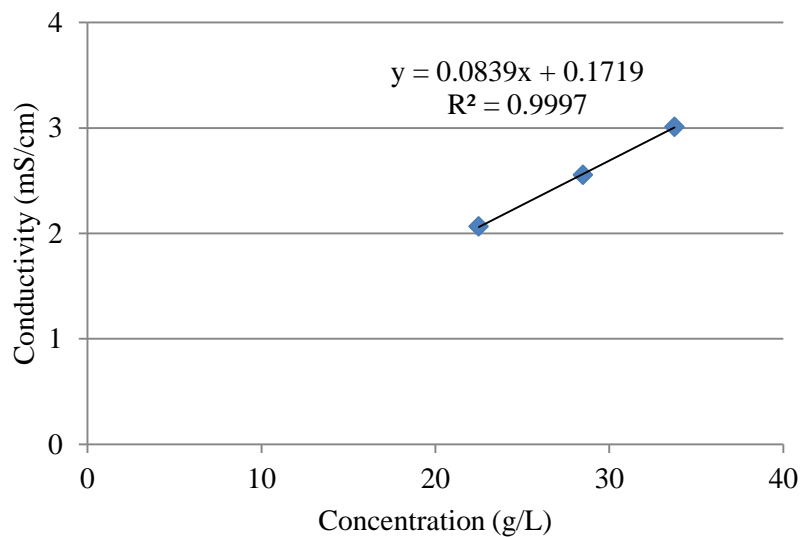


Figure 3.9 Relationship between solution conductivity and concentration of *L*-glutamic acid

resulting equation can be used to convert the probe readings into L-glutamic acid concentration in solution.

3.3 Experimental procedures

3.3.1 Batch crystallisation

3.3.1.1 Nucleation time measurements

The nucleation time of pure and glycine-doped L-glutamic acid solutions was investigated at supersaturation σ of 0.5, 0.6, 0.7, 0.8 and 0.9 at 35°C. The experimental solutions were prepared by dissolution of 11.625 g, 12.400 g, 13.175 g, 13.950 g and 14.725 g of L-glutamic acid in 500 mL of purified and deionised water, respectively. The mass of L-glutamic acid to be used was determined using the solubility data by Kitamura (1989). The effect of the presence of the additive was investigated at four doping levels, namely 1250 ppm, 2500 ppm, 5000 ppm and 7500 ppm (mol/mol). The dissolution was enhanced by agitation with a magnetic stirrer bar at 250 rpm and heating the solution at 60°C for two hours using an IKA-Werke RET Control-Visc hotplate. The vessel was sealed to prevent solvent evaporation. When the dissolution process was complete, the experimental solution was filtered using a pre-heated vacuum filter, transferred into the pre-heated nucleation cell and slowly cooled down to 35°C.

In order to remove any solid residues from previous runs and therefore to minimise the probability of heterogeneous formation of new crystals, the nucleation cell was washed with purified and deionised water at 60°C and stirred for one hour before each experiment. The latter also allows the stirring bar to heat up. After the experimental solution was transferred into the pre-heated cell and after the solution cooled down to 35°C, the laser, stirring and recording of the number of scattered photons were all turned on at the same time. The water bath temperature was set to 35.5°C to compensate for heat losses. The data collection was continuous with the accumulation time of 10 μ s. The recorded signal consists of low intensity background noise, resulting from the density and compositional fluctuations of solution, and a number of large amplitude pulses due to scattering of individual photons. The occasional spikes in the spectrum result from statistical fluctuations due to short sampling time. For the clarity of presentation, throughout this report the recorded data will be plotted as a running average of 20 measurements (*Figure 3.10*).

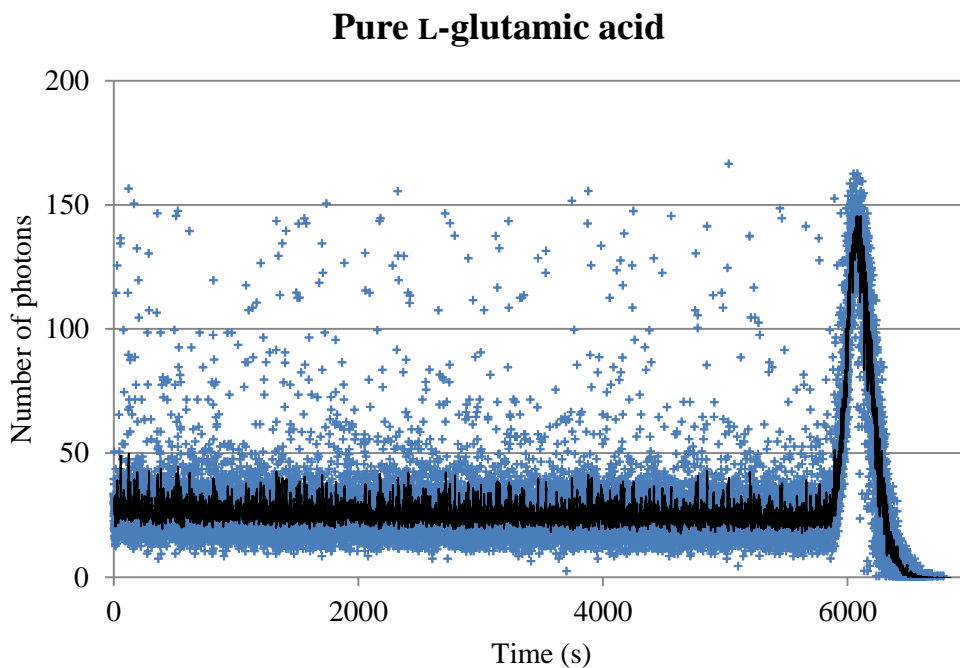


Figure 3.10 Single-photon laser light scattering data on the induction time of L-glutamic acid ($\sigma = 0.5$) obtained in one of the nucleation experiments for pure solution. Blue crosses correspond to individual measurements whereas the black line represents a running average of 20 data points.

The scattering data was recorded until the solution became opaque and the laser light could no longer pass through the cell. The laser beam generator, water bath and stirring were then turned off. After each experimental run, the nucleation cell was rinsed several times with deionised water to ensure complete removal of all chemical residues.

3.3.1.2 In-house studies of polymorphic transformation

The procedure used to prepare pure and glycine-doped solution of L-glutamic acid at supersaturation σ of 0.5 at 35°C for the in-house batch transformation experiments was the same as the one used in the nucleation time studies (*Section 3.3.1.1*).

Prior to each experiment, the crystalliser and the circulation loop were thoroughly rinsed with purified and deionised water to remove any possible contaminants, such as dust or solid residues remaining from earlier runs. After filtration, the solution was transferred into the pre-heated batch crystalliser. Once the solution temperature reached 35°C, the crystalliser vessel was then carefully examined in order to ensure that the solution is free of crystals as these could act as seeds for nucleation. Subsequently, the circulation pump was turned on and, simultaneously, the conductivity and temperature data recording was started. The measurements were taken every 10 seconds. The crystallisation was investigated isothermally

at 35°C and, in order to compensate for heat losses through the glass vessel walls, the water bath temperature was set to 35.5°C.

The probe readings were monitored throughout duration of the experiment to assess the progress of the L-glutamic acid polymorphic transformation. When the polymorphic interconversion was finished, the water bath and the pump were turned off, and the data recording was stopped. The resulting crystals were then filtered off, washed, dried and stored for further investigation. After each of the experiments the equipment was rinsed several times with deionised water to ensure complete removal of all chemical residues.

3.3.1.3 Synchrotron-based studies of growth and polymorphic transformation

The procedure followed to prepare solutions for synchrotron growth and transformation studies and operate the batch crystalliser was similar to that described in *Section 3.3.1.2*. However, in order to increase the polymorphic transformation rate and therefore allow more experimental runs within the allocated synchrotron beam time, the isothermal crystallisation was performed at 45°C.

Pure solution of L-glutamic acid at supersaturation σ of 0.5 at 45°C, corresponding to 16.719 g of solute in 500 mL of water, and solutions in the presence of 2500 ppm, 5000 ppm and 7500 ppm (mol/mol) of glycine were investigated. To compensate for heat losses, the water bath temperature was set to 45.8°C. During the experiment, in addition to conductivity and temperature data, WAXS spectra were also recorded.

3.3.2 Acoustic levitation

The experimental solutions were prepared by dissolution of 2.500 g of L-glutamic acid in 250 mL of purified and deionised water. Pure solution and solution with three other amino acid additives, namely glycine, L-alanine and L-phenylalanine, at two doping levels (2500 ppm and 10000 ppm mol/mol) were prepared. The mass and amount of water that were used correspond to a slightly undersaturated solution at 25°C.

Each solution was heated up and stirred at 45°C for 30 minutes to ensure complete dissolution of the solute. The stirring was then turned off, the solution was filtered using a pre-heated vacuum filter and allowed to cool down. Once the temperature reached 25°C, 5 μ L of solution was drawn into a pipette (Eppendorf, Germany) and injected directly into a node of the standing sound wave generated in the levitator. The collection of WAXS and Raman spectra and recording of the droplet images was then started. Once the solvent had completely evaporated, the solid sample was removed from the levitator.

Table 3.2 *Chemical composition of all investigated solutions*

Expt.	#	Solution volume (mL)	Initial supersat. level (σ)	Mass of L-Glu (g)	Crystallisation temp. ($^{\circ}$ C)	Additive	Additive level (ppm)	Additive mass (g)
Nucleation and transformation time measurements (in-house)	1	500	0.5	11.625	35	—	—	—
	2	500	0.6	12.400	35	—	—	—
	3	500	0.7	13.175	35	—	—	—
	4	500	0.8	13.950	35	—	—	—
	5	500	0.9	14.725	35	—	—	—
	6	500	0.5	11.625	35	Glycine	1250	0.007
	7	500	0.6	12.400	35	Glycine	1250	0.008
	8	500	0.7	13.175	35	Glycine	1250	0.008
	9	500	0.8	13.950	35	Glycine	1250	0.009
	10	500	0.9	14.725	35	Glycine	1250	0.009
	11	500	0.5	11.625	35	Glycine	2500	0.015
	12	500	0.6	12.400	35	Glycine	2500	0.016
	13	500	0.7	13.175	35	Glycine	2500	0.017
	14	500	0.8	13.950	35	Glycine	2500	0.018
	15	500	0.9	14.725	35	Glycine	2500	0.019
	16	500	0.5	11.625	35	Glycine	5000	0.030
	17	500	0.6	12.400	35	Glycine	5000	0.032

Nucleation and transformation time measurements (in-house)	18	500	0.7	13.175	35	Glycine	5000	0.034
	19	500	0.8	13.950	35	Glycine	5000	0.036
	20	500	0.9	14.725	35	Glycine	5000	0.038
	21	500	0.5	11.625	35	Glycine	7500	0.044
	22	500	0.6	12.400	35	Glycine	7500	0.047
	23	500	0.7	13.175	35	Glycine	7500	0.050
	24	500	0.8	13.950	35	Glycine	7500	0.053
	25	500	0.9	14.725	35	Glycine	7500	0.056
Growth and transformation (synchrotron- based)	26	500	0.5	16.719	45	—	—	—
	27	500	0.5	16.719	45	Glycine	2500	0.021
	28	500	0.5	16.719	45	Glycine	5000	0.043
	29	500	0.5	16.719	45	Glycine	7500	0.064
Levitated droplet	30	250	saturated solution	2.500	25	—	—	—
	31	250	saturated solution	2.500	25	Glycine	2500	0.003
	32	250	saturated solution	2.500	25	Glycine	10000	0.013
	33	250	saturated solution	2.500	25	L-Alanine	2500	0.004
	34	250	saturated solution	2.500	25	L-Alanine	10000	0.015
	35	250	saturated solution	2.500	25	L-Phenylalanine	2500	0.007
	36	250	saturated solution	2.500	25	L-Phenylalanine	10000	0.028

Chapter 4

Nucleation and polymorphic transformation studies of pure and glycine-doped L-glutamic acid

In this chapter, we show that glycine used as an additive in the crystallisation of polymorphic L-glutamic acid significantly enhances primary nucleation events and hence solution mediated polymorphic transformation rates with respect to the pure system. This previously unreported effect was observed using single-photon laser light scattering and time-resolved concentration monitoring based on in-situ conductivity measurements of the crystallising solution. An attempt has been made to rationalise, to some extent, the observed effects that accompany the time evolution of the overall complexity, with and without the additive. In parallel, we indicate what, in our opinion, is an essential evolutionary set of the crystallisation stages, the nature of events in each of them and their interdependence.

4.1 Polymorphic transformation of L-glutamic acid in the presence and absence of glycine additive

4.1.1 Pure L-glutamic acid solution

The isothermal batch crystallisation of L-glutamic acid solution at 35°C was investigated using solution conductivity monitoring technique (*Section 3.2.1.2*) that produces data that can easily be translated into concentration evolution information, as described in detail in *Section 3.2.6*. The experiment with pure L-glutamic acid at supersaturation $\sigma = 0.5$ was performed first in order to identify the physical meaning of the recorded concentration plots and to establish a reference for comparison with doped systems.

The concentration evolution data from crystallisation of pure L-glutamic acid solution is shown in *Figure 4.1*. The concentration curve that was derived can be divided into four characteristic regions, for convenience denoted by I, II, III and IV.

At the beginning of the experiment the solution was supersaturated and all L-glutamic acid was present in a dissolved form. Hence, the concentration of L-glutamic acid was initially highest. After the circulation pump was started and following the initial nucleation period, a rapid growth of mainly the metastable α -L-glutamic acid, but also small amounts of the stable β form, occurred, resulting in a sudden drop in solution concentration (region I).

In region II of the curve the L-glutamic acid concentration remained almost constant, suggesting that the overall number of dissolved L-glutamic acid molecules did not change significantly throughout that period. At that stage, dissolution of the α form and growth of the β polymorph were simultaneous, i.e. the polymorphic transformation occurred. Since the concentration curve plateau corresponds to the solubility level of the α form, it can be assumed that the dissolution rate of the α form is much faster than the growth of β -L-glutamic acid. Consequently, it is the growth of the β form that is the driving force for dissolution of α -L-glutamic acid. As no conversion between the polymorphic forms of L-glutamic acid was observed in the solid state, the transformation mechanism is thought to be 'solution-mediated'.

After a complete dissolution of the α crystals, the growth of β form continued, resulting in a further decrease in conductivity (region III of the concentration curve). Once the saturation concentration of β -L-glutamic acid was attained, the growth stopped and therefore the curve is seen to flatten out in the last part of the concentration evolution plot (region IV).

Although the temperature on the water bath was fixed, some small fluctuations in the crystallisation temperature occurred at the beginning of the experiment, shortly after the circulation pump was started, due to the contact of solution with both the pump and tubing that were not temperature controlled. Since the recorded temperature fluctuations were well below 0.5°C , their overall effect on the crystallisation process remains negligible. On the other hand, as electrical conductivity is strongly dependent on temperature, the temperature variations were accounted for using the 'temperature compensation' function on the conductivity meter.

Since the duration of the transformation from the less stable α form to the stable β polymorph is approximately equal to the duration of the plateau (region II), using the concentration evolution plot shown in *Figure 4.1*, it was estimated that the polymorphic interconversion for pure solution of L-glutamic acid was equal to 5.25 hours. The α form of L-glutamic acid ceased to exist in solution 4.79 hours after the beginning of the experiment and the

equilibrium concentration with respect to the more stable polymorph was attained after 5.98 hours.

4.1.2 L-Glutamic acid doped with glycine

In order to investigate the effect of glycine on the L-glutamic acid crystallisation process, further experiments at four additive levels, namely 1250 ppm, 2500 ppm, 5000 ppm and 7500 ppm (mol/mol), were performed for the same supersaturation of L-glutamic acid. The concentration evolution curves obtained for the above-mentioned experimental conditions are shown in *Figures 4.2-4.5*.

Unexpectedly, it was observed that between 0 and 7500 ppm of glycine, the polymorphic transformation rate of L-glutamic acid was increased with respect to the pure system. The extent to which the rate of interconversion was promoted was dependent on the concentration of the additive.

The α to β form interconversion time for solutions doped with 1250 and 2500 ppm of glycine was found to be 4.88 hours and 4.38 hours, respectively. The transition time for solution doped with 5000 ppm of the additive was measured to be 4.25 hours. Upon further addition of glycine, at 7500 ppm, the transformation process took only 3.95 hours.

In all four experiments with glycine used as an additive, minor temperature fluctuations were observed during the first few minutes of the experiments until the pump and the piping attained the temperature of solution. However, since the amplitude of the observed variations was below 0.5°C, the fluctuations were assumed to be negligible and consequently the process was considered to be isothermal in all investigated cases.

It has previously been observed that the introduction of various amino acids additives, such as L-phenylalanine, can successfully be applied in order to hinder the polymorphic transformation (Kitamura and Funahara, 1994, Sano et al., 1997, Cashell et al., 2005). Surprisingly and unexpectedly, in this study it was found that doping the L-glutamic acid solution with glycine can result in an increase of polymorphic transformation rate. To date, this fact has not been reported in the literature.

The increase in polymorphic transformation rate suggests that the presence of glycine may enhance the crystal growth rate of β -L-glutamic acid and/or facilitate the dissolution process of the α form. It is likely that growth/dissolution rates of only certain crystal faces are affected while the formation of the others remains unchanged. The actual mechanism of the

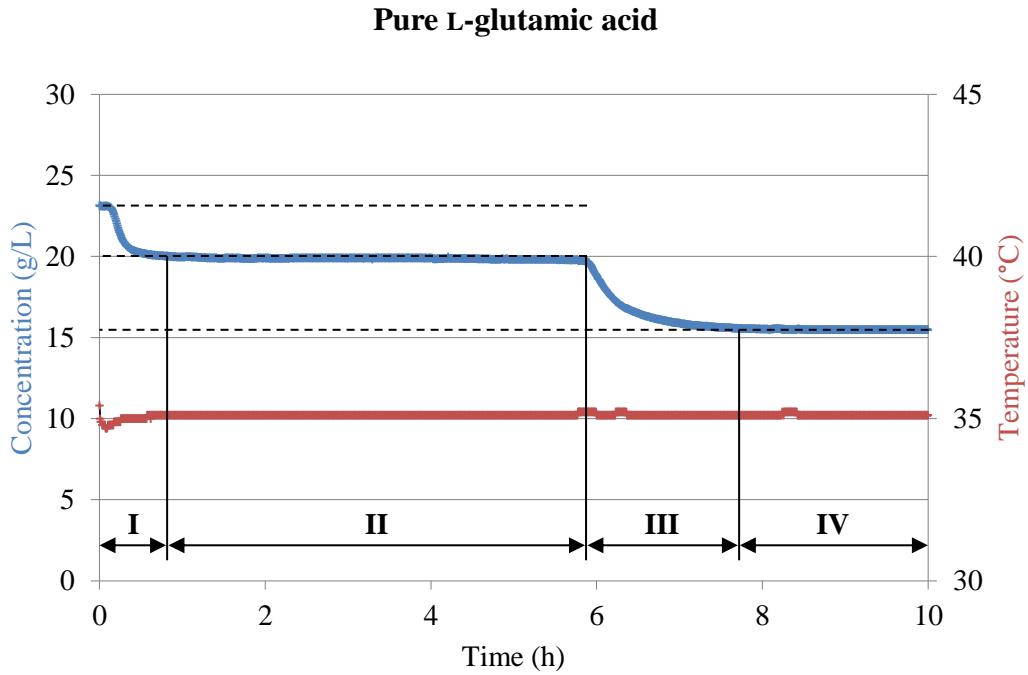


Figure 4.1 Concentration evolution curve for batch crystallisation of pure L-glutamic acid

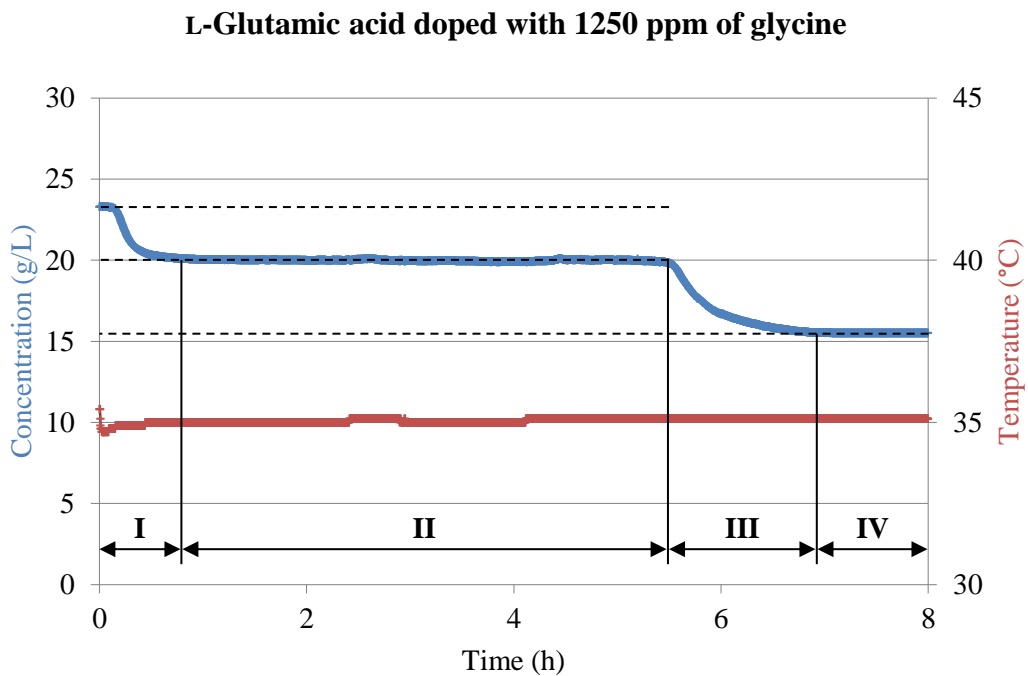


Figure 4.2 Concentration evolution curve for batch crystallisation of L-glutamic acid doped with 1250 ppm of glycine

L-Glutamic acid doped with 2500 ppm of glycine

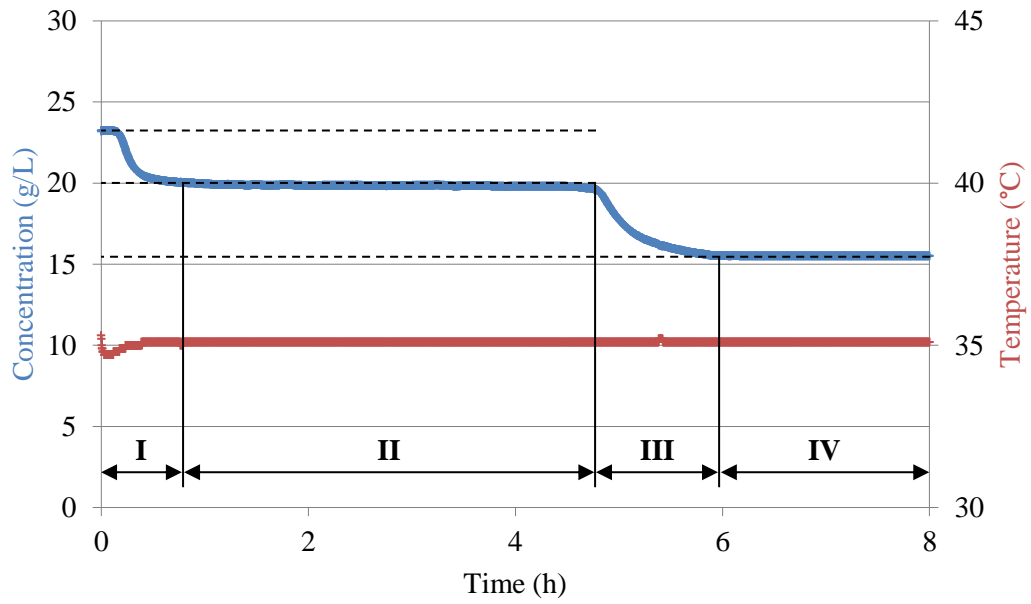


Figure 4.3 Concentration evolution curve for batch crystallisation of *L*-glutamic acid doped with 2500 ppm of glycine

L-Glutamic acid doped with 5000 ppm of glycine

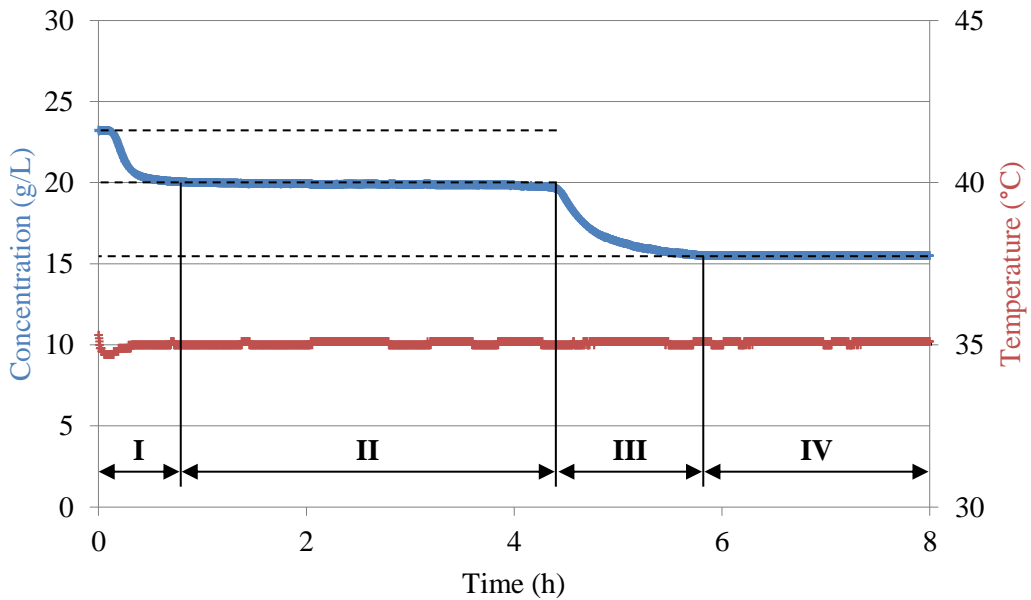


Figure 4.4 Concentration evolution curve for batch crystallisation of *L*-glutamic acid doped with 5000 ppm of glycine

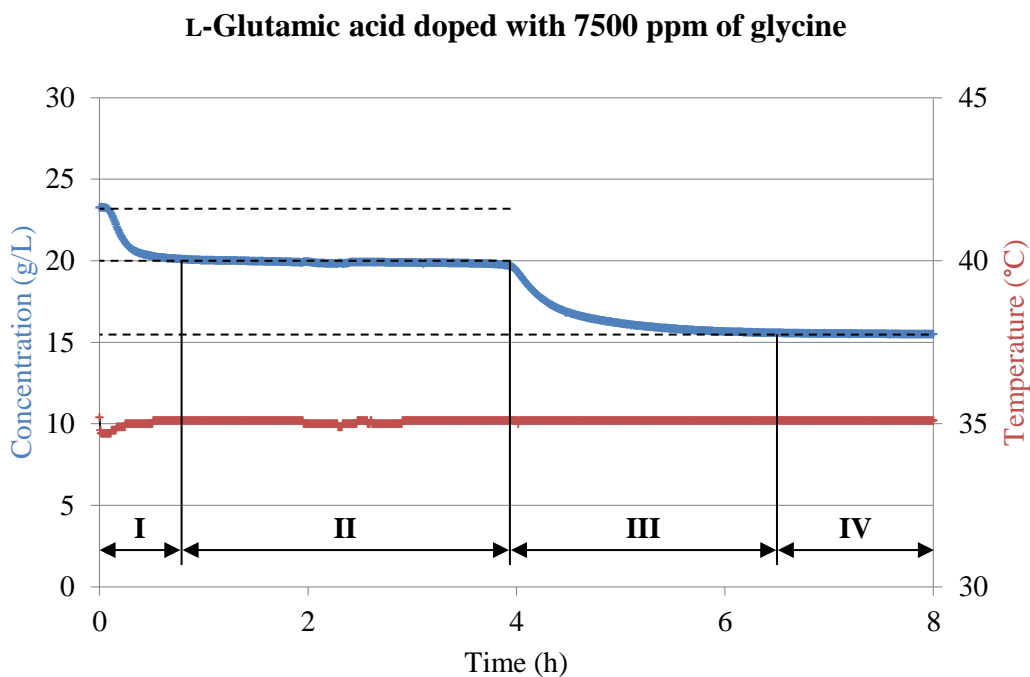


Figure 4.5 Concentration evolution curve for batch crystallisation of *L*-glutamic acid doped with 7500 ppm of glycine

process cannot, however, be determined without further investigation of the process using more advanced techniques such as *in-situ* laser interferometry measurements of crystal faces growth.

Additionally, it was noted that doped solutions where the promoting effect was observed became turbid much earlier than the corresponding solution without glycine, suggesting that the additive may also affect the nucleation stage. The presence of glycine molecules may thus affect the conformation of the hydrated form of *L*-glutamic acid molecules and thus lead to primary nucleation of β -*L*-glutamic acid. Even a small amount of stable β -*L*-glutamic acid would be enough to drive the growth towards that more energetically favoured form and hence increase the polymorphic transformation rate.

While the concentration evolution monitoring technique allows quantitative measurements of the polymorphic transformation time, it was not designed to probe events on a molecular-level and thus cannot be used for investigation of the nucleation phenomena. Therefore, a single-photon laser light scattering technique was employed to investigate the influence of known amounts of glycine additive on the *L*-glutamic acid induction time.

4.2 Nucleation of L-glutamic acid in the presence and absence of glycine additive

4.2.1 The effect of glycine on the nucleation time of L-glutamic acid

A single-photon laser light scattering technique (Kopswerkhoven and Fijnaut, 1981, Dhont et al., 1992) was employed to monitor the isothermal nucleation process from pure and glycine-doped solutions of L-glutamic acid at 35°C. A detailed description of the experimental set-up is given in *Section 3.2.1.1*. Experimental solutions at supersaturations σ between to 0.5 and 0.9 were prepared using the method described in *Section 3.3.1.1*. For each supersaturation level, the nucleation time was measured for pure solution and at various additive levels, namely 1250 ppm, 2500 ppm, 5000 ppm and 7500 ppm (mol/mol). A selection of experimental data from individual experiments is given in *Figures 4.6-4.10* below, whereas a complete set of results is summarised in *Figures 4.11-4.15*.

A laser light was shown through a stirred custom-designed glass cell and the output, which is directly related to the number of scattered photons, was simultaneously recorded. Generally, this time-dependent scattering follows the same pattern irrespective of the additive concentration; the only difference lies in the duration of induction time. The agitated supersaturated solution gives a uniform low-intensity background signal resulting from minor light scattering of solution. At this stage, the clusters that are formed are smaller than the critical nucleus size and hence dissociate. The occasional spikes in the spectrum result from statistical fluctuations due to short sampling time. When the prenuclear clusters become large enough to grow into a thermodynamically stable crystal, the subsequent formation of minute solid bodies in solution leads to increased photon scattering and can be observed as a sudden rise of the signal from the photon counter. The induction time corresponds to the period between the moment when the agitation of supersaturated solution was started and the moment when an appreciable increase in the number of counted photons was detected. The subsequent increase in the number of nucleated crystals results in a further increase of the output signal. As the crystallisation process proceeds, the particle density continues to rise with time and eventually becomes so high that the solution becomes opaque to the laser light and the recorded signal drops to zero.

It was noted that a large scatter in the value of the induction time measured for the same conditions was observed as was expected due to the stochastic nature of the nucleation process (Izmailov et al., 1999). Therefore, in order to reliably assess the effect of the additive

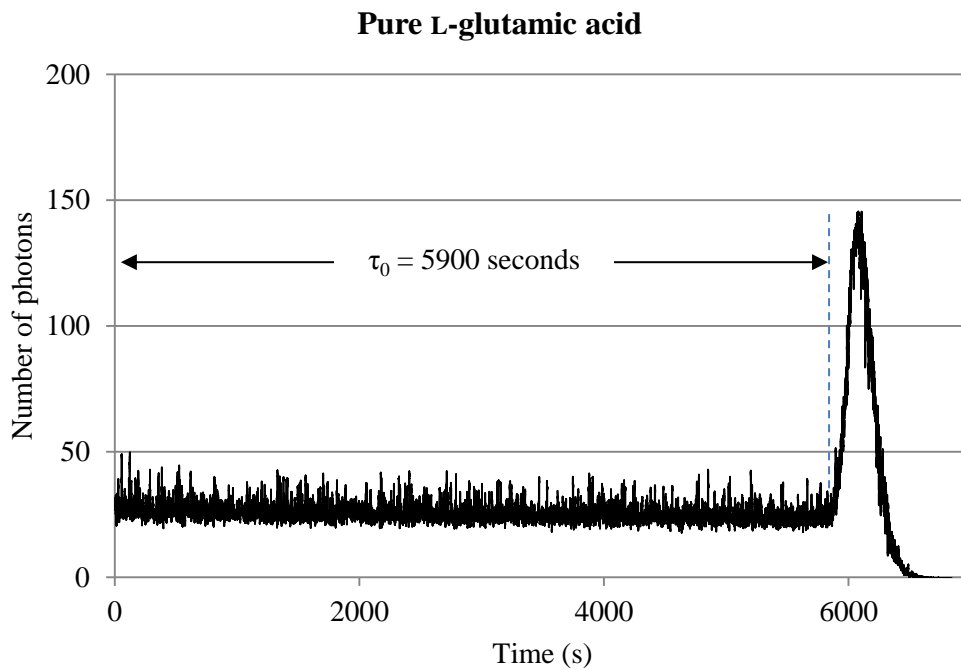


Figure 4.6 Single-photon laser light scattering data on the induction time of L-glutamic acid ($\sigma = 0.5$) obtained in one of the nucleation experiments for pure solution

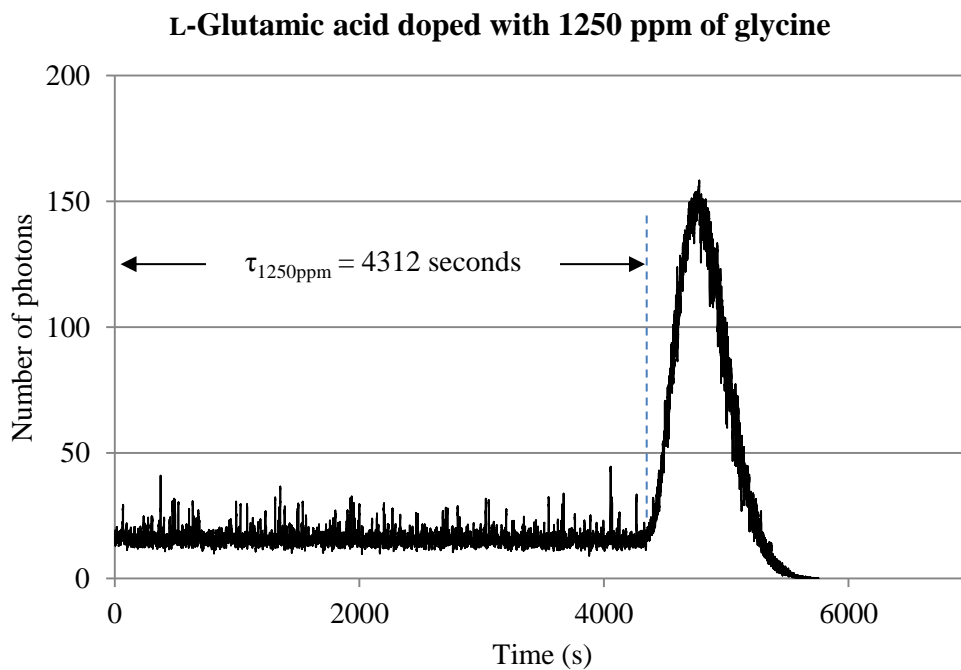


Figure 4.7 Single-photon laser light scattering data on the induction time of L-glutamic acid ($\sigma = 0.5$) obtained in one of the nucleation experiments for solution doped with 1250 ppm of glycine

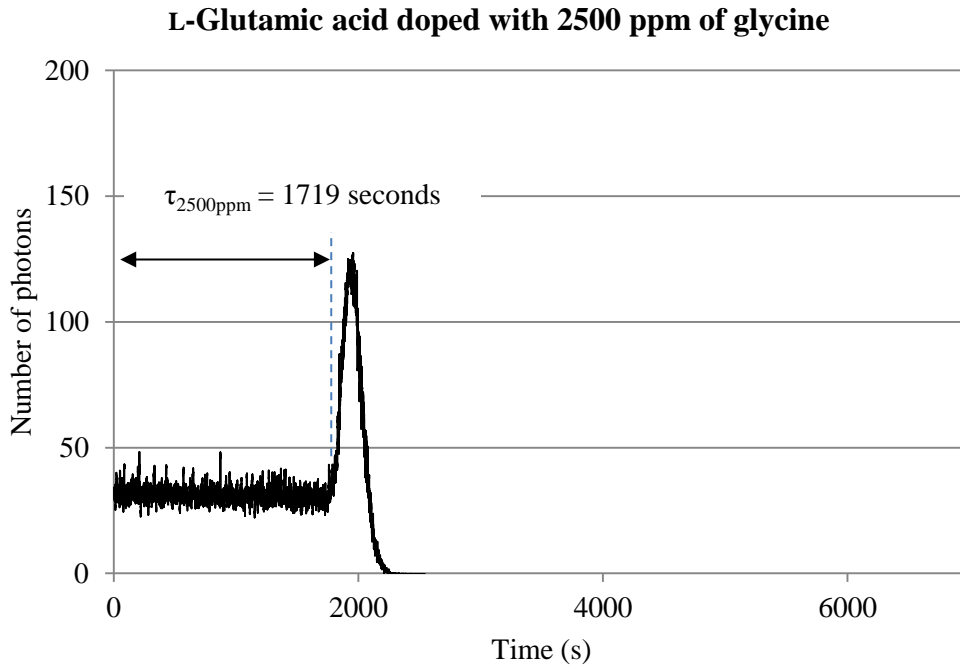


Figure 4.8 Single-photon laser light scattering data on the induction time of L-glutamic acid ($\sigma = 0.5$) obtained in one of the nucleation experiments for solution doped with 2500 ppm of glycine

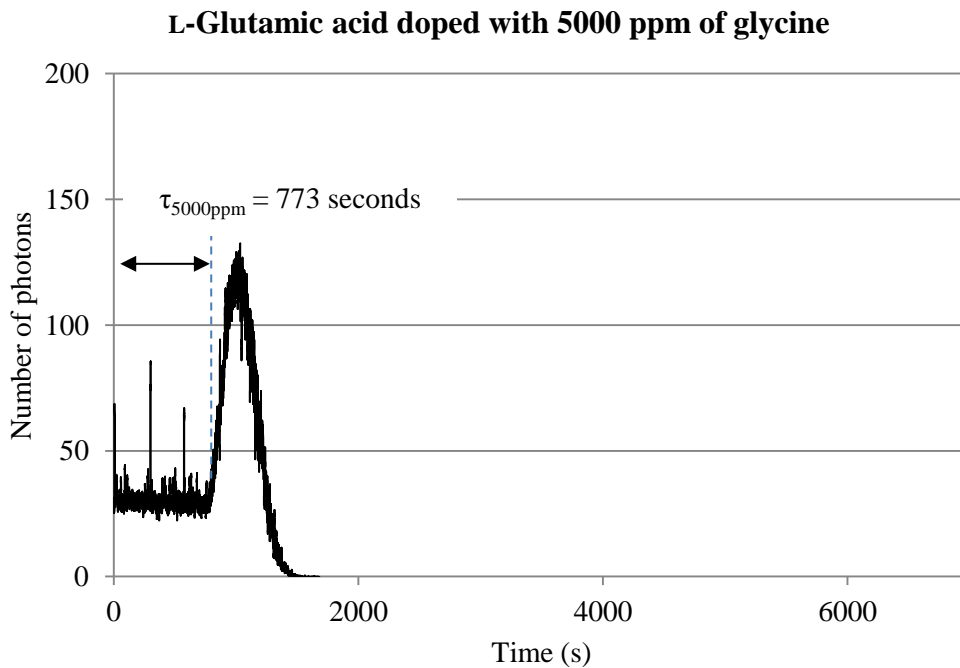


Figure 4.9 Single-photon laser light scattering data on the induction time of L-glutamic acid ($\sigma = 0.5$) obtained in one of the nucleation experiments for solution doped with 5000 ppm of glycine

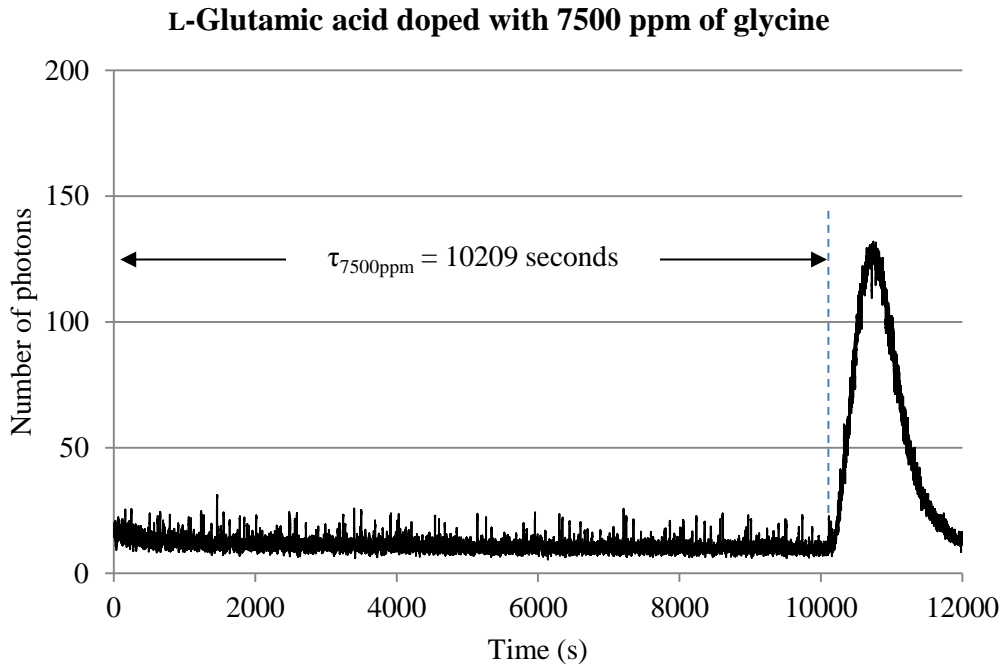


Figure 4.10 Single-photon laser light scattering data on the induction time of L-glutamic acid ($\sigma = 0.5$) obtained in one of the nucleation experiments for solution doped with 7500 ppm of glycine

on the nucleation rate, an average of ten measurements of induction time for a pure solution and for each level of glycine additive was determined.

Unexpectedly, it was found that as the additive concentration was increased, a reduction in the induction time was also observed. The average induction time was measured to be 5780 seconds in pure solution and 4249 seconds in solution doped with 1250 ppm of glycine. An increase in the additive concentration to 2500 ppm and subsequently to 5000 ppm resulted in further reduction of the average nucleation time to only 1840 seconds and 771 seconds, respectively. Since for a given volume of solution, the nucleation rate is inversely proportional to the induction time ($J \propto 1/\tau$) (Van Hook and Bruno, 1949, Nielsen, 1964), the addition of glycine increased the nucleation rate of L-glutamic acid.

4.2.2 The effect of glycine on the surface free energy and critical nucleus radius of L-glutamic acid

Using the data on the nucleation time, τ , as a function of the degree of supersaturation, $S = 1 + \sigma$, plots of $\ln \tau$ against $T^{-3}(\ln S)^{-2}$ can be constructed from which the effect of the additive on the values of surface free energy, γ , and critical nucleus radius, r_{crit} , can be estimated.

As shown in *Equation 1.17*, the slope (m) of the $\ln \tau$ against $T^{-3}(\ln S)^{-2}$ plots can be expressed using the following equation

$$m = \beta \gamma^3 v^2 / k^3 \quad (4.1)$$

Thus, the value of γ for a given additive level is equal to

$$\gamma = \sqrt[3]{m k^3 / \beta v^2} \quad (4.2)$$

Since the critical nucleus radius can be calculated using the following formula

$$r_{crit} = \frac{2 \gamma v}{k T \ln S} \quad (4.3)$$

for a given supersaturation S , the critical nucleus radius is directly proportional to the surface free energy ($r_{crit} \propto \gamma$).

The plots obtained for a range of investigated supersaturation levels and various glycine concentrations are given in *Figures 4.11-4.15* below; the respective slopes were determined using the least squares fit for a line ($y = mx + b$). The calculated values of surface free energies are shown in *Figure 4.16*; the error bars correspond to the standard error returned by the LINEST function in Microsoft Excel.

The value of surface free energy obtained for a pure solution was estimated to be 5.8 mJ/m² and is in good agreement with the values published in the literature (Black and Davey, 1988). The critical nucleus radius calculated for pure solution at $S = 1.5$ was equal to 10.7 Å, which, assuming a spherical nucleus, corresponds to 32 L-glutamic acid molecules. A general decrease in the value of surface free energy and critical nucleus size was noted as the concentration of glycine was increased and for the solution at the same supersaturation doped with 5000 ppm of the additive the values of γ and r_{crit} were reduced to 4.7 mJ/m² and 8.6 Å (i.e. 17 molecules), respectively. This implies that glycine molecules promote formation of L-glutamic acid crystals by lowering the activation energy barrier.

While it has previously been reported that the introduction of various amino acids additives can successfully be applied in order to suppress nucleation of α and β forms of L-glutamic acid (Kitamura and Funahara, 1994), it is the first time when we see the rates of this process being enhanced. At this stage, however, it is not possible to establish which of the two polymorphic forms and to what extent is affected by the presence of the additive. Therefore, further research aimed at understanding the physical mechanism behind the observed effect

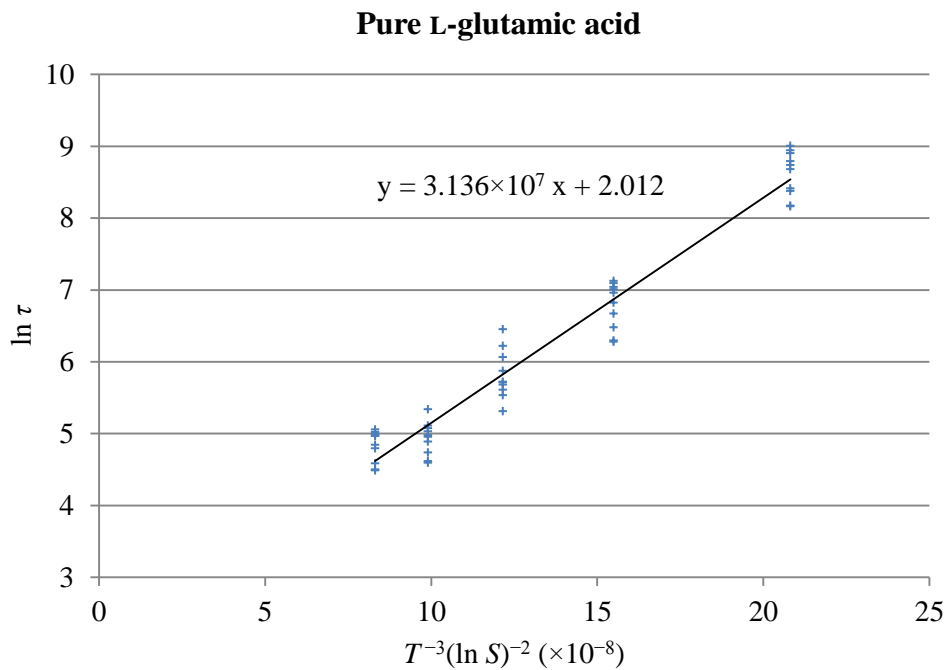


Figure 4.11 Plot of the dependence of $\ln \tau$ on $T^{-3}(\ln S)^{-2}$ obtained for nucleation of pure L-glutamic acid solution

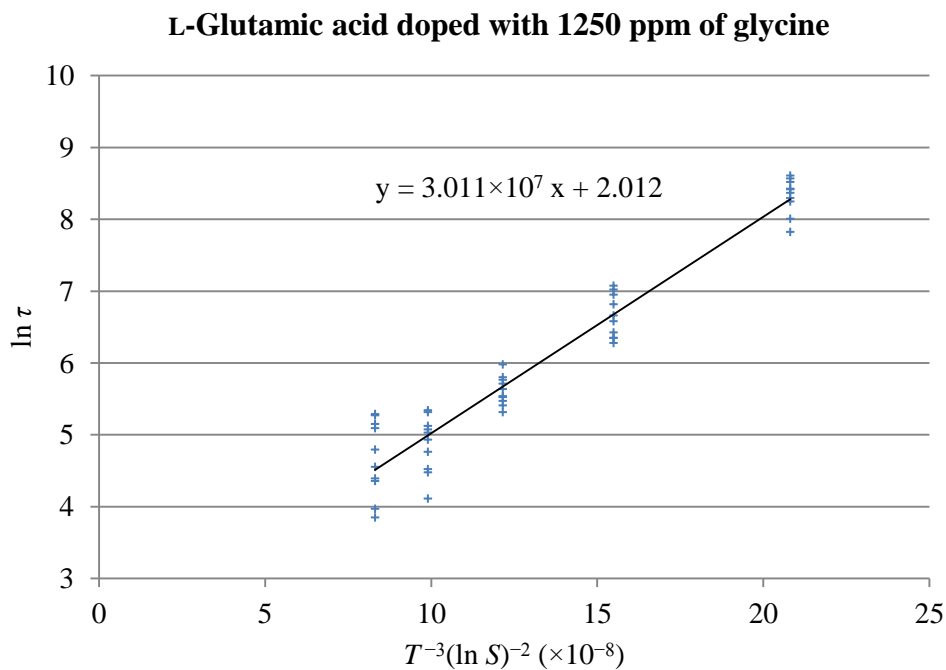


Figure 4.12 Plot of the dependence of $\ln \tau$ on $T^{-3}(\ln S)^{-2}$ obtained for nucleation of L-glutamic acid solution doped with 1250 ppm of glycine

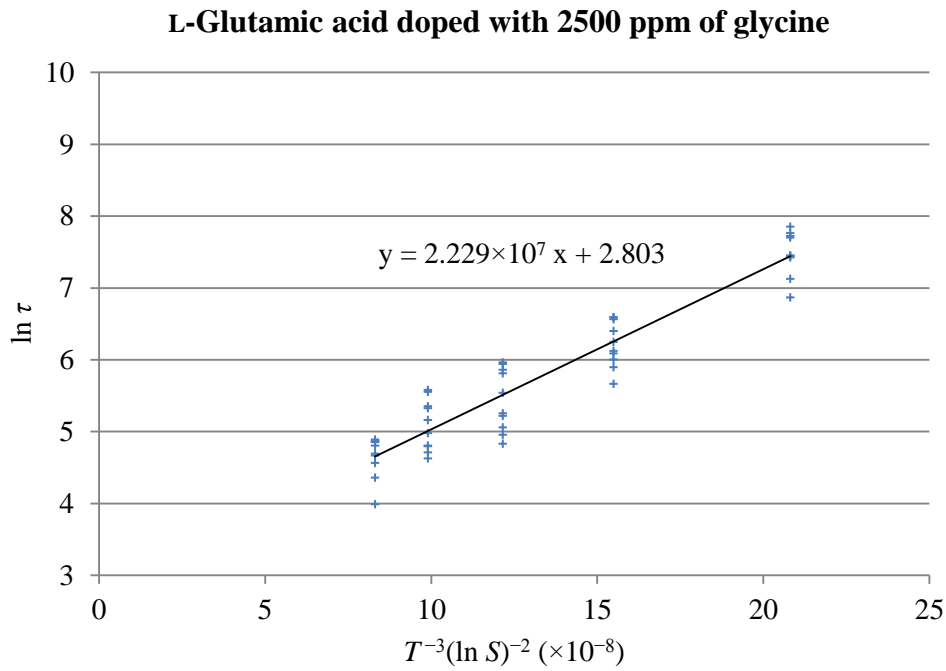


Figure 4.13 Plot of the dependence of $\ln \tau$ on $T^{-3}(\ln S)^{-2}$ obtained for nucleation of L-glutamic acid solution doped with 2500 ppm of glycine

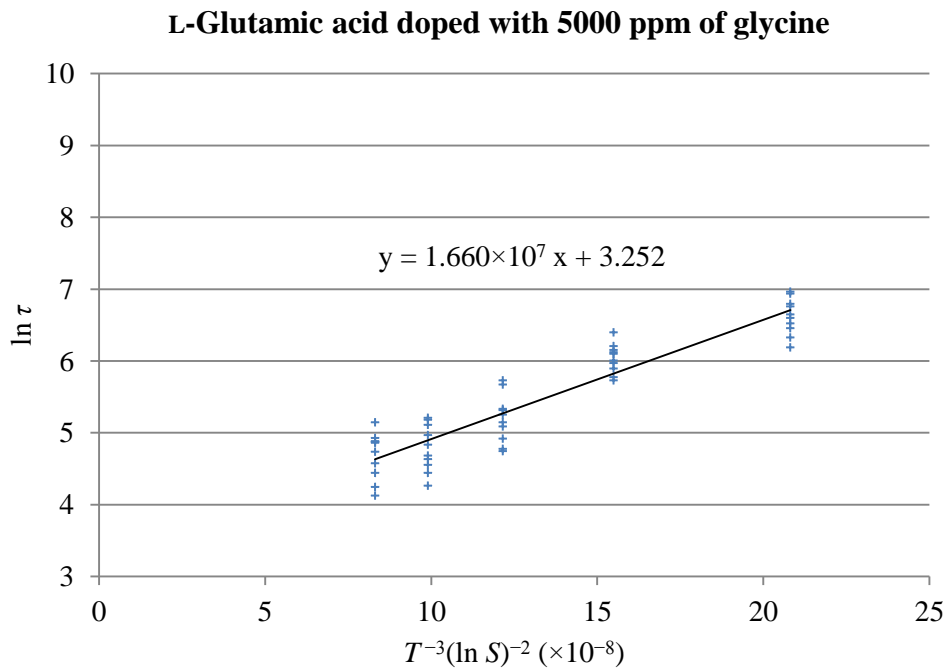


Figure 4.14 Plot of the dependence of $\ln \tau$ on $T^{-3}(\ln S)^{-2}$ obtained for nucleation of L-glutamic acid solution doped with 5000 ppm of glycine

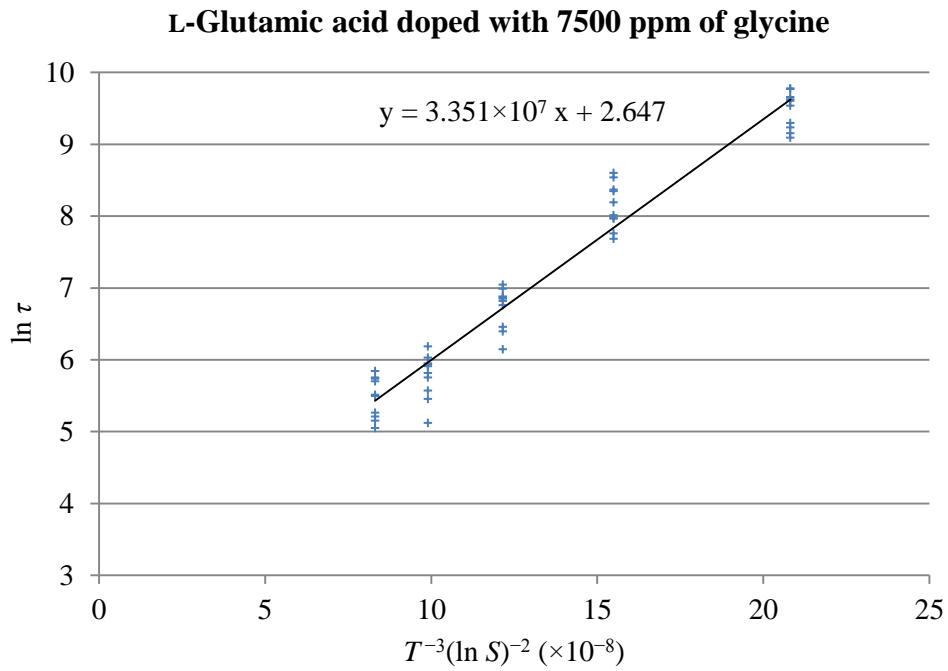


Figure 4.15 Plot of the dependence of $\ln \tau$ on $T^{-3}(\ln S)^{-2}$ obtained for nucleation of L-glutamic acid solution doped with 7500 ppm of glycine

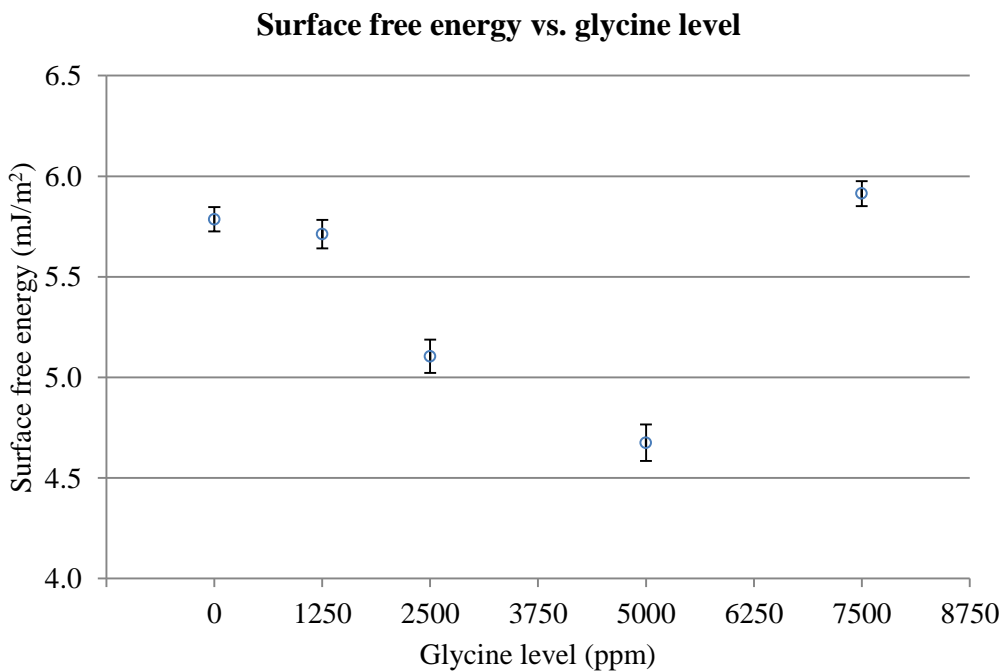


Figure 4.16 Plot of the dependence of surface free energy, γ , on the level of glycine additive

and correlating the nucleation and polymorphic transformation rate enhancements needs to be pursued.

On the other hand, at the highest investigated doping level, i.e. 7500 ppm, it was noted that glycine hinders the nucleation process and the average induction time in the presence of the additive was found to be markedly longer than in the pure solution and the estimated value of γ was increased when compared to the pure solution. It is likely that at high additive concentration glycine molecules act as obstacles in the formation of nuclei of critical size. It is also possible that the additive molecules may become incorporated into some of the growing nuclei and therefore rendering them thermodynamically unstable. As a result, the effective critical nucleus size and the activation energy of the solution containing high levels of glycine would be higher than that of pure solution and the nucleation process would be inhibited.

Since it is generally accepted that molecular modifiers in solution are capable of directing growth morphology, but have only neutral or inhibitory effects on primary nucleation and growth kinetics (Elhadj et al., 2006), and because the nucleation-hindering effect of the additives on crystallisation of L-glutamic acid has already been reported in the literature (Kitamura and Funahara, 1994), further studies presented in this thesis will focus on elucidating the mechanistic insights of the novel promoting effect of glycine and its relation to the polymorphic transformation rate enhancement.

4.3 Scanning Electron Microscopy and High Performance Liquid Chromatography of pure and glycine doped L-glutamic acid samples

Scanning Electron Microscopy was employed to assess visually any possible effect of the additive on the growth behaviour of L-glutamic acid crystals and its potential link to the data presented in *Sections 4.1* and *4.2*. For this purpose, crystalline samples were collected from pure and glycine-doped solutions at equal periods of time, after the crystallisation process began (the beginning of region I in *Figures 4.1* and *4.3*), i.e. before the polymorphic transformation started to occur. As L-glutamic acid is a non-conducting material, the samples were sputter coated with a 20 nm layer of gold using an EmScope Sputter Coater SC-500A (Ashford, England). Scanning Electron Micrographs were taken using Philips XL30 SEM (Netherlands). In both samples, three typical features of the crystalline particles were observed (*Figure 4.17*):

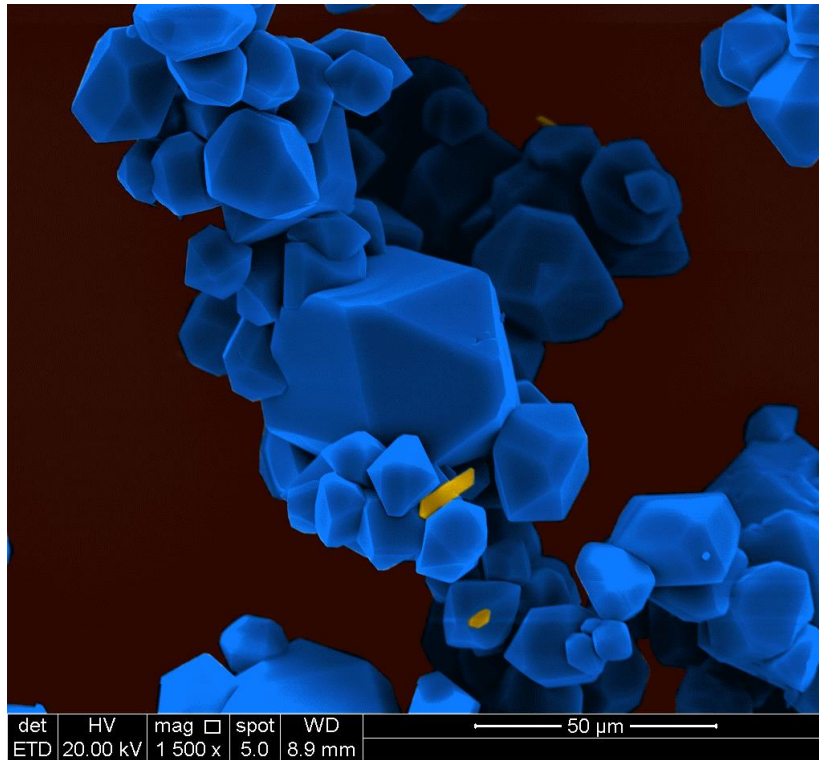
- (i) Almost entirely dominant prismatic shape of α -LGA particles with small traces of needle-like β crystals;
- (ii) An appreciably larger number and average size of β in the glycine-doped sample compared to their counterparts in a pure solution;
- (iii) No noticeable morphological changes of the two forms, regardless of the growth media.

To establish the amount of the additive that is incorporated into the growing crystal lattice, High Performance Liquid Chromatography analysis was carried out using a reversed phase Waters 2695 HPLC system equipped with a Waters 2487 UV absorbance detector at 254 nm. Phase separation was performed using Waters Symmetry Shield RP18 3.5 μ m chromatographic column with a mobile phase of water and acetonitrile (97:3 v/v, flow rate of 1.0 mL/min). It was confirmed that, in all samples grown from doped solutions, the level of glycine being incorporated was less than 1.5%. It is, therefore, unlikely that such a low level of incorporation would be entirely responsible for the observed effect and markedly affect the behaviour of the subsequent crystallisation stages.

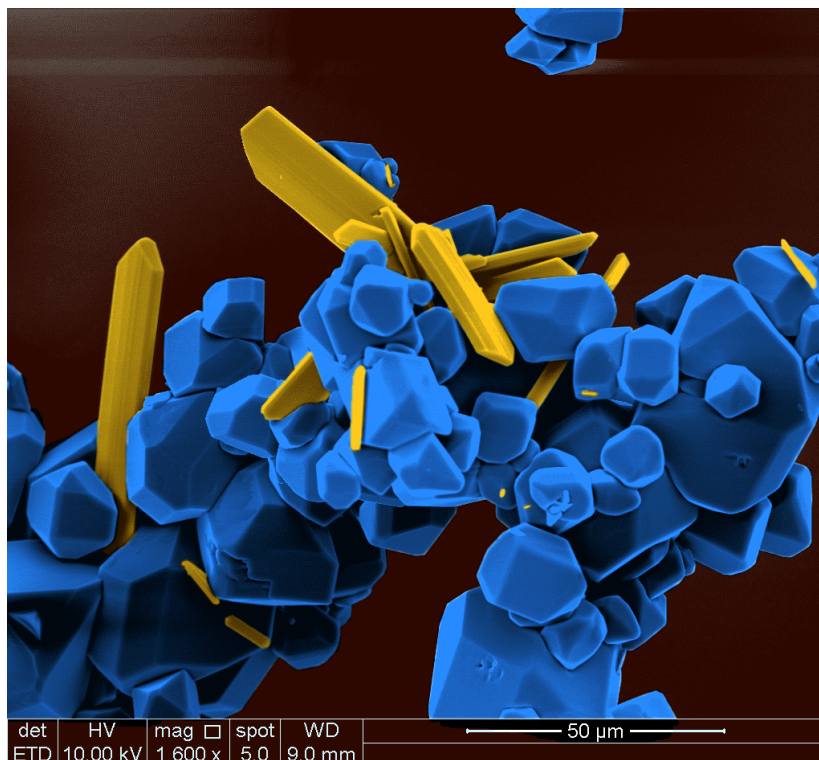
4.4 Discussion

In spite of the fact that in the presence of glycine α was still the principal crystallisation product, there is no experimental evidence that the observed β polymorph nucleation-promoting effect (*Figure 4.17b*) can be solely attributed to the substantial (over three-fold) decrease in the induction time. We do not know which of the two forms is triggered to nucleate first because the applied scattering technique does not differentiate between the polymorphic forms. It is, however, reasonable to assume that glycine molecules accelerate the overall nucleation rate of both α and β forms of L-glutamic acid (*Figures 4.1-4.4* and *4.17*). To account for the observed macroscopic effects brought into play by glycine is rather limited because the molecular-level processes involved are not fully accessible not only to this technique, but also to any other scattering techniques (Burton et al., 2010).

The overall increase of the nucleation rate in the presence of glycine can be rationalised to a certain extent by using quite recently proposed ‘rules for additives that modulate crystal nucleation’ (Anwar et al., 2009). According to the generic rules based on molecular simulations, the promotion of nucleation rate is generally possible and could be considered fast if additive exists as a dimer with the effective size smaller than solute and shows



(a)



(b)

Figure 4.17. SEM images of samples extracted shortly after the crystallisation process was started, i.e. at the beginning of region I: (a) crystallisation without glycine and (b) with 2500 ppm of glycine as an additive. α - and β -L-glutamic acid crystals are indicated in blue and yellow, respectively.

a relatively weak degree of affinity for the solute and solvent particles. A comparison of these criteria with the markedly increased nucleation rate of L-glutamic acid in the presence of the additive suggests that the enhancement of the nucleation process (*Figures 4.6-4.10*) is likely to be caused by the existence of such dimers that confine themselves entirely to the interface and are able to promote nucleation but not inhibit the process (Anwar et al., 2009). However, the design rules do not provide any information about the reasons that may lead to an increase in the nucleation rate of a particular polymorph. In addition, it has recently been reported that glycine exists mainly as monomers (Huang et al., 2008), not dimers (Weissbuch et al., 2005), in supersaturated aqueous solutions. At this stage, we argue that the enhanced nucleation of β (*Figure 4.17b*) may be due to a catalytic role of glycine monomers in the nucleation process.

Generally, when two solutes are dissolved in water, their solvation free energy can depend on their relative positions. This dependence may well be due to the structural change of the hydrogen-bonding network of water around one solute being perturbed by the presence of the other solute (Chandler and Varilly, 2012). Applying this approach to glycine-doped L-glutamic acid implies that there is a probability that molecular dynamics of the solvated monomers may provide a limited range of interactive configurations, with specific values of the electric field generated by the two solutes, at which the initial β conformed cluster could be created. However, without further studies, notably the structural changes of the solution caused by different levels of the additive, we cannot provide deeper insights into the nature of the observed nucleation effects. To investigate the structural response of L-glutamic acid solution imposed by different levels of glycine, combined neutron scattering experiments and modelling techniques are required (Soper, 1996, Soper, 2001, McLain et al., 2006).

A marked reduction in the polymorphic transformation time in the presence of glycine (*Figures 4.1-4.5*) suggests that this process is likely to be caused by a distinguishable increase in the number and average size of β particles (*Figure 4.17b*) promoted by the additive in region I. The former is a result of the glycine-stimulated nucleation whereas the latter suggests that the additive may also enhance the growth rate of these crystals. Generally, for the most insightful information on the influence of different levels of an additive on the growth rate behaviour of a crystal as a whole, the normal growth rates of all habit faces need to be measured separately and accurately using most advanced techniques, e.g. *in-situ* laser interferometry or atomic force microscopy. Once the equilibrium of the metastable α is achieved, these crystals will begin to dissolve due to the continuation of the growth of the

existing β particles (Kitamura, 1989). Initially, the dissolution of α particles will commence at the energetically preferential crystal sites – the locally stressed fields at screw/mixed dislocation outcrops on its facets. The conditions under which some of these localities will be selectively activated for etching are likely to depend on the level of stress field, i.e. the corresponding critical undersaturation, $|\sigma^*|$ (Vanderhoek et al., 1982), and the time needed for increasing undersaturation, $|\sigma(t)|$, to achieve and surpass this barrier. The higher the stress field, the lower the barrier (Cabrera et al., 1954). Bearing in mind that the rate of undersaturation evolution, $d|\sigma(t)|/dt$, is proportional to the overall growth rate, $R_{ov}(t)$, of primary induced β crystals, *Figure 4.17* suggests that these two strongly coupled processes will be appreciably faster for the glycine-doped solution than those induced by their counterparts in the pure solution (smaller number and size of primary β). It is reasonable to assume that a higher rate of undersaturation does not only shorten the time required to achieve and surpass the critical barrier for an etch pit dissolution, but also may activate more etch pits of weaker stress fields (Bennema and Vanenckevort, 1979, Vanenckevort and Vanderlinden, 1979). The most susceptible faces for etching of an α crystal are likely to be those with fast growth rates. Since these rates are directly proportional to the power and density of growth step generators (surface densities of screw/mixed dislocations outcrops) (Chernov, 1989), the related faces should have small areas (low morphological importance, MI). According to the kinetics and MI of a single α crystal (Kitamura and Ishizu, 2000), these faces are either $\{011\}$ or $\{111\}$. We suggest that it is these faces on which an early formation of etch pits and the consequent nucleation and growth of secondary β occurs due to a local increase of concentration with respect to β equilibrium. This proposal seems to be in good agreement with SEM observations of needle-like β crystals on these surfaces (*Figure 4.18*) (Cashell et al., 2003a, Ferrari and Davey, 2004). Due to the fact that at the initial stage of polymorphic transformation a huge number of these faces is simultaneously exposed to etching, it is not surprising that a small increase of primary β and their average size (growth rate) (*Figure 4.17b*) can considerably amplify the overall dissolution/growth process of the two forms and hence reduce the transformation time (*Figures 4.7-4.9*). In other words, the values of these two factors at the transient point (the beginning of region II, where α starts dissolving), can be considered as the initial conditions for solution mediated polymorphic transformation which play a critical role in defining the duration of this process.

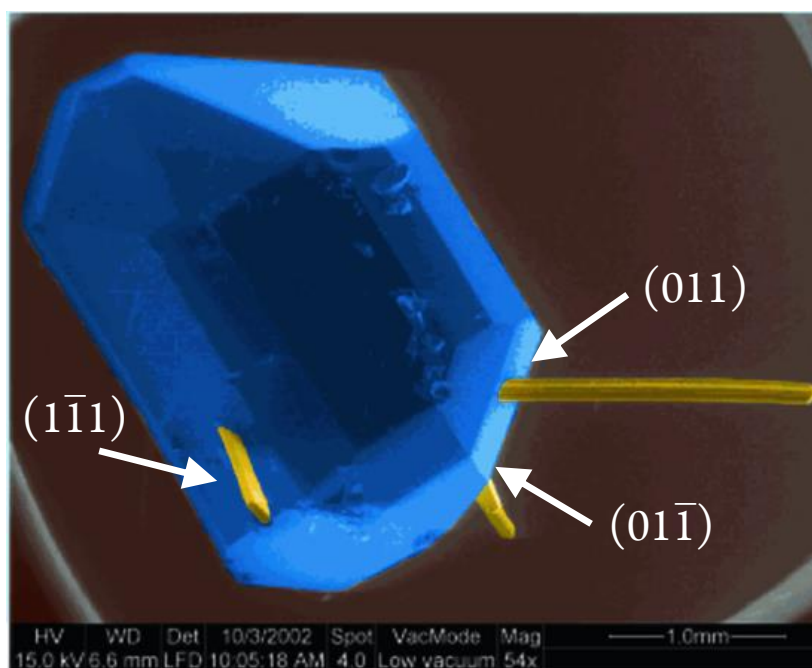


Figure 4.18. SEM image of β crystals growing on the $\{011\}$ and $\{111\}$ type faces of α -L-glutamic acid as a result of secondary nucleation of the more stable polymorph in region II. Image adapted from Ferrari and Davey (2004).

4.5 Conclusions

In summary, a study of nucleation and polymorphic transformation of L-glutamic acid with and without glycine as an additive, presented in this work, shows that both processes are accelerated in the additive range between 0 and 5000 ppm. In addition, it was found that the two are strongly correlated; the more additive promoted primary nucleated β crystals and the faster their growth, the more secondary nucleated β crystals on α surfaces and hence the shorter the polymorphic transformation time. These serendipitous findings suggest that an enhancement of the transformation rate from a metastable to a stable form is feasible when an additive promotes a primary nucleation rate of a stable polymorph, and either has a negligible or enhancing effect on its overall growth rate. Also, we defined a set of most critical issues that we believe need to be addressed in order to get a full appreciation of the complexity of the observed phenomena. Generally, such comprehensive insight may contribute to an improved understanding of diverse polymorphic systems and open the routes for design of new synthetic nucleation/growth modulators. Because of the remarkable effects and intricacies that have emerged in this work, the most general strategy to advance the knowledge in the newly open research avenues would be to treat each issue separately – with great care.

Chapter 5

Evolutionary behaviour of the polymorphic mole fractions during crystallisation of pure and glycine-doped L-glutamic acid

In order to understand the mechanism behind the transformation-promoting effect presented and discussed in Chapter 4, the mole fraction evolutions of the two polymorphs of L-glutamic acid during batch crystallisation of pure and glycine-doped solutions were investigated using synchrotron WAXS technique. Quantitative analysis of the obtained data confirmed that the presence of the additive leads to stimulated nucleation of primary β crystals. The observed effect is in good agreement with the hypothesis postulated earlier and implies the latter is, indeed, the key factor contributing to the enhancement of the polymorphic transformation rate.

5.1 WAXS as a tool to monitor the mole fraction evolutions of the crystallising L-glutamic acid

5.1.1 Evidence of the effect of the additive

The evolution of mole fractions of polymorphs of L-glutamic acid during batch crystallisation from supersaturated solution was examined using time-resolved Wide-Angle X-ray Scattering (WAXS) at BESSY II synchrotron (Berlin, Germany). The experiments were performed isothermally at 45°C and initial supersaturation (σ) equal to 0.5, corresponding to 33.75 g/L, for pure solution of L-glutamic acid and in the presence of glycine additive at three doping levels, namely 2500 ppm, 5000 ppm and 7500 ppm (mol/mol). In addition to the scattering data, the conductivity of solution was also recorded in order to readily assess the extent of the crystallisation process during the experiments. The experimental apparatus is described in detail in *Section 3.2.1.3*.

The typical WAXS spectra recorded as a function of time during crystallisation of supersaturated L-glutamic acid solution in the absence and presence of glycine are given in *Figures 5.1* and *5.2*, respectively.

The preliminary inspection of the recorded scattering spectra allows qualitative evaluation of the crystallisation process and reveals the characteristic features that distinguish the process at the two investigated conditions:

- (i) In the presence of glycine, the α polymorph achieves its maximum concentration, begins to dissolve and eventually ceases to exist earlier than in a pure solution, suggesting that the additive enhances the polymorphic transformation rate.
- (ii) Moreover, the additive stimulates the growth of the β phase and leads to quicker attainment of the maximum concentration of the latter, i.e. the equilibrium with respect to the liquid phase.

The above observations are in a good agreement with the conclusions made in *Section 4.4* and, indeed, confirm that glycine used as an additive has a promoting effect on both the α - to β -L-glutamic acid transformation rate but also enhances crystallisation of the more stable polymorph. However, in order to obtain quantitative information on the mole fraction evolutions of the two polymorphs and consequently get a deeper insight into the mechanism of the promoting mechanism of glycine, a more in-depth analysis of the data is required.

5.1.2 Assessment of the mole fraction evolutions

A batch crystalliser is a thermodynamically closed system where the total number of moles of L-glutamic acid remains constant throughout the experiment. The law of conservation of mass can thus be used to quantify the crystalline mole fraction evolutions of each of the two polymorphs and mole fraction evolution of the material dissolved in solution.

$$m_{\alpha}(t) + m_{\beta}(t) + m_{solution}(t) = m_{initial} \quad (5.1)$$

Where $m_{\alpha}(t)$ and $m_{\beta}(t)$ are the mass evolutions of the crystallised α and β polymorphs, $m_{solution}(t)$ is the mass evolution of the dissolved material, and $m_{initial}$ is the total mass of L-glutamic acid that was initially dissolved during preparation of the experimental solution.

Both sides of the above equation can be divided by the molar mass of L-glutamic acid and hence be expressed in terms of moles:

$$n_{\alpha}(t) + n_{\beta}(t) + n_{solution}(t) = n_{initial} \quad (5.2)$$

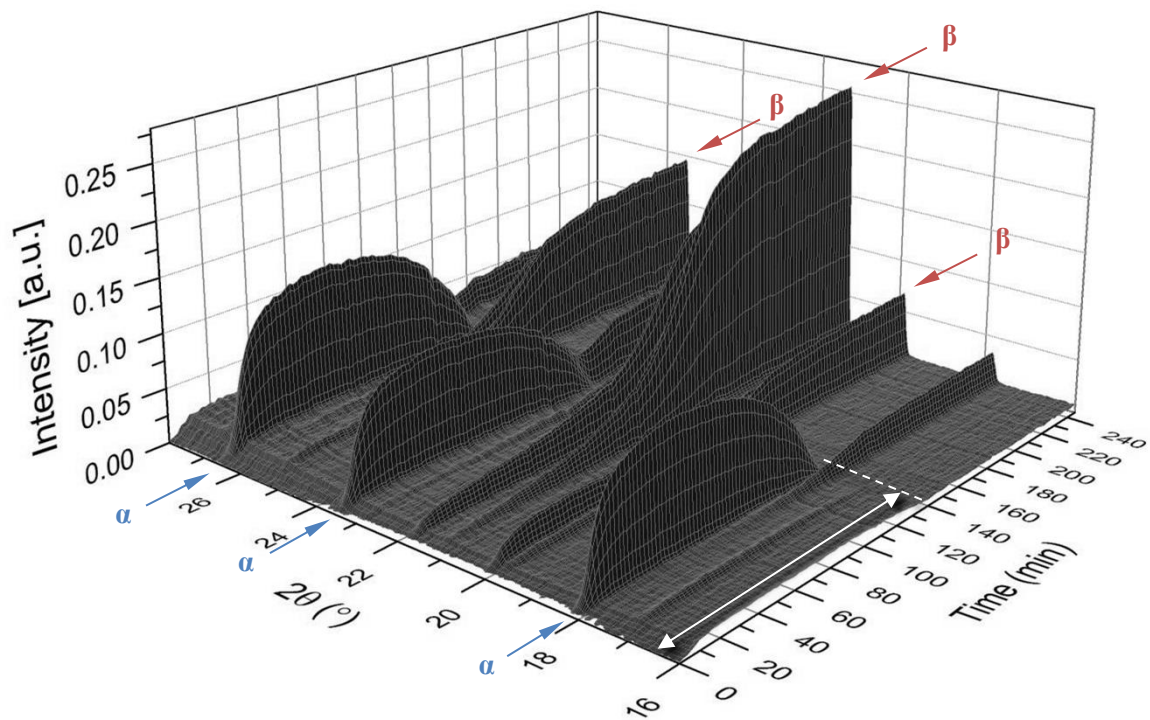


Figure 5.1 Time-resolved WAXS spectra of L-glutamic acid crystallising from pure solution

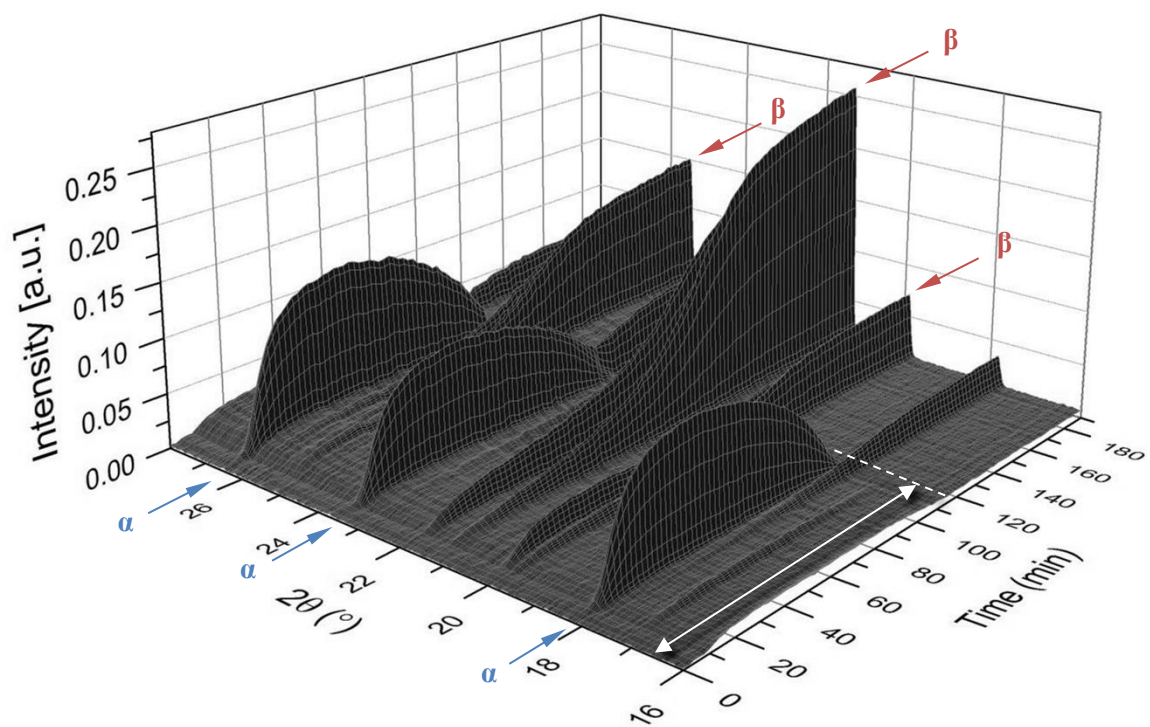


Figure 5.2 Time-resolved WAXS spectra of L-glutamic acid crystallising from solution doped with 5000 ppm of glycine

Thus,

$$n^f_{\alpha}(t) + n^f_{\beta}(t) + n^f_{solution}(t) = \frac{n_{\alpha}(t)}{n_{initial}} + \frac{n_{\beta}(t)}{n_{initial}} + \frac{n_{solution}(t)}{n_{initial}} = 1 \quad (5.3)$$

The scattering intensity of the X-ray beam is proportional to the mass of the corresponding species in the irradiated sample. Additionally, since the intensity is proportional to the area under the diffraction peak (Cullity and Stock, 2001), the following relationships can be written for the two phases of L-glutamic acid:

$$m_{\alpha} \propto I_{\alpha} \propto A_{\alpha} \quad (5.4)$$

$$m_{\beta} \propto I_{\beta} \propto A_{\beta} \quad (5.5)$$

The corresponding proportionality constants, k_{α} and k_{β} , can now be introduced:

$$m_{\alpha} = k_{\alpha}A_{\alpha} \quad (5.6)$$

$$m_{\beta} = k_{\beta}A_{\beta} \quad (5.7)$$

The number of moles of L-glutamic acid in the irradiated section of the flow cell is proportional to the total number of moles in solution with the proportionality parameter K :

$$n_{total} = Kn_{window} \quad (5.8)$$

Where K is the ratio of the total volume of solution to the volume of solution irradiated in the cell. Because of low solubility of L-glutamic acid, the change in the total volume of solution during the crystallisation process is negligible and the value of K can be assumed to be constant.

Therefore, at any time t , the number of moles of each of the crystallised polymorphs can be expressed as:

$$n_{\alpha}(t) = \frac{k_{\alpha}KA_{\alpha}(t)}{k_{\alpha}KA_{\alpha,max}} n_{\alpha,max} = \frac{A_{\alpha}(t)}{A_{\alpha,max}} n_{\alpha,max} \quad (5.9)$$

$$n_{\beta}(t) = \frac{k_{\beta}KA_{\beta}(t)}{k_{\beta}KA_{\beta,max}} n_{\beta,max} = \frac{A_{\beta}(t)}{A_{\beta,max}} n_{\beta,max} \quad (5.10)$$

Where $n_{\alpha,max}$ and $n_{\beta,max}$ correspond to the number of moles of the crystallised material at equilibrium levels and can be determined from the solubility diagram.

Substituting *Equations 5.9* and *5.10* into *Equation 5.3* gives:

$$\begin{aligned} n^f_{\alpha}(t) + n^f_{\beta}(t) + n^f_{solution}(t) \\ = \frac{A_{\alpha}(t) n_{\alpha,max}}{A_{\alpha,max} n_{initial}} + \frac{A_{\beta}(t) n_{\beta,max}}{A_{\beta,max} n_{initial}} + \frac{n_{solution}(t)}{n_{initial}} = 1 \end{aligned} \quad (5.11)$$

Three peaks characteristic to the α form (at 2θ of 18.26° , 23.66° and 26.66°) and three peaks unique to the β polymorph (at 2θ of 21.44° , 22.05° and 25.62°) were integrated in each spectrum. The baseline was defined based on a series of anchor points on both sides of the respective peak and was subsequently subtracted from the collected spectrum. The Peak Analyzer module of the OriginPro software package was used to integrate the area under the peaks. The obtained numerical data was then used to calculate the time evolutions of the mole fractions of the two polymorphs, n^f_{α} and n^f_{β} .

The mole fraction evolution of the number of moles of L-glutamic in solution, $n^f_{solution}$ can now be calculated using the rearranged *Equation 5.11*:

$$n^f_{solution}(t) = 1 - n^f_{\alpha}(t) - n^f_{\beta}(t) \quad (5.12)$$

Since solution conductivity was also recorded throughout the experiments, the latter can alternatively be derived from the molar concentration evolution data, $c_{solution}(t)$, using the following formula:

$$n^f_{solution}(t) = \frac{c_{solution}(t) \times V_{crystalliser}}{n_{initial}} \quad (5.13)$$

The mole fraction evolutions of dissolved L-glutamic acid calculated using *Equations 5.12* and *5.13* are given in *Figure 5.3* and show nearly identical behaviour, confirming the validity of the adopted approach.

It should also be noted that the recorded WAXS peaks result from X-rays scattered over the sampling time. Since every second hundreds of crystals of different size flow through the cell, the statistical fluctuations of the data are inherently included in the recorded spectra. In other words, each peak is a measure of the average signal over the exposure time. Consequently, it is not possible to quantitatively assess the experimental uncertainty. Moreover, even though great care was taken during determination of peak areas, some measurement errors could arise during the integration process, especially for peaks of low intensity that cannot be easily distinguished from the fluctuating background signal.

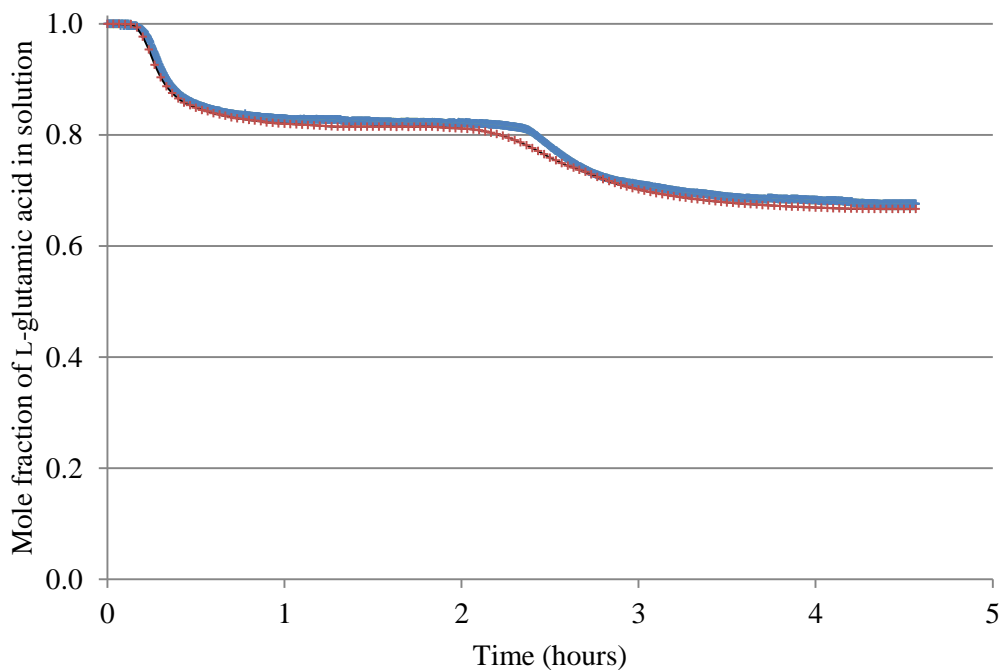


Figure 5.3 Mole fraction evolution of dissolved L-glutamic acid determined using two independent methods: from conductivity data (blue) and from WAXS data (red)

Nevertheless, since there are only a few spectra in which such peaks were integrated, i.e. at the initial stage of the crystallisation process and when the metastable form ceases to exist, the magnitude of the possible measurement error is likely to be negligible and thus a reliable quantitative analysis of the overall evolution of the crystallisation process can be performed.

5.2 Mole fraction evolutions of α and β polymorphs during crystallisation of the pure and glycine-doped solutions of L-glutamic acid

The method described in *Section 5.1.2* was used to quantitatively evaluate the mole fraction evolutions of the two polymorphic phases and the evolution of the mole fraction of L-glutamic acid in solution. The corresponding evolutions and the plots showing geometrical derivations of the rates of change of these evolutions for pure solution and solutions doped with 2500 ppm, 5000 ppm and 7500 ppm of glycine are shown in *Figures 5.4-5.11*, respectively.

The obtained data indicates that the mole fraction evolutions of the two crystallised phases and the evolution of the solution composition are strongly coupled. This implies that the time development of the latter is heavily dependent on the crystallisation/dissolution evolutions of

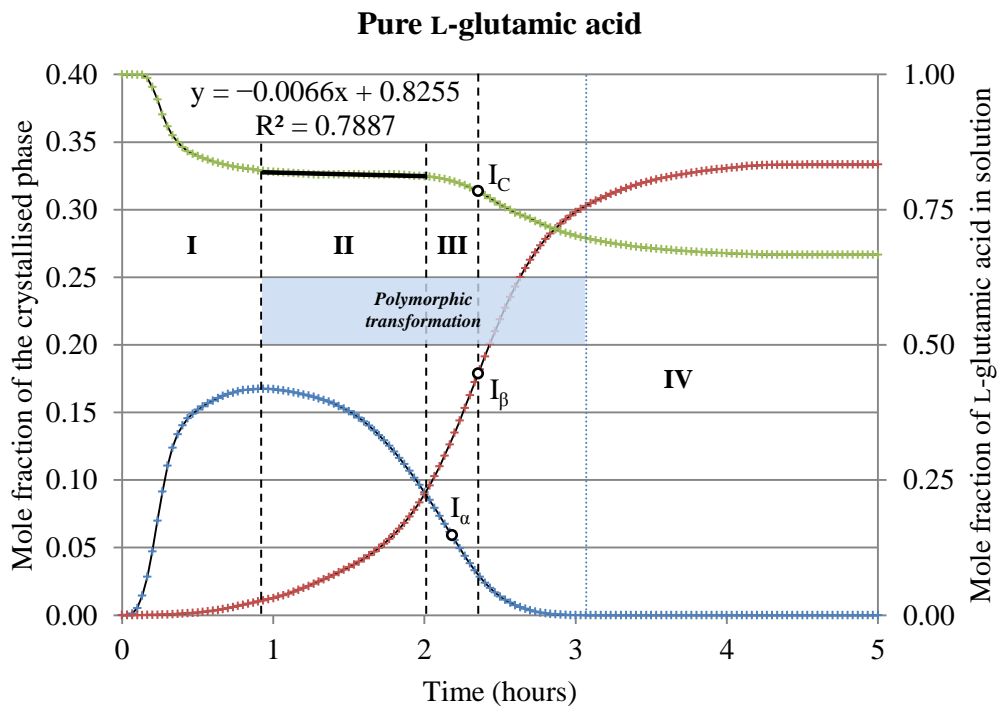


Figure 5.4 Mole fraction evolutions of the crystallised phases and dissolved L-glutamic acid determined for pure solution (blue – α , red – β , green – L-glutamic acid in solution)

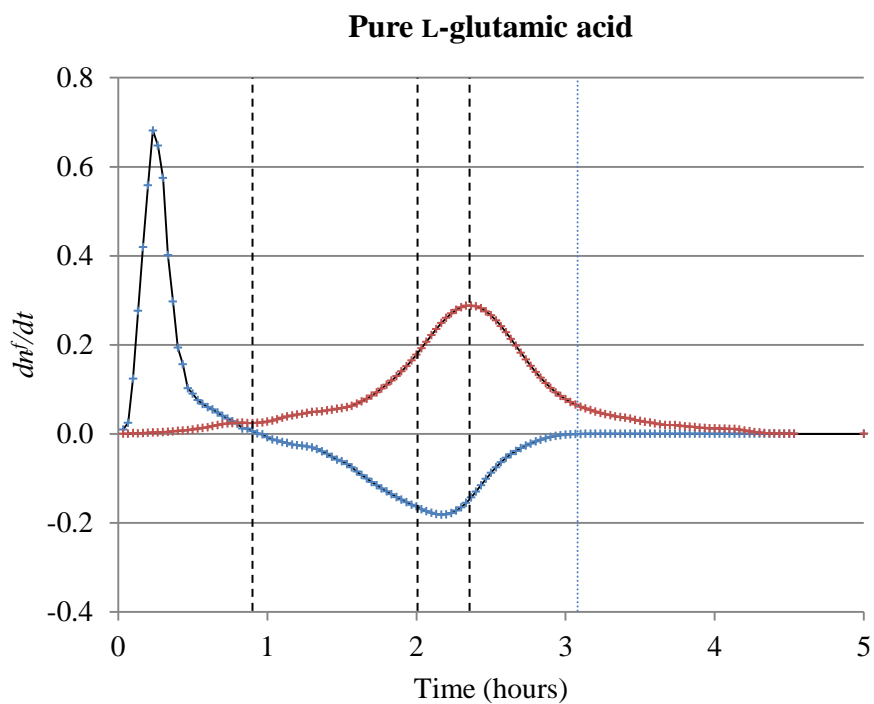


Figure 5.5 The rate of change (first derivative) of mole fraction evolutions of the crystallised phases of L-glutamic acid determined for pure solution (blue – α , red – β -L-glutamic acid)

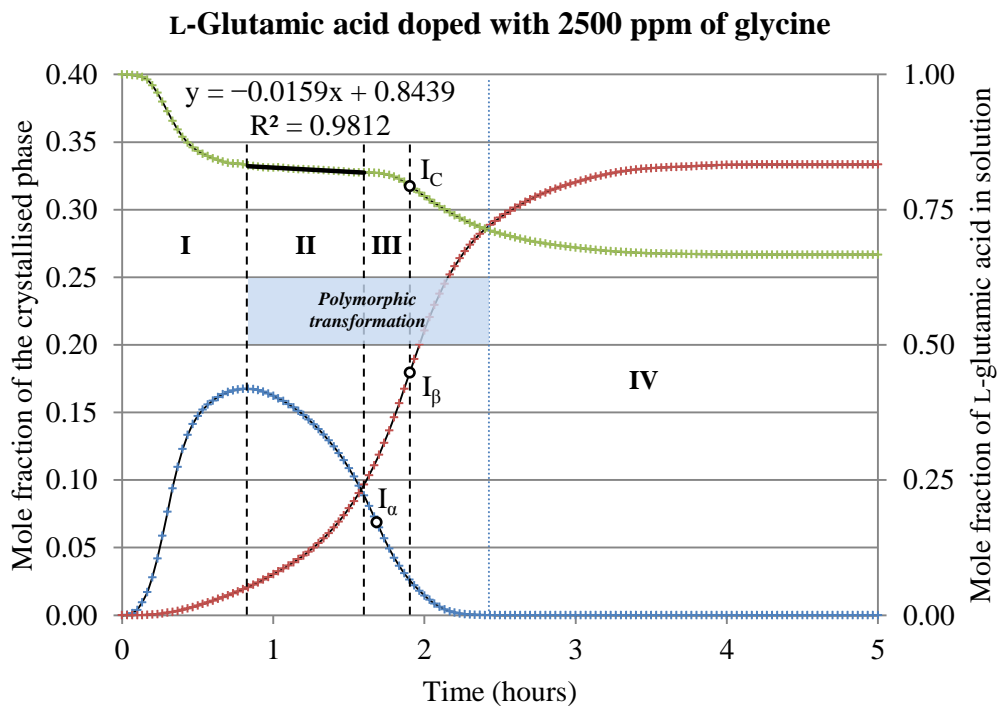


Figure 5.6 Mole fraction evolutions of the crystallised phases and dissolved *L*-glutamic acid determined for solution doped with 2500 ppm of glycine (blue – α , red – β , green – *L*-glutamic acid in solution)

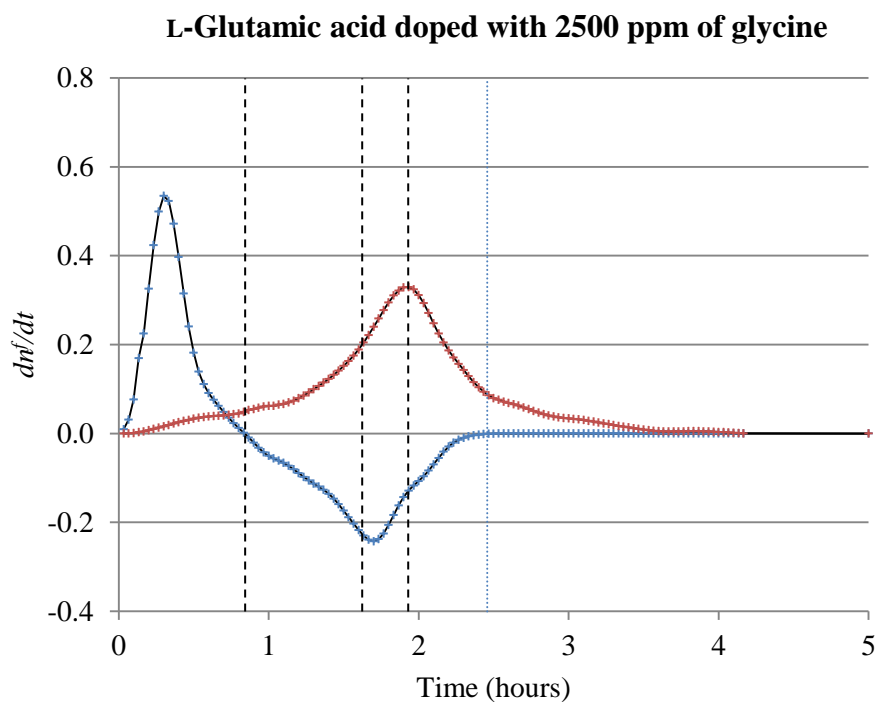


Figure 5.7 The rate of change (first derivative) of mole fraction evolutions of the crystallised phases of *L*-glutamic acid determined for solution doped with 2500 ppm of glycine (blue – α , red – β -*L*-glutamic acid)

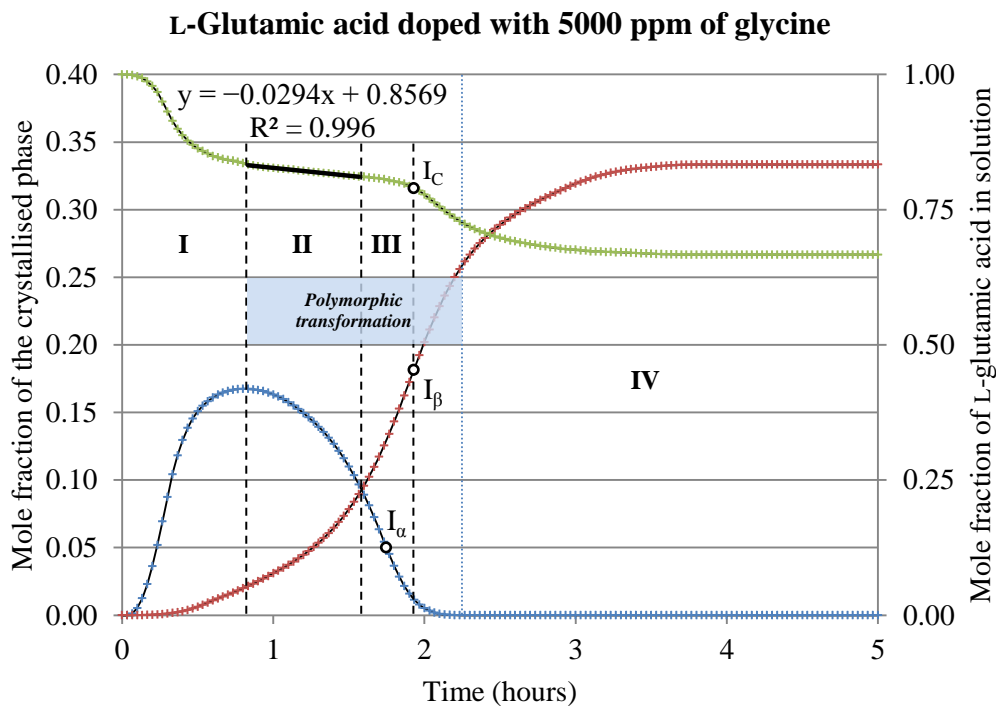


Figure 5.8 Mole fraction evolutions of the crystallised phases and dissolved *L*-glutamic acid determined for solution doped with 5000 ppm of glycine (blue – α , red – β , green – *L*-glutamic acid in solution)

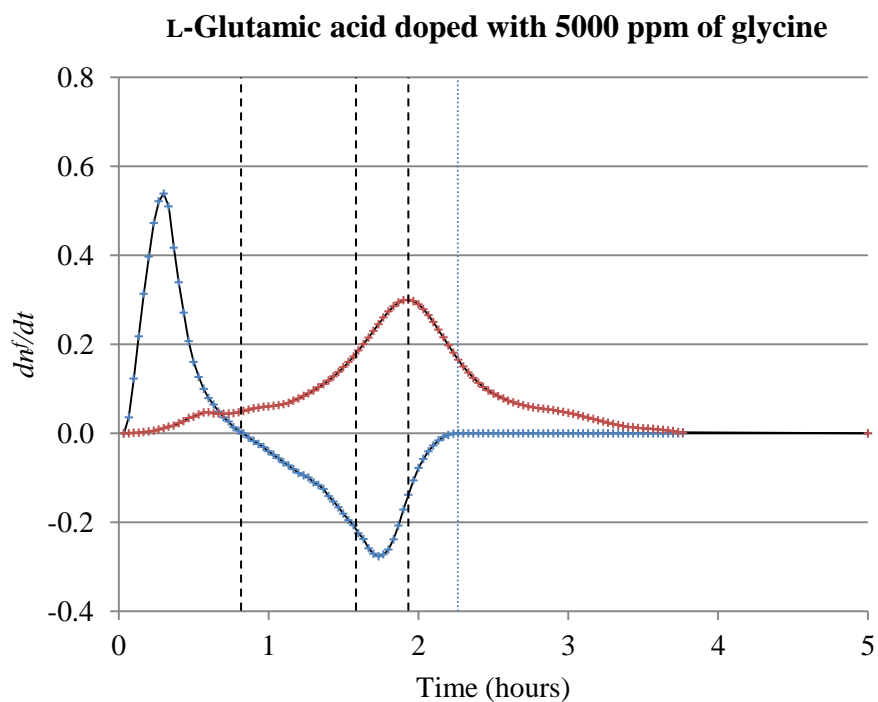


Figure 5.9 The rate of change (first derivative) of mole fraction evolutions of the crystallised phases of *L*-glutamic acid determined for solution doped with 5000 ppm of glycine (blue – α , red – β -*L*-glutamic acid)

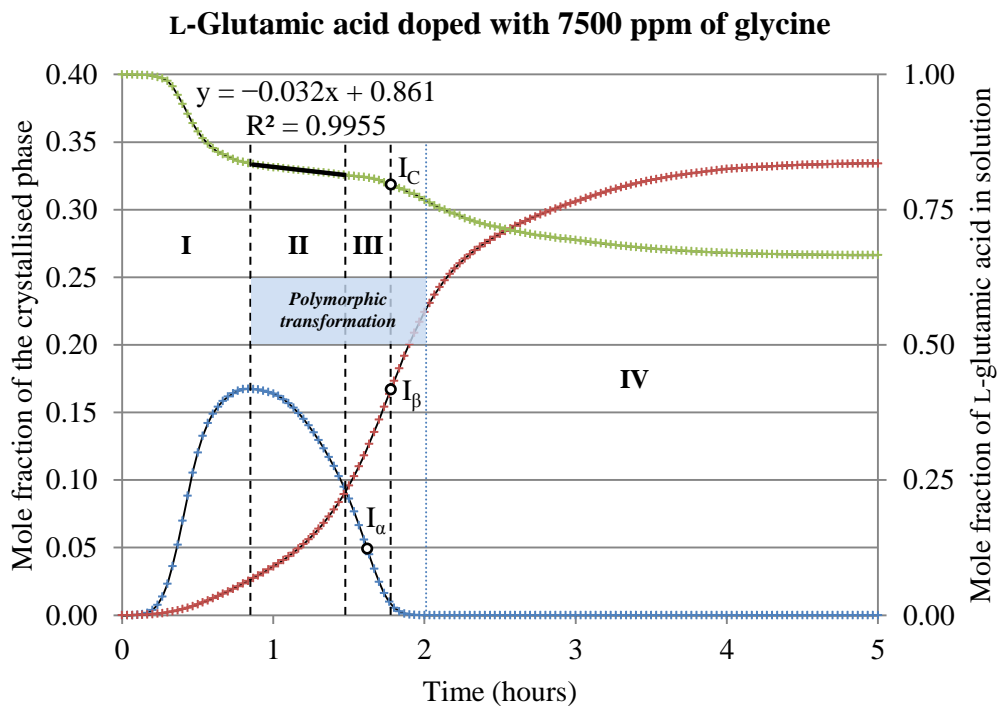


Figure 5.10 Mole fraction evolutions of the crystallised phases and dissolved L-glutamic acid determined for solution doped with 7500 ppm of glycine (blue – α , red – β , green – L-glutamic acid in solution)

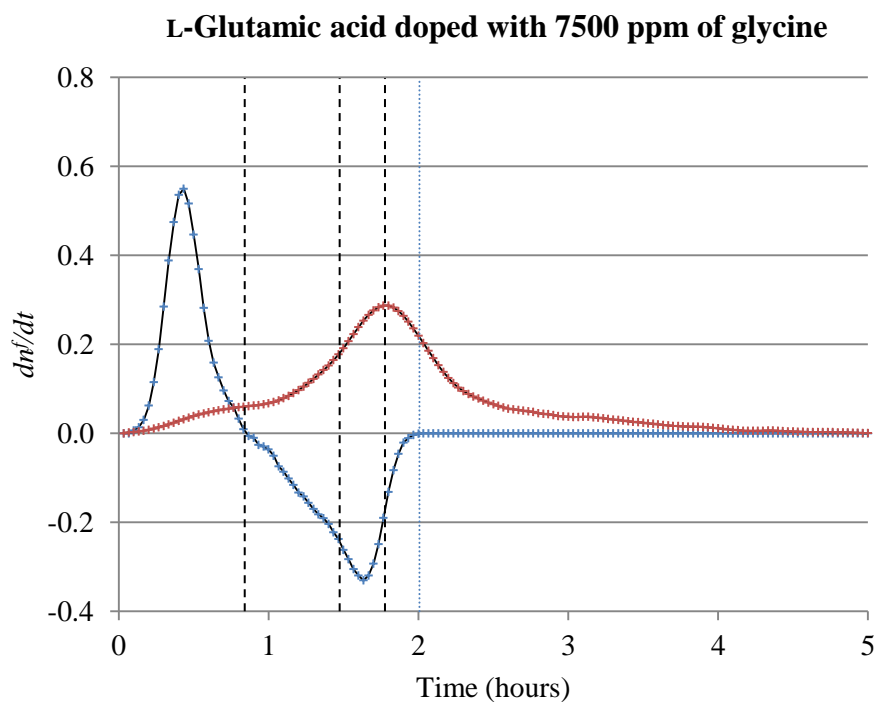


Figure 5.11 The rate of change (first derivative) of mole fraction evolutions of the crystallised phases of L-glutamic acid determined for solution doped with 7500 ppm of glycine (blue – α , red – β -L-glutamic acid)

the two polymorphic phases. Moreover, it was observed that the derived evolution of the mole fraction of the crystallised α phase appears to be heavily dependent on the mole fraction of the crystallised β polymorph.

In the discussion below, we will attempt to find a rationale behind the evolution of the derived mole fraction curves of the crystallised and dissolved phases, explain the reasons for their close mutual interdependence, correlate these evolutions to the crystallisation events and ultimately shed some light on the physical meaning of the obtained curves. Due to the complexity of the data discussed in this chapter, to facilitate the interpretation of the results, it will be convenient to divide the obtained curves into four distinct regions:

- I. From the beginning of the experiment until the point when the crystallised mole fraction of α reaches its maximum value.
- II. From the point of the maximum molar concentration of α to the point where β becomes the dominant crystallised form, i.e. this region corresponds to the plateau on the solution concentration curve.
- III. Between the end of the first concentration plateau and the inflection point on the β mole fraction evolution curve.
- IV. From the inflection point on the curve describing the evolution of the β mole fraction until the attainment of the saturation concentration with respect to the β form, i.e. until the crystal growth stops.

5.2.1 Region I: pure solution of L-glutamic acid

The solution agitation process was started when solution achieved the desired crystallisation temperature. During the first 4 minutes of the experiment no change in solution composition was observed. The period between the beginning of the agitation and the moment when the first diffracted peak was recorded corresponds to the nucleation time. The induction period was followed by concurrent primary nucleation of both α and β polymorphs and an increase in the mole fraction of the respective phase. It was noted that region I was almost entirely dominated by nucleation and growth of the metastable phase. While the increase in the amount of α -L-glutamic acid was rapid, the crystallisation of the β polymorph was significantly slower. It was also noted that the crystallisation of the two polymorphs was accompanied by a fast decrease in the mole fraction of dissolved L-glutamic acid, i.e. a rapid drop of solution concentration.

At the point when n_{α}^f achieved its maximum value ($t_{\alpha, \max, \text{pure}} = 56$ min), the concentration of solution reached the solubility level of the less stable polymorph, i.e. the equilibrium with respect to the α phase. If α was the only form present in solution, the crystallisation process would stop here. However, due to a small amount of β -L-glutamic acid present in solution, the system as a whole is in a non-equilibrium state. The stable form crystals will thus continue to grow at the expense of the α form dissolving.

The calculated mole fraction evolution rates reflect the changes of the corresponding mole fractions with time and are proportional to the crystal growth rates. Due to high solution supersaturation and thus high driving force for crystallisation, the rate of change of the mole fraction of the α crystals, which dominated the initial nucleation stage, was initially rapid. As the crystallisation progressed, the rate of growth of the α crystals started to slow down and, after reaching its maximum value, began to decrease, eventually reaching its zero value, i.e. the point of the maximum mole fraction of the crystallised α polymorph. On the other hand, the mole fraction evolution rate of the more stable β polymorph was slowly but steadily increasing throughout region I.

5.2.2 Region I: L-glutamic acid solution doped with glycine

The general shape of the three mole fraction evolution curves for solutions doped with 2500 ppm, 5000 ppm and 7500 ppm of glycine is similar to that corresponding to a pure solution. However, a number of distinctive features, differentiating between the three doping levels, needs to be pointed out.

The initial nucleation process in the presence of the additive resulted in formation of both polymorphic phases. A careful inspection of the recorded data shows that the determination of the nucleation time using the WAXS technique remains a challenging task. The first peaks of the solid phase in the solutions doped with 2500 ppm and 5000 ppm of glycine appeared approximately after 4 minutes, i.e. no difference in the duration of the nucleation time was noticed in the presence of the additive. A comparison of these results with the laser light scattering data discussed in *Section 4.2*, where over three-fold reduction of the nucleation time was noted, suggests that L-glutamic acid crystals that are initially nucleated in the presence of glycine at 2500 ppm and 5000 ppm are most likely of minuscule size. Such tiny crystals are known to produce broad X-ray peaks and therefore cannot be differentiated from the relatively strong background signal of solution. Accordingly, the scattering signal from crystallised L-glutamic acid is only visible in the recorded data after the crystals had grown to

a certain size and not just after the nuclei were formed. Therefore, one should bear this inherent drawback in mind when considering the WAXS technique as a tool to measure the nucleation time. Moreover, the above observations also imply that single-photon laser light scattering is a more sensitive technique for measurement of the nucleation time in the investigated system.

On the other hand, the nucleation time at 7500 ppm of glycine was noticed to be more than two times longer than in the pure solution ($t_{nucl,7500ppm} = 10$ minutes). The nucleation hindering effect of glycine at the highest doping level agrees with the experimental results presented in the previous chapter. As suggested in *Section 4.2*, the observed induction time retardation is most likely caused by the additive molecules that, at high doping level, are more likely to be present in the vicinity of the developing nuclei, disrupt their growth and consequently increase the time of formation of the critical size nuclei.

While in the presence of glycine α was still the major initial crystallisation product, a noticeable increase in the number of primarily nucleated β crystals was observed when compared to the pure solution. Furthermore, it was noted that the amount of nucleated β crystals increased with increasing concentration of the additive. It was found that in the presence of 2500 ppm of glycine, α -L-glutamic acid attained its maximum concentration earlier than in a pure solution. When the level of the additive was increased to 5000 ppm, the maximum mole fraction of the crystallised α form was also achieved within 50 minutes ($t_{\alpha,max,2500ppm} = t_{\alpha,max,5000ppm} = 50$ minutes). However, due to nucleation hindering, an increase in the level of glycine to 7500 ppm resulted in the time to attain the equilibrium level of the metastable form being slightly delayed ($t_{\alpha,max,7500ppm} = 52$ minutes).

The mole fraction rate evolution curves show similar behaviour irrespective of the additive level. The most noticeable difference in the presence of glycine was a decreased maximum α crystals growth rate when compared to the pure solution. In the latter case, however, the attainment of the maximum growth rate was followed by its sharp decline, whereas in solutions doped with the additive the decrease of the rate was slower. Consequently, the equilibrium level of the metastable form was achieved faster in the presence of the additive. Furthermore, a closer inspection of the mole fraction rate evolution curve of the β polymorph indicated that the growth rate of the primarily nucleated β -L-glutamic acid increases with increasing concentration of the additive.

5.2.3 Region II: pure solution of L-glutamic acid

Once the solubility level of the less stable polymorph of L-glutamic acid is achieved, α crystals begin to dissolve due to the growth of small amounts of homogeneously nucleated β crystals that are metastable with respects to their equilibrium concentration (Kitamura, 1989). The dissolution process will initially occur at the locally stressed fields at screw and mixed dislocation outcrops on the α crystal facets leading to the formation of etch pits (Figure 5.12). The faces most susceptible to dissolution are likely to be those with fast growth rates. It will thus be the fast-growing faces where an early formation of etch pits and a local increase of solution concentration with respect to the β form equilibrium occurs. When the concentration attains an energetically favourable level, secondary nucleation and subsequent growth of β on the dissolving α crystal faces takes place (also see earlier discussion in Section 4.4). The driving force for the dissolution of α is the growth of the β form. Henceforth, two different types of the stable L-glutamic acid crystals can be identified in the experimental solution, i.e. originating from primary and secondary nucleation. Their two distinctive growth pathways should therefore be considered separately. Support for the above hypothesis is evidenced in the collected experimental data.

The rate of dissolution of α crystals depends on the amount and growth rate of β . At the beginning of region II, the β crystals present in solution are almost exclusively resulting from primary nucleation. An inspection of WAXS data shows that the amount of initially nucleated primary β and its growth rate are both fairly low. Since the amount of the latter is small, the dissolution of α and the corresponding heterogeneous nucleation of β crystals on the surface

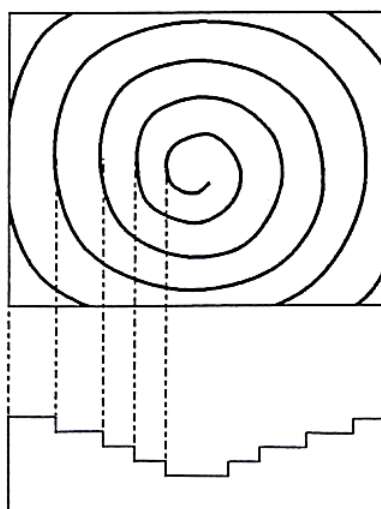


Figure 5.12 Schematic representation of formation of an etch pit at screw dislocation outcrop

of the metastable form are slow. At this stage, the observed change in the mole fraction of the stable polymorph can be predominantly attributed to the growth of the primarily nucleated β crystals. Due to continuous agitation, these crystals are nearly homogeneously dispersed in the experimental solution and thus the probability of overlap between the concentration fields around not only the primarily nucleated β crystals but also between the concentration fields of primary β and the local concentration fields generated at the etch pits of the dissolving α crystal is low. The primary β crystals are thus suspended in the bulk solution of fairly low supersaturation where the driving force is low and hence their growth is slow. Accordingly, the initial increase of n_{β}^f with time in region II was found to be slow. One could argue that since secondary nucleation and growth of the more stable polymorph also takes place in the initial stage of region II, the X-ray scattering from these newly formed β crystals should also affect the intensity of the recorded peaks. However, as pointed out in the discussion above, small crystals are known to produce broad peaks of low intensity and thus their contribution to the recorded WAXS signal is initially likely to be negligible.

It is only approximately 45 minutes after the beginning of the polymorphic transformation when the heterogeneous β crystals, nucleated on the surface of the metastable polymorph, grow large enough to become detectable in the scattering spectrum. One should still keep in mind that the formation of β crystals, in this case the secondary β , is the driving force for dissolution of α -L-glutamic acid. Because of the dissolution of α , the local concentration fields around the etch pits on dissolving α crystal face will be higher than in the bulk solution, and thus the corresponding growth rate of secondary β will be higher than that in the bulk. The latter is manifested by a pronounced rise in the rate of n_{β}^f in the second half of region II.

Further examination of the mole fraction evolutions of α and β polymorphs in region II reveals strong coupling between the growth of the secondary β crystals and the dissolution of the α phase. The fact that the two curves are nearly symmetrical suggests that the number of L-glutamic acid molecules consumed by the growth of the secondary β is approximately equal to the number of molecules released into solution by dissolving α crystals. Consequently, since throughout most of region II the number of dissolved L-glutamic acid molecules does not change significantly with time, the overall concentration of solution remains almost constant and a plateau can be observed on the respective evolution curve. For that reason, the process can be described as solution-mediated polymorphic transformation. However, one should be aware that the plateau is only roughly parallel to the horizontal axis because of the presence of small amounts of primarily nucleated β crystals in the bulk

solution. The slow growth of these crystals, resulting from low supersaturation in the bulk, contributes to the decrease of solution concentration and results in the slope being close to zero on the negative side. The more general point, though, is that the steepness of the slope depends on the amount of primarily nucleated β crystals when the polymorphic transformation process begins, i.e. at the point when the mole fraction of the crystallised α form achieves its maximum value.

Similarly to the mole fraction evolution curves of the two polymorphs, also the respective curves describing the evolutions of their rates show high degree of symmetry, confirming strong coupling between the growth of secondary β and the dissolution α -L-glutamic acid faces. The observed correlation between the rates of these two processes constitutes further evidence supporting the crystallisation mechanism postulated above.

5.2.4 Region II: L-glutamic acid solution doped with glycine

The shape of the curves characterising the time dependence of the crystallised mole fractions of the two polymorphs for solutions doped with glycine bears a certain degree of resemblance to that obtained for the pure solution. Firstly, regardless of the level of the additive, the α and β evolution curves remain symmetrical throughout region II. Moreover, as a consequence of the symmetry between the curves, the characteristic plateau corresponding to the polymorphic transformation process was observed on the concentration evolution plot. Both in the presence and in the absence of the additive, a general trend was also noted that the rates of dissolution of α and growth of β crystals increase as the crystallisation proceeds. The physical reasons behind the observed behaviour of the doped solutions are the same as for the case without glycine and are thoroughly described in the corresponding section above.

Despite the general similarity of the evolutions outlined above, a number of apparent features differentiating between the curves behaviour can be pointed out. While a plateau in the concentration evolution curve is present in the recorded data under all investigated conditions, it was observed that its duration was significantly reduced in the presence of glycine and that the magnitude of the effect appeared to be more pronounced when the concentration of the additive was increased. As shown earlier in the analysis of region I, although at all investigated levels of glycine the initial nucleation process was dominated by precipitation of the α polymorph, the amount of primarily nucleated β was found to increase with increasing concentration of the doping material. When the polymorphic transformation process begins, i.e. at the point where solution reaches the solubility level of the metastable

form, the growth of primary β crystals is the driving force for the dissolution of α . Consequently, in the presence of glycine, the dissolution of the α crystal faces is faster and the resulting local concentration levels around these faces are higher. As a result of the latter, the corresponding rates of nucleation and later growth of secondary β are also increased, leading to a significant reduction in the duration of the polymorphic transformation time. Since the enhancement of the rates of these two processes is related to the amount of the primary β crystals nucleated at the initial stages of the crystallisation process and since the latter is stimulated when the concentration of the additive is increased, the time of the α to β transformation decreases as the level of glycine is increased.

The dissolution of α and consequently enhanced nucleation of secondary β is also likely to be affected by the adsorption of glycine molecules on the surface of the growing α crystal. The attachment of the additive molecules on the growing α faces leads to formation of defects and consequently to an increased concentration of dislocation outcrops on the α crystal faces, promoting dissolution of the less stable form and thus stimulating the formation of secondary β . It is important to note that the adsorbed molecules of glycine are not permanently incorporated into the crystal structure and, after certain period of time, dissolve back into the bulk solution. The hypothesis postulated above is supported by the growth hindering of α observed in region I and by the results of HPLC analysis presented in *Chapter 4* showing that only a negligible amount of the additive becomes incorporated into the α form crystals.

The evolution of the concentration curve in region II exhibits linear behaviour as a result of the polymorphic transformation process, i.e. the growth of the stable polymorph at the expense of the metastable form dissolving. If exactly the same number of molecules dissolving from the surface of α was incorporated into the growing β , the slope would be equal to zero, i.e. the plateau would be exactly horizontal. However, the latter would only be possible if all of the following conditions were met:

- α crystals were the only form present at the beginning of the polymorphic transformation.
- β polymorph was heterogeneously nucleated on the surface of α and no stable form crystals were present in the bulk.
- The growth of β was entirely from the fields of locally increased concentration generated at the expense of the α form dissolving and such field was not perturbed by shear stress due to solution agitation.
- Diffusion from the local fields of high concentration into the bulk was negligible.

In reality, however, the above conditions cannot be satisfied because:

- The α to β transformation process cannot start in the absence of the latter. In real systems, the dissolution of α is triggered by the growth of homogeneously nucleated β .
- Both homogeneously and heterogeneously nucleated β are present in solution and thus scattering from crystals of both origins contributes to the value of n^f_β .
- The agitation of solution perturbs the local concentration fields and helps the diffusion into the bulk.

For these reasons, the absolute value of all slopes is near zero on the negative side. However, due to the complex nature of the process, it is not possible to determine and quantify the individual influence of the above factors on the evolution of the polymorphic transformation.

Nonetheless, it was noted that the slope of the plateau becomes more negative as the level of glycine is increased. Since the amount of primary β was also observed increases with increasing concentration of the additive, the enhanced primary nucleation of the more stable polymorph is therefore the most likely factor leading to the disproportion between the rates of dissolution of α and growth of β . The growth of primary β does not, however, violate the linearity of the concentration evolution curve in region II. As a result of agitation, the primary β crystals are well dispersed in the crystalliser and the supersaturation level around them is relatively low. The growth of the stable form is thus slow and approximately a linear function of time. Accordingly, the linearity of the concentration plateau is maintained.

The change of the additive concentration was found to markedly affect the dissolution rate of α crystals. It was observed that at higher levels of glycine: (i) the increase in the α dissolution rate with time appears to become more pronounced, (ii) the maximum dissolution rate increases and (iii) the latter value is attained earlier. On the other hand, while an increase in the overall growth rate of β was noted, the maximum rate of β growth did not change significantly. One may ask, why, in contrast to the less stable α form, the presence of glycine does not result in an increased formation of defects in the β crystals and thus hindering the growth of the more stable form. The answer to this question can be given on the basis of conformational arguments. It is plausible to suggest that, on average, the conformation of the dissolved glycine molecules resembles, to a certain extent, the conformation adopted by α -L-glutamic acid molecules in the crystalline state and therefore the chance of their attachment to the growing α crystal surface is greater than to the β form. In other words,

glycine molecules treated as growth units are more likely to be 'compatible' with the growing α crystal structure.

Despite the observed significant reduction in the duration of the polymorphic transformation time, the general shape of the mole fraction evolution curves remained almost the same regardless of the doping material level implying that in all cases the underlying mechanism governing the crystallisation process remains largely unchanged. Furthermore, the former shows that even a small perturbation of the initial nucleation conditions may have a pronounced effect on further evolution of the crystallisation process.

5.2.5 Region III: pure solution of L-glutamic acid

The beginning of region III coincides with the point where the curves corresponding to the crystallised mole fractions of α and β polymorphs intersect, i.e. where the number of moles of both polymorphs is equal. From that point on, as a result of further crystallisation, the number of moles of β exceeds the number of moles of α . The latter is followed by a fast dissolution of the metastable crystals and a rapid growth of β .

The rate of dissolution of the metastable α crystals was observed to increase in the initial period of region III and subsequently, after achieving its maximum value, begins to decrease until it eventually reaches zero later in region IV. On the other hand, the growth rate of β crystals increases throughout the entire region III and the moment when the curve attains its maximum value marks the end of the region. Since the coupling between the α and β mole fraction evolutions is no longer present, the symmetry between the two curves breaks. As a result, a fast non-linear decrease of solution concentration was also observed throughout region III.

It is interesting that a significant increase in the rate of growth of β and a marked decrease in solution concentration were observed despite already low supersaturation. Such behaviour of the system can be explained by the fact that the breakage of the acicular β crystals generates particles that act as secondary nuclei for the formation of new β crystals. Since each α crystal has, on average, several β nucleated on its surface (*Figure 4.18*), the number of secondary nuclei of the stable polymorph resulting from breakage of β is significantly greater than that generated by dissolution of α crystals. Additionally, because of their needle-like shape and fragility, the needles of β -L-glutamic acid are prone to further fragmentation and breakage, as evidenced in SEM images of the crystals extracted in region III (*Figure 5.13*), leading to

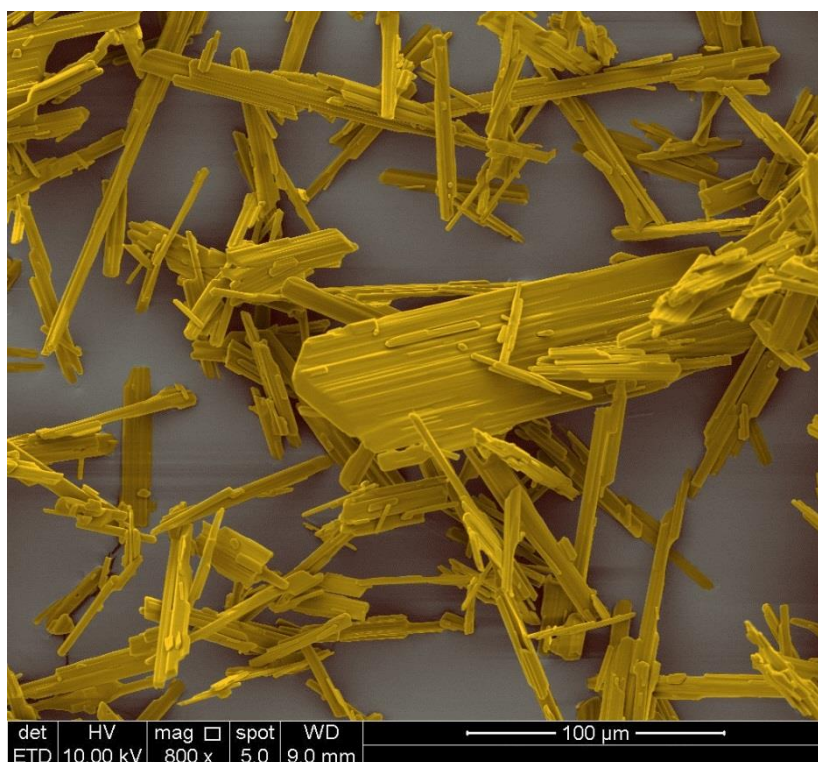


Figure 5.13 SEM image of fragmented β -L-glutamic acid crystals extracted in region III

further increase in the number of secondary β nuclei and further formation and growth of new β crystals.

The breakage of β results from contributions of several factors: (i) shear stress due to agitation, (ii) mutual collisions between the crystallised particles and (iii) collisions with the elements of the crystalliser, i.e. walls of the batch reactor, tubing, pump impeller blades, etc. The breakage conditions vary randomly and the overall process is of stochastic nature, and therefore it does not have a strictly defined starting point. The needles of β are nucleated at different times and grow at different rates. It is not possible to experimentally measure the growth rate of individual crystals. The obtained mole fraction evolutions of the two polymorphic forms are macroscopic quantities, i.e. they are derived from X-ray scattering data for a certain volume of solution and not from individual crystals, and therefore represent the average values. One could argue that it is therefore likely that some breakage events occur earlier, towards the end of region II, but cannot be clearly discerned in the obtained evolution plot. Nevertheless, the high level of symmetry observed in *Figure 5.4* between the mole fraction evolution curves of the α and β form of L-glutamic acid and the linear evolution of the concentration curve in region II both imply that such events, although possible, are rare and their influence on the process is negligible.

The significant increase in the number of secondary nuclei that result from the breakage of β crystals will result in a dramatic increase in the number of sites on crystal facets where molecules of L-glutamic acid can be incorporated. It is important to note that, in parallel, growth of homogeneous and heterogeneous crystals, present in solution prior to the onset of the pronounced fragmentation of β , also occurs. However, because of the abundance of sites for nucleation and attachment of growth units generated during the breakage of β crystals, it is predominantly the first of these processes that is responsible for the observed drop in solution concentration and a fast increase in the number of moles of crystallised β in region III. While the latter two also lead to incorporation of solute molecules from the bulk solution into the crystal structure, their influence on the overall evolution of solution concentration in this region is of considerably less importance.

5.2.6 Region III: L-glutamic acid doped with glycine

The general shape of the mole fraction and solution concentration evolution curves for the solutions doped with glycine is almost identical to that obtained in the pure solution. The arguments presented in the discussion above, when considering the crystallisation of solution without the additive, are therefore also valid here. However, as emphasised earlier, the rate of the polymorphic transformation of L-glutamic acid was observed to increase with increasing concentration of glycine. Accordingly, due to considerably shorter duration of region II in the presence of the additive, a translation of the curves towards the origin of the time axis, i.e. to the left, was noted.

A careful inspection of the data also showed that the rate of dissolution of α increases as the concentration of glycine is increased. Since at higher levels of the additive the number of dislocation outcrops is increased, the nucleation of secondary β on the surface of α is promoted and consequently the population of the former is increased. As discussed above, the majority of these acicular crystals will undergo fragmentation generating sites for further secondary nucleation and growth of β that act as 'sinks' for growth units and therefore further enhance dissolution of α .

On the other hand, the rate of growth of β remained largely independent of the additive level. The latter may suggest that (i) the rate of dissolution of α is not the rate-determining step for the growth of β or (ii) that the increased availability of growth units in solution, generated by faster dissolution of the metastable form, is counterbalanced by the increased level of glycine that hinders the rate of incorporation of L-glutamic acid molecules into the β crystal structure.

5.2.7 Region IV: pure solution of L-glutamic acid

In the boundary area between regions III and IV, the curves describing the evolution of solution concentration, crystallised mole fractions of the two polymorphs of L-glutamic acid and their respective rates were observed to undergo marked changes in their behaviour. These characteristic events are the inflection points on the α and β mole fraction curves and the inflection point on the concentration curve, denoted I_α , I_β , and I_C , respectively. At each inflection point a respective curve changes its concavity, from concave upwards to concave downwards at I_α and I_C , and vice versa at I_β . Moreover, the latter two were found to occur at the same time and coincide with the maximum growth rate of the β polymorph, whereas the former one was observed simultaneously with the maximum dissolution rate of α and slightly earlier than I_β and I_C . The fact that these characteristic points occurred almost simultaneously suggests a high degree of coupling and mutual dependence between the observed evolutionary events.

The coexistence of the inflection points on the mole fraction evolution curves and the extremes on the respective rate curves can be explained on the basis of geometrical consideration since the rates of dissolution of α and growth of β are the first order derivatives of the mole fraction time evolutions of the two polymorphs. However, the fact that the change in the concavity of the curve is observed denotes that the inflection point corresponds to the moment when the system undergoes a substantial change to its physical behaviour.

The growth of β in region III occurs at the expense of the dissolving α form. At the point when the rate of dissolution achieves its maximum value, i.e. when the inflection point on the mole fraction evolution curve of α occurs, the dissolving metastable crystals become too small to solely sustain the delivery of molecules required by the growth of secondary β and the bulk solution gradually becomes the source of L-glutamic acid. While the growth rate of β continues to increase, because of decreasing dissolution rate of α and decreasing solution concentration, the rate of increase of the growth rate cannot be maintained and an inflection point on the β polymorph growth rate curve is observed. At the point when the maximum growth rate of β is attained, corresponding to the inflection point on the β mole fraction evolution curve, the bulk becomes that main molecular supply of L-glutamic acid and consequently an inflection point on the concentration curve is observed.

The remaining small amount of the metastable crystals undergoes fast dissolution since the equilibrium temperature for small crystals and their mother liquor is lower than that for the large ones. The latter is also known as the Gibbs-Thomson effect (Gibbs, 1948). In other

words, the above observation can be attributed to the fact that small particles have higher solubility than the large ones. As a result, the complete dissolution of α was achieved before the solubility level of the more stable polymorph was achieved. Consequently, in the final stage of the crystallisation process, the source of L-glutamic acid molecules for the growth of β was only the bulk solution. Since the solution supersaturation was close to the equilibrium level of the stable polymorph, the driving force for the growth of β was relatively low and thus the growth of β in the final crystallisation stage was very slow. The crystallisation process stopped once the equilibrium concentration with respect to the β form was achieved.

5.2.8 Region IV: L-glutamic acid solution doped with glycine

The α and β mole fraction and concentration curves for solutions doped with glycine exhibit similar evolutionary behaviour to that observed in the pure solution. Therefore, the above discussion on the evolution of the respective curves also holds true for solutions crystallising in the presence of the additive.

It was, however, observed that the higher the level of glycine, the faster the complete dissolution of α is accomplished. The latter effect can be explained by the fact that, as discussed earlier, structural defects, such as dislocations, are more likely to form in the presence of additives. It is also well established that the dissolution process is favoured at such structural imperfections. Accordingly, the increased number of defects in the α form crystals nucleated and grown in solutions doped with glycine results in the dissolution process occurring faster in the presence of the additive than in the pure solution. Since the average number of defects increases with increasing concentration of the additive, the dissolution enhancing effect was observed to become more pronounced as the concentration of glycine is increased.

Moreover, it was observed that, up to 5000 ppm of glycine, the time elapsed after the α form ceased to exist until the solubility level of the stable polymorph was attained was equal to approximately one hour and was largely independent of the additive level. The latter is due to the fact that at low additive levels the molecules of glycine are not likely become incorporated into the growing crystal structure. On the other hand, when the level of the additive was increased to 7500 ppm, a marked inhibition of β growth was noted. At this doping level, the number of additive molecules adsorbing on the surface of the growing β crystal faces is high enough to disrupt the incorporation of L-glutamic acid growth units, lead to an increased formation of defects and consequently noticeably slow down the growth

of the stable polymorph. However, one may ask why similar β growth hindering effect was not observed at 7500 ppm at earlier stages of the crystallisation process. The answer to this question requires consideration of the driving force for crystallisation of β . It should be borne in mind that in regions I, II and III, the supersaturation of solution, and hence the driving force for the growth of the stable form, is relatively high. Consequently, throughout the first three stages of the crystallisation process, the growth of β remains essentially unaffected by the presence of the additive. On the other hand, in region IV, the concentration is nearly equal to the equilibrium value with respect to the β form and thus the relative effect of glycine becomes large enough to become apparent in the recorded data.

5.3 Determination of the polymorphic transformation time from WAXS data

The above findings can now be used to accurately determine the duration of the polymorphic transformation time of L-glutamic acid. In literature, the polymorphic transformation is defined as the process of growth of the stable crystal form at the expense of dissolution of the less stable polymorph. Accordingly, the duration of the transformation is the time between the beginning of the dissolution process of the metastable form due to the growth of the stable polymorph until the complete dissolution of the former is achieved. For many years, there has been a strong belief that that the α form ceases to exist at the end of the first plateau on the concentration evolution curve, i.e. at the end of region II (Kitamura, 1989, Garti and Zour, 1997). In this study, however, using the in-situ Wide Angle X-ray Scattering technique, it was showed that the complete dissolution of α is rather accomplished at the beginning of the second plateau and, hence, this is where the polymorphic transformation process actually ends. Bearing in mind that the synchrotron-based method used in this work is considered to be the most advanced technique available at present to study the evolution of crystallised polymorphs in solution, it can be concluded that the generally accepted criterion for determination of the duration of the polymorphic transformation should be regarded as incorrect as the obtained data clearly demonstrated that the complete dissolution of the less stable polymorph is only accomplished at the beginning of the second concentration evolution plateau and not at the end of the first one as previously believed.

For clarity and convenience, the key findings concerning the evolution of the transformation process are summarised in *Table 5.1*.

Table 5.1 Effect of various levels of glycine on the polymorphic transformation of L-glutamic acid

Level of glycine (ppm)	Onset of the transformation (min)	Polymorphic transformation time (min)	Slope of the plateau in region II	Decrease in the trans. time ($t_{additive} / t_{pure}$)
0	56	128	-0.0066	1.00
2500	50	94	-0.0159	0.73
5000	50	84	-0.0294	0.66
7500	52	62	-0.0320	0.48

5.4 Conclusions

Following the above in-depth analysis of the parameters characterising the behaviour of L-glutamic acid polymorphs during crystallisation from the pure and glycine-doped solutions, it is possible to make conclusive statements regarding the effect of glycine on its polymorphic transformation:

- (i) The growth rate of the α polymorph in region I, and consequently the attainment of its equilibrium level, was enhanced at all investigated levels of glycine.
- (ii) Due to enhanced homogeneous nucleation of the β form crystals in the presence of the additive, an increase in the dissolution rate of α was observed in region II.
- (iii) The effect of the additive was found to depend on the level of glycine and thus the absolute value of the slope of the transformation plateau was note to increase as the level of glycine was increased.
- (iv) As a result, a rapid decrease in the polymorphic transformation time was observed as the concentration of glycine was increased.

Despite the fact that, at present, it is not possible to identify the actual mechanism responsible for the enhanced nucleation of the β polymorph in the presence of glycine, this work demonstrates that even a relatively small amount of the additive can perturb the initial series of nucleation events and ultimately have a significant effect on the subsequent polymorphic transformation and thus on the crystallisation process as a whole. In the investigated system the above was manifested by an appreciable increase in the amount of primarily nucleated β crystals and an increased formation of defects on the growing α form faces. As a result, once the maximum concentration of the metastable polymorph was attained, as

a consequence of the former, and aided by the latter, a significant increase in the dissolution rate of the less stable α was observed, ultimately resulting in a marked reduction of the polymorphic transformation time. Therefore, it was shown that the nucleation and growth events at the initial stage of crystallisation are the major factors influencing further evolution of the process. Since through manipulation of the level of the additive these events can selectively be influenced, it is thus also possible to control the polymorphic transformation process.

Furthermore, although the analysis and discussion presented in this work focuses on the dissolution and growth processes of the dimorphic L-glutamic acid, the approach taken here is of general nature and can be further extended to characterise the transformation process in a wide range of polymorphic materials.

Chapter 6

Crystallisation of L-glutamic acid in an acoustic levitator

Crystallisation of L-glutamic acid is typically investigated in a batch reactor or in a cell. On the contrary, in this chapter, using in-situ WAXS, Raman spectroscopy and droplet size monitoring techniques, we study the nucleation and growth phenomena accompanying crystallisation of L-glutamic acid from a droplet suspended in an acoustic levitator. Interestingly, it was found that the more stable β -L-glutamic acid is the only polymorph that precipitates out from a droplet. Moreover, it was observed that the onset of nucleation and the rate of subsequent growth can, to some extent, be manipulated using molecular additives.

6.1 Containerless crystallisation of pure L-glutamic acid solution

Containerless nucleation and growth of L-glutamic acid were investigated in an acoustic levitator at room temperature using *in-situ* time-resolved WAXS and Raman spectroscopy experiments at BESSY II synchrotron (Berlin, Germany). A digital camera was employed to record images of the evaporating droplet. The images were then used to determine the change in droplet volume with time and hence estimate the evolution of solution supersaturation. A detailed description of the experimental set-up is given in *Section 3.2.2*. Pure solution of L-glutamic acid was investigated first. When a 5 μ L droplet was injected into the levitator, simultaneous recording of WAXS spectra and sample images was started.

6.1.1 Wide Angle X-ray Scattering

Wide Angle X-ray Scattering data recorded as a function of time during crystallisation of pure solution of L-glutamic acid is given in *Figures 6.1* and *6.2*. Selected images of the sample captured during the experiment are shown in *Figure 6.3*.

When the investigation of the crystallisation process was started, the concentration of solution in the droplet was slightly below the saturation level. Initially, broad scattering

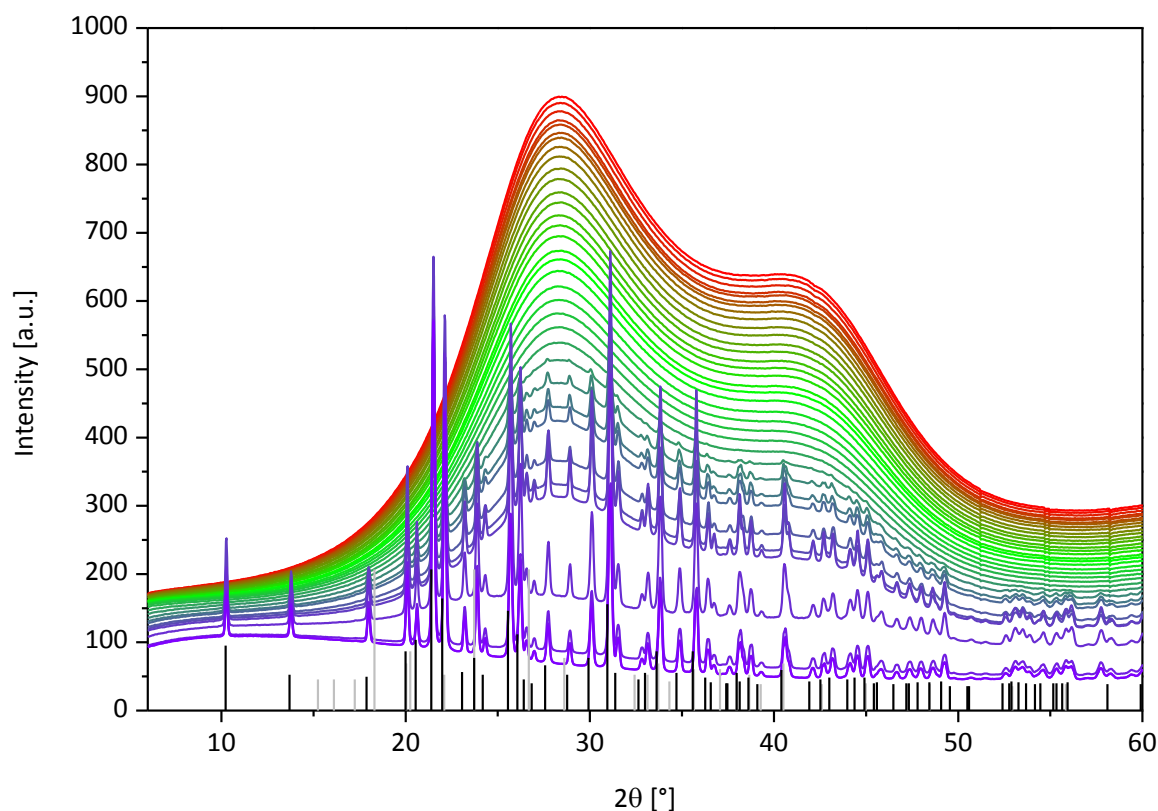


Figure 6.1 Time evolution of WAXS spectra for crystallisation of pure L-glutamic acid. Red and purple curves correspond to solution and the final crystallisation product, respectively. The bar codes represent the powder patterns of the two L-glutamic acid polymorphs, α (grey lines) and β (black lines)

spectrum with high-intensity maximum around $2\theta = 28^\circ$ and low-intensity maximum around $2\theta = 41^\circ$ was observed and can be attributed to the scattering of solution. As the evaporation of the solvent progressed, the intensity of these broad peaks decreased. Since the total number of moles of solute inside the droplet remains constant throughout the experiment, the concentration of solution was gradually increasing what eventually led to the formation of L-glutamic acid crystals. The characteristic peaks of the solid phase were first observed 24 minutes after the beginning of the experiment and were identified to match the XRD pattern of the β polymorph of L-glutamic acid. As the crystallisation proceeded further, the scattering signal from solution decreased in intensity. After approximately 34 minutes all experimental solution had evaporated and only the solid phase peaks of the remaining aggregate of the β -L-glutamic acid crystals were present in the recorded spectrum. No further crystallisation was possible and thus the experiment was stopped. Surprisingly and contrary to the Ostwald's rule of stages, it was found out that the more stable β form of L-glutamic acid was the first and only polymorph that crystallised from a droplet.

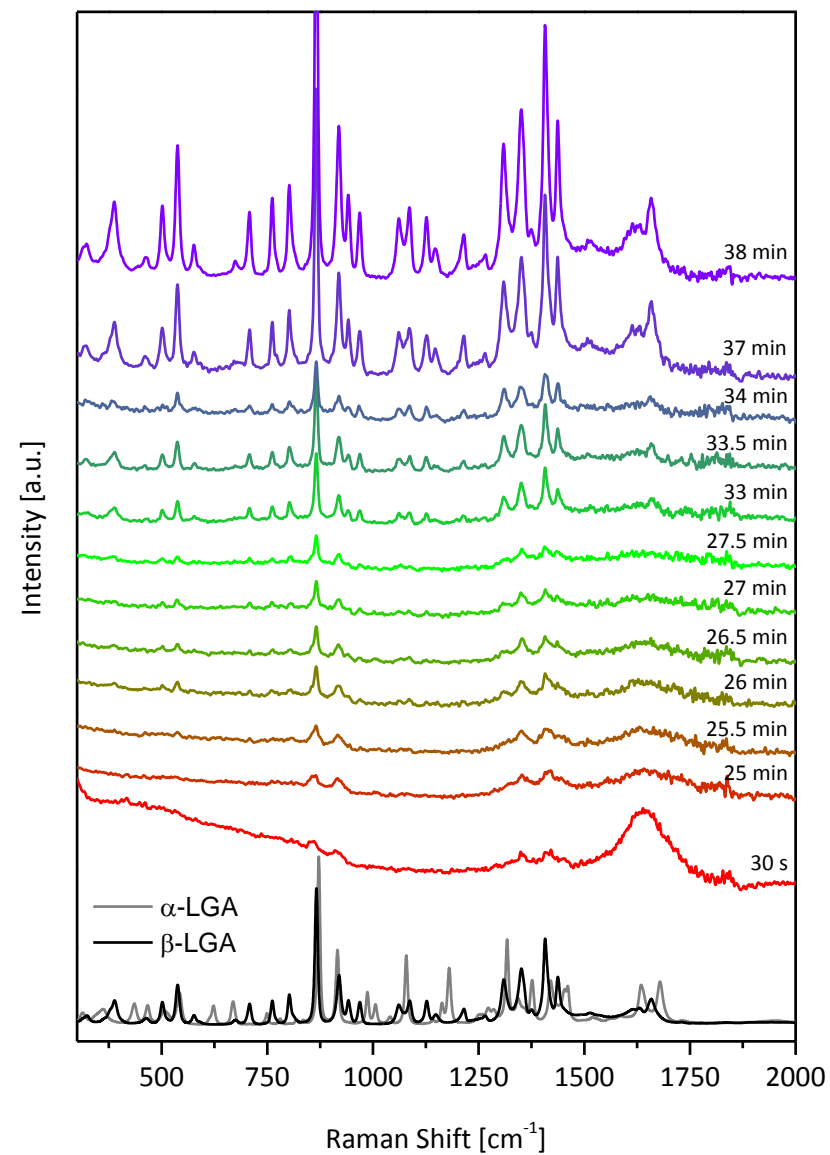
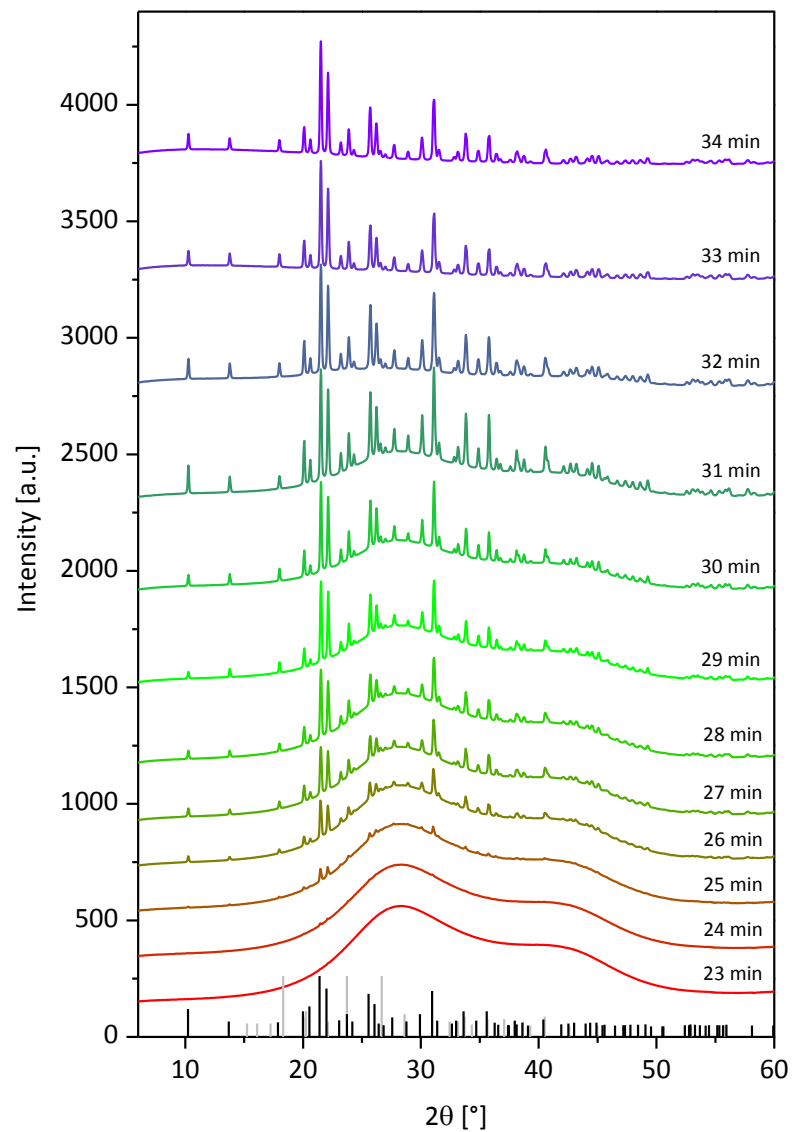


Figure 6.2 Selected WAXS patterns (left) and Raman spectra (right) for crystallisation of pure L-glutamic acid. Red and purple lines correspond to solution and the final crystallisation product, respectively. The bar codes representing powder patterns and reference Raman spectra of the two L-glutamic acid polymorphs, α (grey lines) and β (black lines), are given at the bottom of each figure

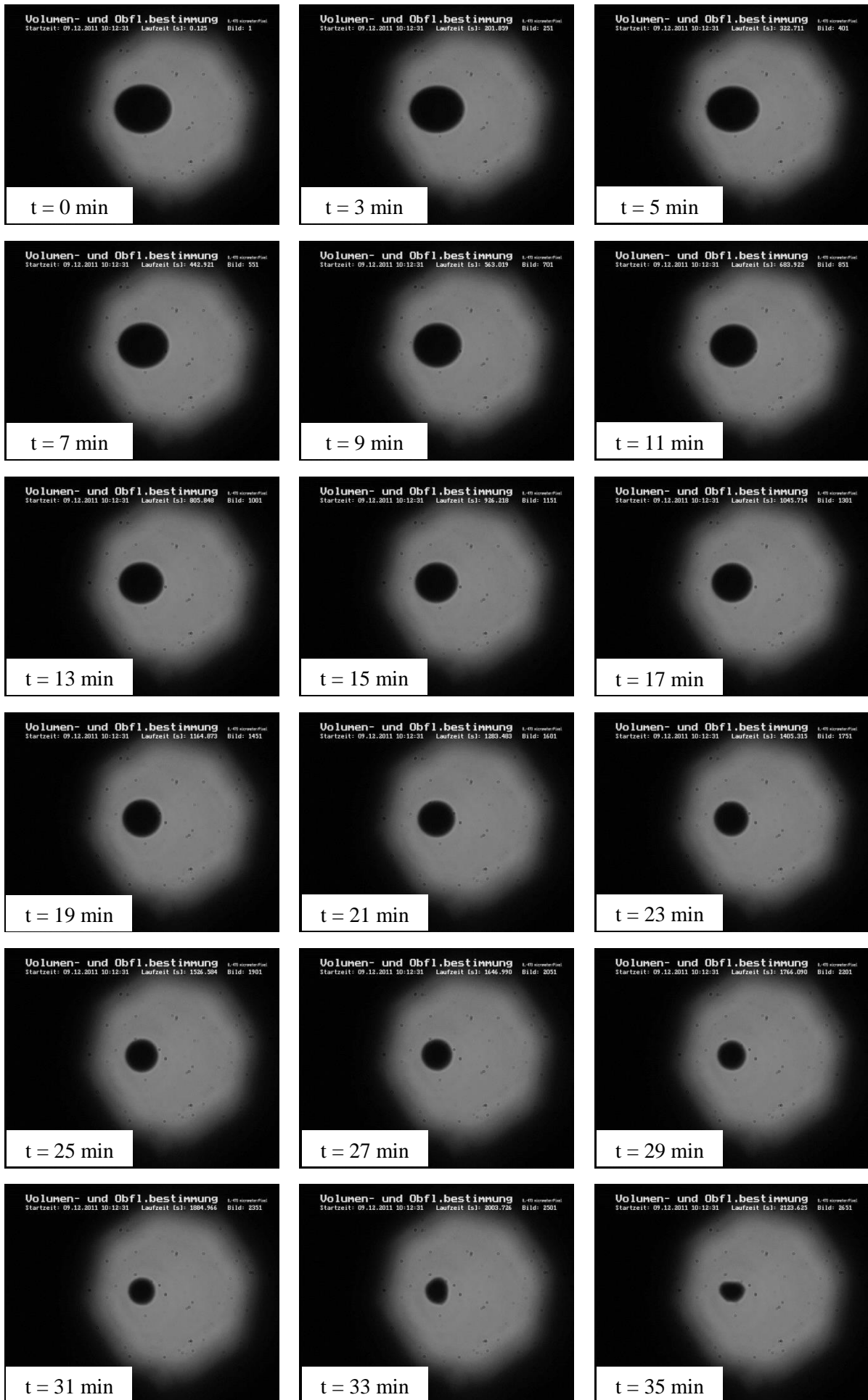


Figure 6.3 Selected images of the shadow of the sample used to determine the change in its volume with time for a typical pure L-glutamic acid crystallisation experiment

One could argue that small short-lived crystals of the metastable α -L-glutamic, on which the stable β polymorph quickly nucleates due to high solution supersaturation, may actually form. Such tiny crystals would produce broad WAXS peaks that could be indistinguishable from the water background. However, since the molecular conformations of the two polymorphs of L-glutamic acid are significantly different through a torsion angle in the main carbon chain, they can, even in solution phase, be distinguished by Raman spectroscopy, as has been shown by Ono et al. (2004). If those tiny metastable crystals were present in solution just before nucleation of the β phase took place, the respective signal should appear in the recorded Raman spectrum. Therefore, in order to further confirm that the β form of L-glutamic acid is indeed the only one that precipitates from a droplet, additional experiments using combined *in-situ* WAXS and Raman spectroscopy were carried out.

6.1.2 Raman spectroscopy measurements

In the beginning of the experiment, the Raman spectra (*Figure 6.2*) display broad signals of water at 1642 cm^{-1} and around 3500 cm^{-1} . During the induction period some additional weak peaks were also noted at 858 cm^{-1} , 917 cm^{-1} , 1357 cm^{-1} and 1419 cm^{-1} . These peaks could result from molecular clusters of dissolved L-glutamic acid but cannot be assigned to a specific polymorph. The existence of such prenucleation clusters in supersaturated solutions has been reported in numerous experimental studies. Most of these studies, however, do not provide direct evidence about the structure of the clusters or their influence on the solid state outcomes (Erdemir et al., 2007). First signal of the crystalline phase appears after 25.5 minutes and corresponds to the β polymorph (characteristic peaks at 575 cm^{-1} , 705 cm^{-1} , 800 cm^{-1} , 1145 cm^{-1} and 1214 cm^{-1}). As the crystallisation process progressed, these peaks were observed to increase while the broad signals of the solvent became less pronounced. No further changes in the Raman spectrum were noted after 37 minutes. The time evolution behaviour of the simultaneously recorded X-ray diffraction pattern was consistent with our previous findings. In both WAXS and Raman data no metastable phase was detected.

The simultaneous WAXS-Raman experiments were subsequently repeated at lower temperature, to investigate precipitation from a droplet when the process is slowed down, and in a stream of dry nitrogen, where the crystallisation rate was increased due to faster evaporation of the solvent. In all of these complementary experiments, the recorded signal of WAXS and Raman could only be assigned to β -L-glutamic acid. The only difference that was noted was the duration of the crystallisation process.

6.1.3 Sample volume and aspect ratio

The images of the sample recorded during the experiment (*Figure 6.3*) were used to determine the change in its volume and aspect ratio (*Figures 6.4* and *6.5*, respectively) as evaporation of the solvent proceeded.

The volume of the sample was observed to decrease with time due to solvent evaporation (*Figure 6.4*). Since at constant external conditions of temperature, pressure and humidity, the total number of moles of solvent leaving the system per unit time is proportional to the surface area of the droplet ($dn_{\text{solvent}}/dt \propto 4\pi r^2$), the evaporation rate was found to decrease with time due to shrinking of the sample. Consequently, the volume evolution curve has a concave shape.

Before crystallisation commences, the recorded change in volume of the sample corresponds solely to the change in volume of solution ($dn_{\text{solvent}}/dt = -\rho_{\text{solvent}} dV_{\text{sample}} / M_{\text{solvent}} dt$, where ρ_{solvent} and M_{solvent} are the density and molar mass of the solvent, respectively, and V_{sample} is the volume of the sample). Thus, for time t less than 24 minutes, a second degree polynomial fit to the experimental data describes the change in volume of the solvent as a function of time. However, one should bear in mind that once crystals start to form on the surface of the droplet, the measured volume of the sample becomes the sum of the volume of solution and the volume of the crystallised material. Thus, a departure from the fit is observed at the final stage of the crystallisation process when the sample consisted mainly of L-glutamic acid crystals. For the latter reason, although no solution phase was present at the end of the experiment, the final volume of the sample was estimated to be approximately 0.3 μL and corresponds to the volume of the crystalline aggregate that remained levitated after all experimental solution had evaporated.

It was noted that initially the width of the levitated sample was greater than its height. This deformation to an ellipsoidal shape is caused by the anisotropic acoustic force field, in which the axial levitation force is some five times greater than the radial one (Trinh and Hsu, 1986). The aspect ratio (D_h / D_v) was found to decrease with time and eventually approach 1.0 as a result of a faster decrease in D_h than in D_v which is caused by an increase in surface tension and hence lower deformability of the droplet as it shrinks during evaporation (Kastner et al., 2001). In the final stage of the experiment the aspect ratio of the sample was observed fluctuate significantly, being either markedly below or above 1.0. These variations can be attributed to the fact that after about 30 minutes the levitated sample comprised

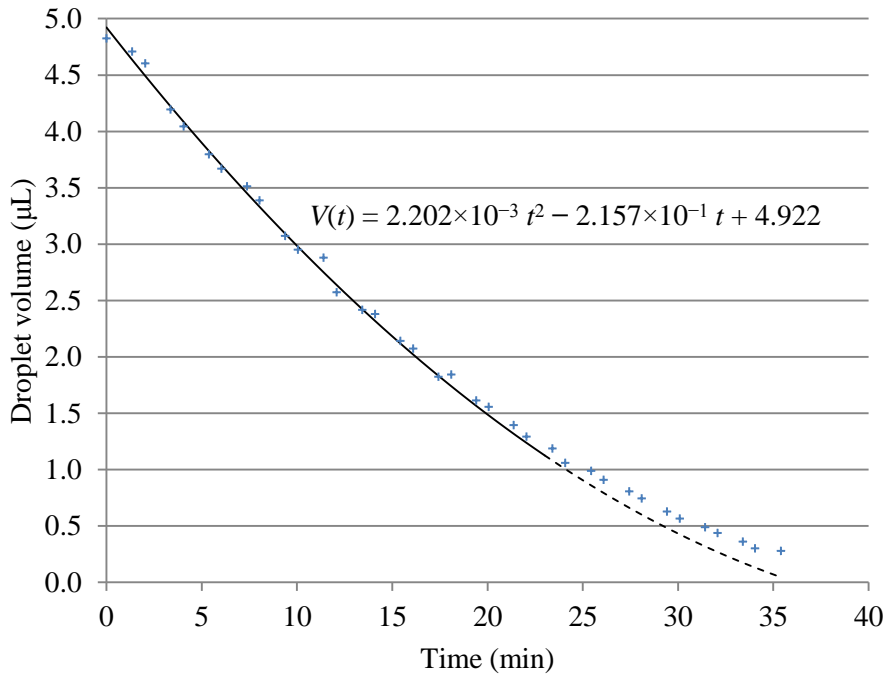


Figure 6.4 Change in volume of the sample as a function of time for a typical pure L-glutamic acid crystallisation experiment

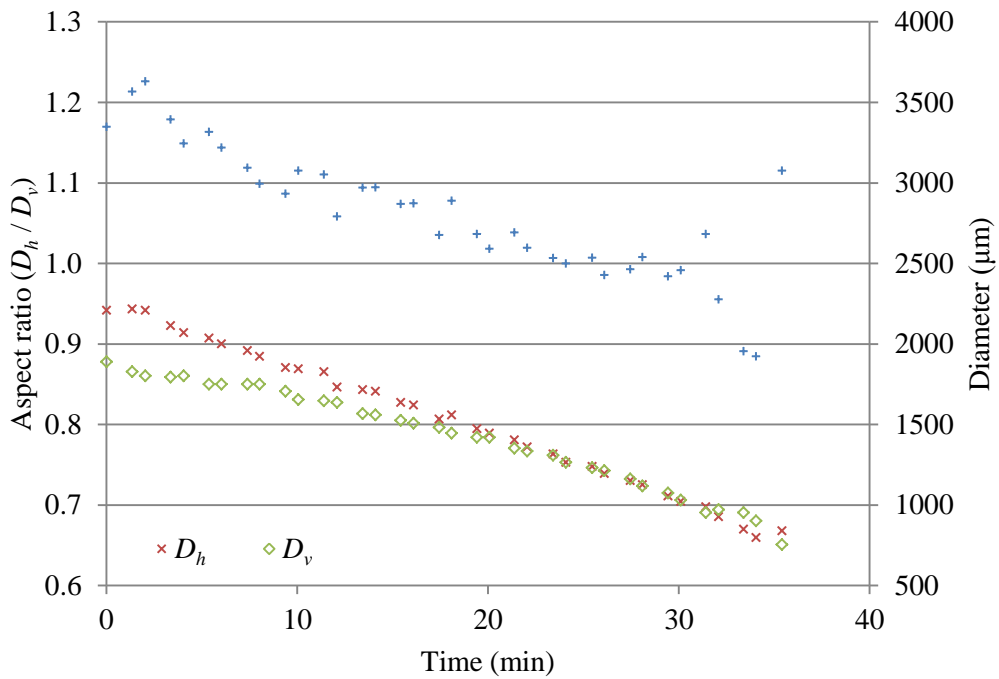


Figure 6.5 Change in the aspect ratio and the horizontal and vertical diameters of the sample as a function of time for a typical pure L-glutamic acid crystallisation experiment

predominantly of a non-spherical β -L-glutamic acid crystal aggregate that was rotating in the acoustic field (cf. *Figures 6.2 and 6.3*).

6.2 Molar concentration and crystallised mole fraction evolutions

6.2.1 Assessment method

Since the total number of moles of L-glutamic acid in the system does not change with time, the sum of the number of moles of L-glutamic acid in solution phase and that in the solid state is equal to the total initial number of moles of L-glutamic acid that was used to prepare the experimental solution. Because the β polymorph was the only form that precipitated, the following relationship can be written:

$$n_{solution} + n_{cryst} = n_{initial} \quad (6.1)$$

Hence,

$$n_{solution} = \left(1 - \frac{n_{cryst}}{n_{initial}}\right) \times n_{initial} \quad (6.2)$$

The integral of the β -L-glutamic acid WAXS peaks (the area under the peaks) is directly proportional to the mass, and therefore the number of moles, of the crystallised material. Thus, assuming that all of the dissolved material crystallised when the solvent has completely evaporated, at any time t , the crystallised mole fraction is equal to:

$$n^f_{cryst}(t) = \frac{n_{cryst}(t)}{n_{initial}} = \frac{A_{cryst}(t)}{A_{final}} \quad (6.3)$$

The volume of the droplet at time t is equal to the sum of the volume of solution and the volume of the crystallised material at time t .

$$V_{sample}(t) = V_{solution}(t) + V_{cryst}(t) \quad (6.4)$$

Thus,

$$V_{solution}(t) = V_{sample}(t) - V_{cryst}(t) \quad (6.5)$$

Since the volume of the crystallised L-glutamic acid is proportional to the mass, and so the number of moles, of the crystallised material, the change in volume of solution with time can be written as:

$$V_{solution}(t) = V_{sample}(t) - n^f_{cryst}(t) \times V_{final} \quad (6.6)$$

Consequently, the evolution of the molar concentration of solution with time can be described using the following equation:

$$c(t) = \frac{n_{solution}(t)}{V_{solution}(t)} = \frac{[1 - (A_{cryst}(t)/A_{final})] \times n_{initial}}{V_{sample}(t) - (A_{cryst}(t)/A_{final}) \times V_{final}} \quad (6.7)$$

The combined WAXS and droplet volume evolution data could thus be used to determine the concentration and crystallised mole fraction evolution curves for the crystallising solution of L-glutamic acid (*Figures 6.6-6.8*). Due to the reasons discussed in *Section 5.1.2*, the experimental uncertainty cannot be quantified but the possible experimental error is likely to be negligible.

6.2.2 Physical meaning of the key points on the evolution curves

The obtained concentration evolution curve can be divided into two segments:

- Region I, before nucleation of β -L-glutamic acid crystals occurred, i.e. when $n_{cryst}^f = 0$, where the increase of solution concentration results solely from the solvent evaporation process. The change in concentration in this region is only a function of the volume of the droplet and can be described using the following equation:

$$c(t) = \frac{n_{initial}}{V_{solution}(t)} \quad (6.8)$$

- Region II, after nucleation and crystal growth of β -L-glutamic acid began to take place, i.e. $n_{cryst}^f > 0$, where the change in concentration is a result of two competing processes: solvent evaporation and incorporation of L-glutamic acid molecules into the structure of growing crystals. Accordingly, additional term accounting for a decrease in the number of molecules available in solution needs to be introduced into the equation describing the concentration evolution curve:

$$c(t) = \frac{n_{initial}}{V_{solution}(t)} - \frac{n_{cryst}(t)}{V_{solution}(t)} \quad (6.9)$$

The concentration of L-glutamic acid in the droplet was initially equal to the saturation level at room temperature, $c_{initial} = 10 \text{ g/L} = 68 \text{ mmol/L}$. As the evaporation of the solvent progressed, the volume of the droplet decreased and thus the concentration of solution was found to gradually increase with time. For the same reason, the rate of change of concentration was observed to increase throughout region I and achieved its maximum at its final stage ($d^2c/dt^2 = 0$ and $dc/dt > 0$), just before crystallisation of the solute began.

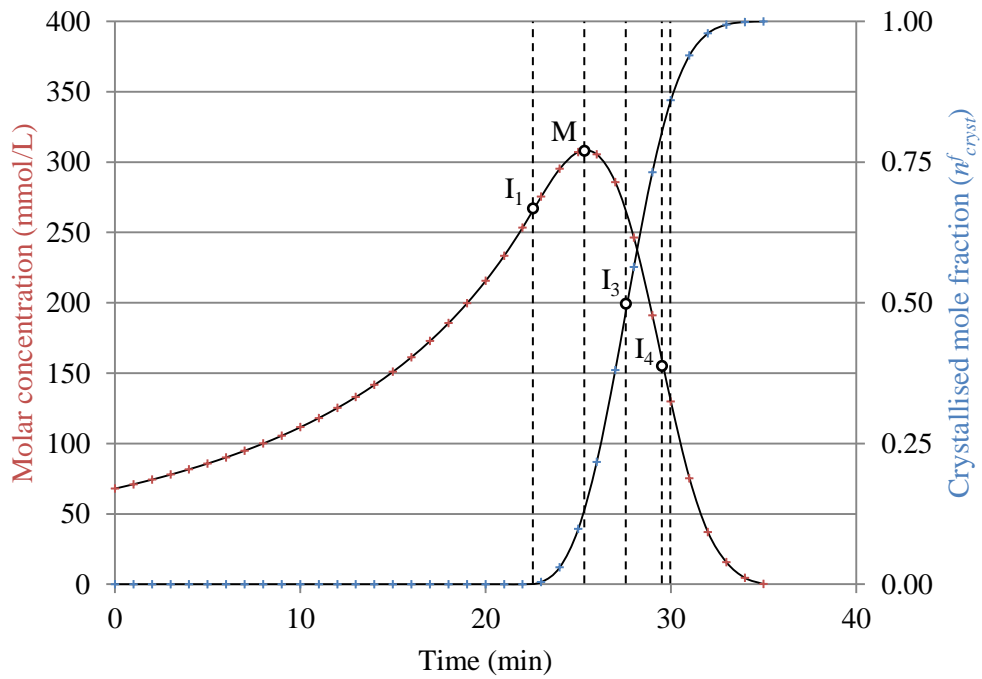


Figure 6.6 Molar concentration and crystallised mole fraction evolution curves determined for a typical pure L-glutamic acid solution crystallising from a droplet

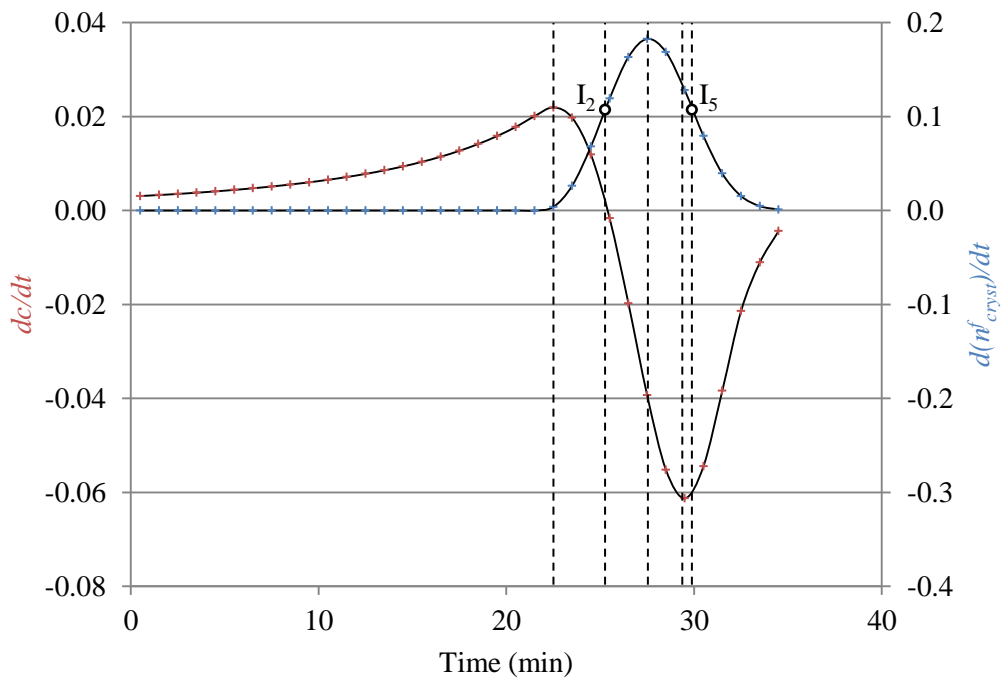


Figure 6.7 The rate of change (first derivative) of concentration and crystallised mole fraction evolution curves determined for a typical pure L-glutamic acid solution crystallising from a droplet

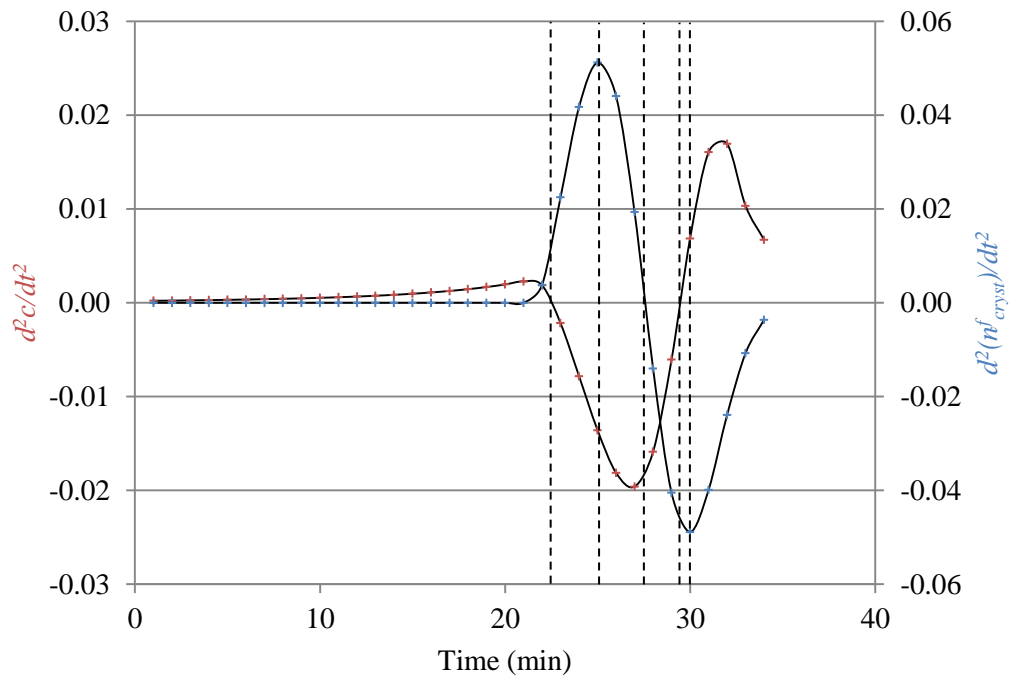


Figure 6.8 The rate of change of the rate of change (second derivative) of concentration and crystallised mole fraction evolution curves determined for a typical pure L-glutamic acid solution crystallising from a droplet

At the beginning of region II, when precipitation of β -L-glutamic acid crystals started to take place, the concentration change rate began to drop due to formation and growth of crystals and thus the inflection point I_1 can be seen on the concentration evolution curve. However, at this stage, solvent evaporation appeared to be still the dominating process and hence the concentration of solution continued to increase until it reached its maximum value ($dc/dt = 0$ and $c > 0$) at point M.

From this point on, the crystallisation component became the key factor defining the behaviour of the concentration evolution curve as the number of molecules per unit volume that leave the solution phase to adsorb on the growing crystals faces exceeded the increase resulting from solvent evaporation. Consequently, concentration of solution began to fall. Since solution supersaturation, which is a function of concentration, is the driving force for crystal growth, point M of the maximum concentration coincides with the inflection point I_2 where the rate of increase of the crystallised mass fraction is highest, i.e. where the value of $d^2(n^f_{cryst})/dt^2$ achieves its maximum.

The total crystallised number of moles of L-glutamic acid continued to increase as crystallisation proceeded. The inflection point I_3 on the crystallised mole fraction evolution curve (*Figure 6.6*) corresponds to the moment when the crystal growth rate was highest ($d^2(n_{cryst}^f) / dt^2 = 0$ and $d(n_{cryst}^f) / dt > 0$). At this point, the effective crystal surface area available for attachment of L-glutamic acid molecules was largest. However, crystal aggregation began to occur at later stages of the experiment. The latter phenomenon resulted in several types of events taking place inside and on the surface of the droplet:

- Inner faces of adjacent crystals becoming unavailable for adsorption of L-glutamic acid molecules due to intergrowth.
- Formation of occlusions where crystal growth proceeds only until saturation concentration of the trapped solution is achieved.
- Peripheral crystals eventually having their surface outside bulk solution.

As a result, the accessible surface area began to decrease and growth hindering was observed.

It was noted that the inflection point I_4 on the concentration evolution curve, where the rate of decrease of solution concentration is highest ($d^2(n_{cryst}^f) / dt^2 = 0$ and $d(n_{cryst}^f) / dt < 0$), lagged in time with respect to the point I_3 corresponding to the maximum rate of crystal growth. As mentioned above, the concentration of solution in region II is a function of the volume of the droplet and the crystallised mass fraction. Even though from point M onwards the latter component is dominating, the former one is also present for the duration of the entire experiment. Evaporation of the solvent effectively increases the concentration of solution and thus shifts the inflection point on its evolution curve later in time. The faster the evaporation rate, the later would the inflection point on the concentration curve occur. Conversely, in a system where the volume of the solvent does not change with time, such as a batch crystalliser, the inflection points I_4 and I_3 on concentration and crystallised mass fraction evolution curves, respectively, would coincide.

The inflection point I_5 on the crystallised β -L-glutamic acid mole fraction evolution curve, i.e. where the rate of decrease of the crystallised mass fraction achieves its maximum, i.e. where the value of $d^2(n_{cryst}^f) / dt^2$ is lowest, corresponds to the moment when solution enters the low supersaturation region. From that point on, assuming spiral growth mechanism, the approximation of the Burton-Cabrera-Frank (BCF) equation changes from $R \propto \sigma$ to $R \propto \sigma^2$ (c.f. *Section 1.5*). In other words, as the supersaturation becomes low, a decrease in the crystal growth rate is observed since the growth law changes from linear to parabolic.

Synchrotron radiation penetrates through the droplet and the obtained WAXS signal is the value resulting from scattering of the entire irradiated volume. However, due to evaporation of solvent from the surface, a gradient of solution concentration exists along the radius of the droplet. The local concentration is always highest at the surface, where removal of the solvent from the system occurs, and decreases towards the centre of the droplet. Therefore, throughout the whole experiment, the chemical potential of the liquid phase at the surface of the droplet is greater than the chemical potential of the solid phase ($\mu_L > \mu_S$). Consequently, the crystal growth and the resulting depletion of concentration continued even after the average concentration of solution calculated using WAXS data fell below the value corresponding to the saturation level at 25°C, until all of solution has completely evaporated.

6.2.3 Chemical potential and the irreversible change in entropy

The chemical potential of a substance in solution can be expressed as:

$$\mu = \mu_0 + RT \ln a_c \quad (6.10)$$

Where R is the ideal gas constant, T is the temperature, μ_0 is the standard chemical potential and a_c is the solute activity expressed on a molar basis, which is related to concentration, c , through the corresponding activity coefficient, γ_L , by:

$$a_c = c\gamma_L \quad (6.11)$$

For non-electrolyte solute in a dilute solution (concentrations about 0.1 molar and lower), the relative activity of the solute can be approximated by its concentration (Foulkes, 2012). Therefore, the following expression for the chemical potential can be used:

$$\mu = \mu_0 + RT \ln c \quad (6.12)$$

Since the maximum concentration of L-glutamic acid in a droplet is of the above order of magnitude, the chemical potential in the liquid phase, μ_L , can be written as:

$$\mu_L = \mu_0 + RT \ln c_L \quad (6.13)$$

Accordingly, the chemical potential of the solute in a solid state is equal to:

$$\mu_S = \mu_0 + RT \ln c_S \quad (6.14)$$

The difference in the chemical potential between the liquid and solid phase, $\Delta\mu$, can thus be expressed as follows:

$$\Delta\mu = \mu_L - \mu_S = RT \ln c_L - RT \ln c_S \quad (6.15)$$

Now, taking the final stage of the droplet crystallisation process as a reference point ($RT \ln c_S = 0$), the difference in the chemical potential with respect to the crystal at a given time t is equal to:

$$\Delta\mu_{cryst}(t) = RT \ln c_L(t) \quad (6.16)$$

Irreversible entropy that is produced by the chemical reactions going on in the system is equal to:

$$\frac{dS_{irr}}{dt} = \frac{A}{T} r \quad (6.17)$$

Where A is the chemical affinity, which is the driving force for the reaction, i.e. the difference in chemical potentials, and r is the net conversion rate, i.e. the net rate of molecule incorporation.

When crystallisation of L-glutamic acid in a levitated droplet is concerned, the chemical affinity corresponds to the difference in chemical potential and the crystallisation rate is equal to the rate of change of crystallised mole fraction. However, since thermodynamics stipulates that at constant conditions of pressure and temperature reactions proceed in a direction that lowers the Gibbs free energy of the system ($\Delta G < 0$), the difference in the chemical potential will be a negative number and hence the absolute value of $\Delta\mu_{cryst}$ should be taken. The irreversible change of entropy with time for the instigated system, from the moment when the nucleation process starts until the solute has completely crystallised, can thus be expressed using the equation below and is shown in *Figure 6.9*:

$$\frac{dS_{irr}}{dt} = \frac{|\Delta\mu_{cryst}(t)|}{T} \frac{d(n^f_{cryst})}{dt} = R |\ln c_L(t)| \frac{d(n^f_{cryst})}{dt} \quad (6.18)$$

The total entropy change of a system is, however, the sum of two contributions:

$$dS = dS_{heat} + dS_{irr} \quad (6.19)$$

Where dS_{heat} results from heat and mass flux with the surroundings and dS_{irr} is the irreversible change of entropy due to the system going from one state to another. Therefore, the total entropy change for an irreversible process depends on how that state is achieved.

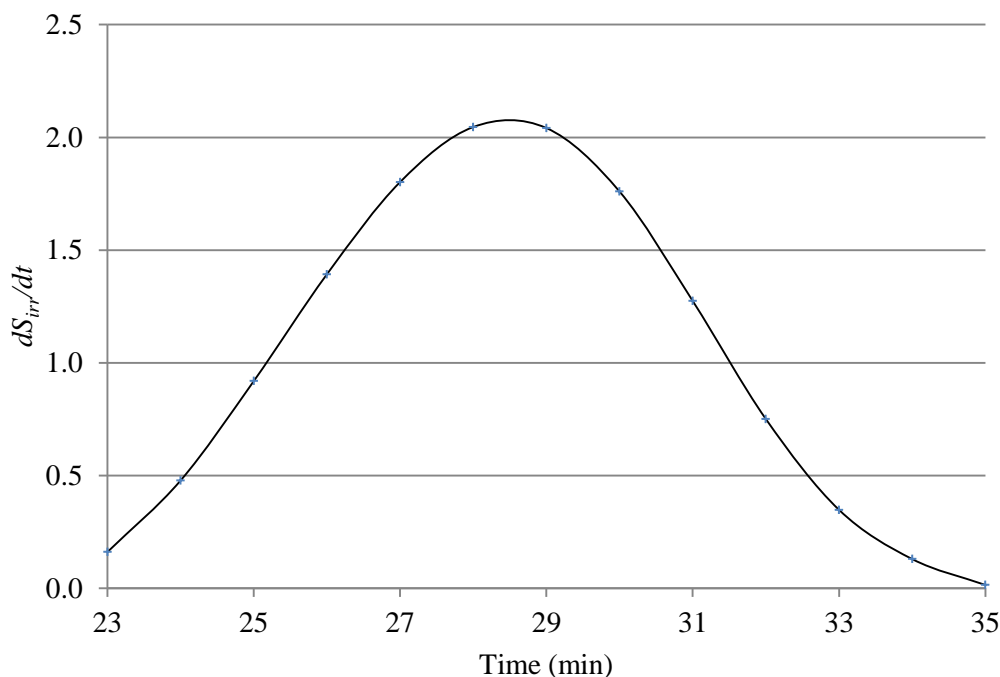


Figure 6.9 Irreversible change of entropy for a typical pure L-glutamic acid solution crystallising from a droplet

6.3 Why is β -L-glutamic acid the only polymorph that forms in an acoustic levitator?

One of the long-standing challenges in organic solid-state chemistry is the ability to predict and control the occurrence of polymorphism, the ability of a molecule to crystallise in more than one crystal structure (Desiraju, 1989). This has broad practical implications to many classes of molecular materials, for example, triglycerides, saturated and unsaturated fatty acids, alkanes, aromatic π -bonded systems, carboxylic acids, amides and amino acids. Generally, the structural variety of any polymorphic material implies its different physical properties which are reflected in crystal morphology, optical characteristics, mechanical properties, and chemical reactivity. For example, solid-liquid separation, comminution, solubility, particle flow, and formulation characteristics are all polymorph dependent (Davey, 1990, Garside, 1994). Therefore, the selection of a polymorph with properties most appropriate for either secondary processing or providing most optimal physical characteristics of a final product is of profound significance to a wide range of industries including pharmaceuticals, healthcare, agrochemicals, pigments, dyestuffs, and foods (Davey et al., 1997). It has been widely accepted that the control of the nucleation process is the ultimate

means of controlling polymorph selection. Despite its fundamental and technological importance, our ability to control polymorph formation is still far from being solved because of our extremely poor understanding of the underlying microscopic kinetic processes occurring during crystallisation of polymorphic systems.

Several approaches for controlling nucleation and selection of polymorphic forms of a compound have been pursued through crystallisation with tailor-made soluble additives (Weissbuch et al., 1991, Lahav and Leiserowitz, 1993), epitaxial growth (Bonafede and Ward, 1995, Mitchell et al., 2001), laser-induced nucleation (Zaccaro et al., 2000), crystallisation in capillaries (Chyall et al., 2002, Hilden et al., 2003), confinement within porous materials (Ha et al., 2004), and more traditional methods, such as varying solvent, temperature, and extent of supersaturation. Most high throughput polymorph generation is limited to combinatorially changing solvent, temperature, and supersaturation conditions (Peterson et al., 2002). Such approaches do not explicitly address the vital role of nucleation despite the fact that this is the critical step in controlling the phenomenon of polymorphism.

In the context of this work, there are two critical questions to be answered: (i) Why at the isothermal conditions only the stable β form crystallises from a levitated droplet and (ii) why the onset of crystallisation occurs at supersaturations which are several times bigger than those that can be achieved by cooling stagnant solution in a closed container?

6.3.1 Thermodynamic consideration of nucleation in the bulk

To begin with, it is worth considering the nucleation process in the bulk solution from the thermodynamic point of view. In general, the change in the Gibbs free energy of a system is a function of the change in its enthalpy and entropy and is defined as:

$$\Delta G = \Delta H - T\Delta S \quad (6.20)$$

Where ΔH is the change in enthalpy, ΔS is the change in entropy and T is the temperature.

The change in enthalpy is negative when heat is being released from a system (exothermic process), whereas the change in entropy is positive when a system is becoming more disordered. While both decrease of enthalpy and increase of entropy are thermodynamically favourable, in order to determine the spontaneity of a process, the overall change in the Gibbs free energy must be taken into consideration. Under constant conditions of temperature and pressure, a process can occur spontaneously only if the change in the Gibbs free energy of the system is negative ($\Delta G < 0$).

The change of the Gibbs free energy during formation of α and β polymorphs of L-glutamic acid can be written as follows:

$$\Delta G^\alpha = \Delta H^\alpha - T\Delta S^\alpha \quad (6.21)$$

$$\Delta G^\beta = \Delta H^\beta - T\Delta S^\beta \quad (6.22)$$

In batch crystallisation, the metastable α polymorph is kinetically favoured and forms first from a supersaturated solution ($|\Delta G^\alpha| < |\Delta G^\beta|$). Since the values of the change in enthalpy during formation are comparable for both L-glutamic acid polymorphs ($\Delta H^\alpha \approx \Delta H^\beta$) (Deij et al., 2007), the absolute change in entropy of formation must be greater for the more stable form of L-glutamic acid ($|\Delta S^\alpha| < |\Delta S^\beta|$). The following energy change diagram for crystallisation of the two polymorphs of L-glutamic acid can thus be produced (*Figure 6.10*).

While the above semi-qualitative explanation shows, to some extent, why, from a thermodynamic point of view, the initial formation of the α polymorph may be favoured in the bulk solution, the principle does not seem to operate for crystallisation from a droplet where the Ostwald's rule of stages is not followed. However, one should bear in mind that these two systems provide two very different environments for the crystallising solutions and consequently should be considered separately.

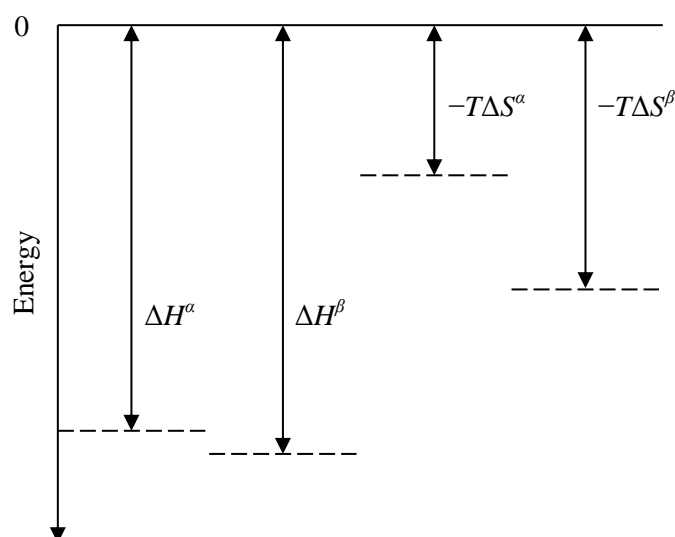


Figure 6.10 Schematic representation of the change of enthalpy and entropy during crystallisation of α and β polymorphs of L-glutamic acid

6.3.2 Crystallisation from a levitated droplet in the light of classical nucleation theory

Figures 6.2 and 6.6 show typical time-dependent evolutions of concentration and WAXS and Raman spectra in the levitated droplet of L-glutamic acid solution. At the same point of time ($t \approx 24$ min), all three undergo the first pronounced change in their evolutionary behaviour. This is manifested by a decrease in the concentration rate (inflection point I_1 in *Figure 6.6*) and simultaneous occurrence of appreciable peaks of the stable β phase on WAXS and Raman spectra (*Figure 6.2*). Further evolution of the latter two spectra indicate that, from this point until the accomplishment of the crystallisation process, the relaxation of the metastable solution of the droplet takes place exclusively through the formation of the β form. This surprising and entirely new effect demonstrates that different experimental techniques and strategies may provide not only a new mode of polymorph selection from a pure solution but also open many fundamental questions on how nature finds intriguing ways to help crystallisation of a stable polymorph, the process that does not follow the most credited and widely accepted Ostwald's rule of stages (Ostwald, 1897). In addition, we find that supersaturation at which the containerless nucleation process begins in a droplet of L-glutamic acid was almost an order of magnitude higher than that in a stagnant solution enclosed in a traditional container such as a growth cell or a batch crystalliser. Here, we shall try to give a brief and purely qualitative rationale for these novel observations by focusing only on the possible prenucleation events that lead to the formation of only the stable β crystals.

At initial point of time ($t_0 = 0$) the solution in the droplet is slightly undersaturated. At this stage the structure of the levitated droplet can be considered as a phase with complete translational and rotational symmetry, and both are isotropic and homogeneous. Because of evaporation of water molecules, the solution enters the state of metastability accompanied with the onset of small density and orientational fluctuations. Further evaporation of the solvent results in two simultaneous and time-dependent processes: (i) a permanent increase in the average supersaturation and (ii) the spatio-temporal changes of the size distribution, density and microstructure of the evolving inhomogeneities. The former one is characterised by somewhat higher concentration of L-glutamic acid at the surface than in the centre of the droplet, whilst the latter is accompanied by the tendency of smaller subcritical nuclei of a new phase to disappear but for the larger ones to grow. The absence of crystallisation of the metastable α form and its consequent solution mediated transformation into a stable β form indicates that factors such as microscopic thermodynamic pathways and kinetics of the

building up supersaturation in a levitated droplet, including its interfacial interaction with air, are quite distinctive from those in a crystallisation cell or a batch crystalliser.

In spite of the fact that classical nucleation theory (CNT) provides some insight into the essential physics of nucleation and growth of crystals (Turnbull, 1969, DeBenedetti, 1996, Onuki, 2002), it cannot provide a rationale for the selective nucleation of only β form of L-glutamic acid during isothermal containerless crystallisation from a levitated droplet. The principle limitation of this theory lies in the assumption that all properties of even very small crystallites (subcritical nuclei) are the same as in their bulk crystals and differ from them only in their relatively large surface-to-volume ratio. For that reason, the classical theory cannot identify or be used to study different crystallisation pathways as various order parameters do not all change at the same time.

6.3.5 Qualitative rationale for selective crystallisation of β -L-glutamic acid in an acoustic levitator

At the beginning of our discussion of why β is selectively formed during containerless crystallisation, it is important to note that a levitated droplet is a thermodynamically open system where water molecules are released from the surface into the surroundings. As a result of evaporation, a radial gradient of concentration is generated inside the droplet with the concentration of L-glutamic acid molecules being highest at the air-droplet interface (*Figure 6.11*). Consequently, nucleation is most likely to take place at the surface. We argue that the freedom of movement of molecules in the prenucleation stage in a droplet is greater than in the bulk because of imbalance of the attractive forces at the interface in the former case (*Figure 6.12*). Accordingly, the probability of L-glutamic acid locally adopting a conformation similar to that of the β form is greater at the surface than in the centrosymmetric bulk. Consequently, we suggest that the resulting reduction in the nucleation barrier for the β phase would be enough to lead to the direct formation of only the more thermodynamically stable polymorph.

However, it should be borne in mind that X-ray scattering from minuscule crystals results in broad peaks that can be indistinguishable from a relatively strong signal of water. Moreover, as observed in *Section 6.1*, when crystallisation of L-glutamic acid is concerned, Raman spectroscopy was found to be a less sensitive method than WAXS as the first Raman peaks corresponding to the solid phase appeared approximately one and a half minutes after than the first signal from the latter technique was recorded. Therefore, one may ask a question:

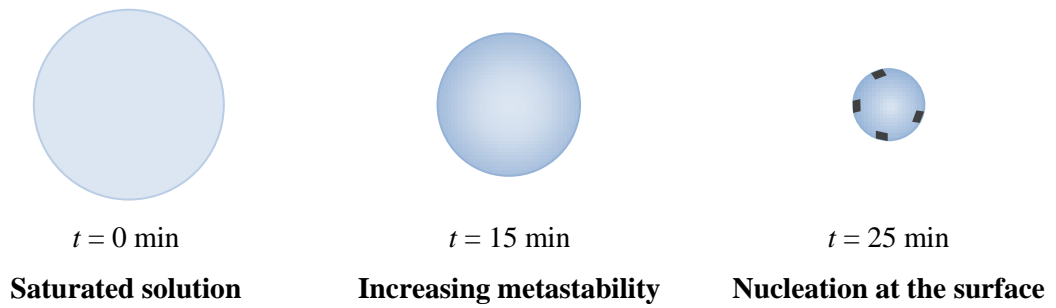


Figure 6.11 Evolution of solution concentration in a levitated droplet

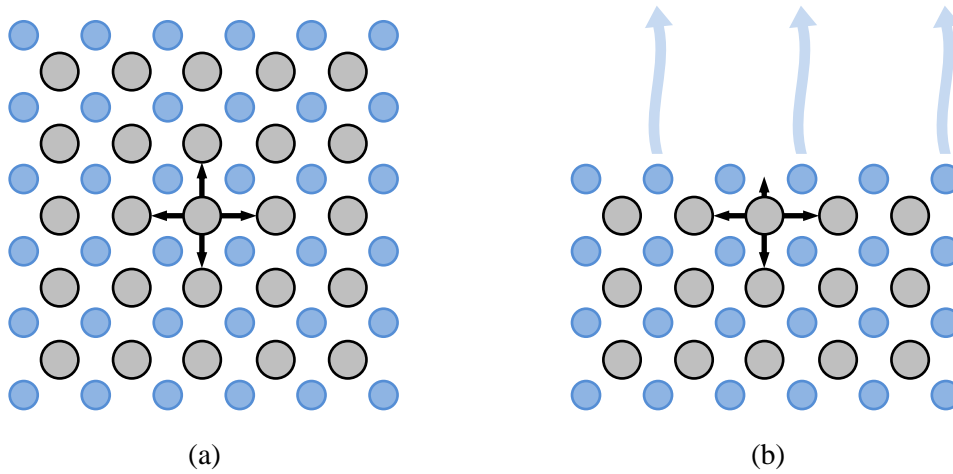


Figure 6.12 Schematic representation of the balance of attractive forces
 (a) in the bulk and (b) at the surface of a droplet

‘How do you know whether small amount of the α form was not present in solution before the first WAXS and Raman signals were observed, i.e. below the detection limit of these techniques?’ To answer this question, we should consider the conditions for the growth of α and the subsequent polymorphic transformation in the interval of time between the moment when solution achieved metastability and when the first WAXS peaks were observed. If the α form was indeed nucleated, because of high and increasing solution supersaturation, the resulting driving force for its crystallisation would lead to its further growth and the respective signal of α would eventually become detectable in the recorded spectra. Furthermore, as shown in *Chapters 4* and *5*, the transformation from α to β is a slow process lasting dozens or even hundreds of minutes. Therefore, we argue that it would be physically impossible for α to completely transform to β within the timescale of the experiment.

It was also observed that the onset of crystallisation in a levitated droplet occurs at supersaturations which are an order of magnitude higher than those that can be achieved by cooling stagnant solution in a closed container. The latter suggests that formation of the new solid phase in a typical batch crystalliser is, in fact, predominantly a heterogeneous process where container walls, tubing and agitator blades act as centres for nucleation. On the other hand, excluding trace amounts ambient dust particles and water or solute impurities that can never be completely removed, solution contained in a droplet is free of contact with any foreign bodies. Consequently, it can be assumed that during containerless crystallisation it is the homogeneous component that plays the key role in the nucleation process.

6.4 Containerless crystallisation of L-glutamic acid solution doped with additives

Further experiments probing crystallisation of levitated samples of L-glutamic acid solution were performed in the presence of three different amino acid additives, namely glycine, L-alanine and L-phenylalanine. Each of the additives was investigated at two doping levels, 2500 ppm and 10000 ppm. Selected WAXS spectra for the range of investigated conditions are shown in *Figures 6.13-6.18*.

6.4.1 Results

In all investigated samples, the WAXS peaks were observed at exactly the same positions corresponding only to the β polymorph of L-glutamic acid. It is particularly interesting that even in the presence of L-alanine or L-phenylalanine, the additives that are generally accepted

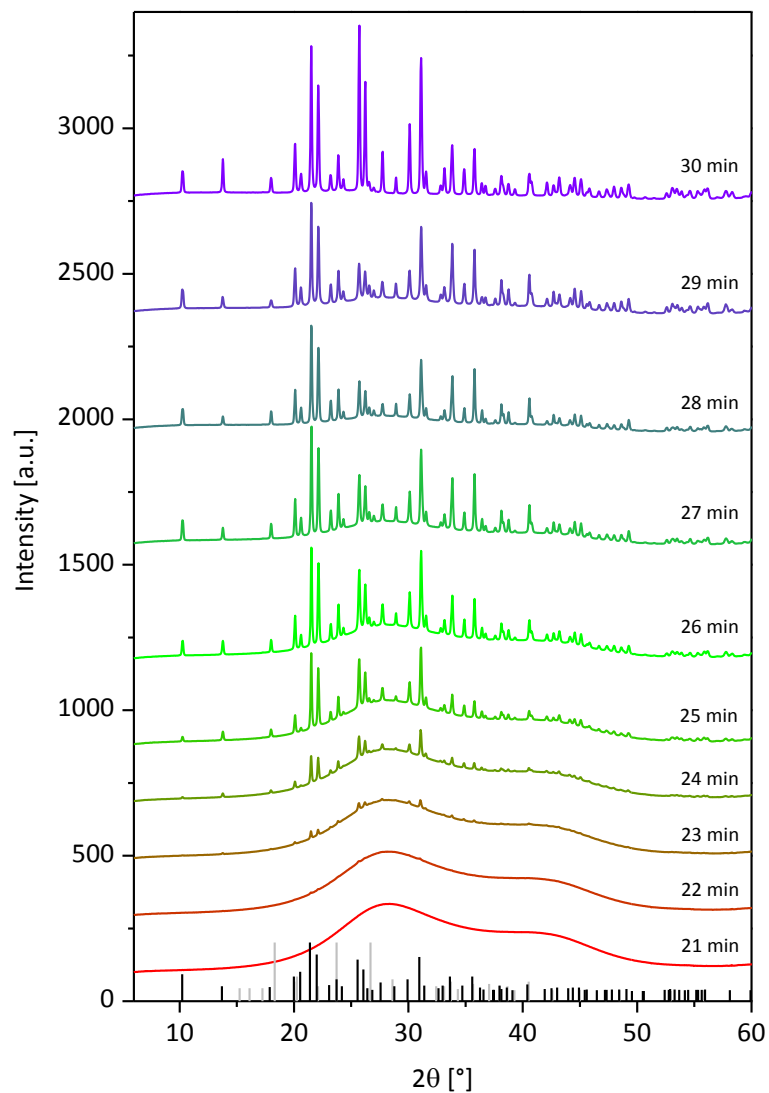


Figure 6.13 Selected WAXS spectra for a typical crystallisation of *L*-glutamic acid doped with 2500 ppm of glycine. Red and purple lines correspond to solution and the final crystallisation product, respectively. The bar codes represent the powder patterns of the two *L*-glutamic acid polymorphs, α (grey lines) and β (black lines).

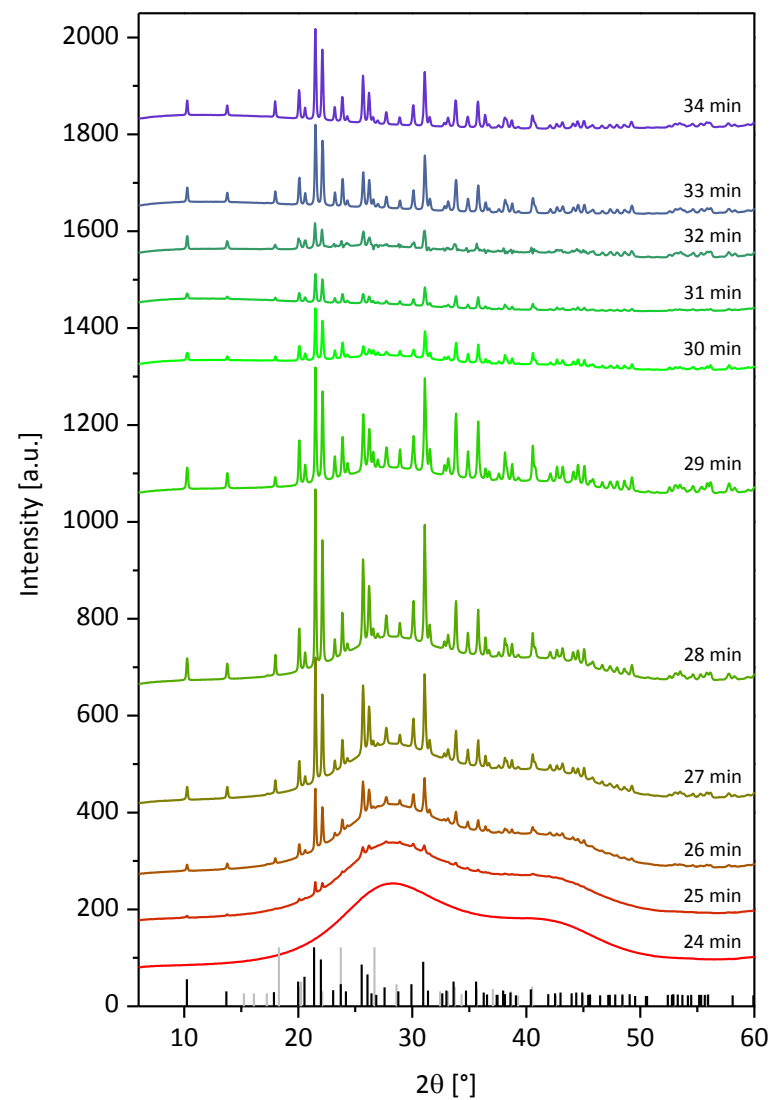


Figure 6.14 Selected WAXS spectra for a typical crystallisation of *L*-glutamic acid doped with 10000 ppm of glycine. Red and purple lines correspond to solution and the final crystallisation product, respectively. The bar codes represent the powder patterns of the two *L*-glutamic acid polymorphs, α (grey lines) and β (black lines).

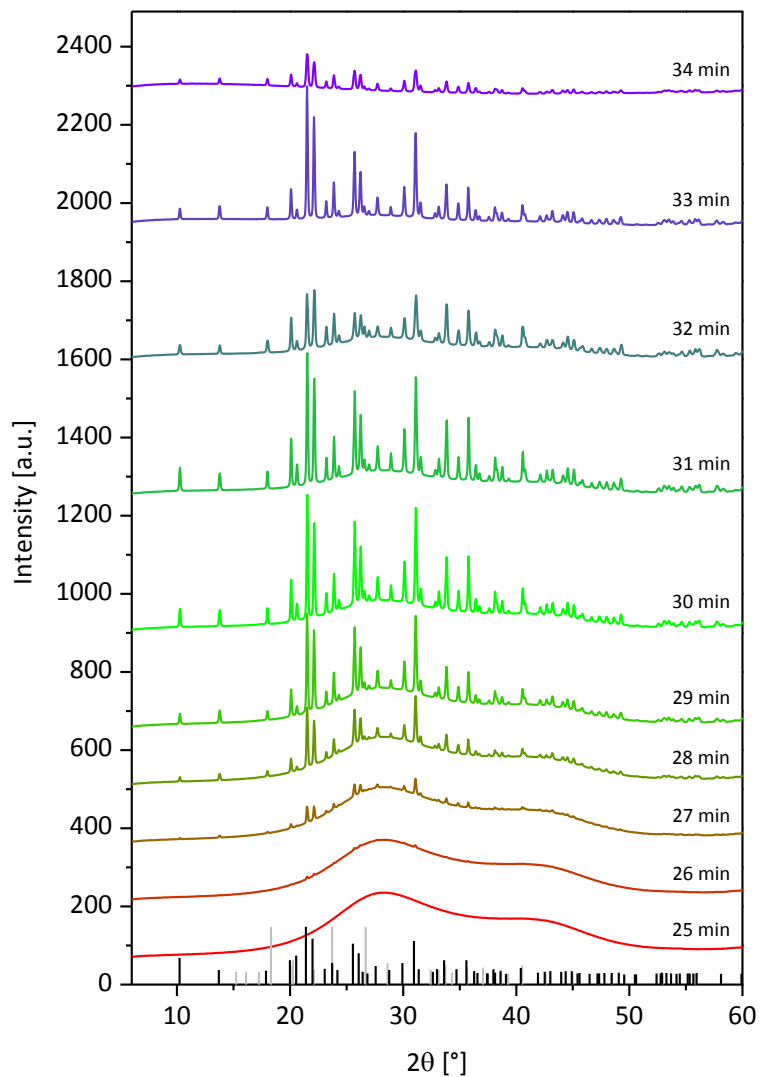


Figure 6.15 Selected WAXS spectra for a typical crystallisation of *L*-glutamic acid doped with 2500 ppm of *L*-alanine. Red and purple lines correspond to solution and the final crystallisation product, respectively. The bar codes represent the powder patterns of the two *L*-glutamic acid polymorphs, α (grey lines) and β (black lines).

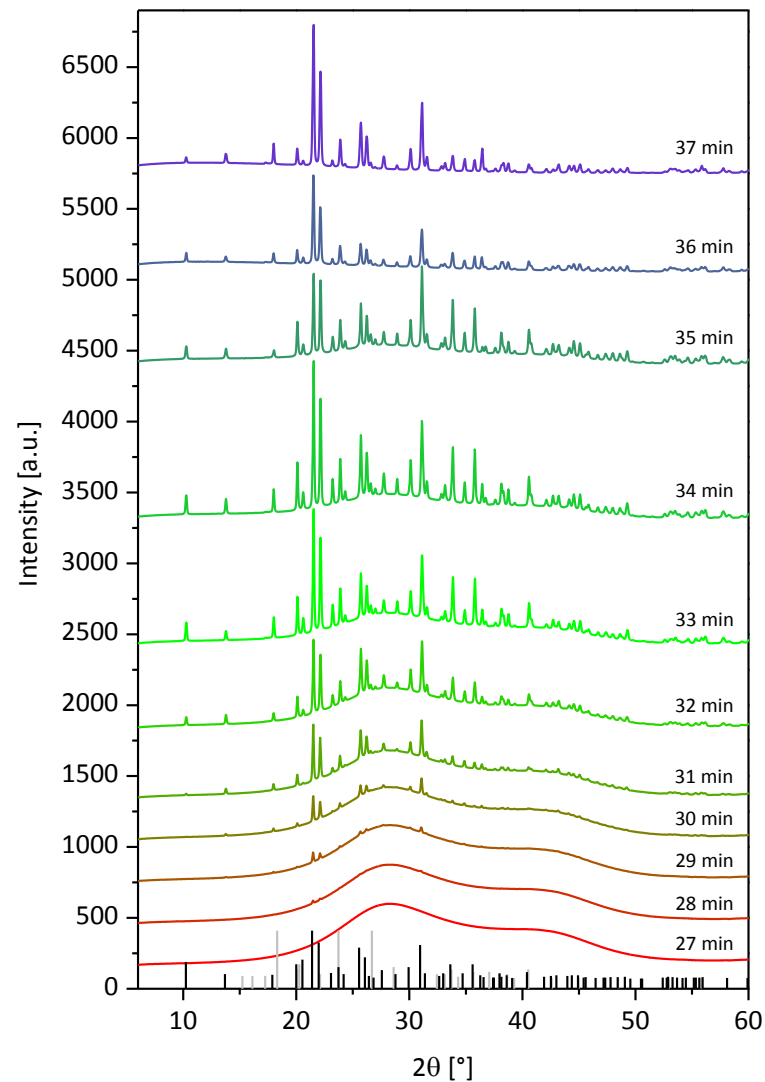


Figure 6.16 Selected WAXS spectra for a typical crystallisation of *L*-glutamic acid doped with 10000 ppm of *L*-alanine. Red and purple lines correspond to solution and the final crystallisation product, respectively. The bar codes represent the powder patterns of the two *L*-glutamic acid polymorphs, α (grey lines) and β (black lines).

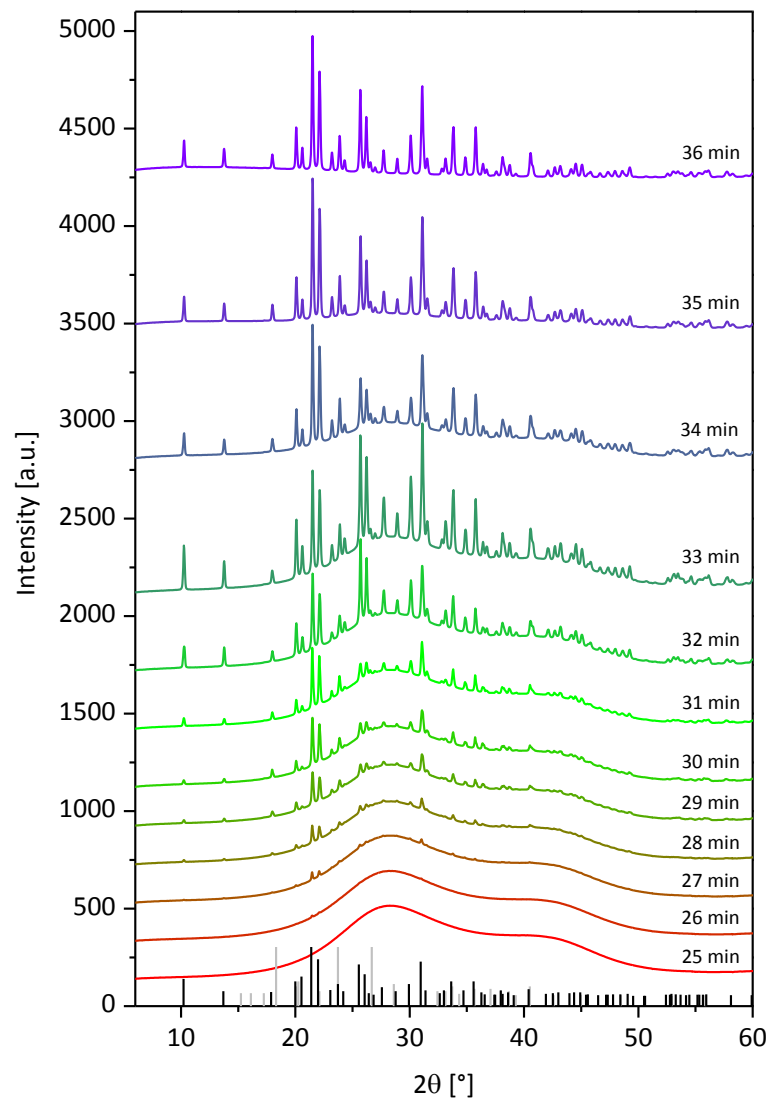


Figure 6.17 Selected WAXS spectra for a typical crystallisation of *L*-glutamic acid doped with 2500 ppm of *L*-phenylalanine. Red and purple lines correspond to solution and the final crystallisation product, respectively. The bar codes represent the powder patterns of the two *L*-glutamic acid polymorphs, α (grey lines) and β (black lines).

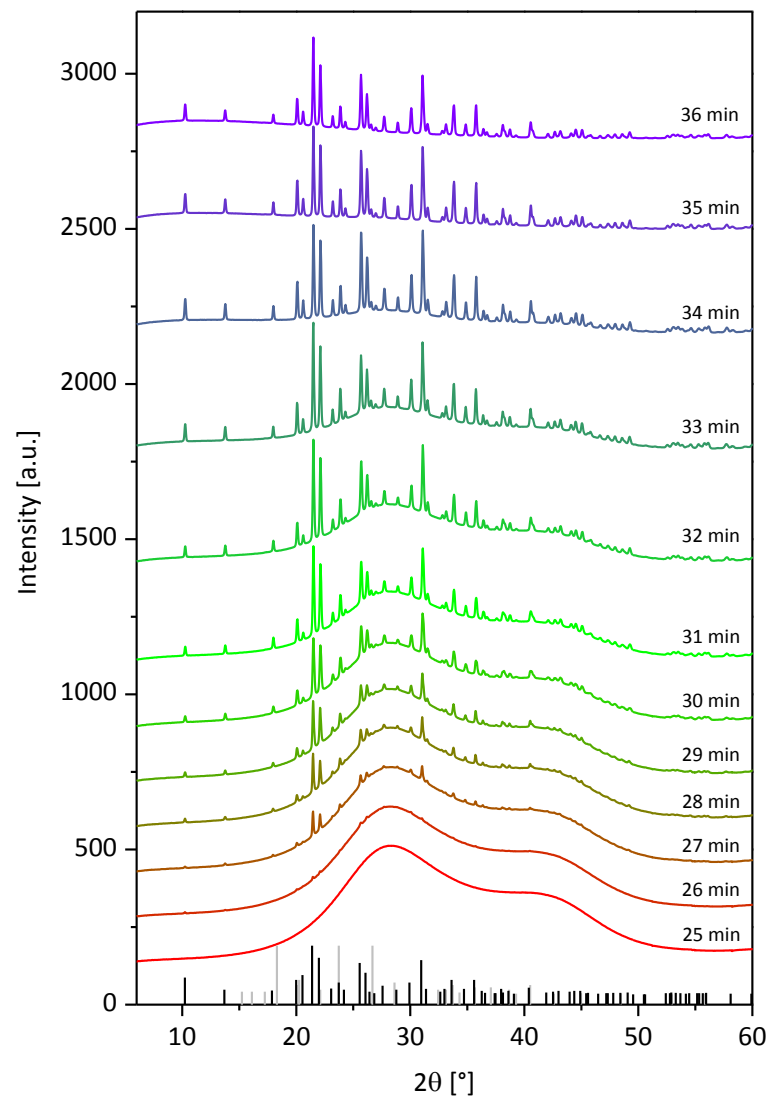


Figure 6.18 Selected WAXS spectra for a typical crystallisation of *L*-glutamic acid doped with 10000 ppm of *L*-phenylalanine. Red and purple lines correspond to solution and the final crystallisation product, respectively. The bar codes represent the powder patterns of the two *L*-glutamic acid polymorphs, α (grey lines) and β (black lines).

to hinder the nucleation and growth rates of β -L-glutamic acid and thus stabilise the α polymorph (Staab et al., 1990, Weissbuch et al., 1994, Kitamura and Funahara, 1994), no peaks that could be attributed to the metastable form were observed. As noted in the discussion below, the above-mentioned doping materials were also found to suppress the onset of the crystallisation process. Consequently, due to longer evaporation time, the background signal of the solvent at the moment of nucleation in the doped sample is weaker than in a pure solution. For these reasons, if small α form crystals were formed in a droplet, they would be likely to give an appreciable signal in the recorded spectrum. Thus, the lack of the α -L-glutamic acid peaks in the presence of the transformation hindering agents further supports the hypothesis postulated in *Sections 6.1.1* and *6.1.2* that the metastable polymorph does not nucleate during crystallisation in the acoustic levitator.

The scattering intensity is proportional to the volume of the irradiated sample. Because the solid material that precipitates out from a droplet forms a non-uniform crystalline aggregate, the intensity of the scattering peaks depends on the spatial orientation of the sample in the standing wave node. In *Section 6.1.3* it was noted that the levitated sample was in constant rotational motion caused by the acoustic field. Therefore, a variation of the maximum scattering intensity between different samples and fluctuations of the peak intensity for different measurements of the same sample were observed. The time evolution of the recorded peaks has been discussed in detail in *Section 6.2* and thus will not be discussed further here.

The obtained WAXS spectra were used to determine the nucleation time and the crystal growth time for each sample. Since nucleation is a stochastic process, each experiment was repeated multiple times (between 2 and 6, depending on the additive). The average values were then calculated and are presented in *Table 6.1*.

In pure solution, the average induction time was measured to be 26 minutes. It was found that upon addition of 2500 ppm of glycine, the nucleation time was reduced to approximately 22 minutes. However, when the level of the additive was increased to 10000 ppm, the effect of glycine on the nucleation rate was found to be negligible. At 2500 ppm of L-phenylalanine and both levels of L-alanine, the effect of the additive on the nucleation process was negligible or slightly hindering. A significant retardation of the nucleation process was only noted when the concentration of L-phenylalanine was increased to 10000 ppm. In the latter case, the average nucleation time was increased to 32 minutes.

Table 6.1 Average values of the nucleation and crystal growth time during crystallisation of L-glutamic acid in the acoustic levitator in the presence of additives. The estimated error is the standard deviation of the average.

Additive	Additive level (ppm)	Average nucleation time (min)	Average crystal growth time (min)
Pure L-glutamic acid	–	25 ± 3	7 ± 2
Glycine	2500	22 ± 1	7 ± 1
Glycine	10000	26 ± 2	7 ± 2
L-Alanine	2500	26 ± 2	8 ± 1
L-Alanine	10000	27 ± 2	9 ± 1
L-Phenylalanine	2500	26 ± 2	10 ± 1
L-Phenylalanine	10000	32 ± 3	5 ± 1

The average crystal growth time in pure solution was determined to be approximately 7 minutes and did not change significantly upon addition of 2500 ppm or 10000 ppm of glycine. L-alanine appeared to slow down the growth process and the effect was found to become more pronounced as the concentration of the additive was increased; the average crystal growth time was found to be 8 and 9 minutes at low and high level of L-alanine, respectively. It was determined that in the presence of 2500 ppm of L-phenylalanine the crystal growth was hampered even further and stopped, on average, 10 minutes after the nucleation of L-glutamic acid was noted. However, the crystal growth time recorded at 10000 ppm of L-phenylalanine was measured to be only 5 minutes.

6.4.2 Discussion

The presence of the additive was observed to markedly affect the nucleation rate of L-glutamic acid from a droplet only at 2500 ppm of glycine, where acceleration of the nucleation process was noted, and at 10000 ppm of L-phenylalanine, where hindering effect of the additive was observed. Interestingly, in the batch crystallisation both low level of glycine and high concentration of L-phenylalanine were found to affect the process in the same direction, markedly stimulating and retarding the nucleation of L-glutamic acid, respectively. Despite the obvious differences between the two systems, it is plausible to suggest that the mechanism of action of the additives and their effect on L-glutamic acid molecules in the solution phase could be similar. If that indeed was the case, low levels of

glycine would increase the nucleation rate by promoting formation of the β polymorph (c.f. *Chapter 4*). On the other hand, the increased nucleation time in the presence of high levels of L-phenylalanine would result from the additive molecules incorporating into the structure of the pre-nuclear clusters and consequently disrupting the formation of a stable nucleus.

The other investigated doping materials were, however, found to affect the nucleation rate only insignificantly. Therefore, the question that arises is why, in contrast to the batch crystallisation process, do high levels of glycine, the presence of L-alanine and low concentrations of L-phenylalanine not have a pronounced effect on the nucleation time of L-glutamic acid during crystallisation from a droplet? The answer requires consideration of solution concentration at the point when the nucleation process begins. Since crystallisation from a levitated droplet is essentially containerless, the number of external factors that could potentially affect the nucleation barrier and hence trigger the nucleation events is limited. On the other hand, in a batch crystalliser, the nucleation barrier is lowered by the interaction of the agitated solution with the vessel walls and the stirrer. As a result, when crystals begin to form, the concentration of solution in a droplet is several times higher than can be achieved in a conventional batch crystalliser. The nucleation process in the former system is thus almost entirely dominated by the drive towards the thermodynamic equilibrium and its behaviour approaches that of the pure system. Consequently, although the nucleation rate promoting/hindering effect in a droplet is likely to operate to some extent for all of the investigated additives, it is evident in the experimental data only for the conditions where the corresponding effect in the batch system would be most pronounced.

The overall effect of additives on L-glutamic acid crystallising from a droplet appears to be similar to that in the bulk also when the growth rate of the already nucleated crystals is concerned. In batch crystallisation, both L-alanine and L-phenylalanine were reported to hinder the crystal growth of β -L-glutamic acid (Sano et al., 1997, Kitamura and Ishizu, 1998). The growth retardation is considered to be due to the steric hindrance of the side groups of the additives that adsorb on the crystal faces. As suggested by Sano et al. (1997), the strength of the inhibition depends on the multiplication of the two factors that affect the surface diffusion of the growth units: (i) the similarity in the hydrogen bond formation and (ii) the bulk of the side group that hinders the next molecule to be adsorbed. It was indeed observed that both L-alanine and L-phenylalanine slow down the growth of the β -L-glutamic acid polymorph that precipitates out in a droplet. As expected, for the same doping level of

2500 ppm, L-phenylalanine, containing a bulky phenyl side chain, was observed to have a more pronounced hindering influence on the growth rate than L-alanine, whose molecules are relatively small. Moreover, it was found that the effect increases with increasing concentration of L-alanine. Interestingly, in the presence of 10000 ppm of L-phenylalanine, where the growth rate was expected to be also dependent on concentration and thus markedly reduced when compared to the pure solution, the crystallisation process was observed to cease much earlier than for the other solutions. However, one should bear in mind that the levitated droplet is an open system where the amount of solvent decreases with time due to evaporation. On average, at 10000 ppm of L-phenylalanine, the nucleation process did not begin until the 32nd minute of the experiment thus leading to a much higher supersaturation at the point of nucleation when compared to the other solutions. Additionally, as was observed by monitoring of the size of the droplet (*Section 6.1.3*), after approximately 36 minutes, hardly any water is still present in the experimental sample. Consequently, the growth driving force in this region, caused by high solution supersaturation and decreasing amount of solvent, would overbalance any, even a very prominent, effect of the additive and lead to complete precipitation of L-glutamic acid earlier than otherwise expected. Lastly, despite its potential incorporation into the crystal structure, especially at higher additive levels, the disrupting effect of glycine on the overall growth rate remains negligible, be it at 2500 ppm or 10000 ppm. It can thus be concluded that the experimental observations are in good agreement with the proposed hypothesis. The mechanism of the additives action that is believed to be present in batch crystallisation is therefore also likely to be in operation during crystallisation from a droplet using an acoustic levitator.

6.5 Conclusions

Crystallisation of L-glutamic acid from a droplet of supersaturated solution suspended in an acoustic field was investigated using simultaneous *in-situ* WAXS, Raman spectroscopy and droplet size monitoring techniques. It was observed that, unlike in a typical batch crystalliser, the more stable β is the first and only polymorph that nucleates from the droplet. Despite the inherent complexity of the problem, we made an attempt to provide a qualitative rationale explaining why the Ostwald's rule of stages is not followed and why the nucleation process does not lead to the initial formation of the metastable polymorph. Bearing in mind that the nucleation process is most likely to take place at the air-droplet interface, we argue that the freedom of movement of molecules in the prenucleation stage in a droplet is greater

than in the bulk. Accordingly, during containerless crystallisation, the probability of L-glutamic acid locally adopting a conformation similar to that of the β form is increased. We suggest that the resulting reduction in the nucleation barrier for the β phase would be enough to lead to the direct formation of only the more stable polymorph.

Additionally, in order to probe the effect of additives on the crystallisation from a droplet, further experiments were performed in the presence of glycine, L-alanine and L-phenylalanine at two doping levels, 2500 ppm and 10000 ppm. It was shown that the rates of both nucleation and crystal growth can be manipulated using selectively chosen amino acid additives. Since similar result has also been observed during batch crystallisation of L-glutamic acid, it was suggested that the mechanism responsible for the observed effect is of similar nature, i.e. the additive molecules adsorb on the crystal faces and are subsequently incorporated into the growing crystal structure. However, because the driving force for crystallisation in a droplet is markedly greater than during the batch process, the effect of the additives in the former case is much less pronounced.

Chapter 7

Conclusions

In the first part of this work, batch crystallisation of L-glutamic acid was investigated.

- Using single-photon laser light scattering and concentration monitoring techniques, it was observed that both nucleation and polymorphic transformation rates were enhanced in the presence of glycine additive. It was the first time when it was demonstrated that the crystallisation rates of one amino acid can be promoted using another amino acid as an additive.
- The nucleation-promoting effect was found to be concentration dependent and increase up to 5000 ppm of glycine. The critical nucleus radius was estimated to decrease with increasing concentration of the additive. The latter implies that glycine molecules promote formation of L-glutamic acid crystals by lowering the activation energy barrier. On the other hand, hampering of the nucleation process was observed at 7500 ppm. It was suggested that at the highest investigated doping level the molecules of glycine may become incorporated into some of the growing nuclei, rendering them thermodynamically unstable, increasing the activation energy barrier and consequently inhibiting the nucleation process.
- Scanning Electron Microscopy of the crystalline samples collected at the beginning of the crystallisation process showed that although in both pure and glycine-doped samples the α form crystals were dominant, an appreciably larger number and average size of β was present in the sample crystallised in the presence of the additive.
- Wide Angle X-ray Scattering measurements were carried out to quantify the observed polymorphic transformation enhancing effect. Time-resolved diffraction patterns were used to derive mole fraction evolutions of the two polymorphs of L-glutamic acid and their respective rates. Consequently, the evolution of the growth and dissolution of each polymorph could be monitored.

- A noticeable increase in the number of primarily nucleated β crystals was observed during crystallisation from solution doped with glycine. Furthermore, it was found that the growth rates of both α and β polymorphs were promoted in the presence of the additive. The crystallisation promoting effect of glycine was found to increase with increasing concentration of the doping material.
- Due to an increased amount of homogeneously nucleated β in the presence of glycine, the dissolution rate of the metastable α crystals was promoted leading to increased formation of secondary β . Consequently, a significant increase in the polymorphic transformation rate was observed. The former also results in the slope of the plateau on the concentration evolution curve becoming more negative as the level of glycine is increased.
- An improved method for determination of the polymorphic transformation time from the concentration evolution curves was proposed since the obtained data showed that the generally accepted criterion is not reliable.
- In general, this work demonstrated that even a relatively small amount of the additive can perturb the initial series of nucleation events and ultimately have a significant effect on the subsequent polymorphic transformation and thus on the crystallisation process as a whole.

The second part of this thesis considered, for the first time, crystallisation of L-glutamic acid from a droplet of supersaturated solution suspended in an acoustic field.

- Containerless nucleation and growth were investigated using *in-situ* time-resolved WAXS, Raman spectroscopy and droplet size monitoring techniques. It was found that, contrary to the Ostwald's rule of stages, the more stable β was the first and only polymorph that forms during crystallisation from a levitated droplet. The metastable polymorph did not nucleate even in the presence of the additives that were reported to stabilise the α form.
- It was postulated that the freedom of movement of molecules on the surface of a droplet, where the nucleation process takes place, is greater than in the bulk solution. Accordingly, the nucleation barrier for the β phase is lowered resulting in the direct formation of only the more thermodynamically stable polymorph.
- It was observed that the onset of crystallisation in a levitated droplet occurs at supersaturations which are an order of magnitude higher than those that can be achieved in a conventional crystalliser. The latter implies that it is the homogeneous

component that plays the key role in the nucleation process during containerless crystallisation, whereas crystallisation in a closed container is predominantly a heterogeneous process.

- Further experiments revealed that the rates of both nucleation and growth can, to some extent, be manipulated using other amino acids as additives. It was postulated that the observed effect is due to adsorption of the additive molecules on the growing crystal faces. However, since the driving force for crystallisation in a droplet is greater than during the batch process, the magnitude of the observed effect in the former case is much less pronounced.
- The presented results indicate that factors such as microscopic thermodynamic pathways and kinetics of the building up supersaturation in a levitated droplet, including its interfacial interaction with air, are quite distinctive from those in a crystallisation cell or a batch crystalliser.
- This entirely new effect demonstrates that different experimental techniques and strategies may provide not only a new mode of polymorph selection but also open many fundamental questions on how nature finds intriguing ways to help crystallisation of a stable polymorph.

Chapter 8

Further work

The results and their critical consideration presented in this work have not only markedly advanced the knowledge in the area of nucleation and crystal growth of the polymorphic materials but also opened new research avenues for more comprehensive appreciation of the overall complexity of the crystallisation process. Although a considerable effort was made to find a rationale for these new phenomena, several puzzling questions still remain. The following chapter outlines the experimental strategies that, in our opinion, should be adopted in order to shed more light on the molecular mechanisms of the underlying processes and answer (i) why under certain conditions primary nucleation of the stable β form of L-glutamic acid is promoted and (ii) why crystallisation of the latter from a droplet suspended in an acoustic field does not follow the Ostwald's rule of stages.

8.1 Investigation of the mechanism leading to the enhanced primary nucleation of β -L-glutamic acid in the presence of glycine additive

The results from the WAXS experiment provided valuable qualitative insight into the nature of the α to β transformation-promoting effect and showed that it is the enhanced nucleation of primary β that is primarily responsible for the observed increase in the polymorphic transformation rate. However, the exact mechanism leading to the increased nucleation of the more stable form of L-glutamic acid remains an open question. To tackle this problem, two different approaches can be taken: (i) neutron diffraction studies of L-glutamic acid solution with and without glycine additive and (ii) molecular modelling of the respective solutions.

Previous studies on two-component solutions (McLain et al., 2006, Burton et al., 2008, Burton et al., 2009, Burton et al., 2010) showed that neutron scattering experiments with isotope substitution and empirical potential structure refinement (EPSR) can provide detailed atomistic level data on the structure of saturated and supersaturated solutions. Most notably, these techniques have also been used to extract structural information for a three component

system, L-glutamic acid dissolved in a two molar sodium hydroxide solution (Soper, 1996). The above approach demonstrated a significant role of the nature of the solvent-solute interactions in determining the viability of the nucleation clusters and hence the structural crystallisation outcome.

In the aforementioned work, however, the investigated materials were highly soluble in the respective solvents and consequently the experimental solution contained more solute than solvent molecules. On the other hand, solubility of amino acids in water, including L-glutamic acid, is much lower and therefore the resulting solution would be too dilute for any diffraction method to directly probe the local solvation of these species. Nonetheless, the neutron diffraction experiment, a technique that is the accepted standard for production of the most accurate models of water structure (Soper, 2007), would provide detailed insights into the time-averaged environment of solvent and solute molecules in pure and glycine-doped solutions of L-glutamic acid and, hence, shed some light on understanding of the molecular aggregating events leading to the direct formation of the stable β polymorph and their nature at the initial, most critical, stage which defines the overall time-dependent crystallisation evolution of the system.

Experimental investigation of crystallisation kinetics in molecular systems is a challenging task since the formation of crystal nuclei in a supersaturated solution is a rare event but, when it happens, the process is typically very fast. On the other hand, a detailed investigation of short time processes can, in general, be performed using molecular dynamics (MD) modelling. Conventional MD simulations cannot, however, be used to study crystal nucleation under realistic conditions. Crystallisation in a molecular system may take minutes or hours. In a simulation, the situation would be worse because the volume that can be studied is several orders of magnitude smaller, and the probability of crystal formation is decreased by the same amount. Moreover, the computational cost of molecular dynamics simulations that cover more than 10^{-8} s becomes prohibitive (tenWolde and Frenkel, 1997).

One way to circumvent this problem is to simulate a system at a much higher supersaturation, where the free energy barrier for the crystal nuclei formation is sufficiently low to allow the system to crystallise spontaneously on a time scale that is accessible to MD simulation. However, Auer and Frenkel (2005) point out that at such extreme supersaturations crystallisation may proceed differently than at moderate levels, i.e. many crystal nuclei may form simultaneously and may interact in an early stage of their development. Instead, in order to study crystal nucleation at moderate supersaturations, Auer and Frenkel (2004) suggest

using a combination of numerical techniques, including umbrella sampling and a local bond-order analysis for the identification of crystal nuclei, to compute the shape and the height of the nucleation barrier and to study the structure of critical nuclei.

While molecular dynamics simulations can provide atomistic-level information on the structure and dynamics of the forming nucleus, one should also be aware of several limitations of this approach. Firstly, the computational techniques use a set of parameters defining equilibrium bond lengths, bond and torsional angles, partial charge values, force constants and van der Waals parameters, collectively known as force fields. Although an extensive effort is made to adjust these parameters to accurately represent specific aspects of a physical system, the relatively complex systems, such as solutions of amino acids, remain notoriously difficult to estimate (Oostenbrink et al., 2004). Secondly, the commonly used models assume the nucleation process to be homogeneous and steady-state, while, in the real world, crystallisation is usually initiated by heterogeneous nucleation.

8.2 Molecular dynamics modelling to determine the order parameters leading to selective nucleation of β -L-glutamic acid in a levitated droplet

Since the phenomena occurring at the surface of a crystallising droplet of L-glutamic acid are very rapid and of atomic scale, probing the nucleation events using the experimental techniques available at present is virtually impossible. For that reason, in order to try to answer why β is the only polymorph that nucleates in a levitated droplet, one should, in our opinion, tackle the problem by employing molecular dynamics (MD) simulations. The goal of the modelling approach would be to describe the sequence of events preceding the formation of critical nuclei using two parameters: (i) positional order parameter (density) and (ii) orientational order parameter. The questions that additionally arise are: ‘How are these parameters coupled, are they acting simultaneously, and which one is more important?’

However, modelling of the nucleation process remains a very difficult task. In addition to a number of apparent challenges arising during simulation of the formation of crystals in the bulk solution, discussed in *Section 8.1*, modelling of a levitated droplet requires consideration of significantly more complex conditions for which the order parameters are to be estimated: (i) the levitated droplet is a thermodynamically open system where water molecules are released from the surface into the surroundings, (ii) a radial gradient of concentration is

present inside the droplet, (iii) the nucleation process occurs at the surface and (iv) due to constant solvent evaporation, the composition at the surface of the droplet is changing with time. Furthermore, as revealed by Kawasaki and Tanaka (2010), the existence of additional transient medium-ranged structural order states that help crystallisation beyond the simplified model should not be ruled out.

References

- ADDADI, L., BERKOVITCH-YELLIN, Z., DOMB, N., GATI, E., LAHAV, M. & LEISEROWITZ, L. 1982. Resolution of conglomerates by stereoselective habit modifications. *Nature*, 296, 21-26.
- ANWAR, J., BOATENG, P. K., TAMAKI, R. & ODEDRA, S. 2009. Mode of Action and Design Rules for Additives That Modulate Crystal Nucleation. *Angewandte Chemie-International Edition*, 48, 1596-1600.
- AUER, S. & FRENKEL, D. 2004. Numerical prediction of absolute crystallization rates in hard-sphere colloids. *The Journal of Chemical Physics*, 120, 3015-3029.
- AUER, S. & FRENKEL, D. 2005. Numerical Simulation of Crystal Nucleation in Colloids. In: HOLM, C. & KREMER, K. (eds.) *Advanced Computer Simulation*. Springer Berlin Heidelberg.
- BAYES-GARCIA, L., CALVET, T., CUEVAS-DIARTE, M. A., UENO, S. & SATO, K. 2011. In situ synchrotron radiation X-ray diffraction study of crystallization kinetics of polymorphs of 1,3-dioleoyl-2-palmitoyl glycerol (OPO). *CrystEngComm*, 13, 3592-3599.
- BECKER, R. & DÖRING, W. 1935. Kinetische Behandlung der Keimbildung in übersättigten Dämpfen. *Annalen der Physik*, 416, 719-752.
- BECKER, W. 2010. *Advanced Time-Correlated Single Photon Counting Techniques*, Springer.
- BENNEMA, P. & VANENCKEVORT, W. J. P. 1979. Occurrence of a critical driving force for dissolution - theory and experimental-observation on KDP and other crystals. *Annales De Chimie-Science Des Materiaux*, 4, 451-459.
- BERNAL, J. D. 1931. Short notifications and notes - The crystal structure of the natural amino acids and related compounds. *Zeitschrift Fur Kristallographie*, 78, 363-369.
- BERNSTEIN, J. 1991. Polymorphism of L-glutamic acid: decoding the-phase relationship via graph-set analysis. *Acta Crystallographica Section B: Structural Science*, 47, 1004-1010.
- BERNSTEIN, J. 2002. *Polymorphism in molecular crystals*, Oxford University Press, Incorporated.
- BLACK, S. N. & DAVEY, R. J. 1988. Crystallization of amino-acids. *Journal of Crystal Growth*, 90, 136-144.
- BLACK, S. N., DAVEY, R. J. & HALCROW, M. 1986. The kinetics of crystal growth in the presence of tailor-made additives. *Journal of Crystal Growth*, 79, 765-774.

- BONAFEDE, S. J. & WARD, M. D. 1995. Selective Nucleation and Growth of an Organic Polymorph by Ledge-Directed Epitaxy on a Molecular Crystal Substrate. *Journal of the American Chemical Society*, 117, 7853-7861.
- BUGAY, D. E. & WILLIAMS, A. C. 1995. Physical Characterization of Pharmaceutical Solids. In: BRITTAIN, H. G. (ed.). New York: Marcel Dekker, Inc.
- BUNN, C. W. 1949. Crystal growth from solution. II. Concentration gradients and the rates of growth of crystals. *Discussions of the Faraday Society*, 5, 132-144.
- BURTON, R. C., FERRARI, E. S., DAVEY, R. J., FINNEY, J. L. & BOWRON, D. T. 2009. Relationship between Solution Structure and Phase Behavior: A Neutron Scattering Study of Concentrated Aqueous Hexamethylenetetramine Solutions. *Journal of Physical Chemistry B*, 113, 5967-5977.
- BURTON, R. C., FERRARI, E. S., DAVEY, R. J., FINNEY, J. L. & BOWRON, D. T. 2010. The Relationship between Solution Structure and Crystal Nucleation: A Neutron Scattering Study of Supersaturated Methanolic Solutions of Benzoic Acid. *Journal of Physical Chemistry B*, 114, 8807-8816.
- BURTON, R. C., FERRARI, E. S., DAVEY, R. J., HOPWOOD, J., QUAYLE, M. J., FINNEY, J. L. & BOWRON, D. T. 2008. The structure of a supersaturated solution: A neutron scattering study of aqueous urea. *Crystal Growth & Design*, 8, 1559-1565.
- BURTON, W. K., CABRERA, N. & FRANK, F. C. 1951. The Growth of Crystals and the Equilibrium Structure of their Surfaces. *Philosophical Transactions of the Royal Society of London. Series A, Mathematical and Physical Sciences*, 243, 299-358.
- CABRERA, N., LEVINE, M. M. & PLASKETT, J. S. 1954. Hollow dislocations and etch pits. *Physical Review*, 96, 1153-1153.
- CARDEW, P. T. & DAVEY, R. J. 1985. The kinetics of solvent-mediated phase-transformations. *Proceedings of the Royal Society of London Series A-Mathematical Physical and Engineering Sciences*, 398, 415-428.
- CASHELL, C., CORCORAN, D. & HODNETT, B. K. 2003a. Secondary nucleation of the beta-polymorph of L-glutamic acid on the surface of alpha-form crystals. *Chemical Communications*, 374-375.
- CASHELL, C., CORCORAN, D. & HODNETT, B. K. 2004. Control of polymorphism and crystal size of L-glutamic acid in the absence of additives. *Journal of Crystal Growth*, 273, 258-265.
- CASHELL, C., CORCORAN, D. & HODNETT, B. K. 2005. Effect of amino acid additives on the crystallization of L-glutamic acid. *Crystal Growth & Design*, 5, 593-597.
- CASHELL, C., SUTTON, D., CORCORAN, D. & HODNETT, B. K. 2003b. Inclusion of the stable form of a polymorph within crystals of its metastable form. *Crystal Growth & Design*, 3, 869-872.
- CHANDLER, D. & VARILLY, P. 2012. Lectures on Molecular- and Nano-scale Fluctuations in Water. *Proc. Internat. School Phys. Enrico Fermi, Course CLXXVI*, 176, 75-111.
- CHEN, C. L., QI, J. H., ZUCKERMANN, R. N. & DEYOREO, J. J. 2011. Engineered Biomimetic Polymers as Tunable Agents for Controlling CaCO₃ Mineralization. *Journal of the American Chemical Society*, 133, 5214-5217.

- CHERNOV, A. A. 1989. Formation of crystals in solutions. *Contemporary Physics*, 30, 251-276.
- CHYALL, L. J., TOWER, J. M., COATES, D. A., HOUSTON, T. L. & CHILDS, S. L. 2002. Polymorph Generation in Capillary Spaces: The Preparation and Structural Analysis of a Metastable Polymorph of Nabumetone. *Crystal Growth & Design*, 2, 505-510.
- CLAYDEN, J. 2001. *Organic chemistry*, Oxford University Press.
- CONSTABLE, R. F. S. 1968. *Kinetics and Mechanism of Crystallization*, Academic Press.
- CRACKNELL, A. P. 1969. *Crystals and their structures*, Pergamon Press.
- CULLITY, B. D. & STOCK, S. R. 2001. *Elements of X-ray diffraction*, Prentice Hall.
- DAVEY, R. J. 1982. Solvent Effects in Crystallization Processes. In: KALDIS, E. (ed.) *Current Topics in Materials Science*. North-Holland.
- DAVEY, R. J. 1990. *Manufacturing Chemist*.
- DAVEY, R. J., BLAGDEN, N., POTTS, G. D. & DOCHERTY, R. 1997. Polymorphism in molecular crystals: Stabilization of a metastable form by conformational mimicry. *Journal of the American Chemical Society*, 119, 1767-1772.
- DAVEY, R. J., BLAGDEN, N., RIGHINI, S., ALISON, H. & FERRARI, E. S. 2002. Nucleation control in solution mediated polymorphic phase transformations: The case of 2,6-dihydroxybenzoic acid. *Journal of Physical Chemistry B*, 106, 1954-1959.
- DAVEY, R. J., BLAGDEN, N., RIGHINI, S., ALISON, H., QUAYLE, M. J. & FULLER, S. 2001. Crystal polymorphism as a probe for molecular self-assembly during nucleation from solutions: The case of 2,6-dihydroxybenzoic acid. *Crystal Growth & Design*, 1, 59-65.
- DAVEY, R. J., CARDEW, P. T., MCEWAN, D. & SADLER, D. E. 1986. Rate controlling processes in solvent-mediated phase-transformations. *Journal of Crystal Growth*, 79, 648-653.
- DAVEY, R. J. & GARSIDE, J. 2000. *From Molecules to Crystallizers: An Introduction to Crystallization*, Oxford University Press.
- DAVEY, R. J., GUY, P. D. & RUDDICK, A. J. 1985. The IV - III polymorphic phase-transition in aqueous slurries of ammonium-nitrate. *Journal of Colloid and Interface Science*, 108, 189-192.
- DEBENEDETTI, P. G. 1996. *Metastable liquids: concepts and principles*, PRINCETON University Press.
- DEBYE, P. & SCHERRER, P. 1916. Interference on inordinate orientated particles in roentgen light. *Physikalische Zeitschrift*, 17, 277-283.
- DEIJ, M. A., TER HORST, J. H., MEEKES, H., JANSSENS, P. & VLIEG, E. 2007. Polymorph Formation Studied by 3D Nucleation Simulations. Application to a Yellow Isoxazolone Dye, Paracetamol, and l-Glutamic Acid. *The Journal of Physical Chemistry B*, 111, 1523-1530.
- DELISSSEN, F., LEITERER, J., BIENERT, R., EMMERLING, F. & THUNEMANN, A. F. 2008. Agglomeration of proteins in acoustically levitated droplets. *Analytical and Bioanalytical Chemistry*, 392, 161-165.

- DENBIGH, K. G. & WHITE, E. T. 1966. Studies on liquid inclusions in crystals. *Chemical Engineering Science*, 21, 739-753.
- DESIRAJU, G. R. 1989. *Crystal engineering: the design of organic solids*, Elsevier.
- DHAMELINCOURT, P. & RAMÍREZ, F. J. 1991. Polarized micro-Raman and Fourier transform infrared spectra of L-glutamic acid. *Journal of Raman Spectroscopy*, 22, 577-582.
- DHONT, J. K. G., SMITS, C. & LEKKERKERKER, H. N. W. 1992. A time resolved static light-scattering study on nucleation and crystallization in a colloidal system. *Journal of Colloid and Interface Science*, 152, 386-401.
- ELHADJ, S., DE YOREO, J. J., HOYER, J. R. & DOVE, P. M. 2006. Role of molecular charge and hydrophilicity in regulating the kinetics of crystal growth. *Proceedings of the National Academy of Sciences of the United States of America*, 103, 19237-19242.
- ERDEMIR, D., CHATTOPADHYAY, S., GUO, L., ILAVSKY, J., AMENITSCH, H., SEGRE, C. U. & MYERSON, A. S. 2007. Relationship between self-association of glycine molecules in supersaturated solutions and solid state outcome. *Physical Review Letters*, 99.
- FERRARI, E. S. & DAVEY, R. J. 2004. Solution-mediated transformation of alpha to beta L-glutamic acid: Rate enhancement due to secondary nucleation. *Crystal Growth & Design*, 4, 1061-1068.
- FOULKES, F. R. 2012. *Physical Chemistry for Engineering and Applied Sciences*, CRC Press, Taylor & Francis Group.
- FRANK, F. C. 1949. The influence of dislocations on crystal growth. *Discussions of the Faraday Society*, 5, 48-54.
- FU, G., QIU, S. R., ORME, C. A., MORSE, D. E. & DE YOREO, J. J. 2005. Acceleration of calcite kinetics by abalone nacre proteins. *Advanced Materials*, 17, 2678-+.
- GALKIN, O. & VEKILOV, P. G. 2000. Control of protein crystal nucleation around the metastable liquid-liquid phase boundary. *Proceedings of the National Academy of Sciences of the United States of America*, 97, 6277-6281.
- GARSIDE, J. 1994. *Separation Technology: The Next Ten Years*, Institution of Chemical Engineers.
- GARSIDE, J. & DAVEY, R. J. 1980. Secondary contact nucleation - kinetics, growth and scale-up. *Chemical Engineering Communications*, 4, 393-424.
- GARTI, N. & ZOUR, H. 1997. The effect of surfactants on the crystallization and polymorphic transformation of glutamic acid. *Journal of Crystal Growth*, 172, 486-498.
- GIBBS, J. W. 1876. On the equilibrium of heterogeneous substances. *Trans. Connecticut Acad. Arts Sci.*, 3, 108-248.
- GIBBS, J. W. 1878. On the equilibrium of heterogeneous substances. *Trans. Connecticut Acad. Arts Sci.*, 3, 343-524.
- GIBBS, J. W. 1948. *Collected Works*, New Haven, Yale University Press.
- GLATTER, O. & KRATKY, O. 1982. *Small Angle X-ray Scattering*, Academic Press.

- HA, J.-M., WOLF, J. H., HILLMYER, M. A. & WARD, M. D. 2004. Polymorph Selectivity under Nanoscopic Confinement. *Journal of the American Chemical Society*, 126, 3382-3383.
- HARTEL, R. W. 2001. *Crystallization in Foods*, Springer.
- HENCK, J.-O. & KUHNERT-BRANDSTATTER, M. 1999. Demonstration of the terms enantiotropy and monotropy in polymorphism research exemplified by flurbiprofen. *Journal of Pharmaceutical Sciences*, 88, 103-108.
- HILDEN, J. L., REYES, C. E., KELM, M. J., TAN, J. S., STOWELL, J. G. & MORRIS, K. R. 2003. Capillary Precipitation of a Highly Polymorphic Organic Compound. *Crystal Growth & Design*, 3, 921-926.
- HILFIKER, R. 2006. *Polymorphism*, Wiley.
- HIRAYAMA, N., SHIRAHATA, K., OHASHI, Y. & SASADA, Y. 1980. Structure of alpha form of L-glutamic acid - alpha-beta transition. *Bulletin of the Chemical Society of Japan*, 53, 30-35.
- HIROKAWA, S. 1955. A new modification of L-glutamic acid and its crystal structure. *Acta Crystallographica*, 8, 637-641.
- HUANG, J., STRINGFELLOW, T. C. & YU, L. 2008. Glycine exists mainly as monomers, not dimers, in supersaturated aqueous solutions: Implications for understanding its crystallization and polymorphism. *Journal of the American Chemical Society*, 130, 13973-13980.
- HUMPHREYS-OWEN, S. P. F. 1949. Crystal Growth from Solution. *Proceedings of the Royal Society of London. Series A. Mathematical and Physical Sciences*, 197, 218-237.
- IZMAILOV, A. F., MYERSON, A. S. & ARNOLD, S. 1999. A statistical understanding of nucleation. *Journal of Crystal Growth*, 196, 234-242.
- JACKSON, K. A. 1958. Liquid metals and solidification. In: DOREMUS, R. H. (ed.) *Growth and perfection of crystals*. American Society for Metals.
- JANCIC, S. J. & GROOTSCHOLTEN, P. A. M. 1984. *Industrial Crystallization*, Springer.
- JETTEN, L. A. M. J., HUMAN, H. J., BENNEMA, P. & VAN DER EERDEN, J. P. 1984. On the observation of the roughening transition of organic crystals, growing from solution. *Journal of Crystal Growth*, 68, 503-516.
- KASTNER, O., BRENN, G., RENSINK, D. & TROPEA, C. 2001. The acoustic tube levitator - A novel device for determining the drying kinetics of single droplets. *Chemical Engineering & Technology*, 24, 335-339.
- KAWASAKI, T. & TANAKA, H. 2010. Formation of a crystal nucleus from liquid. *Proceedings of the National Academy of Sciences of the United States of America*, 107, 14036-14041.
- KITAMURA, M. 1989. Polymorphism in the crystallization of L-glutamic acid. *Journal of Crystal Growth*, 96, 541-546.
- KITAMURA, M. 2002. Controlling factor of polymorphism in crystallization process. *Journal of Crystal Growth*, 237-239, Part 3, 2205-2214.

- KITAMURA, M. & FUNAHARA, H. 1994. Effect of L-phenylalanine and D-phenylalanine on crystallization and transformation of L-glutamic acid polymorphs. *Journal of Chemical Engineering of Japan*, 27, 124-126.
- KITAMURA, M. & ISHIZU, T. 1998. Kinetic effect of L-phenylalanine on growth process of L-glutamic acid polymorph. *Journal of Crystal Growth*, 192, 225-235.
- KITAMURA, M. & ISHIZU, T. 2000. Growth kinetics and morphological change of polymorphs of L-glutamic acid. *Journal of Crystal Growth*, 209, 138-145.
- KITAMURA, M. & NAKAMURA, T. 2001. Inclusion of amino acids and the effect on growth kinetics of l-glutamic acid. *Powder Technology*, 121, 39-45.
- KITAMURA, M. & ONUMA, K. 2000. In Situ Observation of Growth Process of α -L-Glutamic Acid with Atomic Force Microscopy. *Journal of Colloid and Interface Science*, 224, 311-316.
- KLIMAKOW, M., LEITERER, J., KNEIPP, J., ROSSLER, E., PANNE, U., RADEMANN, K. & EMMERLING, F. 2010. Combined Synchrotron XRD/Raman Measurements: In Situ Identification of Polymorphic Transitions during Crystallization Processes. *Langmuir*, 26, 11233-11237.
- KOPSWERKHOVEN, M. M. & FIJNAUT, H. M. 1981. Dynamic light-scattering and sedimentation experiments on silica dispersions at finite-concentrations. *Journal of Chemical Physics*, 74, 1618-1625.
- KOSSEL, W. 1934. Zur Energetik von Oberflächenvorgängen. *Annalen der Physik*, 413, 457-480.
- LAHAV, M. & LEISEROWITZ, L. 1993. Tailor-made auxiliaries for the control of nucleation, growth and dissolution of 2-dimensional and 3-dimensional crystals. *Journal of Physics D-Applied Physics*, 26, B22-B31.
- LARKIN, P. 2011. *Infrared and Raman Spectroscopy: Principles and Spectral Interpretation*, Elsevier Science.
- LEHMANN, M., KOETZLE, T. & HAMILTON, W. 1972. Precision neutron diffraction structure determination of protein and nucleic acid components. VIII: the crystal and molecular structure of the β -form of the amino acid L-glutamic acid. *J. Cryst. Mol. Struct*, 2, 225.
- LEHMANN, M. S. & NUNES, A. C. 1980. A short hydrogen bond between near identical carboxyl groups in the [alpha]-modification of l-glutamic acid. *Acta Crystallographica Section B*, 36, 1621-1625.
- LEITERER, J., LEITENBERGER, W., EMMERLING, F., THUNEMANN, A. F. & PANNE, U. 2006. The use of an acoustic levitator to follow crystallization in small droplets by energy-dispersive X-ray diffraction. *Journal of Applied Crystallography*, 39, 771-773.
- MCKIE, D. & MCKIE, C. 1974. *Crystalline solids*, Wiley.
- MCLAIN, S. E., SOPER, A. K. & WATTS, A. 2006. Structural studies on the hydration of L-glutamic acid in solution. *Journal of Physical Chemistry B*, 110, 21251-21258.
- MCMURRY, J. 1996. *Organic chemistry*, Brooks/Cole Pub. Co.

- MITCHELL, C. A., YU, L. & WARD, M. D. 2001. Selective Nucleation and Discovery of Organic Polymorphs through Epitaxy with Single Crystal Substrates. *Journal of the American Chemical Society*, 123, 10830-10839.
- MULLIN, J. W. 2001. *Crystallization*, Oxford, Butterworth-Heinemann.
- NIELSEN, A. E. 1964. *Kinetics of precipitation*, New York, Pergamon Press.
- OHARA, M. & REID, R. C. 1973. *Modeling crystal growth rates from solution*, Prentice-Hall.
- ONO, T., TER HORST, J. H. & JANSENS, P. J. 2004. Quantitative measurement of the polymorphic transformation of L-glutamic acid using in-situ Raman spectroscopy. *Crystal Growth & Design*, 4, 465-469.
- ONUKI, A. 2002. *Phase Transition Dynamics*, Cambridge University Press.
- OOSTENBRINK, C., VILLA, A., MARK, A. E. & VAN GUNSTEREN, W. F. 2004. A biomolecular force field based on the free enthalpy of hydration and solvation: The GROMOS force-field parameter sets 53A5 and 53A6. *Journal of Computational Chemistry*, 25, 1656-1676.
- OSTWALD, W. 1893. *Lehrbuch der allgemeinen Chemie*, W. Engelmann.
- OSTWALD, W. 1897. Studien über die Bildung und Umwandlung fester Körper. *Zeitschrift für Physikalische Chemie*, 22, 289.
- PETERSON, M. L., MORISSETTE, S. L., MCNULTY, C., GOLDSWEIG, A., SHAW, P., LEQUESNE, M., MONAGLE, J., ENCINA, N., MARCHIONNA, J., JOHNSON, A., GONZALEZ-ZUGASTI, J., LEMMO, A. V., ELLIS, S. J., CIMA, M. J. & ALMARSSON, Ö. 2002. Iterative High-Throughput Polymorphism Studies on Acetaminophen and an Experimentally Derived Structure for Form III. *Journal of the American Chemical Society*, 124, 10958-10959.
- RADNIK, J., BENTRUP, U., LEITERER, J., BRÜCKNER, A. & EMMERLING, F. 2011. Levitated Droplets as Model System for Spray Drying of Complex Oxides: A Simultaneous in Situ X-ray Diffraction/Raman Study. *Chemistry of Materials*, 23, 5425-5431.
- ROELANDS, C. P. M., TER HORST, J. H., KRAMER, H. J. M. & JANSENS, P. J. 2005. The unexpected formation of the stable beta phase of l-glutamic acid during pH-shift precipitation. *Journal of Crystal Growth*, 275, e1389-e1395.
- ROELANDS, C. P. M., TER HORST, J. H., KRAMER, H. J. M. & JANSENS, P. J. 2007. Precipitation mechanism of stable and metastable polymorphs of L-glutamic acid. *AIChE Journal*, 53, 354-362.
- SAKATA, Y. 1961a. Studies on Polymorphism of L-Glutamic Acid Part 1. Effects of Coexisting Substances on Polymorphic Crystallization. *Agricultural and Biological Chemistry*, 25, 829-834.
- SAKATA, Y. 1961b. Studies on Polymorphism of L-Glutamic Acid Part 2. Measurement of Solubilities. *Agricultural and Biological Chemistry*, 25, 835-&.
- SAKATA, Y. & TAKENOUCI, K. 1963. Studies on Polymorphism of L-Glutamic Acid Part 7. Enthalpy Differences between Alpha- And Beta-crystals. *Agricultural and Biological Chemistry*, 27, 615-&.

- SANO, C., KASHIWAGI, T., NAGASHIMA, N. & KAWAKITA, T. 1997. Effects of additives on the growth of L-glutamic acid crystals (beta-form). *Journal of Crystal Growth*, 178, 568-574.
- SOPER, A. K. 1996. Empirical potential Monte Carlo simulation of fluid structure. *Chemical Physics*, 202, 295-306.
- SOPER, A. K. 2001. Tests of the empirical potential structure refinement method and a new method of application to neutron diffraction data on water. *Molecular Physics*, 99, 1503-1516.
- SOPER, A. K. 2007. Joint structure refinement of x-ray and neutron diffraction data on disordered materials: application to liquid water. *Journal of Physics-Condensed Matter*, 19.
- STAAB, E., ADDADI, L., LEISEROWITZ, L. & LAHAV, M. 1990. Control of polymorphism by 'tailor-made' polymeric crystallization auxiliaries. Preferential precipitation of a metastable polar form for second harmonic generation. *Advanced Materials*, 2, 40-43.
- TENWOLDE, P. R. & FRENKEL, D. 1997. Enhancement of protein crystal nucleation by critical density fluctuations. *Science*, 277, 1975-1978.
- TRINH, E. H. & HSU, C.-J. 1986. Equilibrium shapes of acoustically levitated drops. *The Journal of the Acoustical Society of America*, 79, 1335-1338.
- TURNBULL, D. 1969. Under What Conditions Can a Glass Be Formed. *Contemporary Physics*, 10, 473-&.
- VAN HOOK, A. & BRUNO, A. J. 1949. Nucleation and growth in sucrose solutions. *Discussions of the Faraday Society*, 5, 112-117.
- VANDAELE, V., LAMBERT, P. & DELCHAMBRE, A. 2005. Non-contact handling in microassembly: Acoustical levitation. *Precision Engineering*, 29, 491-505.
- VANDERHOEK, B., VANDEREERDEN, J. P. & BENNEMA, P. 1982. Thermodynamical stability conditions for the occurrence of hollow cores caused by stress of line and planar defects. *Journal of Crystal Growth*, 56, 621-632.
- VANENCKEVORT, W. J. P. & VANDERLINDEN, W. H. 1979. Relation between etch pits or growth hillocks and dislocations on the (111) faces of potassium aluminum alum. *Journal of Crystal Growth*, 47, 196-202.
- VOLMER, M. 1939. *Kinetics of Phase Formation (Kinetik Der Phasenbildung)*, Air Force Cambridge Research Center, Geophysics Research Division, Atmospheric Physics Laboratory.
- WEISSBUCH, I., ADDADI, L., LAHAV, M. & LEISEROWITZ, L. 1991. Molecular recognition at crystal interfaces. *Science*, 253, 637-645.
- WEISSBUCH, I., LEISEROWITZ, L. & LAHAV, M. 1994. Tailor-made and charge-transfer auxiliaries for the control of the crystal polymorphism of glycine. *Advanced Materials*, 6, 952-956.
- WEISSBUCH, I., TORBEEV, V. Y., LEISEROWITZ, L. & LAHAV, M. 2005. Solvent effect on crystal polymorphism: Why addition of methanol or ethanol to aqueous solutions induces the precipitation of the least stable beta form of glycine. *Angewandte Chemie-International Edition*, 44, 3226-3229.

- WINICK, H. 1995. *Synchrotron Radiation Sources: A Primer*, World Scientific Publishing Company Incorporated.
- WOLF, S. E., LEITERER, J., KAPPL, M., EMMERLING, F. & TREMEL, W. 2008. Early Homogenous Amorphous Precursor Stages of Calcium Carbonate and Subsequent Crystal Growth in Levitated Droplets. *Journal of the American Chemical Society*, 130, 12342-12347.
- ZACCARO, J., MATIC, J., MYERSON, A. S. & GARETZ, B. A. 2000. Nonphotochemical, Laser-Induced Nucleation of Supersaturated Aqueous Glycine Produces Unexpected γ -Polymorph. *Crystal Growth & Design*, 1, 5-8.